Second Series *May 15, 1932* *Vol. 40, No. 4*

THE

PHYSICAL REVIEW

The Shape of an X-ray Line

By ARCHER HOYT
Department of Physics, Cornell University

(Received March 28, 1932)

An x-ray emission line as measured by the double-crystal spectrometer ("anti-parallel" position) can be represented very accurately by means of a simple empirical formula. Some uses for the formula are (1) location of background under the $K\alpha$ doublet, (2) the calculation of the separation of close components from measured points used in the empirical formula. This formula appears to be a function of a very useful type since it is also a good representation of rocking curves obtained in the "parallel" position of the spectrometer. A search for theoretical justification of this type of formula has brought to light the curious result that although the application of the Dirac quantum theory of the radiation field yields a formula of the same type, the maximum ordinate predicted is independent of the spontaneous transition probability; whereas, certain experimental work indicates that the maximum ordinate is a good measure of the line intensity. This is very disturbing since the assumption is usually made that the line intensity *is* proportional to this Einstein coefficient of spontaneous transition.

AN X-RAY emission line can be represented very accurately by means of a simple empirical formula of the type

$$y = \frac{a}{1 + (x/b)^2} \tag{1}$$

where the ordinate y represents the intensity $I(\lambda)$ as a function of $x \equiv (\lambda_0 - \lambda)$, b the *half-width at half-maximum*, a the maximum ordinate of the spectral line, and λ_0 the wave-length of that ordinate.

If one integrates Eq. (1) to get the total area under the emission line contour, which of course is a measure of the intensity of the x-ray line which it represents, one has

$$I = 2ab \int_0^\infty \frac{b\,dx}{b^2 + x^2} = \pi ab. \tag{2}$$

Since Eq. (1) really fits very nicely an x-ray emission line as measured with a double crystal spectrometer, (2) indicates that for a given line the maximum ordinate of an x-ray line is a correct measure of its intensity (i.e., as a function of excitation voltage as in work by Wooten,[1] and DuMond and Hoyt[2]) pro-

[1] Wooten, Phys. Rev. **13**, 71 (1919).
[2] DuMond and Hoyt, Phys. Rev. **36**, 799 (1930).

vided of course that b, the half-width at half-maximum, is not affected markedly (i.e., as by different excitation voltages).

Eqs. (1) and (2) are general formulae which can be specialized and simplified by taking $b=1$ as the natural unit of the abscissa scale. This gives

$$y' = \frac{a}{1+(x')^2} \qquad (1)'$$

$$I = \pi a. \qquad (2)'$$

In this form the work of plotting is somewhat simplified. A table of the function $1/(1+x^2)$ is very useful in that most of the computation involved need only be done once although the computed results are to be applied to many line structures.

As an example of the kind of fit one gets with this type of formula, Fig. 1 gives an actual emission line Mo $K\alpha_1$ measured with a double crystal spectrometer in the first order. To make the fit, one measures the maximum ordinate a, and the half-width at half-maximum b, (which is taken as the unit of the abscissa scale in (1)′) and calculates the various points which fit as indicated.

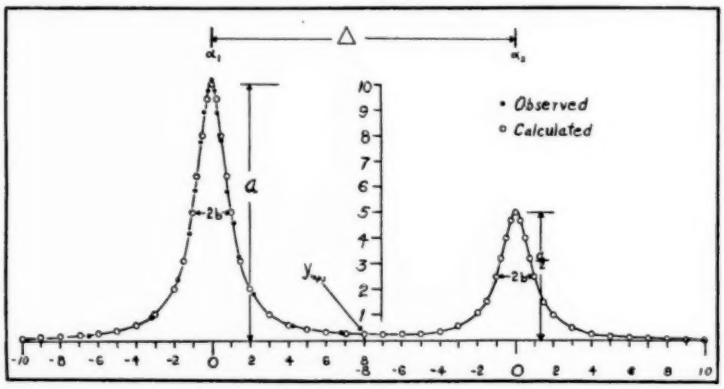

Fig. 1. An actual spectral line (Mo $K\alpha_1$ real—α_2 artificial) measured by means of the double crystal spectrometer by Richtmyer and Barnes. The Mo $K\alpha$ doublet was excited at 50 k.v. and 10 m.a. The vertical divergence of the x-ray beam was less than 30 minutes of arc; hence the measured curve must closely approach the natural structure of the x-ray line. The solid dots represent observed points while the open circles represent the calculated points obtained from the empirical Eq. (1).

The author has applied this formula to the following x-ray lines as measured with the double-crystal spectrometer: Mo $K\alpha_1$, α_2, γ, Cu $K\alpha_1$, α_2, all of which were x-ray emission lines. The formula was also applied to the scattered radiation lines Mo $K\alpha_{1,2}$ unmodified and Mo $K\alpha_{1,2}$ modified radiation. In this latter case the fit may well be fortuitous. However, in all cases available the fit was exceedingly good for first order lines. In every case cleavage faces of a calcite crystal were used in the spectrometers.

Uses for the Empirical Formula

Several uses for the empirical formula immediately present themselves.

(1) The several orders of a spectral line can be compared as can also different spectral lines. Of course this is not essentially different from a direct graphical comparison except that one has an actual, workable, analytic equation of the line contour instead of merely a functional curve $I(\lambda)$.

(2) In the $K\alpha$ doublet, for example, one can use the analytic equation of two partially superposed lines of different intensity to determine just where to locate the continuous background since the midpoint ordinate of the saddle between the two lines always bears a definite ratio to the maximum ordinate, being in the case of Mo $K\alpha$ about 2.3 and 4.6 percent of the maximum ordinate of α_1 and α_2 respectively. In this case one has

$$y' = \frac{a}{1 + (x')^2} + \frac{a/2}{1 + (x' - \Delta)^2} \tag{3}$$

where $\Delta \approx 16$ times the half-width at half-maximum. (See Fig. 1). (Δ is taken as 16 b for the purpose of illustration only. It is determined graphically in

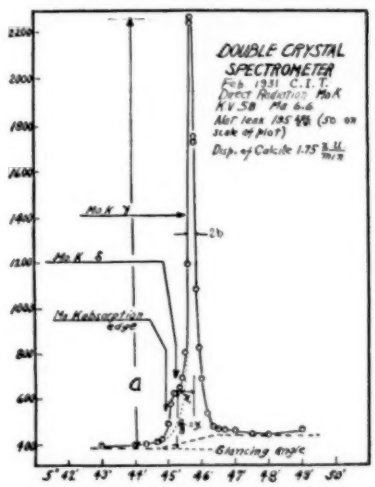

Fig. 2. This illustrates the use of the empirical formula in determining the separation of partially resolved components of an observed line structure of simple form.

this case. It varies to values as high as 25 b for some spectral lines depending on the perfection of the crystals of the spectrometer and the kind of corrections one applies to the experimental data.) To obtain the midpoint ordinate, one puts $x' = \Delta/2 = 8$ and $\Delta = 16$ in Eq. (3) and solves for y_{mp_3}', the ordinate of the midpoint of the saddle. One gets

$$y_{mp_3}' = 0.023a \tag{4}$$

where a is the maximum ordinate of $K\alpha_1$. This relation (4) gives a method of locating the background which is better than a guess since one has from the experimental observations both the peak of α_1 and the midpoint of the saddle as places to measure down from.

(3) In case there is partially resolved structure in the experimentally observed curve, one can attempt to get at its real nature by measuring the

location of maxima, minima and inflection points, and calculating their location as a function of intensity ratios and separations of the various components in an assumed empirical equation of the type (3). In general, this is laborious, but in clear cut special cases the labor is much reduced. In the case shown in Fig. 2, one measures the ordinate of the inflection point (or any other) on the delta line and finds it to be $a/9$ where a is the maximum ordinate of the γ line, and determines the intensity ratio of the two as 7:1 by means of a planimeter. (In Fig. 2 one interpolates the dotted background for the δ line by Eq. (1) applied to the γ line or by a graphical means such as a spline. One next measures with a planimeter the area under the δ line and above the dotted line and compares this with the area measured under the γ line proper and above the background. The ratio of these areas is about 7.3:1, for purposes of illustration, say 7:1.) The equation of the two superposed is, for the point y_1

$$y_1 = \frac{a}{1 + x_1^2} + \frac{a/7}{1 + (x_1 + \Delta)^2} \tag{5}$$

y_1 is measured as $a/9$, and x_1 as $-5\ b$. Solving (5) numerically, one gets $-\Delta = 3.88b$, and since $b = 0.2$ x.u., $-\Delta = 0.675$ x.u. Assuming that the lines

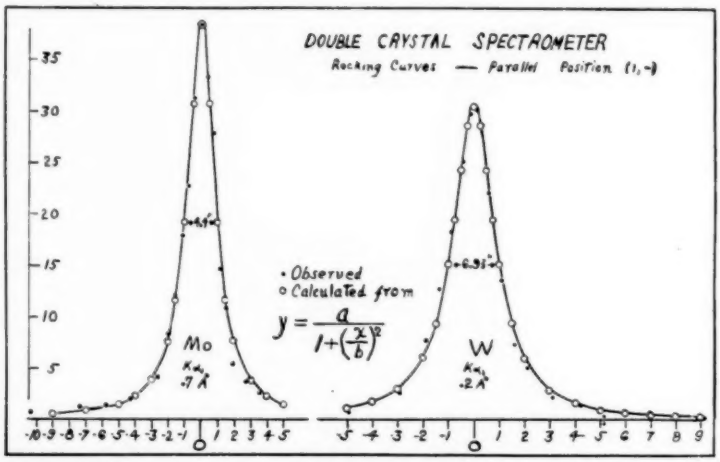

Fig. 3. The rocking curves shown are for a pair of calcite crystals in the parallel position (1, −1). The curves are selected from a series of curves which were taken in the process of making the axes of rotation prallel. The particular curve chosen from each series is the one which gives the minimum width at half-maximum ordinate. The observations, made by Richtmyer and Barnes are represented by solid dots; while the full line curves and the open dots are from the empirical formula. The figure shows the type of fit obtainable for two widely different wavelength regions, Mo $K\alpha_1$ and W $K\alpha_1$.

γ and δ are similar, this value for the separation should be much better than a graphical guess. Of course this value hangs on the assumption that the lines are similar.[3]

Eq. (1) is a curve which is determined by fixing the values of two constants. Obviously one need not be able to measure the maximum ordinate and the half-maximum half-width to get the exact analytic equation of the

line. One need only measure the coördinates of any two points anywhere on the curve. A method of getting b and a from a series of measurements on two or more points has been devised by the author.

Rocking Curves—Parallel Position of Crystals

Eq. (1) appears to be a formula of a very useful type since it also fits the rocking curve obtained with the crystals of the spectrometer in the "parallel" $(n, -n)$ position. The author has applied the formula to many of the rocking curves published in the literature. Great difficulty was often encountered here because the background of the rocking curves was frequently not given. An example of the type of fit one gets with a rocking curve for the parallel position of the crystals is given in Fig. 3. The fit is made for the narrowest rocking curves obtained when the crystal axes were being given their final adjustment for exact parallelism.

Theoretical Justification of Eq. (1)

After using Eq. (1) for some time, a search of the literature was made to justify it. In the case of resonance lines, Weisskopf and Wigner,[4] and F. Hoyt[5] have made the calculation of the intensity function from the viewpoint of the Dirac quantum theory of the radiation field. These investigators get formulae which are essentially the same:

$$I(\nu)d\nu = \frac{\gamma^2 h\nu_0 d\nu}{(\gamma/2)^2 + 4\pi^2(\nu - \nu_0)^2} \tag{6}$$

where γ is the Einstein probability coefficient of spontaneous transition and ν_0 is the frequency of the peak of the emission line. A constant factor $\gamma h\nu_0$ was added to the numerator of Eq. (6) as given by Weisskopf and Wigner to make it dimensionally correct, and to make the total intensity of the spectral line be

$$I = \int_{-\infty}^{\infty} I(\nu)d\nu = \gamma h\nu_0.$$

Taking

$$I(\lambda)d\lambda \equiv I(\nu)d\nu$$
$$\nu\lambda = c$$
$$d\nu = (c/\lambda^2)(-d\lambda)$$

Eq. (6) becomes

$$I(\lambda)d\lambda = \frac{4hc^2(-d\lambda)/\lambda_0\lambda^2}{1 + (\lambda_0 - \lambda)^2(4\pi c)^2/(\lambda_0\lambda\gamma)^2}. \tag{6'}$$

Since Eq. (1) has appreciable values only when $\lambda \approx \lambda_0$, it is indistinguishable from (6)′ and hence (6). These equations give the maximum ordinate and the half-maximum *half-width* in wave-length units

[3] DuMond and Hoyt, Phys. Rev. **38**, 839 (1931).
[4] Weisskopf and Wigner, Zeits. f. Physik **63**, 54 (1930).
[5] F. Hoyt, Phys. Rev. **36**, 860 (1930).

$$a = 4hc^2/\lambda_0\lambda^2 \tag{7}$$

$$b = \Delta\lambda = (\lambda_0 - \lambda) = \gamma\lambda\lambda_0/4\pi c. \tag{8}$$

In deriving expression (6), γ was assumed proportional to the intensity of the emission line. It is found experimentally that the maximum ordinate of a particular x-ray emission line is a good measure of its intensity.[1,2] *Hence it is very disturbing to note in Eq.* (7) *that the maximum ordinate is independent of* γ, while the half-maximum half-width is proportional to γ. However, it is quite pleasing to find that (1) and (6)′ are practically indistinguishable in form.

From classical theory on the basis of a damped linear oscillator, one gets a similar type of formula with a damping factor $\gamma/2$ and a half-width at half-maximum of $\gamma\lambda\lambda_0/4\pi c$ in wave-length units. On the classical theory of radiation damping

$$\gamma/2 = 4\pi^2e^2/3mc\lambda^2. \tag{9}$$

Substituting (9) in (8)

$$b = \Delta\lambda = 2\pi e^2/3mc^2 = 0.06 \text{ x.u.} \tag{10}$$

which leaves the half-maximum half-width ascribable to radiation damping independent of wave-length.[6]

In making the experimental measurements, the line contour observed is made up of three parts, one the natural or real line width; the others are spurious widths due to geometrical causes such as vertical divergence of the x-ray beam and crystal perfection. The width due to vertical divergence can be made negligible by the use of a vertical slit system since for the small angles involved, it is dependent on the square of the angle of vertical divergence. To correct for the crystal imperfection, one takes observations on the transmission of the crystals in the "parallel"[7] position. Expressing the *half-widths* W_1 and W_2 for the rocking curves of the two crystals in angular measure, the *half-width* of the line W_λ in linear measure, and the dispersion D as $d\theta/d\lambda$, one has, following Schwarzschild[8] and Allison and Williams,[7] for the *observed width* of a spectral line measured in any of the "anti-parallel"[7] positions

$$W^2 = W_1^2 + W_2^2 + D^2W_\lambda^2 = 2W_1^2 + D^2W_\lambda^2 \tag{11}$$

where all curves involved were assumed Gaussian in shape. This of course is only approximately true. A more exact method of making this type of correction has been worked out by Spencer.[9] He finds that Eq. (11) does not give a large enough correction. Typical experimental data appear in Table I. One notes from the data given that by Eq. (11) the effect of the rocking curve (parallel position) makes up about a quarter or less of the observed width. A comparison of Eq. (10) with the last column of the table is also of interest. A

[6] Allison and Williams, Phys. Rev. **35,** 1490 (1930).
[7] Allison and Williams, Phys. Rev. **35,** 149 (1930).
[8] Schwarzschild, Phys. Rev. **32,** 162 (1928).
[9] Spencer, Phys. Rev. **38,** 625 (1931).

TABLE I.

Observer	Half-widths W_1 of rocking curves, parallel position (1, −1)	Half-widths W_λ of spectral lines. Anti-parallel position (1, 1)	
		Mo $K\alpha_1$	
Spencer[10] Crystals No. 2	2.6–4.5 sec.	9.15 sec.	0.267 X.U.
Allison and Williams[6]	2.1	5.4 sec.	0.155 "
		Ag $L\alpha_1$	
Spencer[10] Crystals No. 1	6.	105. sec.	2.25 "
		Cu $K\alpha_1$	
Spencer[10] Crystals No. 1	6.	21.5 sec.	0.61 "
		U $L\alpha_1$	
Williams[11]	2.6	15.7 sec.	0.44 "

more extensive collection of data on line widths can be found in the second edition of "X-ray Spectroscopy" by Siegbahn.

DISCUSSION

The discrepancies between theory and experiment are real. These *may* indicate (1) that the line widths measured with the double crystal spectrometers are not the natural widths but are in part ascribable to the crystals themselves (although the rocking curves in the parallel position seem to preclude this), (2) that unresolved structure is present, (3) that the radiating atom is appreciably disturbed at its interior by neighboring atoms in the solid target, and hence that (4) further refinements of the theory of the radiation processes are required to account for this greater natural breadth observed; and also to relate the maximum ordinate to the intensity of the line.

Other investigators have used the type of analytical representation given in Eq. (1) for emission lines. J. H. Williams[11] used a formula of approximately[12] this type since he was comparing the measured shape of the uranium $L\alpha_1$ line with the shape predicted by the classical theory. In his case (L series lines) he found that the fit was good except at the "tail" or foot of the line where measured values were less than calculated values of the intensity. The same type of departure takes place for higher order reflection from crystals. Williams used a double crystal calcite spectrometer. The fact that a curve of type (1) fits well the measurements of DuMond and Hoyt and Richtmyer and Barnes but not so well (?)[12] the work of Williams indicates that the shape *may* not be independent of the particular pair of crystals used, and it may be premature to ask theorists for broader lines.

The author is indebted to F. K. Richtmyer and E. H. Kennard for encouragement and consultation.

[10] Spencer, Phys. Rev. **38**, 630 (1931).

[11] Williams, Phys. Rev. **37**, 1442 (1931).

[12] There *appears* to be an error in the formula used by Williams in that it includes a term of the type $[(2\pi\nu)^2-(2\pi\nu_0)^2]$ instead of the proper term $(2\pi\nu-2\pi\nu_0)^2$ as in Eq. (6) of this paper.

The Compound Photoelectric Effect of X-rays in Light Elements*

By GORDON L. LOCHER
The Rice Institute

(Received March 24, 1932)

The K fluorescence yields of oxygen, neon, and argon have been found from the numbers of double photoelectron tracks (produced by auto-ionization), and the numbers of single tracks, on 1950 stereopictures made in a Wilson cloud chamber, with atmospheres containing small amounts of the gases under investigation. From the data of this experiment and the K absorption data collected by Wien and Harms, the yields are: oxygen 8.2 percent, neon 8.3 percent, and argon 14.9 percent, for 0.709A x-rays. The K yields previously found for heavier elements by A. H. Compton, M. I. Harms, and L. H. Martin, and those given here, mostly lie on a smooth curve. Auger's value for krypton seems to be 13 percent to low, and that for argon, at least 45 percent too low. The most probable values of the K yields of 47 elements are considered to be, at present, as follows: O 8.2, F 8.5, Ne 8.8, Na 9.3, Mg 9.9, Al 10.5, Si 11.2, P 12.0, S 12.8, Cl 13.8, A 14.9, K 16.0, Ca 17.2, Sc 18.5, Ti 20.0, Va 21.7, Cr 23.6, Mn 25.5, Fe 28.4, Co 31.2, Ni 34.4, Cu 37.8, Zn 41.2, Ga 44.3, Ge 47.4, As 50 5, Se 55.3, Br 55.8, Kr 58.2, Rb 60.2, Sr 62.2, Y 64.0, Zr 65.5, Nb 67.0, Mo 68.0, Ma 69.1, Ru 70.0, Rh 70.8, Pa 71.7, Ag 72.5, Cd 73.0, In 73.5, Sn 74.0, Sb 74.5, Te 74.8, I 75.0, Xe 75.3, expressed as percentages of the K quanta that escape from K ionized atoms. The L yield of argon is estimated to be between zero and 20 percent, on the basis of the numbers of tracks counted. A new type of double track has been observed; its components are of similar energy, but produce very unequal ionization. They are believed to be due to krypton atoms with metastable lives of the order of 0.01 second. The cloud method can be used for detecting heavy gases in light ones. It is shown that 15 parts of krypton in 10^5 of oxygen, or 50 parts of xenon in 10^6 of oxygen, will give 2 percent of characteristic double tracks due to the heavy element.

INTRODUCTION

THE compound photoelectric effect consists in the almost simultaneous ejection of two or more electrons from an atom by a single photon, as a result of the atom's absorption of its own fluorescent radiation. Using the Bohr atom model, the mechanism of this phenomenon is as follows: when a K electron is ejected by x-rays, an outer one drops into the vacant orbit, accompanied by the emission of a K quantum characteristic of the atom. But this fluorescence quantum is in the interior of the atom and has a considerable chance of being absorbed by one of the outer electrons before emerging, thereby ejecting it with energy characteristic of the atom and level concerned. The net result is that two electrons are set free by one photon. In sufficiently heavy elements, three or more may be successively liberated by similar action in the several electronic shells. This effect was recognized in 1925 by Auger[1] as the explanation of certain types of multiple photoelectron

* This research was supported, in part, by a Grant-in-Aid from the National Research Council.

[1] P. Auger, Comptes Rendus **180,** 65 (1925); Jour. de Physique et Radium **6,** 205 (1925); also Ann. de Physique **6,** 183 (1926).

tracks that he found in a Wilson cloud chamber. C. T. R. Wilson[2] had previously observed similar tracks and commented on them at some length, but it appears that he did not fully understand their origin.

Compound action does not follow every K ionization, else fluorescent x-rays would never be observed, but it greatly reduces x-ray fluorescence, especially from elements of low atomic number. In this connection, the "K fluorescence yield" is conveniently defined as the fraction of all K quanta that escape from the atoms in which they originate, without producing compound action. Similarly, the L fluorescence yield is the fraction of the fluorescent L quanta that escape, and so on. The K yield is the most important of these, particularly for hard x-rays and light elements, because 85 percent or more of all primary photoelectrons come from K levels. It might be supposed that a quantum of fluorescent radiation would have a greater chance to escape if there were but few peripheral electrons between it and the outside of the atom, but the opposite is true: the K yield *increases* with atomic number, instead of decreasing. It seems desirable to determine the fluorescence yields of as many elements as possible, for it is only by knowing these and the relative absorption of the incident radiation by the K L, M, and N rings that one can predict the number of photoelectrons liberated by any given number of quanta, and the ionization resulting therefrom.

Auger[1] deduced values for the K yields of argon, krypton, and xenon, by counting the numbers of single and double tracks formed in cloud-chamber atmospheres containing these gases. The double tracks originate from compound action, while the single ones are made by electrons ejected (from any orbit) by the ordinary process. His measurements were followed by those of Harms[3] and A. H. Compton,[4] who determined the K yields of 8 elements between 26 and 42 by measuring the relative intensities of incident and the corresponding fluorescent x-rays from solid fluorescers, using ionization chambers. Martin[5] explored the same range and also found the K yield of iodine, with a special ionization method. The approximate agreement of the results of these careful experiments, seems to fix the values for elements between 26 and 42, with considerable certainty. The present paper describes cloud-method determinations of the yields of oxygen, neon, and argon, and a correlation of the results with previous ones. In this way, a continuous range is made available for elements 8 to 54. The cloud method is somewhat more direct than those using ionization chambers, and seems preferable when the material investigated is a suitable gas or vapor. On the other had, it is much slower because it involves the collection and minute examination of large numbers of stereoscopic pictures.

Apparatus and Procedure

Fig. 1 shows the general arrangement of the apparatus. X-rays generated in a tube A, pass through filters into the expansion chamber of a Wilson cloud

[2] C. T. R. Wilson, Proc. Roy. Soc. **A104,** 1 (1923).

[3] M. I. Harms, Ann. d. Physik **82,** 87 (1926).

[4] A. H. Compton, Phil. Mag. **8,** 961 (1929). This paper contains a good summary of preceding work on this subject, and makes some necessary corrections of Harms' data.

[5] L. H. Martin, Proc. Roy. Soc. **A115,** 420 (1927).

machine *B*, producing photoelectron tracks that are photographed by a pair of cameras *C*, while illuminated by the arc *D*.

The x-rays were taken from a water-cooled molybdenum Coolidge tube, operated for 0.04 sec. at 25 m.a. and 37 k.v.p., at each expansion. A Seeman spectrogram of the radiation showed intense *K* lines and negligible background. The rays were filtered through 0.2 mm of aluminum, a "balanced filter"[6] containing strontium carbonate and zirconium oxide in equal atomic concentrations of the metals, and 5 mm of Pyrex glass; the wave-length transmitted is taken as 0.709A. The work of Compton,[4] Martin,[5] and Auger[1] indicates that the *K* yield is independent of the wave-length of the exciting rays, so that small variations in this should certainly have no effect. Intensity requirements of the experiments were met by varying the diameter of the x-ray beam through the chamber from 1 to 3 mm.

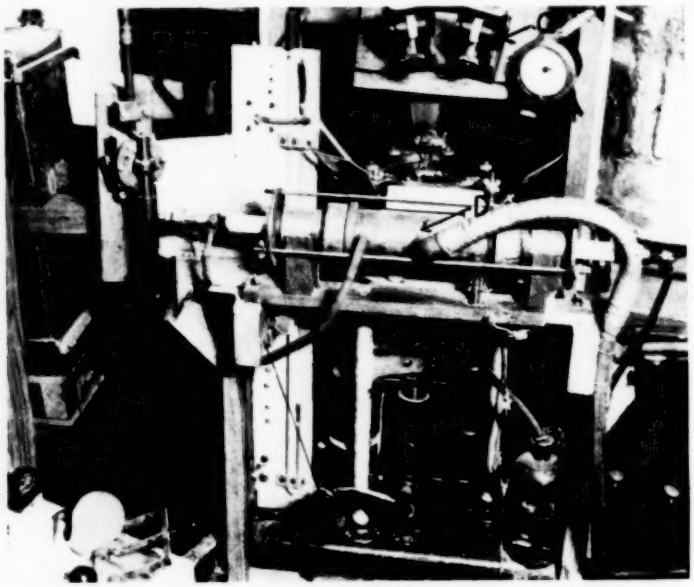

Fig. 1. Experimental arrangement.

Details of the cloud machine have already been published,[7] although some improvements have since been made. The apparatus is operated by turning a crank that mechanically drives the expansion mechanism and times the events connected with the cycle of operation. Once adjusted, hundreds of pictures may be taken without any appreciable change in the quality of the tracks. About 9000 pairs of pictures have been made with this outfit, including tracks originating from x-rays, cosmic-rays, and radioactive γ-rays.

Matched "Leica" cameras, mounted with their optic axes intersecting at 22° in the cloud chamber, served as a stereoscopic camera. Their regular

[6] Similar to that of P. A. Ross, J.O.S.A. and R.S.I. **16,** 433 (1928).

[7] G. L. Locher, J.O.S.A. and R.S.I. **19,** 58 (1929). The chamber is 15.6 cm across; a flexible diaphragm replaces the customary cylinder and piston arrangement.

lenses which have an aperture of f. 3.5, were supplemented with auxiliary ones for close photography. The developed negatives (2.5 by 3.5 cm, each) were viewed in a Zeiss stereoscope equipped with achromatic lenses of 8 cm local length. It was found that the gain in contrast resulting from the use of "positive" motion picture film, instead of the customary negative film, much more than compensates for the smaller sensitivity of the former, which was used in this work.

A convenient high-intensity mercury arc has been invented by the author to meet the unusual intensity requirements of cloud-track photography. Details of the arc, including its optical and electrical characteristics, will presently be submitted for publication in The Review of Scientific Instruments. In this machine, a fine stream of mercury, issuing from a small hole in one electrode and impinging on the other, is continuously exploded in an iron chamber for 1/60 to 1/30 sec., at the time of photographing the tracks, with power consumption estimated at 10 to 15 k.w. The luminosity of this source is enormous, greatly exceeding that got from any of the high-intensity carbon arcs, or by exploding tungsten wires, or mercury vapor, previously tried.

In order that the low-energy components of the compound action tracks should be as long as possible, the atmospheres used in the cloud-chamber were mainly composed of hydrogen. Tracks in hydrogen are much thinner and less persistant than in air, because of the lower density and viscosity of hydrogen, so the photographic exposure has to be short and the illumination strong. The expansion ratio that gave best results was found by trial to be about 1.25, at 33°C. Recoil electrons from hard γ-rays were found convenient for such adjustment, since their tracks are very thin.

Results for Oxygen, Neon and Argon

In these experiments the temperature of the cloud chamber was kept at 33° and the total pressure at 68 cm. It might be supposed that the increased lengths of the low-energy tracks, got by using lower gas pressure, would make their identification easier, but this apparent advantage is offset by increased diffuseness and thinness of the tracks formed at reduced pressures, especially in hydrogen.

It was often difficult or impossible to identify the short tracks from oxygen and neon. (Their energies are respectively $528-50=478$ volts, and $864-22=842$ volts; track lengths <0.5 mm).[8] All tracks were discarded that could not be definitely classified as single or double, or in connection with which there was any other uncertainty. About as many were lost for various reasons as were kept.

Oxygen

The source of oxygen was the water vapor of the cloud chamber; pure hydrogen constituted the remainder of the atmosphere. Calculation of the relative amounts of the incident radiation absorbed by these two elements was

[8] F. Holweck, "De la Lumiere aux Rayons X" 134 (1927); also Compton and Mohler, "Critical Potentials," 103 and 87 (1924).

based on the assumption that the vapor was saturated, although no appreciable error arises if this was not the case. The atomic fluorescence absorption coefficient of oxygen is 410 times that of hydrogen, which makes the hydrogen absorption almost negligible. The data for oxygen are as follows:

Atmosphere	Oxygen	2.72 percent
	Hydrogen	97.28 percent, of the total number of atoms
Number of tracks identified		644, on 900 pairs of pictures
Single tracks		93 or 14.5 percent
Double tracks		551 or 85.5 percent

Absorption of incident x-rays[9] oxygen 99.3 percent, hydrogen 0.7 percent

Neon

In this case it was desirable to know the exact composition of the atmosphere, because the tracks due to oxygen are indistinguishable from those due to neon. The numbers of single and double tracks due to neon alone had to be deduced from the total numbers counted, by means of simple calculations based on the relative absorption coefficients of neon and oxygen, the relative numbers of atoms present, and the relative numbers of single and double tracks formed in oxygen alone. The last mentioned are 14.5 percent and 85.5 percent, as shown above. Although the accuracy possible in this experiment is thought to be somewhat less than in the other two, because of the uncertainty about the saturation of the water vapor, the error is diminished by the proximity of neon to oxygen in the periodic table. The similarity of their K yields, which this suggests, is borne out by the results given later on in this paper. The principal data for neon are as follows:

Atmosphere	Neon	7.36 percent
	Water vapor	5.5 percent
	Hydrogen	87.14 percent, of the total pressure
Number of tracks identified		1018, on 603 pairs of pictures
Single tracks		182 or 17.88 percent
Double tracks		836 or 82.12 percent
Double tracks due to compound action in krypton, about 35		

Absorption of incident x-rays[9] neon 72.0 percent, oxygen 28.0 percent (hydrogen <0.4 percent)

Argon

The short components of the double tracks counted in this case come from three sources: argon K photons (energy about 2930 volts), argon L photons (230 volts), and oxygen K photons (480 volts). The first are listed as "tracks with long companions", and the other two as "tracks with short companions". The data for argon are:

Atmosphere	Argon	5.1 percent
	Water vapor	5.5 percent
	Hydrogen	89.4 percent, of the total pressure

[9] Calculated from Owen's formula, Proc. Roy. Soc. **A94,** 510 (1918), as modified by Richtmyer and Warburton, Phys. Rev. **22,** 539 (1923).

Number of tracks identified	1828, on 450 pairs of pictures
Tracks with long companions	1334 or 73.0 percent
Tracks with short companions	224 or 12.2 percent
Tracks with no companions	270 or 14.8 percent
Sum of last two classes	494 or 27.0 percent

Double tracks due to compound action in krypton, about 37

Absorption of incident x-rays[9] argon 96.0 percent, oxygen 4.0 percent (hydrogen <0.05 percent)

To find the K yields, one must also know the relative absorption of the incident x-rays by the K, L, and M electrons of the atoms concerned. Unfortunately, adaquate data are not available on this subject, probably because of the experimental difficulties involved in determining them. So it has been found necessary to extrapolate the relative absorption data found for heavier elements, to get values for the light ones. This is, evidently, not very satisfactory procedure, but there is reasonably good agreement of the values of the yields found by applying three sets of these data. Two of the sources were the atomic fluorescent absorption coefficients found by Richtmyer and Warburton[10] and by Gray.[11] The former are expressed by the formulae

$$\tau_a = 2.24Z^4\lambda^3 \times 10^{-26} \cdots 0.1A < \lambda < \lambda_K \tag{1}$$

$$\tau_a = 0.33Z^4\lambda^3 \times 10^{-26} \cdots \quad \lambda_K < \lambda < \lambda_{L3}. \tag{2}$$

Gray's formulae are derived by comparing (1) and (2) with similar ones given by Allen,[12] and are as follows

$$\tau_a = 1.92(1 + 0.008Z)(1 - \lambda/4\lambda_K - \lambda/50\lambda_K{}^2)Z^4\lambda^3 \times 10^{-26} \cdots 0.1A < \lambda < \lambda_K \tag{3}$$

$$\tau_a = 0.255Z^4\lambda^{2.7} \times 10^{-26} \cdots \quad \lambda_K < \lambda < \lambda_{L2} \tag{4}$$

$$\tau_a = 0.058Z^4\lambda^{2.6} \times 10^{-26} \cdots \quad \lambda_{L_1} < \lambda < \lambda_{M5}. \tag{5}$$

A third set of values, which are probably the best ones, were got by interpolation (for argon), and by a very reasonable extrapolation (for oxygen and neon), of values collected in Wien and Harms' Handbuch.[13]

On the basis of these, Table I was prepared:

TABLE I. *Relative absorption of 0.709A x-rays by K, L, and M electrons.*

Source	Absorption, percent		Absorption, percent	
	Oxygen K	Oxygen L	Neon K	Neon L
(a)	87.8	12.3	86.2	13.8
(b)	93.3	6.7	92.8	7.2
(c)	85.3	14.7	85.3	14.7
	Argon K	Argon L	Argon M	
(a)	88.6	8.3	3.1	
(b)	90.8	9.2		
(c)	85.3	14.7		

(a) Calculated from Gray's formulae.
(b) Interpolated and extrapolated from Wien and Harms' collected data
(c) Calculated from Richtmyer and Warburton's formulae

[10] F. K. Richtmyer and F. W. Warburton, Phys. Rev. **22,** 539 (1923).
[11] J. A. Gray, Trans. Roy. Soc. of Canada **21,** 179 (1927).
[12] S. J. M. Allen, Phys. Rev. **27,** 226 and **28,** 907 (1926).
[13] "Handbuch der Experimentalphysik", 24, part 1, 256 (1930).

From these and the data previously given, we get the following values for the K fluorescence yields of oxygen, neon, and argon, expressed as percentages of K quanta that escape from K ionized atoms:

	Oxygen	Neon	Argon
(a)	2.34	2.84	12.75
(b)	8.21	8.29	14.88
(c)	0	1.82	9.40

Calculation of the K yield of neon, from (a), above, is given as an illustration of the method used.

Let S_n and S_0 = number single tracks from neon and oxygen; C_n and C_0 = number double tracks from neon and oxygen; S = total number single tracks observed; S_1 = total number single tracks due to oxygen and neon; C = total number double tracks due to oxygen and neon; $S_1 = S - 35$ (estimated number of single tracks due to krypton, on the basis of the number of double tracks)

$$S_1 = 147 \quad S_n + S_0 = 147 \quad S_n + C_n = 0.72(836 + 147) = 707.8$$
$$C = 836 \quad C_n + C_0 = 836 \qquad S_0 = 0.145(S_0 + C_0).$$

These give $S_n = 115$, $C_n = 593$, $S_0 = 32$, $C_0 = 243$. Of the 708 neon tracks, 13.8 percent should come from the L shells, so the number of single tracks from the K shells, S_k, is $S_n - 0.138\ (S_n + C_n) = 17.3$. The total number of tracks from the K shell is $S_k + C$, so the K yield is

$$W_K = S_K/(S_K + C) = (S_n - 0.138(S_n + C_n))/(S_n - 0.138(S_n + C_n) + C_n)$$
$$W_K = 0.0284, \text{ or } 2.84 \text{ percent}.$$

Equivalent procedure is followed for getting the yields of oxygen and argon. It is somewhat more complex in the case of argon, because the M electrons have to be dealt with.

TABLE II. *K fluorescence yields, collected data.*

Element	Observer	Method	K yield, percent	
8 O	Locher	Cloud	(a) 2.3	(b) 8.2†
10 Ne	Locher	Cloud	(a) 2.8	(b) 8.3
18 A	Locher	Cloud	(a) 12.8	(b) 14.9
18 A	Auger	Cloud	7.	
26 Fe	Harms*	Ioniz.	28.2	
26 Fe	Martin	Ioniz.	29.	
28 Ni	Compton	Ioniz.	37.	
28 Ni	Martin	Ioniz.	35.	
29 Cu	Harms	Ioniz.	37.8	
29 Cu	Martin	Ioniz.	40.	
30 Zn	Harms	Ioniz.	40.3	
30 Zn	Martin	Ioniz.	46.	
34 Se	Compton	Ioniz.	54.	
34 Se	Harms	Ioniz.	51.7	
34 Se	Martin	Ioniz.	59.	
35 Br	Compton	Ioniz.	56.	
35 Br	Martin	Ioniz.	59.	
36 Kr	Auger	Cloud	50. 51.	
38 Sr	Harms	Ioniz.	61.5	
42 Mo	Compton	Ioniz.	68.	
53 I	Martin	Ioniz.	75.	
54 Xe	Auger	Cloud	71.	

* Harms' values are corrected by Compton.
† The values (*b*) are preferred.

Variation with Atomic Number

Table II is a collection of the experimental values of the K yields of 14 elements, that seem to be the most reliable data now available. Fig. 2 shows

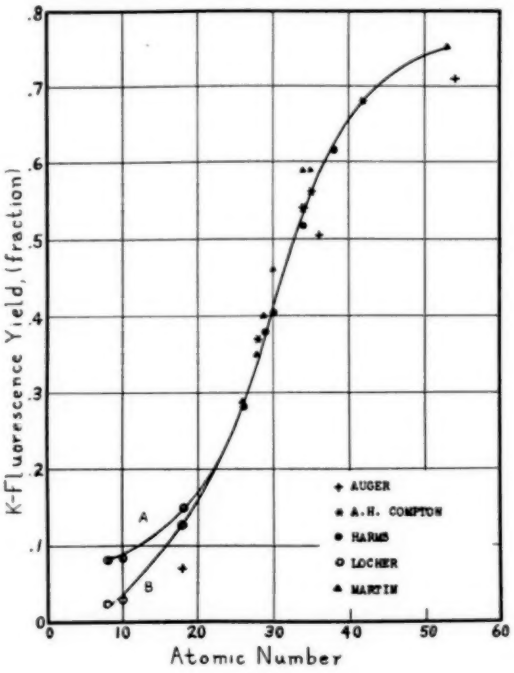

Fig. 2.

Table III. *K fluorescence yields, interpolated values.*

Element	K yield, percent (a)	(b)	Element	K yield, percent
8 O	2.3	8.2	33 As	50.5
9 F	2.9	8.5	34 Se	53.3
10 Ne	3.6	8.8	35 Br	55.8
11 Na	4.5	9.3	36 Kr	58.2
12 Mg	5.4	9.9	37 Rb	60.2
13 Al	6.4	10.5	38 Sr	62.2
14 Si	7.6	11.2	39 Y	64.0
15 P	8.8	12.0	40 Zr	65.5
16 S	10.1	12.8	41 Nb	67.0
17 Cl	11.4	13.8	42 Mo	68.0
18 A	12.8	14.9	43 Ma	69.1
19 K	14.3	16.0	44 Ru	70.0
20 Ca	16.0	17.2	45 Rh	70.8
21 Sc	17.8	18.5	46 Pa	71.7
22 Ti	19.7	20.0	47 Ag	72.5
23 Va	21.6	21.7	48 Cd	73.0
24 Cr	23.7	23.6	49 In	73.5
25 Mn	26.0	25.5	50 Sn	74.0
26 Fe	28.4	28.4	51 Sb	74.5
27 Co	31.2		52 Te	74.8
28 Ni	34.4		53 I	75.0
29 Cu	37.8		54 Xe	75.3
30 Zn	41.2			
31 Ga	44.3			
32 Ge	47.4			

that they mostly lie on a smooth curve. In plotting this curve, a little more weight has been given to the data of Harms and Compton than to those of Martin, because of the difference in their experimental methods. The lower branch (B), corresponds to the data (a), of Table II, while the upper branch

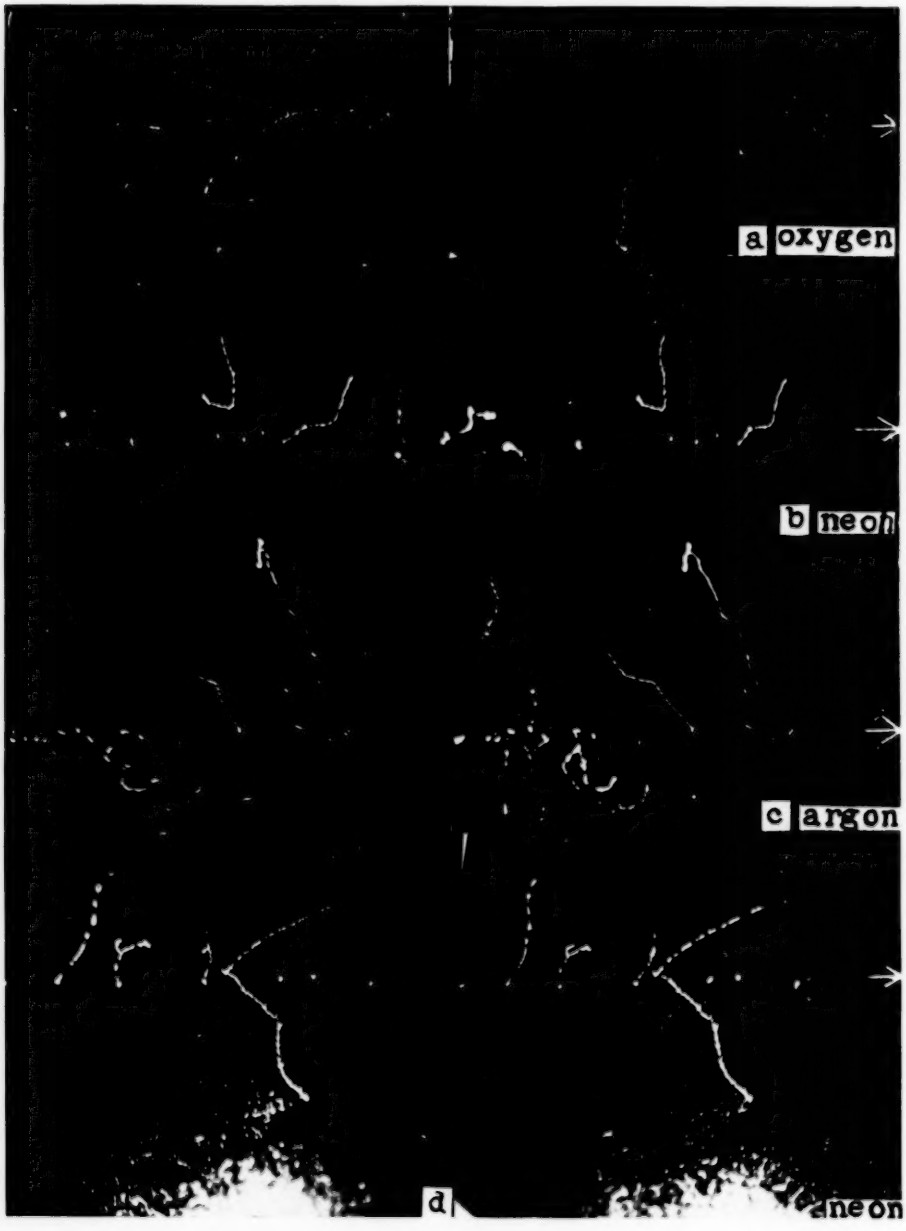

Fig. 3. a, b, and c. Cloud tracks showing compound photoelectric action of x-rays in oxygen neon, and argon, respectively. d, also shows a diffuse track of an α-particle and a compound track, due to krypton. The arrows indicate the direction of the x-ray beam. Mag. $\times 0.73$.

(*A*), which corresponds to the data (*b*), is believed to give the best representation of the actual variation. Auger's values were the first determined, and seem to be too low.

It is interesting to notice that there is still an appreciable yield for very light elements, contrary to the expectation of Martin, whose extrapolated curve intersected the axis at $Z = 21$. There is no evidence for believing that discontinuities exist in this curve, although the possibility of their existance makes interpolation between experimental points a little uncertain, and prohibits extrapolation to elements of lower atomic number.

Experimental work might well be extended to heavier elements, in which the auto-ionization is less conspicuous, by the use of ionization methods, or Geiger counters. The small x-ray absorption of very light elements, and the smallness of the energies of the short components of their compound tracks, casts much doubt on the feasibility of attempting to extend the measurements to lighter elements, except, perhaps, by spectroscopic methods. It seems possible, however, that the yields might be deduced by measuring the intensities of spark lines, since these intensities are believed to be altered by auto-ionization.

Discussion

Fig. 3, a, b, and c, are typical pictures taken in atmospheres containing oxygen, neon, and argon, respectively. Fig. 3, d, taken in neon, shows 4 compound tracks due to neon or oxygen, 1 single track (very diffuse), 3 recoil electrons, 1 compound track due to krypton (with the long branch), and 1 very diffuse α-particle track; two of the tracks are branched, and two others have spiral paths.

The formation of compound tracks in a gaseous mixture provides a sensitive way of detecting small amounts of heavy gases, such as krypton, among light ones. One can rather easily identify the double tracks that hard x-ray produce under such circumstances, by the low-energy components whose lengths are characteristic of the parent atoms. Their relative numbers are simple functions of the absorption coefficients and the fluorescence yields. As an example, consider how the relative numbers of krypton and oxygen atoms, n_k and n_0, can be found from the total number of tracks, N, in a krypton-oxygen atmosphere, by using total number of double krypton tracks, N_d, (which is p percent of N), and the K yield of krypton, W_k, the fraction of the krypton-absorbed incident x-rays, f_k, that are absorbed by K-electrons,the atomic fluroescent absorption coefficients, τ_k and τ_0, and the atomic numbers, Z_k and Z_0, all of which are known. If the total numbers of krypton and oxygen tracks are N_k and N_0, we may write

$$N_d = N_K f_K (1 - W_K). \tag{1}$$

From Owen's law

$$\tau_K/\tau_0 = Z_K{}^4/Z_0{}^4, \text{ whence}$$
$$N_K/N_0 = n_K Z_K{}^4/n_0 Z_0{}^4. \tag{2}$$

Also,

$$N_d/N = p\% = 0.0p = N_K f_K (1 - W_K)/(N_0 + K_K), \text{ or}$$
$$N_K/N_0 = 0.0p/(f_K - f_K W_K - 0.0p). \tag{3}$$

From (2) and (3)

$$n_K / n_0 = 0.0pZ_0^4 / (f_K - f_K W_K = 0.0p)Z_K^4. \tag{4}$$

If, for example, $p = 2$ percent,

$$n_K / n_0 = \frac{0.02 \times 8^4}{(0.85 - 0.85 \times 0.58 - 0.02)36^4} = 0.000145 = 0.015 \text{ percent}.$$

The neon and argon used in the present experiment were contaminated with about 0.02 percent of krypton, as found by similar calculations. Using Auger's value for the K yield of xenon, we see that $n_x / n_0 = 0.000044$, or 0.0044 percent of xenon atoms in oxygen will give 2 percent double xenon tracks, if sufficiently hard x-rays are used. The existence of this percentage would be readily noticed.

Several curious types of tracks were found on the pictures taken in this experiment. Perhaps the most interesting that are not known to have been

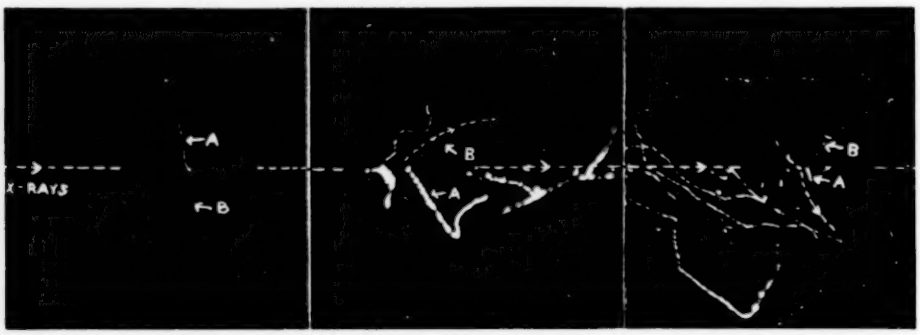

Fig. 4. Compound tracks whose components are of similar energy but very unequal density. Mag. ×0.73.

previously described, are double tracks resembling compound krypton tracks in all respects except that the two components are of unequal density. At first, these were regarded as cases of accidental coincidence of the starting points of two ordinary tracks, but their frequent occurrence presently made this improbable. A possible explanation is that they are due to K ionized krypton atoms that have a metastable life comparable with the time of sensitivity of the cloud chamber (0.01 to 0.04 sec.), so that the formation of the second component took place after the sensitivity of the atmosphere had appreciably diminished. Fig. 4 shows the beginnings of three tracks of this type; the density differences of the components vary considerably. In case the proposed explanation should prove correct, the approximate lives of individual excited krypton atoms could be found by measuring the displacements of the charged drops in the two tracks, resulting from the application of a suitable horizontal electric field in the chamber. The performance of this experiment is contemplated. Another possibility in this connection, is that two fast electrons that have about the same velocity may produce very different amounts of ionization per cm path. This might be explained by supposing that one was

spinning and the other not, or that some other abnormal condition affected the production of ions by one of them. Evidence for an effect of this type was seen in connection with the pictures recently examined: tracks of definitely established origin were occasionally observed, along which the ionization *suddenly diminished*, accompanying a sharp bend in the track, and later increased in the normal manner as the electron slowed down.

A rough determination of the L yield of argon places it between zero and 20 percent. This is not of much value, because the number of L tracks dealt with is small, and especially because the numbers of oxygen K compound tracks and argon L compound tracks have to be separately counted. Their short components have energies that differ only by 100 percent, whereas in getting the K yield, the smallest energy difference is about 600 percent. However, the accuracy seems good enough to show that the L yield is small.

When γ-rays are scattered by K electrons, compound action may follow. This is shown by the fact that most recoil electron tracks from hard γ-rays scattered in the gas of the cloud chamber, were double, just as the x-ray tracks were. Likewise, tracks produced by scattered x-ray quanta were observed to be double, usually. Neither of these observations is in the least surprising, because the auto-ionization that follows K ionization is an atomic phenomenon that should be independent of the particular type of radiation that sets it in motion.

The author wishes to express his best thanks to Professor H. A.Wilson for his interest and advice throughout the course of this investigation.

The Ionization Potential of Molecular Hydrogen

By WALKER BLEAKNEY*
Palmer Physical Laboratory, Princeton University
(Received April 6, 1932)

A description is given of a mass spectrograph designed to work with gases at very low pressures. The metal parts are made entirely of tantalum and tungsten enclosed in an all glass system which may be baked out quite thoroughly, making it possible to work with gases at pressures of the order of 10^{-6} mm. The apparatus has been applied to the study of the ionization potential of molecular hydrogen yielding a value of 15.37 ± 0.03 volts. A discussion of all the previous measurements of this quantity is given.

INTRODUCTION

THE ionization potentials of molecules and in particular that of molecular hydrogen have been of considerable interest for the last twenty years, and its measurement has been the object of more than twenty experiments. At first it was believed that a stable H_2^+ ion did not exist and the efforts were directed toward learning the nature of the mechanism of ionization and how the energy was distributed between the various components. Now we know that as the velocity of the impinging electrons is increased from zero, the first ion formed in pure molecular hydrogen is the stable H_2^+ configuration which may be changed subsequently by collisions with other molecules. The minimum energy required to produce this ion by electron impact from hydrogen in the normal state has lately become of importance because of its relation to the host of facts now known about the potential energy curves, vibrational levels, heats of dissociation and band spectra of this molecule and the limitations imposed by the Franck-Condon principle. Probably all the physicists who have worked in this field now agree that this ionizing potential lies in the neighborhood of 16 volts. Considering the number of different determinations scattered over a period of several years and the accuracy claimed for them, the values obtained are surprisingly discordant. In Table I will be found a list of all the values of any importance known to the writer.

Smyth[1] after a critical survey of all the best values rejected the author's recent determination (and justifiably so) but hoped the experiment would be repeated using argon as the calibrating gas. Kallmann and Rosen[2] on the other hand have given full credence to this value in their report. This experiment has now been repeated using an entirely new setup and it is the object of this paper to present the results. The author hopes he is not adding to the confusion by contributing a value which lies outside the range of all the other observations!

* National Research Fellow.
[1] Smyth, Rev. Mod. Phys. **3**, 347 (1931).
[2] Kallmann and Rosen, Phys. Zeits. **32**, 534 (1931).

TABLE I. *Observed I. P. for molecular hydrogen.*

I. P. (volts)	Observer[3]	Reference
15.8	Davis and Goucher	Phys. Rev. **10,** 101 (1917).
15.7	Bishop	Phys. Rev. **10,** 244 (1917).
17.1	Franck, Knipping, and Krüger	Ber. d. D. phys. Ges. **21,** 728 (1919).
15.1	Found	Phys. Rev. **16,** 41 (1920).
16.5 ±0.5	Mohler and Foote	Bur. Stan. Bull. **16,** 669 (1920).
16.9	Horton and Davies	Proc. Roy. Soc. **A97,** 23 (1920).
15.9	Compton and Olmstead	Phys. Rev. **17,** 45 (1921).
17.1 ±0.2	Krüger	Ann. d. Physik **64,** 288 (1921).
15.6 ±0.1	Boucher	Phys. Rev. **19,** 189 (1922).
16.0	Foote and Mohler	Origin of Spectra, p. 68
16.0	Mohler, Foote, and Kurth	Phys. Rev. **19,** 414 (1922).
16.0	Olmstead	Phys. Rev. **20,** 613 (1922).
15.8	Mackay	Phil. Mag. **46,** 828 (1923).
15.9	Horton and Davies	Phil. Mag. **46,** 872 (1923).
16.7	Olson and Glockler	Proc. Nat. Acad. Sci. **9,** 122 (1923).
15.8	Mackay	Phys. Rev. **24,** 319 (1924).
15.7	Hogness and Lunn	Proc. Nat. Acad. Sci. **10,** 398 (1924).
16.0	Smyth	Phys. Rev. **25,** 452 (1925).
16.0	Hogness and Lunn	Phys. Rev. **26,** 44 (1925).
16.5	Dorsch and Kallmann	Zeits. f. Physik **44,** 565 (1927)
16.1	Langmuir and Jones	Phys. Rev. **31,** 357 (1928).
16.5	Vencov	C. R. **189,** 27 (1929).
15.4 ±0.1	Bleakney	Phys. Rev. **35,** 1180 (1930).
15.6 ±0.1	Smith	Phys. Rev. **39,** 270 (1932).
15.37 ±0.03	Bleakney	This paper

APPARATUS

The apparatus employed was in the form of a mass spectrograph to which reference has already been made[4] but one which has never been described in detail. The basic principles are the same as the one previously used by the author[5] with the exception of the analyzer. A large water-cooled solenoid was made in the Palmer Laboratory shops one meter in length and 5 inches bore capable of producing a field of 1500 gauss continuously without the introduction of any iron in the magnetic circuit. With such a field it was possible to employ the semicircular type of analyzer as first introduced by Dempster.[6] An isometric drawing of the metal parts of the vacuum tube is shown in Fig. 1. Electrons from the filament F are accelerated between the first two diaphragms of the electron gun G and pass between the plates A and B as shown by the dotted lines. They are finally collected on the inclined plate P which is maintained about 100 volts positive with respect to the rest of the trap T in order to prevent the escape of secondary electrons. The electron beam is kept accurately lined up with the apparatus by the longitudinal magnetic field H. The positive ions formed along the electron path are accelerated through the two slits S_1 and S_2 by a small field between A and B and a stronger one between B and C. The ions then travel on the arc of a circle due to the influence of the magnetic field H. The radius r of the circle is

[3] The values listed in this table were reported, in many cases, merely as critical potentials and it was only later that the true explanation became apparent.

[4] Bleakney, Phys. Rev. **39,** 536 (1932); **40,** 130 (1932).

[5] Bleakney, Phys. Rev. **34,** 157 (1929).

[6] Dempster, Phil. Mag. **31,** 438 (1916).

determined by the relation,

$$m/e = r^2H^2/2V$$

where V is the velocity expressed in equivalent volts which the ion has acquired before passing through S_2. Obviously the value of r may be determined by adjusting V such that ions having a particular value of m/e will pass through the third slit S_3 and fall upon the plate K which is connected to a Compton electrometer having a sensitivity of 5000 mm per volt. When several different types of ions are present they may be passed in succession before the slit S_3 by varying the accelerating potential V. The plate L may also be connected to the electrometer and serves to measure the total number of ions in a particular beam when the potential V is adjusted so that the totality of the beam falls upon it. The whole apparatus within the vacuum tube is made of the two metals tantalum and tungsten with Pyrex glass insulation. The tube is entirely free of wax and grease joints and is permanently mounted within a furnace. The furnace itself is mounted inside the water-

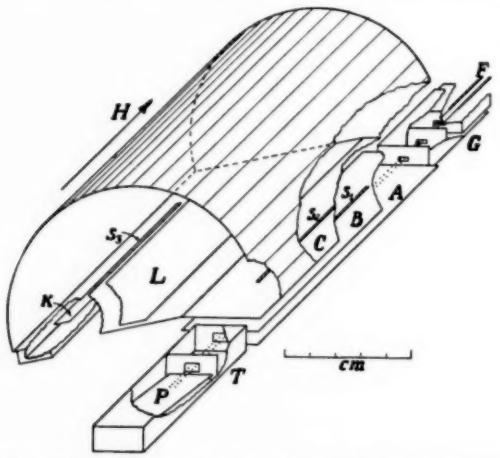

Fig. 1. Isometric drawing of the apparatus with sections cut away to show the interior. All dimensions are to scale except the widths of the slits which are *1.0*, *0.2*, and *0.5* mm for S_1, S_2 and S_3 respectively.

cooled solenoid so that the tube may be baked out at any time without disturbing anything. With this apparatus it is possible to study ionizing potentials with pressures ranging from 10^{-4} to 10^{-7} mm Hg.

Procedure and Results

After the tube had been evacuated and baked until the residual pressure was less than 10^{-7} mm Hg as measured by using the tube itself as an ionization gauge, a mixture of hydrogen and argon was admitted and allowed to flow continuously out through the pumps. The hydrogen was admitted through a palladium tube and the argon, which had been purified in a misch metal arc, was allowed to leak through a fine capillary. The pressure of the argon in the reservoir as well as the temperature of the palladium tube could be controlled and hence the partial pressures of the two gases in the ionizing

chamber could be varied at will. For a given steady mixture the analyzer was set to catch the H_2^+ ion and a run was made studying the intensity of this ion as a function of the electron velocity. Immediately thereafter the field between B and C was changed so that the intensity of the A^+ ions could be submitted to a like study, everything else remaining as nearly constant as possible. In the region AB the paths of the ions are bent slightly before enter-

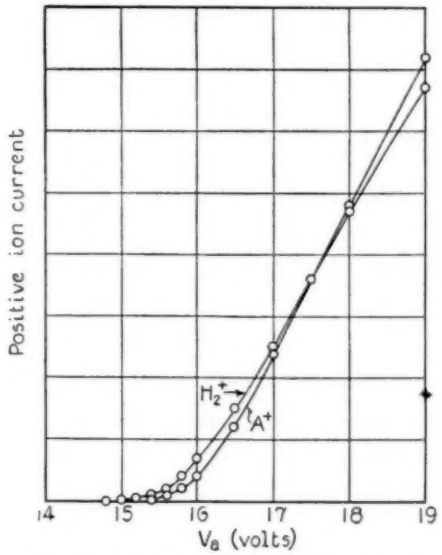

Fig. 2. Typical ionization potential curves showing the positive ion current as a function of the electron velocity (uncorrected).

ing S_1 due to the magnetic field and since the electric field between A and B is held constant throughout it follows that the H_2^+ ions will be deflected more than the heavier A^+. Hence in order to enter the slit S_1 the H_2^+ and A^+ ions must start from different points. The electron velocity will not be the same at these two points due to the potential drop in the filament. However this discrepancy will be reversed in sign when the filament current is reversed and the mean should be free of any such error. The shift observed on reversing the filament current was about 0.2 volts. Eight different runs were made to determine the difference between the ionizing potentials of H_2^+ and A^+. Each of these runs was checked by varying the electron velocity in the opposite direction making really sixteen runs in all. Of the eight values four were made with the filament current reversed so that on averaging corresponding pairs four independent values of the difference were obtained. They were 0.40, 0.25, 0.35, and 0.30. In every case argon showed the higher I.P. In Fig. 2 is shown a typical run. Assuming the value for argon to be 15.69 the I.P. for H_2^+ is

$$\text{I.P.} = 15.37 \pm 0.03 \text{ volts}$$

where the probable error is calculated from the internal consistency of the data. Measurements taken under a variety of conditions representing changes

in pressure of one-hundred fold, in electron current of tenfold, and in magnetic field of twofold failed to show any consistent variations in the ionization potential. In all cases the relative pressures were adjusted so that the intensities of the two ion peaks were of the same order of magnitude.

Discussion

The results of this experiment agree very satisfactorily with those previously reported by the author.[7] There seems to be no obvious systematic error in this method although it differs from all the other work. In many of the older experiments the effect of velocity distribution of electrons and contact potential was unknown. Usually the apparatus was calibrated by admitting a gas whose I.P. was known. This gas was then removed before admitting the hydrogen and it is possible that the contact potential changed at the same time. This would not account for the results obtained by Dorsch and Kallmann, Hogness and Lunn, Smith, and Mackay however since in these experiments the two gases were mixed together. In these cases the discrepancy may be entirely due to the sensitivity of the apparatus. A study of the potential energy curves in the light of the Franck-Condon theory shows that the most probable excitation is one to a higher vibrational state involving a total energy change of about 15.9 volts and the probability of transitions on either side of this value falls off. This probability is even appreciable at 18 volts[7] where the ion is just able to dissociate and it is believed that this experiment shows that this range may extend as low as 15.4 volts or lower. It may be well to point out that these results offer no contradiction to those of Harnwell[8] which showed that $H_2^+ + A \rightarrow H_2 + A^+$ because the H_2^+ ion may have any energy from 15.4 to 17.9 volts and most of the hydrogen ions will have energies above the I.P. of argon. The theoretical minimum should be that energy required to transform the normal molecule from its lowest vibrational state to the corresponding lowest vibrational state of the ion assuming no change in rotation energy. This ionization potential has been calculated many times, both from band spectra and theory, with varying degrees of accuracy. Perhaps the best values are those calculated by Birge[9] from Richardson's data on the band spectra and a later value given by Richardson and Davidson.[10] These were 15.34 and 15.381 volts respectively. The agreement with the result of this experiment, 15.37, seems to indicate that transitions by electron impact from the ground level of normal hydrogen to the ground level of the molecular ion are possible.

In measuring the difference between the I.P.'s of H_2 and A it is perhaps well to point out that the latter has two I.P.'s differing by 0.18 volts according as the argon ion is left in the $^2P_{1\frac{1}{2}}$ or the $^2P_{\frac{1}{2}}$ state. It seems safe to assume however that the minimum observed is the lower of these two, cor-

[7] Bleakney, Phys. Rev. **35,** 1180 (1930).

[8] Harnwell, Phys. Rev. **29,** 830 (1927).

[9] Birge, Proc. Nat. Acad. Sci. **14,** 14 (1928).

[10] Richardson and Davidson, Proc. Roy. Soc. **A123,** 466 (1929); Richardson, The Faraday Society, *Molecular Spectra and Molecular Structure,* Sept. 1929, p. 686.

responding to an I.P. of 15.69 volts. The slight "foot" at the end of the argon curve in Fig. 2 is probably due partly to the two I.P.'s and partly to the velocity distribution of the electrons. In helium which has only one I.P. to contend with the foot is less pronounced. The effect is quite marked in the case of H_2^+ and is probably explained by excitation to the higher vibration levels of the molecular ion as the electron velocity is increased.

The author is indebted to the National Research Council for the grant of a fellowship to carry on this work and to the Palmer Physical Laboratory for its facilities. He also gratefully acknowledges many helpful discussions with Professor H. D. Smyth and Professor R. Ladenburg.

Double Stern-Gerlach Experiment and Related Collision Phenomena

By N. ROSEN AND C. ZENER*
Massachusetts Institute of Technology and Princeton University
(Received April 2, 1932)

The theory of the double Stern-Gerlach experiment is developed where the rate of rotation has a maximum at $t=0$ and goes gradually to zero at $t=\pm\infty$. The negative results of the experiments of Phipps and Stern are completely accounted for. The same analysis is applied to those collision phenomena where only two quantum states need be considered, and where their difference of energy, ΔE, is so much smaller than the relative kinetic energy of the two systems that the positions of the centers of gravity of the two systems may be regarded as time parameters. If $f(t)=2\pi/h$ times the matrix element of the perturbation, and if $A=\int_{-\infty}^{\infty}f(t)dt$, then the transition probability is

$$\left|\frac{\sin A}{A}\int_{-\infty}^{\infty}f(t)e^{2\pi i(\Delta E/h)t}dt\right|^2$$

for the cases investigated, and this probably holds for all experimental cases.

I. DOUBLE STERN-GERLACH EXPERIMENT

1. Introduction

A BEAM of alkali atoms all having the same spatial quantization may be obtained by the Stern-Gerlach experiment. The question arises, if such a beam of atoms is sent through a weak magnetic field which is rapidly rotating, will the spatial quantization remain unaltered, or will transitions occur which will separate the beam when it is subjected to a second Stern-Gerlach experiment? This question has been examined both theoretically[1] and experimentally.[2]

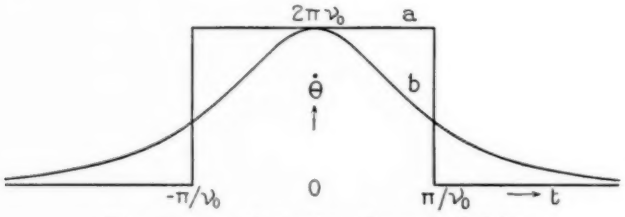

Fig. 1. Rate of rotation of magnetic field.

In view of the lack of agreement between the theoretical calculations of Güttinger and the experiments of Phipps and Stern, it is of interest to re-examine the theory of transitions in spatial quantization. An obvious improvement is to replace the discontinuous rate of rotation of the magnetic field used by Güttinger, curve *a* in Fig. 1, by a continuous rate of rotation,

* National Research Fellow.
[1] P. Güttinger, Zeits. f. Physik **73**, 169 (1932).
[2] T. E. Phipps and O. Stern, Zeits. f. Physik **73**, 185 (1932).

such as curve b in Fig. 1. In the following section the analysis is carried through for such a rotating magnetic field. The results are in complete agreement with experiment in predicting no transitions in the particular arrangement of Phipps and Stern where the magnetic field rotates through an angle of 2π.[3]

2. Analysis

Since the only dynamical variable of an alkali atom which is appreciably affected by the weak magnetic field, H, is the electron spin, the Hamiltonian may be written simply as $H \cdot \sigma$, where σ is the magnetic moment of the spin. This spin variable can have only two quantum states, so the wave function may be written as the linear combination $\psi = A(t)\psi_\alpha + B(t)\psi_\beta$, where ψ_α, ψ_β are the Pauli spin functions with reference to an arbitrary axis. In particular, if we choose this axis to be parallel to the magnetic field, which makes an angle θ with the fixed z axis, these functions will satisfy the wave equations

$$\begin{aligned}(H\cdot\sigma - h\nu)\psi_\alpha &= 0\\ (H\cdot\sigma + h\nu)\psi_\beta &= 0\end{aligned} \tag{1}$$

where ν is the frequency of the Larmor precession. By means of the transformation relations which relate ψ_α, ψ_β to the spin functions ψ_α', ψ_β' referring to a fixed z axis, namely[4]

$$\begin{aligned}\psi_\alpha &= \cos(\theta/2)\psi_\alpha' - i\sin(\theta/2)\psi_\beta'\\ \psi_\beta &= -i\sin(\theta/2)\psi_\alpha' + \cos(\theta/2)\psi_\beta',\end{aligned}$$

we see that ψ_α, ψ_β are related by

$$\begin{aligned}\dot{\psi}_\alpha &= -i(\dot{\theta}/2)\psi_\beta\\ \dot{\psi}_\beta &= -i(\dot{\theta}/2)\psi_\alpha.\end{aligned} \tag{2}$$

The exact wave equation is

$$\left(H\cdot\sigma - \frac{h}{2\pi i}\frac{d}{dt}\right)\{C_1 e^{2\pi i\nu t}\psi_\alpha + C_2 e^{-2\pi i\nu t}\psi_\beta\} = 0. \tag{3}$$

Corresponding to our knowledge that the spin is initially antiparallel, say, to the magnetic field, this equation is given the boundary conditions

$$C_1(-\infty) = 0 \tag{4a}$$

$$|C_2(-\infty)| = 1. \tag{4b}$$

The answer to our problem, namely the fraction, P, of atoms which change their spatial quantization upon passing through the rotating field, will be given by

$$P = |C_1(\infty)|^2.$$

[3] The observed change of quantization caused by impurities may be interpreted as caused by an exchange of electrons having opposite spins.

[4] W. Pauli, Zeits. f. Physik **43**, 601 (1927).

Upon applying the relations (1) and (2) to the wave Eq. (3), we obtain[5]

$$\dot{C}_1 = i\frac{\dot{\theta}}{2}e^{-2\pi i\Delta\nu t}C_2 \tag{5a}$$

$$\dot{C}_2 = i\frac{\dot{\theta}}{2}e^{2\pi i\Delta\nu t}C_1 \tag{5b}$$

where $\Delta\nu = 2\nu$. Elimination of C_2 leads to the second order equation

$$\ddot{C}_1 + (2\pi i\Delta\nu - \ddot{\theta}/\dot{\theta})\dot{C}_1 + \left(\frac{\dot{\theta}}{2}\right)^2 C_1 = 0. \tag{6}$$

In order that the results of this analysis may be legitimately compared with an actual experiment, $\dot{\theta}$ and $\ddot{\theta}$ must be continuous functions of time. Our choice of $\dot{\theta}$ is limited, however, to such functions that render (6) reducible to a known type of differential equation. Such a function is

$$\dot{\theta} = 2\pi\nu_0 \operatorname{sech} \pi t/\tau, \tag{7}$$

the plot of which is b of Fig. 1. The constants ν_0, τ have been so chosen that the total change in θ,

$$\Delta\theta = \int_{-\infty}^{\infty}\dot{\theta}dt = 2\pi\nu_0\tau,$$

is that produced by a constant rotation of frequency ν_0 and of duration τ.

This function, together with the transformation

$$z = [\tanh(\pi t/\tau) + 1/2],$$

reduces (6) to the hypergeometric equation

$$z(1-z)\frac{d^2C_1}{dz^2} + \{c - (a+b+1)z\}\frac{dC_1}{dz} - abC_1 = 0 \tag{8}$$

where $a = -b = \Delta\theta/2\pi$ and $c = \frac{1}{2} + i\tau\Delta\nu$. As t goes from $-\infty$ to ∞, z goes from 0 to 1. The general solution of (8) which is defined in this range is

$$C_1 = AF(a, b, c, z) + Bz^{1-c}F(a+1-c, b+1-c, 2-c, z).$$

In order that the boundary condition (4a) be satisfied, we must set $A = 0$. Using Eq. (5a) we find that the boundary condition (4b) is satisfied when

$$B = \frac{(\Delta\theta/2\pi)}{|c|}.$$

The desired transition probability is thus given by

$$\begin{aligned} P &= \left|\frac{\Delta\theta/2\pi}{c}F(a+1-c, b+1-c, 2-c, 1)\right|^2. \\ &= \sin^2\frac{\Delta\theta}{2}\operatorname{sech}^2(\pi\tau\Delta\nu). \end{aligned} \tag{9}$$

[5] This direct method of obtaining this simultaneous set of equations was suggested to the authors by Professor H. P. Robertson.

3. Discussion

We have found the fraction (9) of electrons which change their spatial quantization when subjected to a rotating magnetic field of the type (7). It is reasonable to expect that any experimentally realizable rotating magnetic field of the same general type as (7), Fig. 1b, will lead to the same general results.

The fraction, P, is zero whenever the total rotation is a multiple of 2π. In the experiment of Phipps and Stern, where the total rotation was 2π, no transition was observed. Even if their rotation had not been quite 2π the "sech" in (9) would probable have given a result with their apparatus too small to be observed.

Another equally surprising result is, that if we multiply $\dot{\theta}$ by an arbitrarily large number, we do not change P, apart from the sine factor.

The dependence of P upon the duration of the rotation τ and upon the difference in energy of the two states, $\Delta E = 2h\nu$, is of a type to be expected from previous studies on transitions.[6] The decrease of P with increasing values of the product $\tau\Delta\nu$ is much more marked than as found by Güttinger. A comparison is given in Fig. 2.

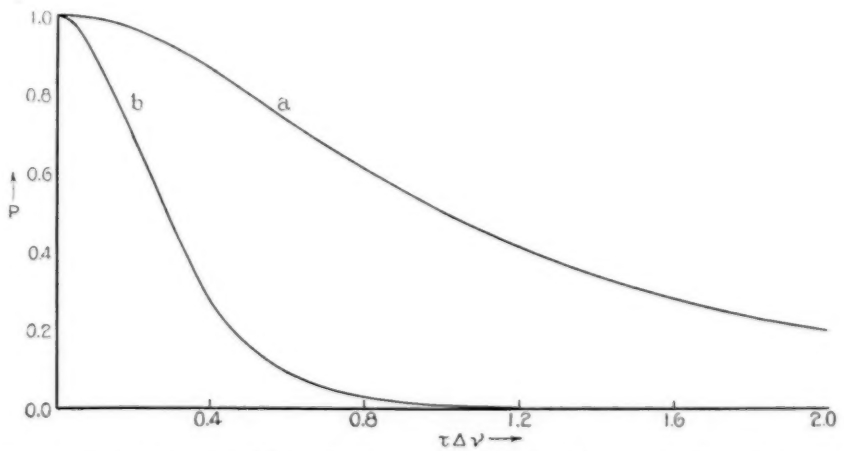

Fig. 2. Transition probabilities. Curve a, $P = 1/[1+(\tau\Delta\nu)^2]$; curve b, $P = \mathrm{sech}^2\, \pi\tau\Delta\nu$.

II. Related Collision Phenomena

The Born-Dirac collision method has been applied with success to numerous high velocity collision problems. No such general method has been found for collisions which involve low velocities. The best that can be hoped for at present is to have a variety of techniques each restricted to a limited class of collisions. Such special techniques are being rapidly developed.

The most obvious procedure is to use the Born-Dirac method with modifications which reduce the perturbations by keeping the colliding systems apart. One method is to consider only grazing incidences.[7] Another is to use

[6] C. Zener, Phys. Rev. **38**, 277 (1931).

[7] O. K. Rice, Proc. Nat. Acad. Sci. **17**, 34 (1931).

as the initial solutions those corresponding to elastic collisions.[8] Even then the perturbation method is not applicable if the eigenwert of the initial state is very close to an eigenwert of another state.

Fortunately in this case a simplification is introduced by the legitimacy of considering only the two states which are in close resonance. The problem may then be reduced to the solution of two simultaneous equations of the second order in the coordinates of the centers of gravity of the two systems.[9] These can at present be handled only by a perturbation method starting from the adiabatic solutions. This is, however, exceedingly cumbersome.

These complications may be avoided in those cases in which the difference in energy between the two quantum states is small in comparison with the relative energy of translation. We are then justified in treating the positions of the centers of gravity not as dynamical variables but as parameters dependent upon time. This is in the spirit of the pioneer work of Kallmann and London.[10] The problem is then reduced to the solution of two simultaneous equations of the first order.

The initial wave equation is of the form

$$\left\{H_0(x) + V(t, x) - \frac{h}{2\pi i}\frac{d}{dt}\right\}\{C_1(t)e^{2\pi i(E_1/h)t}\psi_1(x) + C_2(t)e^{2\pi i(E_2/h)t}\psi_2(x)\} = 0. \tag{10}$$

H_0 is the unperturbed Hamiltonian for the internal coordinates x. V is the perturbation energy. Since the relative coordinates are here being regarded as definite functions of time, V is a function of t and x. The wave functions ψ_1, ψ_2 satisfy

$$(H_0 - E_n)\psi_n = 0.$$

The two simultaneous equations are obtained by multiplying (10) by ψ_1^* and by ψ_2^* and integrating.

$$\dot{C}_1 = ife^{-2\pi i\Delta\nu t}C_2 \tag{11a}$$

$$\dot{C}_2 = ife^{2\pi i\Delta\nu t}C_1. \tag{11b}$$

Here

$$f(t) = \frac{2\pi}{h}\int \psi_1 V(t/x)\psi_2^* dx$$

and $\Delta\nu = (E_1 - E_2)/h$. We must specify that V be such that $(n|\ V|\ n) = 0$.

The analysis of the preceding section has shown that this set of equations can be solved exactly if we give f the form

$$f(t) = f_0 \operatorname{sech}(\pi t/\tau). \tag{12}$$

[8] C. Zener, Phys. Rev. **37**, 556; **38**, 277 (1931); P. M. Morse and E. Stueckelberg, Ann. d. Physik **9**, 579 (1931).

[9] O. K. Rice, Phys. Rev. **37**, 1187; 1551; **38**, 1943 (1931); F. London, Zeits. f. Physik **74**, 143 (1932).

[10] H. Kallmann and F. London, Zeits. f. physik. Chem. **2B**, 207 (1929).

In particular, we have seen that the solution which satisfies the boundary conditions

$$C_1(-\infty) = 0$$
$$|C_2(-\infty)| = 1$$

gives for the asymptotic value of the transition probability

$$P = |C_1(\infty)|^2 = \sin^2 A \operatorname{sech}^2(\pi\tau\Delta\nu),$$

where

$$A = \int_{-\infty}^{\infty} f(t)dt.$$

This may be written in the more general form

$$P = \left| \frac{\sin A}{A} \int_{-\infty}^{\infty} f(t) e^{2\pi i \Delta\nu t} dt \right|^2. \tag{13}$$

If we retain only the first term in the expansion of $\sin A$, we obtain the P given by the perturbation method of setting $C_2 = 1$ in (11a). This simple relationship between the exact solution and that obtained by the perturbation method suggests that (13) is not confined to the particular $f(t)$ given by (12), but is the general expression for all non-singular f's, i.e., all functions which are continuous and whose first derivatives are continuous. This is borne out by the fact that for $\Delta\nu = 0$, it is found that for *any* f, P is given by $\sin^2 A$. This generalization, applied to (9), says that the factor $\sin^2(\Delta\theta/2)$ is present for all experimentally obtainable θ's.

As an example, let

$$f(t) = f_0/(1 + \pi^2 t^2/\tau^2).$$

Then (13) gives

$$P = \sin^2(\tau f_0) e^{-2\tau\Delta\nu/\pi}.$$

The Absolute Values of the Mobility of Gaseous Ions in Pure Gases

By NORRIS E. BRADBURY
Physical Laboratory, University of California

(Received March 17, 1932)

The absolute method of measuring the mobilities of gaseous ions developed by Tyndall and Grindley has been employed to study the ionic mobility in gases of high purity. The method was slightly altered to improve the resolving power. An intense source of high voltage x-rays previously used in recombination measurements provided an external source of ionization for the Pyrex glass mobility chamber. Under these conditions a high degree of gas purity could be maintained in the baked out chamber, and definite knowledge concerning the existence of a velocity spectrum could be obtained from the shape of experimental curves. Careful purification and drying by liquid air was employed for all gases. At time intervals of the order of 4×10^{-2} seconds only a single class of each ion was found for the positive and negative ion in air. The mobility, 1.60 cm/sec. per volt/cm for the positive ion and 2.21 cm/sec. per volt/cm for the negative ion is in agreement with other absolute values. Oxygen prepared from $KClO_3$ gave an anomalous high mobility of 2.65 for the negative ion, due probably to the presence of chlorine oxides. Oxygen from $KMnO_4$ and from a commercial tank source carefully purified gave the values 1.58 for the positive ion and 2.18 for the negative ion. Nitrogen, as finally prepared by extreme purification of the commercial tank gas gave no negative ions and a positive ion of mobility 2.09. Hydrogen was found to give no negative ions and a predominating positive ion of mobility 8.2. Indications of a higher mobility ion at 13.1 were also found. This is in agreement with the results of Loeb on Na^+ ions in H_2. Helium gave no negative ions and a positive ion of mobility 17.0. This agrees with an approximate value observed by Tyndall and Powell for lower pressures and shorter ion ages. For pure gases and ion ages of the order of magnitude of those employed in these experiments (0.04″ to 0.07″) sharp peaks, indicative of a single class of ion, were always observed.

INTRODUCTION

SINCE the initial experiments of Rutherford and J. J. Thomson[1] in 1896 on the conductivity of air ionized by x-rays, the mobilities of the normal gaseous ions have been studied by many investigators. The results of these measurements, however, have by no means resulted in a series of accurate and absolute values of ionic mobilities for different gases. So great has been the discrepancy between different observers with different experimental procedures that, lacking a standard of comparison or interpretation, it was necessary in the compilation of the International Critical Tables[2] to include all published values of even moderate reliability. In the case of hydrogen, which is typical, this has resulted in the listing of seven different values for the mobility of the positive ion ranging from 4.96 to 6.70. Similarly discordant values are to be found for the other common gases. Under such circum-

[1] Thomson and Rutherford, Phil. Mag. **42,** 392 (1896).
[2] L. B. Loeb, Int. Crit. Tables, **6,** 111 (1929).

stances, it is obviously impossible to compare theory with experiment, exact values for substitution and calculation in other theoretical equations are lacking, the values obtained by one method cannot be compared with those given by another under slightly different conditions, and the whole situation is incompatible with the facilities and means for investigation of modern research. It is for these reasons that the experiments to be described were carried out to obtain a series of accurate absolute values of ionic mobilities under conditions of high gaseous purity.

A consideration of the experimental methods and techniques which have been employed in mobility measurements in the past shows that most of the causes of the discrepancies noted above may be classified under two headings. These are: (1) experimental idiosyncracies either uncontrollable or neglected; (2) the degree of gas purity maintained. Although in any given experiment it may be difficult to assign either one or both of these conditions as having been operative, yet they form a valuable means of evaluating the reliability of a proposed method.

Under (1) we have such phenomena as turbulence, which is usually unavoidable in all air blast methods, interpenetration of fields in methods employing gauzes, volumes of ionization vaguely defined and seriously affected by diffusion, and similar difficulties. In addition, conditions of low resolving power, abnormally high fields, contact potentials, and the like must be considered and guarded against.

Under (2) it is only necessary to mention the well-known effect of traces of water vapor on the mobility of the ion, and the work of Loeb[3] on mixtures. The latter studies have shown that extremely minute traces of certain impurities can exert a marked effect on the mobility of the ion, and that furthermore such traces are frequently difficult to eliminate. The large volumes required in blast methods make adequate purification of the gas under such circumstances impossible. Radioactive materials, when employed as means of ionization, have been sources of contamination in certain gases. Metal parts that cannot be carefully cleaned are constant sources of impurities due to films of oil and grease of high vapor pressure. Hard rubbers, shellacs, stopcock greases, etc. that can come in contact with the gas to be studied are almost invariably sufficient sources of contamination to affect seriously the values of the mobility obtained.

Of the few absolute methods of mobility measurement that are relatively free from criticisms of the first type, the method of Tyndall and Grindley[4] is the only one adaptable to a large number of different gases and ions. As originally designed with α particle ionization, failing a better source, the method was not able to yield the beautiful results of which it was capable. The availability of the splendid high tension d.c. source of x-rays, built for studies on ionic recombination furnished the possibility of developing the Tyndall and Grindley method to the limit of its usefulness. With the powerful constant *external* ionizing source it became possible to measure mobilities

[3] L. B. Loeb, Phys. Rev. **32,** 81 (1928).

[4] Tyndall and Grindley, Proc. Roy. Soc. **A110,** 341 (1926).

by an absolute method in a baked out glass chamber with a minimum of metal parts, and so to alter the method that the mobility curves were composed of linear elements with a sharp peak and therefore had perhaps the highest resolving power of any method yet used. In addition a slight change in the cycle of potentials applied to the measuring field was made to permit the measurement of positive ion velocities in gases in which free electrons existed. The same change permitted negative ions, if any, to be observed in supposedly free electron gases. Another minor variation in the method allowed a simplification of the theory, thus permitting a clearer interpretation of the experimental curves. The results obtained with this method quite transcended expectations and will constitute the contents of this paper.

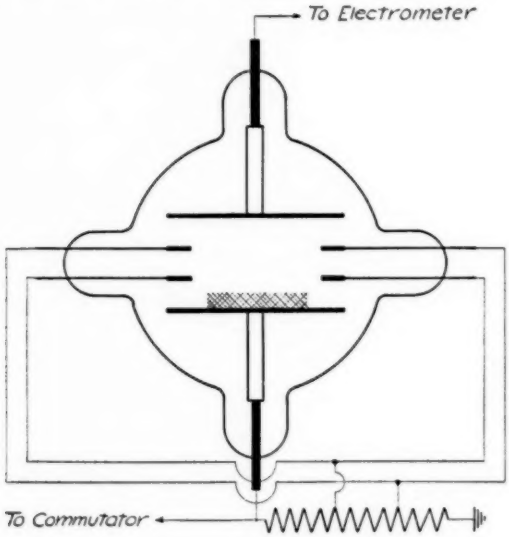

Fig. 1a. End view of ionization chamber showing sheath of ionization along the lower plate and equipotential vanes to maintain a uniform field.

Apparatus

The source of ionization was a homogeneous beam of intense, hard x-rays from a Coolidge tube under a potential of 80 k.v. pure d.c. An elaborate control and filter system enabled the potential on the tube and the current drawn to be kept constant to within 0.3 percent. This equipment, previously used in recombination measurements, formed an invaluable source of constant ionization for these experiments.

The ionization chamber was constructed of Pyrex glass as shown in Fig. 1. The plates were 7×15 cm and 3.5 cm apart. The plates, as well as the equipotential guard rings mounted equally spaced between the plates, were kept in position and accurately parallel by a carefully made spacing block kept in place during the necessary glass blowing. When the plates were fixed in position, this spacer could be withdrawn and the remainder of the glass blowing completed. The alignment and parallelism of the plates was further checked by cathetometric measurements. All metal parts were of Monel

metal save the ground shield in the front part of the chamber through which the x-rays had to pass. This was of thin aluminum. The entire plate system was surrounded by a grounded Monel metal screen to protect the measuring fields from external electrostatic disturbances. The chamber was then mounted behind an adjustable lead slit through which the ionizing x-rays could pass in a thin sheath parallel to and grazing the lower plate. Connections to the diffusion pump and gas purifying train were made as shown.

The upper plate, on which the ions were collected, was kept at ground potential and connected to the electrometer. The lower plate was connected to ground through a 30,000 ohm resistance, at the upper end of which was applied the necessary potential to produce the required field between the plates. The equipotential guard rings were then connected 10,000 ohms above ground and 20,000 ohms above ground respectively. A sensibly uniform field was thus maintained between the plates over a much larger area

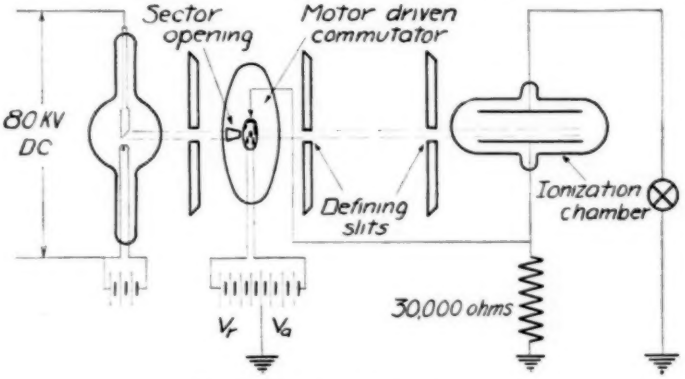

Fig. 1. Diagram of apparatus.

than otherwise. Since, however, the ions follow the lines of force, and only the ions which get across *first* (i.e., along the straightest lines or the most uniform field) are important in the measurements, these guard rings are of importance only in increasing the intensity of the observed currents.

A lead shielded brass disk, in which two variable sector openings had been cut, was mounted in the path of the x-ray beam so that its rotation permitted a flash of x-rays to pass through at each revolution. Affixed to this disk was a commutator with suitable segments and brush system for applying the potential cycle to the plates of the ionization chamber. The position of this commutator with respect to the x-ray flash could be varied. This cummutator and disk assembly were driven by a large, variable speed d.c. motor through reduction gears. The constancy and absolute value of this speed was determined by voltage readings from an accurate magneto tachometer directly connected to the motor. The entire arrangement is similar to that employed in aging experiments on ions in air, and is shown in Fig. 1. The potential cycle applied to the plates at each revolution is shown in Fig. 2. The dotted lines represent an addition to the cycle employed when it was desired to measure positive ions in gases in which electron attachment does not occur over appreciable periods of time.

Theory of the Method

The theory of the method has been given by Tyndall and Grindley. Inasmuch as the present experiments following a different and somewhat simpler procedure, the theory will be given as it here applies.

An individual cycle takes place as follows. A flash of x-rays in a thin sheath parallel to the lower plate occurs at the point marked γT in Fig. 2 with respect to the potential cycle. At this time the space between the plates is field free and ions accumulate in uniform layer above the lower plate. Let us suppose we are measuring positive ions. The flash of x-rays is followed by the application to the lower plate of a *negative* potential V_r which drags the positive ions *downwards* for a time δT, where T is the time of a revolution and δ a fraction. Necessarily the lower part, or even all, of the sheath may be caught by the lower plate during this phase. Those ions which are not caught at the conclusion of this phase are then drawn across the space, by an advancing potential V_a, towards the upper plate for a time αT which, if sufficiently long, will permit all the ions not caught at the end of γT to be received at the upper plate and noted as a current to the electrometer. If V_a is not

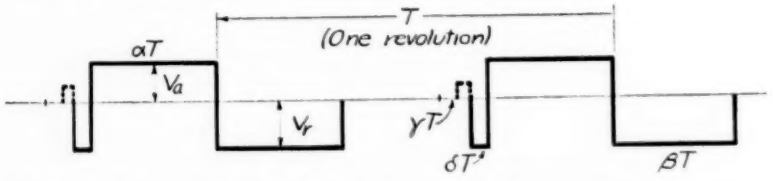

Fig. 2. Cycle of potentials applied to the lower plate. Ions are formed during γT, drawn towards the lower plate during δT, and drawn across the volume to the upper plate during αT, Volume cleared of all ions not caught during βT. Free electrons, if present, are swept out by the small potential shown in dotted lines.

great enough, or αT too short, those ions which are not caught at this time are swept out of the field by V_r acting during βT. The space between the plates is now free of ions (the negative ions having been swept out to the lower plate during αT) and the cycle may be repeated.

In practice V_a is set at a definite value and V_r at a somewhat higher value. The speed of revolution, which directly determines the time of application of αT, βT and γT, is then varied and the relative current received at the electrometer at different frequencies noted. We can now consider the variation of the electrometer current with frequency as it is related to the mobility of the ions, the time of application and magnitude of V_a, and the distance between the plates.

Suppose the x-ray beam forms Q ions per cc per second in the sheath above the lower plate. Then during the time of application of the x-rays, γT, at A there will be formed $Q\gamma TAd$ ions in the sheath if A is its area and d its thickness. The sheath is then acted on by V_r for a time δT. If the mobility of the ions is k, the sheath will then move downwards a distance $kV_r\delta T$ and only $(d-kV_r\delta T)Q\gamma TAd$ ions remain above the plate. V_a now acts for a time αT. If V_a is great enough or αT long enough all these ions will be caught at the upper plate and the quantity received at the electrometer per

cycle will be that amount. Over a series of cycles this corresponds to a current of $(d-kV_r\delta T)\,Q\gamma Ad$.

Suppose, however, we increase the frequency so that αT is no longer sufficiently long to permit all the ions to reach the upper plate. A certain fraction of the ions remaining after δT will also escape capture at the upper plate and will subsequently be swept from the field. It is easily shown that the amount now received at the electrometer in terms of current is

$$(d - kV_r\delta T - D + kV_a\alpha T)Q\gamma Ad$$

where D is the distance between the plates. We may now consider the variation of these two expressions with T, the period of one revolution. When

$$T = (D - d)/(kV_a\alpha - kV_r\delta)$$

the current will be zero and will remain so for all shorter T's. As T increases di/dT is given by $Q\gamma Ad(kV_a\alpha - kV_r\delta)$ which is positive since $\alpha/\delta > V_r/V_a$. When $D = kV_a\alpha T$, the second expression reduces to the first for which the di/dT is seen to be $Q\gamma Ad(-kV_r\delta)$. This is negative and hence the current decreases with increasing period. Obviously, there is a point of discontinuity, whose evidence is a maximum in the electrometer current-frequency curve at

$$D = kV_a\alpha T.$$

Hence if we measure the electrometer current for different periods or frequencies of the commutator, we will find a linear *increase* in i with increasing T (decreasing N where N is the frequency) until the point

$$D = kV_a\alpha T$$

is reached. At this point there will be a linear *decrease* in current until the point $d = kV_r\delta T$ is reached beyond which the current will be zero. Since we can measure D, V_a, α, and T (at the maximum) we can easily calculate k from the above equation, and this will form our method of procedure.

In the case of gases in which free electrons exist, a change in the cycle had to be made shown by the dotted lines in Fig. 2. Otherwise, during the time of application δT of the retarding phase for positive ions, the free electrons, having an approximate mobility of 10,000 cm per sec., would be entirely swept across the field to the upper plate and completely mask the following positive current. Hence it was necessary to insert a small *positive* potential (2–20 volts) *before* the application of δT. This is sufficient to sweep the electrons entirely from the field to the lower plate, causing a negligible change in the effective d of the positive ion sheath.

It is interesting to notice that k so determined is independent of V_r and d-two variables whose effects it is extremely desirable to eliminate. Moreover it can easily be shown that the same results are obtained if the beam does not exactly graze the plate but passes a short distance above it. This theory shows, then, that the mobility can be calculated from easily measured variables and it is independent of those factors whose value would be difficult to determine. Moreover, it predicts a definite type of curve for a single

mobility and hence enables easy comparison with experiment. It may be mentioned here that the independence of the position of the peak with respect to V_r and d was amply verified by experiment. The resolving power of the method can be increased at will by making d as small as is compatible with the intensity of ionization and the sensitivity of the detecting system.

Purification of the Gases Used

The chamber was surrounded by a wire-wound resistance furnace enabling the chamber and metal parts to be baked out under a vacuum at a temperature of 350°C. The dimensions of the metal parts precluded their being made so as to permit outgassing with an induction furnace. By prolonged baking out, however, it was felt that most of the *adsorbed* gases on the surfaces were removed. A liquid air trap was mounted between the chamber and the remainder of the pumping and purifying system to prevent any possible diffusion of stopcock grease vapors into the chamber when filled with pure gas. This trap was kept at liquid air temperatures during the filling of the chamber and the course of a run. It was, of course, removed when baking out was in process. Under such conditions the chamber could be pumped out to better than 10^{-6} mm.

The method of purification of the gases used varied with the different gases. Liquid air was always used for drying where possible. Oxygen, which condenses at atmospheric pressure and liquid air temperatures, was dried by a freezing alcohol bath. Two or more such drying traps were always employed, in addition to the trap on the chamber itself. Even under such conditions, it was found necessary to pass the gas through the purifying train extremely slowly.

Air, upon which the first measurements were made, was purified by passing it through the usual purifying train consisting of NaOH, $CaCl_2$, and P_2O_5 followed by liquid air traps. A later series of experiments was made in which the air was purified only by passing very slowly through three liquid air traps in series. Apparently both methods were equally satisfactory.

Oxygen was first prepared by heating $KClO_3$, condensing the oxygen in a liquid air trap, and subsequently distilling through the purifying train into the chamber. In another preparation the same procedure was followed save that $KMnO_4$ was substituted for the $KClO_3$. Finally, tank oxygen was condensed by liquid air and fractionated using the middle third for filling the chamber. The latter two methods were apparently the more satisfactory, though extreme care had been taken to purify the $KClO_3$ by recrystallization and to keep out organic matter.

Nitrogen was obtained from a commercial tank. Preliminary results obtained by passing it through the usual purifying train plus a small heated tube filled with copper shot and powder showed the presence of a large number of negative ions. The value for the mobility of the positive ion was, however, higher than expected. The preparation of nitrogen was then carried out by the decomposition of sodium azide, which, after passing through liquid air traps, was led directly into the chamber. This had the gratifying result of

giving only free electrons but evidences of some impurity (probably organic ammonia like compounds due to the method of preparation of the azide) were still present in a lower (though normal) positive ion mobility. Drastic purification of tank nitrogen was then attempted. A Pyrex tube one meter in length was filled with glass wool and precipitated copper powder which was thoroughly reduced by passing hydrogen through the heated tube. In addition, a tube containing metallic sodium, vaporized under vacuum, was placed in the purifying line. Liquid air traps before and after the copper tube and after the metallic sodium completed the purifying train. Under these circumstances nitrogen was obtained which gave no negative ions and every evidence of extreme purity.

Hydrogen was obtained from a commercial tank of considerable purity and passed through the usual purifying train plus a heated copper tube. With the usual liquid air drying, this hydrogen appeared to be of highly satisfactory purity.

Helium was first obtained from a small cylinder donated several years before by the U. S. Navy. Purification by the ordinary train gave a product of very doubtful purity, which was probably due to the condition of the gas employed. Another tank of the gas, stated to be of 95 percent purity, was then obtained and a specially designed purifying train constructed. Heated tubes containing precipitated copper and powdered copper oxide were put in to remove hydrogen and oxygen. In addition, the helium was sparked between magnesium electrodes to remove nitrogen and passed over heated metallic sodium. The gas, after this treatment plus absorption in two charcoal traps in liquid air, gave results indicative of high purity. Spectroscopic examination of both the hydrogen and helium showed nothing but the ordinary line spectrum.

Before filling with any gas, the chamber and purifying train were pumped out to high vacuum and the chamber was baked out. The train was then shut off from the chamber, slowly filled with gas, quickly pumped out, and slowly filled with gas again. The chamber itself was then flushed out with the purified gas, and finally filled to atmospheric pressure. Approximately two hours was required for the purification of the two liters of gas required to fill the chamber.

Results

It was noted under the theory that the theoretical shape of the commutator frequency-electrometer current should be that of two straight lines intersecting in a maximum value or peak at a value of T such that

$$D = kV_a\alpha T.$$

This was deduced for ions supposedly of a single unique mobility. It has previously been shown that if there is a uniform distribution or spread of mobilities about some average value, the top of this peak will be rounded off or flattened. Naturally, it is impossible to obtain an absolutely sharp maximum with such factors as diffusion and self-repulsion, and finite separation of observed points, yet in pure gases with a single type of ions where the ioniza-

tion intensity was sufficient to permit adjustment for high resolving power, very satisfactory sharp peaks could be obtained. Occasionally when it was necessary to widen the slit to too great an extent in order to secure measurable electrometer currents, the sides of the peak would drop off to zero too rapidly owing to ions of the opposite sign coming across during δT, or which were not entirely removed during αT. This resulted in an outward "bow" in the curves. Such curvature, however, was never found to influence the position of the peak, and only rendered the observed curves a little more difficult to interpret. None of the results to be reported were obtained under these conditions.

The observed values of mobility in the different gases are given below. All values have been reduced to 760 mm. The temperature of these measurements was 22°C.

Air. Typical curves for the positive and negative ions in air are shown in Fig. 3. These ions were observed at an age of 0.07 seconds and it is clear that they show a unique velocity. In general the negative curves are sharper than

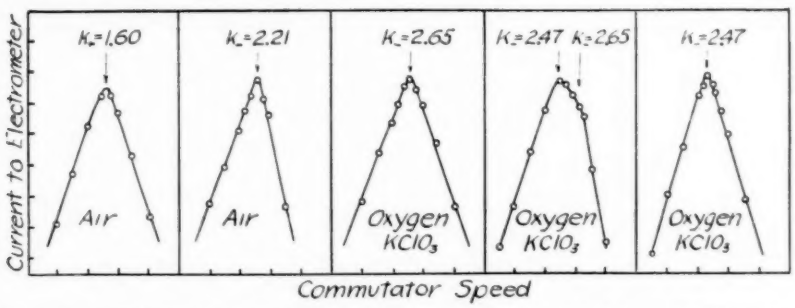

Fig. 3. Experimental curves for air and for oxygen prepared from $KClO_3$. The arrows indicate the position of the peak for calculation.

the positive. This is probably due to an incipient aging effect in the case of positive ions, enhanced by the products of ionization formed by the intense x-rays. The average of all values obtained for the positive ion was 1.60 cm/sec. per volt/cm and for the negative ion 2.21 cm/sec. per volt/cm. These values are in exact agreement with those obtained for "new" ions in the aging experiments previously reported and are also in good agreement with the values obtained by Loeb with photoelectric ions, and by Tyndall and Grindley with radioactive ionization. Apparently the complex chemical reaction products formed by the x-rays in a mixed gas such as air are sufficient to cause the lowered mobility in spite of the elaborate precautions taken to insure purity. These values in air are practically the same as those found with much more casual methods of purification. The value obtained by Loeb[5] of 2.16 was in air of somewhat questionable purity as was the 2.18 value of Tyndall and Grindley. Schilling[6] has worked in very pure air, but used a gauze method which gave results dependent on the auxiliary field strength.[7] Luhr and Brad-

[5] L. B. Loeb, Journ. Frank. Inst. **196,** 537 (1923).
[6] H. Schilling, Ann. d. Physik **83,** 23 (1927).
[7] Cf. footnote, Int. Crit. Tables **6,** 112 (1929).

bury[8] with a Langevin method obtained values in agreement with those reported here. Zeleny[9] has made recent accurate studies on ions of different ages in dry and moist air in an apparatus which was not outgassed using an air blast method. His results were thus obtained under conditions which make comparison difficult. In view of the agreement of the values here obtained with the other recent values given by the absolute methods cited, *one must accept as the standard values for air the values of 1.60 and 2.21 cm/sec. per volt/cm for the positive and negative ions respectively.* These are in place of the previously accepted values of 1.36 and 1.87 obtained in 1901.[10]

Oxygen. Oxygen was first prepared, as described, by the decomposition of $KClO_3$. Under these circumstances rather remarkable values were obtained. The negative ion showed an initial high mobility—reaching values of 2.65—which subsequently decreased to 2.47 as the gas was allowed to remain in the chamber. The positive ion showed a similarly high mobility which decreased with the age of the gas from 1.71 to values approximating 1.6 with more than one type of ion present. The curves in this case are shown in Fig. 3, for the negative ion, and Fig. 4, for the positive ion. Frozen alcohol was maintained

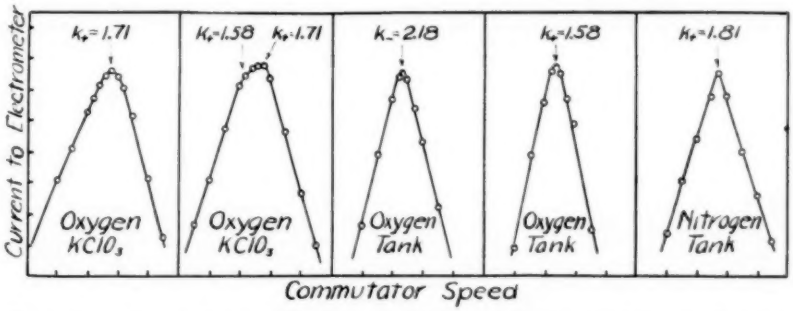

Fig. 4. Experimental curves for oxygen and an initial curve on impure nitrogen.

on the trap during the time the gas was in the chamber. The shift of the maximum indicates either the appearance or disappearance of some impurity. The possibility of the decomposition of the $KClO_3$ resulting in traces of chlorine oxides were any traces of foreign matter present in the salt makes the latter case seem the more probable. This method was used as it had been recommended as that method giving the purest O_2 for molecular weight determinations. It is seen that the ions are sensitive to impurities which do not affect the most accurate chemical technique. The preparation of oxygen from $KMnO_4$ was therefore carried out, in spite of the fact that Baker's C.P. chemical contained, by their analysis, 0.004 percent Cl and ClO_3. These were evidently in the form of salts which did not decompose at the low temperatures required by $KMnO_4$. In this case the average of the runs taken gave 2.19 for the negative mobility and 1.58 for the positive ion. These values did not change as the gas remained in the chamber over 24 hours, and seem much

[8] Luhr and Bradbury, Phys. Rev. **36,** 1394 (1930).
[9] J. Zeleny, Phys. Rev. **34,** 310 (1929); **36,** 35 (1930); **38,** 969 (1931).
[10] J. Zeleny, Phil. Mag. **195,** 193 (1901).

more understandable than those obtained from $KClO_3$ oxygen when compared with the values obtained in air.

Finally, in spite of the practical impossibility of removing all the N_2 in the purification of liquid oxygen by fractionation, this means of preparation was attempted. The values obtained in this case were the same as those given by the $KMnO_4$ prepared gas, and lend weight to the assumption as to its purity. Typical curves obtained are shown in Fig. 4. The absolute values for the mobility of the positive and negative ion in pure oxygen at atmospheric pressure may then be taken to be 1.58 and 2.19 cm/sec. per volt/cm respectively. The only values that exist in the literature are those of Zeleny[10] (1.36 and 1.80 which may be compared with his values for air), and those of Franck[11] using his gauze modification of the Rutherford method. He obtained 1.29 and 1.79 but the gauze method makes comparison in this case futile.

Nitrogen. The first runs were made on nitrogen taken from an ordinary commercial tank and gave a positive ion of 1.82 and a rather sharp curve as shown in Fig. 4. This value was somewhat higher than that to be expected from the air and oxygen measurements, and it was rather surprising to find that there was only about 30 percent free electrons. These results are in agreement with those noted by Luhr[12] in recombination measurements whose nitrogen was purified in much the same manner. Luhr, believing his N_2 pure, ascribed his negative ions to possible attachment of electrons to atoms or molecules activated by the x-rays. These results and those to follow show in reality that the N_2 was impure and that the Cu was apparently not removing all the oxygen. Similar conditions apply to Luhr's work in argon and probably explain the results of Mario da Silva[13] who believed that attachment might take place between electrons and activated atoms of N and molecules of N_2. Since the attachment experiments of Cravath had shown that under ordinary conditions electron attachment should not take place in pure nitrogen, the existence of negative ions of a mobility 2.21 gave definite evidence that some impurity was present which could attach electrons. In consequence, the preparation of nitrogen from sodium azide was carried out. In this gas a mobility of 1.62 for the positive ion was obtained with the curve shown in Fig. 5a. No negative ions could be detected, the free electrons being removed by the application of the small auxiliary phase mentioned above.

Although the value obtained for the mobility of the positive ion in the case of the azide nitrogen seemed plausible, yet the higher value obtained in tank nitrogen and the suspected contamination of the azide by organic compounds, led to the feeling that still higher values might be obtained were purification methods more strenuous. The tank nitrogen was consequently purified as previously described with very satisfactory results. No negative ions could be detected in the gas even after standing four days in the chamber. Furthermore a mobility of the positive ion of 2.09 was found and initial curves showed an asymmetry on the high mobility side which may be com-

[11] Franck, Zeits. f. Physik **12,** 291 (1910).
[12] O. Luhr, Phys. Rev. **36,** 24 (1930).
[13] M. A. da Silva, Ann. d. Physik **12,** 100 (1929).

pared with the high values found by Loeb[14] for the Na ion in short time intervals in nitrogen. Fig. 5b shows the type of curve obtained and Fig. 5c that obtained after the gas had been in the chamber 36 hours, though no negative ions were detected even after three days.

The mobilities of ions in nitrogen have been measured by Franck[15] and by Yen,[16] who also used the Franck method. Their results agreed within their limits of error giving a positive mobility of about 1.3 and a negative mobility of 1.8. The impurity of the gases used and the unknown effect of the gauzes make comparison futile. Tyndall and Powell,[17] however, have measured the mobility of the positive ion in nitrogen (in which they found no negative ions) at low pressures and short time intervals. They could not determine absolute values but found a mobility for the positive ion of about 2.1 with indications of a subsidiary peak at 1.6. These investigations confirm the

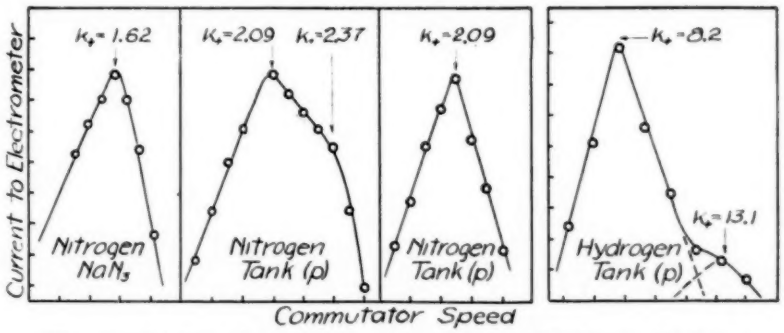

Figs. 5 and 6. Experimental curves for nitrogen and hydrogen; the latter showing the presence of the 13.1 mobility.

existence of this high mobility, however, at greater ion ages and atmospheric pressures. Loeb has measured the mobility of Na^+ ions in nitrogen and found an initial mobility of 3.75 at ages less than 5×10^{-3} seconds. Following this there is a moderately abrupt decrease to a mobility of about 3.0 and a subsequent decrease to the value 1.6 at ages of 0.01 second. The uncertain temperature correction in the experiments make his absolute values somewhat doubtful, but the appearance of the hump on the high mobility side of Fig. 5 at 2.37 is an interesting confirmation of his results. Several attempts were made to detect a higher mobility than 2.09, but were unsuccessful. Hence it may be said that the mobility of the more stable positive ion in pure nitrogen at atmospheric pressure measured within 10^{-2} seconds is 2.09 cm/sec. per volt/cm. No negative ion exists in pure nitrogen, the carriers being free electrons. It is to be noted that the 2.09 cm/sec. positive ion in nitrogen may be the unaged positive ion of mobility approximately equal to that of the negative ion observed by Erikson[18] and by Mahoney[19] in impure gases in the aging experiments.

[14] L. B. Loeb, Phys. Rev. **38,** 549 (1931).
[15] Franck, Zeits. f. Physik **12,** 613 (1910).
[16] K. L. Yen, Proc. Nat. Acad. Sci. **4,** 91 (1918).
[17] Tyndall and Powell, Proc. Roy. Soc. **A129,** 162 (1930).
[18] H. A. Erikson, Phys. Rev. **30,** 339 (1927).
[19] J. J. Mahoney, Phys. Rev. **33,** 217 (1929).

Hydrogen. The results obtained in pure hydrogen gave a curve of the shape shown in Fig. 6 for the positive ion. The peak mobility is at 8.2 and there is definite indication of a subsidiary peak at a mobility of 13.1. No negative ions could be detected in the gas under these conditions. Loeb has measured the mobility of Na^+ ions in H_2 as a function of their age[14] and found a mobility of 8.4 at ages greater than 10^{-2} seconds. He found, however, that the initial value of 17.5 at ages less than 10^{-5} seconds dropped sharply to a value of about 13.5 at 10^{-4} seconds. As mentioned above, the heating correction is somewhat doubtful, and his resultant values may not be exact. The values obtained by the method of this experiment, however, confirm the results, and furnish more accurate absolute values. The existence of the high mobility ion at 13.1 is gratifying evidence as to the purity of the gas. The detection of the 17.5 ion is beyond the limits of the experiment with the ion ages necessarily employed.

Since the values of the mobility for the hydrogen positive ion have generally been reported between 4.96 and 6.70, measurements were made on hydrogen that had been purified by merely passing through liquid air. In this case a curve was obtained with a mobility at 6.8.

Zeleny in his original measurements obtained a value of 6.70 for the mobility of the positive ion. If this is multiplied by 1.21, which is the approximate error in his standard values for air, we obtain a value of 8.1 which is in fair agreement with the results mentioned above. His hydrogen, however, maintained negative ions, and it is doubtful if the purity was sufficient for him to have observed this high value. Loeb and DuSault[20] have obtained 6.5 by the Franck method in a gas sufficiently pure so that free electrons were observed.

The negative ion mobility was measured as a matter of interest in mixture experiments for impure hydrogen. The value obtained in this case, 9.6, is in agreement with that obtained by Loeb and DuSault and by Wellisch.[21] The values for the positive ion obtained by the latter, however, are much too low. Whether this was due to field distortion or to impurities cannot be said.

In the light of these experiments and those of Loeb on Na^+ ions the mobility of the most stable positive ion in hydrogen under normal times of 10^{-2} seconds can be said to be 8.2 cm/sec. per volt/cm. In *pure* hydrogen, no negative ions are found.

Helium. The first experiments on what was evidently relatively impure helium gave the curve shown in Fig. 7 which after 24 hours in the chamber changed to one with a high mobility peak at 14.1. The main peak at 7.2 corresponds roughly to the value of 5.09 observed by Franck[22] when corrected to the new standard scale, and the 17.3 and 14.1 values are in rough agreement with results of Tyndall and Powell[17] who found the transient existence of an ion of mobility 17. They also found that, after their gas, which was of considerable purity contained in a glass chamber, had been in the apparatus for

[20] Loeb and duSault, Proc. Nat. Acad. Sci. **14,** 192 (1928).
[21] E. M. Wellisch, Am. Journ. Sci. **44,** 1 (1917.)
[22] Franck, Jahrbuch der Rad. und Elek. **9,** 235 (1912).

several days, that their curves indicated the appearance of an ion of mobility approximately 7.

These results indicated that the helium was of insufficient purity, and accordingly its further purification as previously described was carried out. The results in this case gave the curve shown in Fig. 8—with a single mobility at 17.0. This value remained unchanged after the gas had been in the chamber three days. The curve lacks symmetry because of the exceptional width of the slit which was necessary with the very feeble ionization in helium. Great difficulty was experienced in obtaining measurable currents with even the highest intensity of x-rays that it was feasible to employ, without rebuilding the electrometer system for measuring currents.

Tyndall and Powell[23] have since detected an ion in helium at low pressures and ages of 10^{-5} seconds of mobility 21. No such ion could be found in these experiments where the ion ages are of the order of magnitude of 0.04 seconds and are measured at atmospheric pressures.

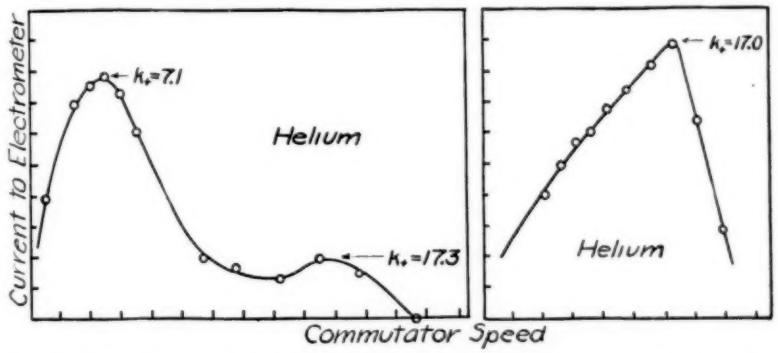

Figs. 7 and 8. Experimental curves for positive ions in impure and pure helium.

Discussion and Conclusion

In the setting up of the theory for the experiment it was tacitly assumed that the amount of ionization was proportional to T. This is the case provided we are sufficiently far removed from the steady state between ion production and recombination. Although this seemed certain to be the case, it was verified by taking electrometer currents for different frequencies with the commutator so arranged as to collect *all* the ions of one sign formed. No change in the electrometer current with frequency could be observed. The lack of dependence of the position of the peak on slit widths and V_r was verified by taking runs on the same sample of gas at varying values of each. The x-ray beam was necessarily slightly divergent, but since the position of the peak is independent of d, this is of no importance. Diffusion of the ions during times of the order of magnitude of these measurements is negligible. The time constant of the chamber and electrometer system and high resistance to ground was of the order of magnitude of 10^{-5} seconds and entirely negligible. The plates of the chamber were parallel and of known distance apart to 1

[23] Tyndall and Powell, Proc. Roy. Soc. **A134,** 125 (1931).

percent. The commutator speed could be read and kept constant to approximately 2 percent. It was checked from time to time with a revolution counter and stopwatch. The advancing voltage was measured on an instrument calibrated against the laboratory standard. It is believed that the mobilities measured in this manner are accurate to 3 percent.

In spite of the chemical purity which has been maintained in these experiments, it is extremely doubtful if any of the measurements are those for a monomolecular ion moving in its own gas and the significance of the values obtained as indicating any real characteristics of the gas other than its inherent common impurities may be questioned. The experiments of Loeb have shown that the attachment by the ion of some foreign molecule takes place with extreme rapidity. Even when the gas purity is high, the times of measurement required in these experiments are sufficient to allow many impacts of ions and impurity molecules with an estimated purity of as high as 1 part in 10^5. The measurements in the case of hydrogen, which though presenting experimental difficulties because of the low ionization, is relatively easy to prepare with high purity, show the probable limits of this method of attack. In this case the predominating ion is one which has probably attached one or two fairly bulky molecules of impurity during the course of the measurements, but sufficient ions which have possibly formed monomolecular attachments (probably to water molecules) are present in detectable quantities. In the case of nitrogen and helium, the high values obtained show that at least some impurity which has been present in the earlier experiments has been successfully eliminated. What impurities remain, and what their amounts are it is impossible to say as their limits are below those of either chemical or spectroscopic detection. This is, of course, unfortunate, as it leaves one still uncertain as to the exact character of the particular ion—that is to say, its size—at these time intervals. It is therefore impossible to make adequate comparison with theory. The value of the mobility of the positive ion in helium alone begins to approach that demanded by the complete Langevin equation, and, as indicated by the recent experiments of Tyndall and Powell, may not even then represent a true He^+ in helium. It is therefore necessary to assert

TABLE I. *Values of the absolute mobility of normal gaseous ions.*

Gas	Source	Purity	k	k
Air	—	p	2.21*	1.59*
Oxygen	$KClO_3$	i (?)	2.65	1.71
Oxygen	$KMnO_4$	p	2.18*	1.58*
Oxygen	Tank	p	2.18	1.58
Nitrogen	NaN	i	1.60	e
Nitrogen	Tank	i	1.81	2.21
Nitrogen	Tank	p	2.09* 2.37	e
Hydrogen	Tank	p	8.2* 13.1	e
Hydrogen	Tank	i	6.7	9.6
Helium	Tank	i	7.1 14.0	e
Helium	Tank	p	17.0*	e

* Values for the more stable ion.

that while values such as found in these experiments serve to give useful absolute standard values for mobilities in pure gases as usually prepared, they are of little theoretical significance. They will, however, serve in all calculations requiring a knowledge of the mobility under ordinary conditions.

The results detailed above may be presented in a condensed form in Table I which gives the absolute values of the mobility of the normal gaseous ions in the gas in question. The method of purification and probable purity is also indicated. The starred values are those for the more stable ion to be found in the gas.

In conclusion it is desired to thank Professor L. B. Loeb, under whose direction the experiments were carried out, for his continual interest and invaluable suggestions concerning all phases of the work.

Mobility Experiments in Gaseous Mixtures and Aging Experiments in Pure Gases

By NORRIS E. BRADBURY
Physical Laboratory, University of California

(Received March 17, 1932)

Gases to which a trace of NH_3 has been added have been known to show an abnormally high value for the mobility of the positive ion. In the experiments reported here, the method of Tyndall and Grindley for measuring ionic mobilities under conditions of high gas purity and resolving power has been employed to determine the ion spectra in the case of H_2-NH_3 and N_2-NH_3 mixtures. In the former case when the partial pressure of NH_3 was reduced to 0.15 mm, a positive ion of mobility 9.4, which is substantially equal to that of the negative ion in impure H_2, was observed. In the case of the N_2-NH_3 mixtures, a positive ion of mobility 1.83 was observed in addition to the normal positive ion in the pure gas of mobility equal to 2.09. No negative ions were observable. The aging experiments reported previously (Phys. Rev. **37**, 1311 (1931)) have been continued under conditions of high gas purity using the Tyndall and Grindley method. No aging was observed in pure N_2 at ion ages as great as 0.5 seconds. Air, however, where chemical reaction products could be formed by the x-ray ionization source, showed similar aging effects to those reported previously.

A. Mixture Experiments

SINCE the mobility measurements on pure gases reported in another paper had resulted almost uniformly in only a single class of ion at ages of 4×10^{-2} seconds, it was of interest to investigate the nature of the mobility curves of certain gaseous mixtures which had been observed to indicate specific molecular attachments to ions. The Tyndall and Grindley method, as it has been employed in these and the pure gas experiments with x-ray ionization, and high gas purity and resolving power, gives an admirable method of testing for the simultaneous appearance of several ions. The shape of the curves, normally having straight sides and a sharp apex, permits more than a single class of ions to be readily observable. The same apparatus and methods of measurement as used in the experiments in pure gases have been employed here, and the same discussion applies. The two mixtures studied were hydrogen and ammonia, and nitrogen and ammonia. Previously Loeb[1] observed an abnormally high value for the positive ion when traces of NH_3 were present in air.

The nitrogen and hydrogen were prepared as described in the preceding paper. The ammonia was formed by the interaction of C.P. $(NH_4)_2SO_4$ and a concentrated solution of NaOH. The gas so formed was passed through a trap cooled to $-35°$, through a long tube filled with broken sticks of KOH, and condensed in a trap surrounded by liquid air. The ammonia was distilled off by removing the liquid air, and was then refrozen in another trap. Subsequent fractional distillation yielded NH_3 relatively free from water vapor.

[1] L. B. Loeb, Proc. Nat. Acad. Sci. **12**, 677 (1926).

The resulting curves for the nitrogen-ammonia mixtures are shown in Fig. 1. Curve *A* shows the sharp peak for pure nitrogen with a maximum corresponding to a mobility of 2.09. Addition of 1 mm partial pressure of NH_3 gave curve *D* with a very broadened peak indicating two or more mobilities.

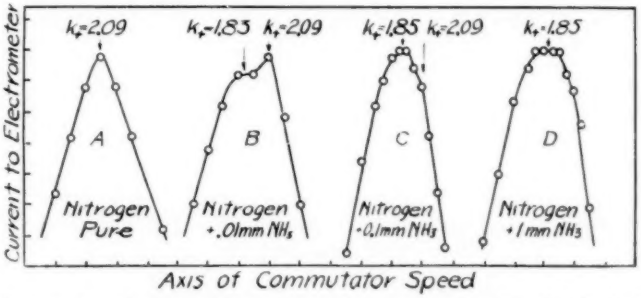

Fig. 1. Curves for mixtures of nitrogen and ammonia showing the deviation from the type of curve obtained with the pure gas.

Reduction of the ammonia to 0.1 mm gave the curve shown in *C* in which the appearance of the 2.09 peak is indicated on the high mobility side of the curve. Further reduction of the ammonia present to 0.01 mm gave the curve shown in *B* which is intermediate between *A* and *C*. Evidently in the case of nitrogen-ammonia mixtures an ion of mobility 1.85 exists in addition to the normal mobility of 2.10. This is in agreement with the results of Loeb who found an anomalous high mobility for the positive ion of 1.8 in the case of ammonia-air mixtures. The action of ammonia was found by him to be specific for the positive ion. Since in these measurements no negative ions could be detected, this effect could not be verified. It was, however, definitely verified in the case of impure hydrogen.

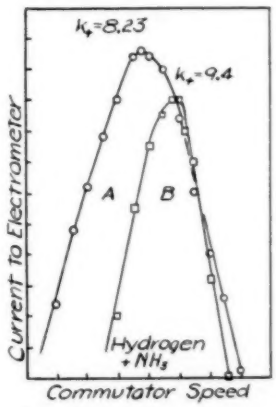

Fig. 2. Hydrogen and ammonia mixtures showing the increase in mobility of the positive ion as the percentage of ammonia is decreased.

The hydrogen-ammonia mixtures gave curves of the type shown in Fig. 2. The curve *A* corresponds to a partial pressure of 1.5 mm NH_3 and a mobility of 8.23. Curve *B* is that obtained for 0.15 mm NH_3 and corresponds to a mobility of 9.4. Its appearance is perhaps predicted by the slight asymmetry

in curve *A* on the high mobility side. A preliminary series of runs in which the purification of the ammonia was not entirely satisfactory gave the 8.3 value and indications of a hump at the usual 6.7 value.

The results were then repeated in impure hydrogen in which negative ions were present. The hydrogen in this case was dried merely by passing over liquid air. In these experiments a mobility of 9.6 was obtained for the negative ion and curves very similar to those in Fig. 2, for the positive ion with a final high mobility of 9.4. *This is seen to be practically equal to that for the negative ion.* Such a result is not, however, surprising in the light of Erikson's[2] and Mahoney's[3] experiments, who found a mobility of the positive ion in air-ammonia mixtures equal to that of the negative. No change in the mobility of the negative ion could be detected which confirms Loeb's results on the specificity of the effect of the ammonia on the positive ion. He found 7.88 for the positive ion where traces of ammonia were present and 9.36 for the negative ion.

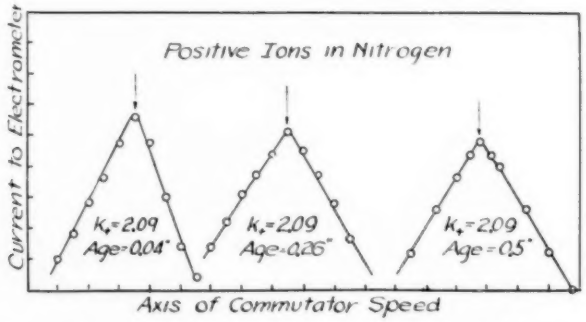

Fig. 3. Aging experiments in nitrogen. No noticeable change in the shape of the curves or a shift of the position of the maximum is present.

It can thus be said from these experiments that the mobility of the positive ion in pure hydrogen has a value of 8.2; that the addition of traces of ammonia raises this value to 9.4; and that this value is substantially equal to that for the negative ion in the case of impure hydrogen.

Aging Experiments

Aging experiments have previously been reported on air in a metal chamber.[4] In these experiments it was found that with ion ages greater than a tenth of a second the average mobility appeared to decrease and become spread out over a wide range as if the ions had attached a wide variety of impurities or reaction products of the x-rays. The existence of the glass chamber used in the above measurements made it possible to test these effects under conditions of greater gas purity. Two series of runs were carried out—one on positive ions in pure nitrogen and the other on positive and negative ions in air. The results in the case of nitrogen are shown in Fig. 3. In this case, with a gas

[2] H. A. Erikson, Phys. Rev. **30,** 339 (1927).
[3] J. J. Mahoney, Phys. Rev. **33,** 317 (1929).
[4] N. E. Bradbury, Phys. Rev. **37,** 1311 (1931).

of high purity, and no chance of reaction products such as nitric oxides, ozone, and the like formed by the x-rays, we obtain *no decrease in mobility*, and *no noticeable broadening* of the maximum of the peak. But one class of ion is formed and remains so throughout the aging time up to 0.5″. The measurements were not carried beyond this as the air experiments had shown very apparent aging effects at these times.

The results for the positive ion in air are shown in Fig. 4. The results are much the same in magnitude and appearance as those previously reported. The broadening and shift of the maximum of the peak in the case of the positive ions shown is very noticeable. The breadth of the spectrum is not quite

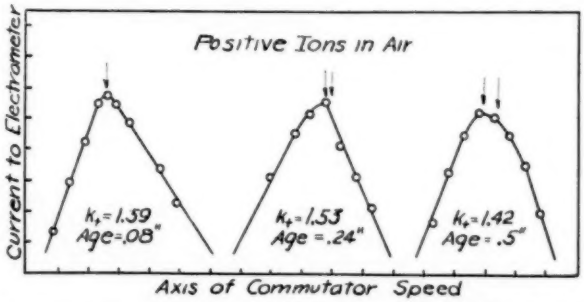

Fig. 4. Aging experiments on positive ions in air. The right hand arrow indicates the position of the peak for *new* ions. The shift and flattening of the curves is evident.

as great as in the earlier experiments, owing, doubtless, to the increased purity of the gas. The aging of the negative ions was not quite as great as that for the positive which is to be expected in view of the greater electrochemical affinity of the positive ion for the type of impurity liable to be present.

The comparison of the two results, for air and nitrogen, rather definitely confirms the scheme of ionic behavior under such circumstances which has been advanced by Loeb and the author.[5] The results in air are in agreement with those of Zeleny[6] who, however, was forced to work under conditions permitting no great control of gas purity.

Conclusion

The results in the mixture experiments may be summarized in Table I.

Table I. *Summary of results.*

Gas	Purity	k	k
Nitrogen + NH_3 (trace)	p	1.83 2.09	e
Hydrogen + NH_3 (trace)	p	9.4	e
Hydrogen + NH_3 (trace)	i	9.4	9.6

The chemically stable NH_4^+ ion in many compounds presents, perhaps, an explanation of the specific effect of NH_3 on the positive ion alone. The re-

[5] Loeb and Bradbury, Phys. Rev. **38**, 1716 (1931).
[6] J. Zeleny, Phys. Rev. **38**, 969 (1931).

sultant effect is evidently the protection of the positive ion from attachment by some bulkier molecule with a consequent increase in the observed mobility of the final ion. The extent of this protective effect has been discussed by Loeb.

In conclusion, it is desired to thank Mr. Daniel Posin, who assisted in taking some of the measurements, and Professor L. B. Loeb for his suggestions and assistance in the interpretation of the experimental data.

Predissociation in the Spectrum of Iodine Chloride

By WELDON G. BROWN* AND G. E. GIBSON**

Ryerson Physical Laboratory, University of Chicago, and Chemical Laboratory, University of California

(Received April 2, 1932)

A study of an unusual group of bands lying just beyond the convergence of the ordinary visible absorption bands of iodine chloride has revealed an interesting case of predissociation, and has made possible a new interpretation of the electronic states in accordance with Mulliken's theory of the halogens.

Electronic states and dissociation products. Spectroscopic evidence provided by the new band systems, together with thermodynamic data recently obtained by Yost and McMorris, definitely prove that the dissociation products of the ordinary absorption system (system I) are normal atoms. The upper level of this system is now interpreted as a $^3\Pi_1$ state, an interpretation which is supported by the recent analysis of these bands by Curtis. The *3,1*, *2,0*, and *3,0* band of a new system (system II) have been analyzed. These bands show *P* and *R* branches only, and furnish rotational constants for the normal state which are in good agreement with those obtained by Curtis from bands of system I. The upper electronic state lies 3600 cm^{-1} above the $^3\Pi_1$ state, appears to be derived from normal iodine and excited chlorine ($^2P_{1/2}$) atoms, and is classified as the O^+ member of the $^3\Pi$ multiplet. The existence of this state is in satisfactory confirmation of Mulliken's theory of the halogens. The *4,1* and *4,0* bands of system II appear as bands of continuous absorption, except for certain lines, and at this point a new series of closely spaced vibrational levels begins, giving rise to faint and diffuse band heads (system III) which converge to give normal iodine and excited chlorine ($^2P_{1/2}$) atoms as dissociation products. The rotational structure of this system, as observed in absorption, is incomplete, consisting of *P* and *R* branches extending over narrow ranges of *J* values, and all lines are diffuse except the central lines in these short series. The sharp lines in these series can also be interpreted as belonging to system II.

Predissociation. These phenomena can be explained by assuming that the predissociation, which sets in sharply above the $v'=3$ level of System II ($^3\Pi_{0^+}\leftarrow{}^1\Sigma$), is due to interaction with a repulsive O^+ state derived from two normal atoms, and that, at the intersection of the potential energy curves, a new set of levels (system III) originates. In absorption transitions to this new O^+ state result in sharp lines only where the rotational levels coincide, at the same rotational quantum number, with predicted levels of the original $^3\Pi_{0^+}$ state. This is interpreted as due to momentary existence of the molecule in the $^3\Pi_{0^+}$ state as an intermediate step in the absorption process, a step which is followed either by predissociation giving normal atoms, or by a radiationless transition into the new O^+ state, the latter being highly probable only when rotational levels with the same *J* value are coincident or very close.

* National Research Fellow.

** This investigation was begun as a joint research at the University of California in continuation of experiments carried out by the undersigned at Göttingen where the predissociation bands were first photographed. The completion of the rotational analysis and the interpretation of the fine structure of system III are the work of Brown at Chicago to whom the credit for this part of the paper is due. G. E. Gibson.

I. Introduction

THE visible absorption spectrum of ICl is similar in appearance to those of the other halogens in that it consists of a number of series (v' progressions) of band heads extending throughout the red and yellow. The $v''=0$ progression converges in the neighborhood of 5755A and at this point a broad band of continuous absorption, having a maximum at 4700A, sets in and extends into the near ultraviolet. In the region just beyond the convergence a number of faint bands are to be seen, two of which were discovered by Gibson and Ramsperger,[1] and several others by Gibson.[2] The first of these bands, 5730A, is sharp and shows fine structure clearly while the succeeding bands appear diffuse, or at best show only irregular patches of fine structure.

Gibson and Rice[2] noted the fact that the lines in the 5730A band, sharp near the head, become broadened at higher rotational quantum numbers at a point in the spectrum corresponding roughly to the convergence limit of the first system. They found subsequently, however, by microphotometry of this band (hitherto unpublished) that this correspondence is accidental, as the broadening of lines is here due to the gradual separation of two branches which are coincident near the head. Furthermore the analysis shows conclusively that this band has $v''=1$ and so the upper rotational levels lie considerably above the dissociation point. Nevertheless, predissociation-like phenomena make their appearance in the succeeding bands.

The band at 17,577 cm^{-1} is quite remarkable. Under the highest dispersion we have been able to employ (0.8A/mm) it appears only as a narrow unsymmetrical region of continuous absorption, superimposed on which are four distinct series of widely and almost equally spaced lines. These series occur in two pairs, one pair with 5 members each, and one pair with 8 members. In each series the central lines are sharp and in each direction they become rapidly diffuse and fade out. Beyond this band the lines become extremely numerous and very faint. A fairly strong and sharp band head appears at 17,665 cm^{-1} and another at 17,828 cm^{-1}. The latter is obviously the $v''=0$ band corresponding to the 17,446 band and at this point the spectrum begins to repeat itself. Between 17,765 cm^{-1} and 17,828 cm^{-1} a converging series of closely spaced bands can be seen which are obviously not a continuation of the 17,446–17,577 series. These closely spaced bands are extremely faint, so faint that their reality might be doubted were it not for the fact that a similar series can be observed between 17,960 and 18,200 cm^{-1}, which one would expect if the former series was a $v''=1$ progression. No structure was found beyond 18,180 cm^{-1}.

II. Experimental

Relative to the ordinary visible bands of iodine chloride the bands of the predissociation group are faint and require considerably more absorbing vapor. However, they lie in the region of continuous absorption from the ordinary system and at high pressures are completely obscured by this continuous

[1] G. E. Gibson and H. C. Ramsperger, Phys. Rev. **30**, 598 (1927).
[2] G. E. Gibson and O. K. Rice, Nature **123**, 347 (1929).

absorption. We have obtained them using a 50 cm absorption tube containing excess liquid iodine chloride heated to temperatures up to 100° C, also with a 150 cm tube at room temperature. The latter was used in obtaining the high dispersion photographs from which the fine structure analysis has been made. Iodine chloride was prepared by passing chlorine gas over pure iodine until after conversion to the monochloride was complete so that the material contained, in addition, some iodine trichloride. The presence of the latter appeared to be necessary to suppress completely all traces of free iodine. This material was placed in the absorption tube and frozen with liquid air while the tube was evacuated and sealed.

Preliminary experiments to determine the optimum conditions for observing these bands were carried out with a Steinheil prism spectrograph and a 10′ concave grating at the University of California. The high dispersion photographs were obtained by one of us in the second and third orders of a 21′ grating at the University of Chicago. The exposures were from 30 to 48 hours, roughly eight times that which would have been necessary had there been no continuous absorption in this region.

III. Analysis of the 17,446, 17,664, and 17,828 cm^{-1} Bands

The three bands, 17,446, 17,664, and 17,828 cm^{-1}, show no anomalies in their fine structure. In appearance they are like the well-known bands of chlorine or bromine in that they consist of two branches (coincident near the heads) which can be described at once as P and R branches. The combination differences which can be obtained in each band are

$$\Delta_2F''(J) = R(J-1) - P(J+1), \text{ and } \Delta_2F'(J) = R(J) - P(J).$$

From the relative positions one predicts beforehand that 17,446 and 17,828 have the same upper vibrational state, and that 17,665 and 17,828 have the same lower vibrational state. The analysis then becomes merely a matter of obtaining combination differences which agree for the proper vibrational level. The frequencies, in cm^{-1}, of lines in these bands and the combination differences are given in Tables I, II, and III. If any further proof for the correctness of the analysis of these bands were needed it lies in the agreement of the B'' values so obtained with those obtained by Curtis and Patkowski[3] in their analysis of the ordinary absorption bands.

The measurements of the 17,664 band are less accurate than those of 17,446 and 17,828, because the lines in this band are extremely faint and because of overlapping lines from other bands. Only one second-order plate shows these lines strong enough for measurement, and then only with difficulty. The question as to how high the upper rotational levels extend is of importance but is not easily answered. In the 17,446 band the lines can be observed up to $J' = 52$ in each of the P and R branches, and in the neighborhood of this point diffuseness gradually sets in. However, there is overlapping here from the converging bands of the main system and it is not possible to state definitely whether any undue influence is operating to make higher

[3] W. E. Curtis and J. Patkowski, Nature **127**, 707 (1931).

TABLE I. *3, 1 band,* $\nu^0 = 17{,}446.26\ cm^{-1}$.

J	P	R	Δ_2F''	Δ_2F'	J	P	R	Δ_2F''	Δ_2F'
1	17,445.95*				24	422.52	430.35	11.08	7.83
2	445.63*				25	420.69	428.87	11.52	8.18
3	445.30*				26	418.83	427.30	12.00	8.47
4	444.87*				27	416.87	425.67	12.43	8.80
5	444.37*				28	414.87	423.96	12.89	9.09
6	443.83*	17,445.95*		2.12	29	412.78	422.23	13.30	9.45
7	443.17*	445.63*	3.44	2.41	30	410.66	420.39	13.82	9.73
8	442.46*	445.30*	3.86	2.79	31	408.41	418.50	14.27	10.09
9	441.71*	444.87*	4.36	3.10	32	406.12	416.50	14.73	10.38
10	440.88*	444.37*	4.79	3.43	33	403.77	414.46	15.17	10.69
11	440.01*	443.83*	5.23	3.75	34	401.33	412.36	15.59	11.03
12	439.06*	443.17*	5.69	3.98	35	398.87	410.18	16.07	11.31
13	438.06*	442.46*	6.10	4.27	36	396.29	407.93	16.55	11.64
14	436.93*	441.71*	6.51	4.63	37	393.63	405.61	16.98	11.98
15	435.90	440.88*	6.99	4.92	38	390.95	403.23	17.42	12.28
16	434.66	440.01*	7.45	5.28	39	388.19	400.80	17.87	12.61
17	433.37	439.06*	7.92	5.61	40	385.36	398.27	18.35	12.91
18	432.02	438.06*	8.38	5.96	41	382.45	395.69	18.78	13.24
19	430.60	436.93*	8.86	6.24	42	379.49	393.03	19.23	13.54
20	429.12	435.69	9.29	6.57	43	376.46	390.29	19.68	13.83
21	427.56	434.43	9.73	6.87	44	373.35	387.57	20.11	14.22
22	425.96	433.12	10.17	7.16	45	370.18	384.69		14.51
23	424.26	431.77	10.60	7.51					
	$B_1''=0.1132$	$B_3'=0.0800$							

* $P-R$ doubling not resolved.

TABLE IA. *ICl^{37} 3, 1 band,* $\nu^\circ = 17{,}447.09\ cm^{-1}$.

J	P	R	J	P	R
8	17,443.52*		15		442.03*
9	442.80*		16		441.18*
10	442.03*				
11	441.18*		39	391.91	
12			40	389.24	
13		17,443.52*			
14		442.80*	44		391.50
			45		388.73

* $P-R$ doubling not resolved.

TABLE II. *3, 0 band.* $\nu^\circ = 17{,}827.76\ cm^{-1}$.

J	P	R	Δ_2F''	Δ_2F'	J	P	R	Δ_2F''	Δ_2F'
19	17,811.74				33	17,784.44	17,795.20	15.27	10.76
20	810.19				34	781.96	793.02	15.79	11.06
21	808.59				35	779.41	790.77	16.16	11.36
22	806.98				36	776.86	788.50	16.63	11.64
23	805.33				37	774.14	786.10	17.08	11.96
24	803.45	17,811.34		7.89	38	771.42	783.73	17.52	12.31
25	801.63	809.78	11.61	8.15	39	768.58	781.18	17.94	12.60
26	799.73	808.18	12.07	8.45	40	765.79	778.70	18.55	12.91
27	797.71	806.56	12.48	8.85	41	762.63	776.07		13.44
28	795.70	804.86	13.01	9.16	42		773.37		
29	793.55	802.98	13.46	9.43	43		770.57		
30	791.40	801.17	13.87	9.77	44		767.70		
31	789.11	799.23	14.30	10.12	45		764.92		
32	786.87	797.23	14.79	10.36	46		761.82		
	$B_0''=0.1140$	$B_3'=0.0800$							

TABLE III. *2, 0 band.* $\nu^\circ = 17{,}664.04$ *cm*$^{-1}$.

J	P	R	Δ_2F''	Δ_2F'	J	P	R	Δ_2F''	Δ_2F'
16	17,652.86				34	17,621.33*	17,632.87*	15.91	11.54
17	651.73				35	618.93	630.83	16.32	11.90
18	650.31				36	616.71	628.73	16.72	12.18
19	649.00				37	614.11	626.61	17.09	12.50
20	647.58				38	611.64	624.45	17.50	12.81
21	646.19	17,653.31		7.12	39	609.11	622.15*	17.95	13.04
22	644.69	652.15	10.23	7.46	40	606.50	619.77	18.38	13.27
23	643.00	650.83	10.72	7.75	41	603.77	617.38	18.78	13.61
24	641.50	649.52	11.15	8.09	42	600.99	614.94	19.26	13.95
25	639.68	648.16	11.60	8.48	43	598.12	612.44	19.72	14.22
26	637.92	646.69	12.07	8.77	44	595.22	609.84	20.22	14.62
27	636.09	645.27	12.46	9.08	45	592.22	607.19	20.54	14.97
28	634.23	643.54	12.92	9.37	46	589.30	604.49*	21.07	15.19
29	632.25*	641.95	13.39	9.70	47	586.12	601.83		15.66
30	630.21	640.27	13.84	10.06	48		598.94		
31	628.11	638.56	14.36	10.45	49		595.99		
32	625.91	636.74	14.90	10.83	50		593.05		
33	623.66	634.84	15.41	11.18					

$B_0'' = 0.1140$ $B_2' = 0.0829$

* Line not measured; value smoothed in.

members of these branches diffuse. The fact that the sharpness of the P and R branches ends at the same quantum number rather than at the same place in the spectrum may have some significance, particularly since Curtis and Patkowski were able to observe up to $J = 80$ in the main bands. The band at 17,828 is less intense and there is overlapping here also, particularly by the 17,769 band, but the appearance at quantum numbers above 50 is very similar to the 17,446 band.

From these three bands some very necessary information can be derived, particularly with regard to the vibrational numbering, frequency of vibration, and the rate of convergence of the upper electronic state. From the combination differences of the 17,446 band one can estimate the value of the coefficient D in the rotational energy expression, and hence $\omega(D = -4B^3/\omega^2)$. The value of D turns out to be so small that one can only deduce that ω lies between 150 and 200 cm^{-1}. This serves, however, to show that 17,664 and 17,828 are successive members in a v' progression, being separated by 164 cm^{-1}. One can now proceed to utilize the isotope effect to determine the vibrational numbering. Rotational lines of the ICl^{37} band corresponding to the 17,446 band of ICl^{35} are given in Table I. To be sure, the number of lines listed is small, but several others have been observed visually and a faint head 0.8 cm^{-1} on the short wave-length side of 17,446 agrees well with the calculated separation of origins, 0.83 cm^{-1}. The isotope separation for the lower state can be calculated by means of the well known formulae, and we find for $v'' = 1$, $\delta G'' = -12.19$ cm^{-1}. Hence, $\delta G' = -12.19 + 0.83 = -11.36$ cm^{-1}. This is to be equated as follows

$$\delta G' = \omega_e(\rho - 1)(v + \tfrac{1}{2})$$

where $(\rho - 1)$ is known accurately, and ω_e is something slightly less than 163 cm^{-1}. Only the value $v' = 3$ comes into consideration, and on substituting

in the above expression we find $\omega_e = 152$ cm^{-1}. A second approximation gives $\omega_e = 151$ cm^{-1}. The numbering of bands, therefore, is as follows: 17,466 (*3, 1*); 17,665 (*2, 0*); 17,828 (*3, 0*).

We now have two values of ω, namely: $\omega_{2.5} = 164$, and $\omega_3 = 151$. These give an approximate value of $\omega_e x_e = 13$ cm^{-1} indicating not only that the series is converging with great rapidity but also that the 17,577 band is the next member of the $v'' = 1$ series.

IV. Diffuse Bands

As seen under low or moderate dispersion the band heads of the predissociation group are shown in Table IV in order of decreasing wave-length:

Table IV.

cm^{-1}	Estimated intensity	Remarks	cm^{-1}	Estimated intensity	Remarks
17,446.5	10	Sharp. (*3, 1*)	17,769*	2	Sharp
447.3	2	ICl^{37} (*3, 1*)	790	1	Sharp
474	1	Probably (*1, 0*)	807	0	Doubtful
577	8	Diffuse	820.6	2	Sharp ICl^{37} (*3, 0*)
665	5	Fairly sharp	828.0	5	Sharp, (*3, 0*)
696	2	Diffuse	885	0	Doubtful
722	2	Diffuse	952	3	Diffuse
743	2	Diffuse	981	1	Diffuse

* This band coincides with a strong I_2 band, but it remains when every other trace of I_2 bands has been eliminated.

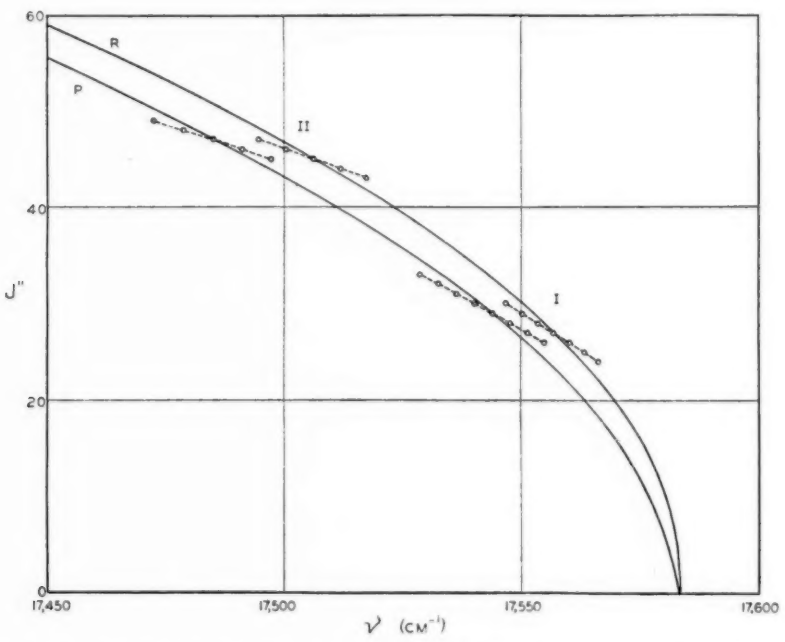

Fig. 1. Showing the relation between the observed lines of series I and II to the predicted structure (solid lines) of the *4,1* band of system II.

Under high dispersion the diffuse bands become less conspicuous while the fine structure in the region 17,446–17,828 cm^{-1} appears in irregular groups of sharp and diffuse lines. Between 17,446 and 17,577 cm^{-1} there are the four especially prominent series of lines (series I and II of Table V), mentioned

TABLE V. *Incomplete branches of system III bands.*

J	P	R	Δ_2F''	Δ_2F'	B'
		Series I, $\nu^\circ = 17{,}600.8$ cm^{-1}			
24		17,566.23*uu*			
25		563.40*uu*	11.33		
26	17,554.90*uu*	560.12*u*	12.00	5.22	0.0491
27	551.40*uu*	556.87*s*	12.39	5.47	0.0497
28	547.73	553.58	12.91	5.85	0.0512
29	543.96*s*	550.25*u*	13.41	6.29	0.0532
30	540.17	546.80	13.87	6.63	0.0543
31	536.38*u*		14.25		
32	532.55*uu*				
33	528.65				
		Series II, $\nu^\circ = 17{,}632.6$ cm^{-1}			
43		517.30*uu*			
44		511.86*u*	20.14		
45	497.16*uu*	506.15*s*	20.69	8.99	0.0494
46	491.17*u*	500.39*u*	21.06	9.22	0.0495
47	485.09*s*	494.73*uu*	21.48	9.64	0.0507
48	478.91*u*				
		Series III, $\nu^\circ = 17{,}696.8$			
27	640.27*				
28	636.09*	640.85		4.76	0.0417
29	631.93	636.74*	13.37	4.81	0.0407
30	627.48	632.53	13.83	5.05	0.0413
31	622.91	628.11*	14.35	5.20	0.0412
32	618.18	623.66*	14.68	5.48	0.0421
33	613.43	618.93*	15.32	5.50	0.0411
34	608.34	614.11*	15.64	5.77	0.0417
35	603.29	609.11*		5.82	0.0409

* Line overlaps line of *2, 0* band.

Series IV, not identified

17,584.14*uu*, 17,577.35*u*, 17,570.60*u*, 17,563.40*uu*.

s = sharp, *u* = broad, *uu* = very broad.

in the introduction. Overlapping the *2, 0* band, the head of which is at 17,665 cm^{-1}, is another pair of series (series III), so obscured by the *2, 0* lines that it is impossible to determine its full extent or the character of the lines. Another widely spaced series (series IV), consisting of four strong diffuse lines, is to be observed in the neighborhood of 17,577 cm^{-1}. Between 17,665 and 17,769 cm^{-1} there are numerous diffuse lines with no obvious regularities.

The occurrence of these series in pairs suggests that each pair consists of a P and an R branch, and since the phenomenon causing diffuseness must be one affecting the upper level one is led to assume that each branch extends over the same range of upper rotational quantum numbers. However it is difficult to determine the extent of each series, and, following the same argument, we assume that the sharpest lines in each pair correspond to the same J'. That this analysis of series I and II yields correct values of the combination differences for the lower vibrational state is shown in the table. These

differences also establish the rotational numbering. On plotting these lines on the usual type of Fortrat diagram (Fig. 1) it appears that series I and II are segments of two successive bands, the upper level of which is characterized by a very large moment of inertia (small B value) and a small frequency of vibration. The ν^0 values calculated in the usual way are 17,601 and 17,633 cm^{-1} for series I and II respectively. On the other hand the sharpest lines of series I and II correspond very well with the structure one would expect for the *4, 1* (shown by the solid lines in Fig. 1). This interpretation yields $B_4' = 0.073$ $\nu^0(4, 1) = 17{,}583$ cm^{-1}, and implies perturbations of the diffuse lines of a nature which can be inferred from Fig. 1, i.e., positive at one end of a series changing to negative at the other, and amounting to as much as 6 cm^{-1}. It is to be noted that this is much greater than the width of a diffuse line so that the diffuseness cannot be the result of crossing of the *4, 1* branches by branches of some other band.

Series III consists of at least 15 members, each a narrow doublet. Of these 8 have been measured and are given in Table V together with an assignment of rotational quantum numbers which leads to correct $\Delta_2 F''$ values. The corresponding B' value is somewhat lower than for series I and II, and the ν^0 value is 17,697 cm^{-1}.

One would expect that, like series I, II, and III, series IV should be double. If the observed lines are R lines, the corresponding P lines should be present at longer wave-lengths, or vice versa. Another possibility is that the P and R branches are coincident giving a single series of lines. We are inclined toward the belief that these lines are R lines, and the corresponding P lines are present but lost in the complicated group of *2, 0* and series III lines. If this is the case the ν^0 value is somewhat greater than 17,697, the B' value somewhat smaller than that for series III, that is, series IV bears the same relation to series III that series II does to series I.

These ν^0 values fit remarkably well into the series of closely spaced band heads observed under low dispersion, and one can arrange both in a vibrational analysis, assuming for the present that they constitute an independent band system (system III). (Table VI.) Unfortunately, it has not been possi-

TABLE VI. *Vibrational analysis, system III.*

v' \ v''	0	1
0	17,981 (*h*)	17,601 (ν^0)
1	obs.	17,633 (ν^0)
2	obs.	17,665 (*h*)
3	obs.	17,697 (ν^0)
4	obs.	17,722 (*h*)
5	obs.	17,743 (*h*)
6	obs.	17,769 (*h*)
7		17,790 (*h*)
8		17,807 (*h*)

ble to observe the isotope shifts, either of the rotational lines, or of the band heads. As a result the v' numbering of system III is arbitrary.

V. Dissociation Limits

There has been a good deal of discussion as to whether the convergence of system I correspond to dissociation into two normal atoms, or into normal iodine and an excited chlorine atom in the $^2P_{\frac{1}{2}}$ state. The experimental thermodynamic data, upon which Gibson and Ramsperger based their conclusion that the latter is the case, are open to some criticism, and on the photochemical side the evidence is somewhat conflicting. (The statement by Mulliken[4] to the effect that the experimental evidence favors excited chlorine as a dissociation product is obviously the opposite of what the author intended.) Recently, Yost and McMorris[5] have obtained accurate thermodynamic data for the reaction, $\frac{1}{2}I_2(g)+\frac{1}{2}Cl_2(g)=ICl(g)$, that are in beautiful agreement with the results calculated from band spectrum data on the assumption that the convergence at 5755A corresponds to dissociation into two normal atoms.

The actual point of convergence of the bands of system I is known to a high degree of accuracy. As Darbyshire[6] has recently shown, the earlier extrapolations by Gibson and Ramsperger, 17,410 cm^{-1} (convergence of the $v''=0$ progression), and of Wilson, 17,430 cm^{-1}, are probably too high. From their data he obtains 17,340 cm^{-1}. From new measurements which we have made we obtained a slightly higher value 17,365 cm^{-1}, or 2.143 volts.

From the data for the $v'=2$ and $v'=3$ levels of system II we can perform a linear extrapolation and so obtain a rough value for the dissociation limit. The result is 18,270 cm^{-1}. Similarly an extrapolation can be made from the known levels of system III. The extrapolation here is much shorter and gives $18,250\pm 20$ cm^{-1}. If the dissociation products of system I were normal iodine and excited chlorine the next lowest limit would be two excited atoms, or $17,365+7600=24,965$ cm^{-1}. On the other hand if normal atoms are the products of system I, the limit for dissociation into normal iodine and excited chlorine would lie at $17,365+880=18,245$ cm^{-1}; which is in excellent agreement with the above extrapolations.

VI. Character of the Electronic States

As mentioned above, there is no longer any reason for believing that the ICl bands (system I) are analogous to the bands of the homonuclear halogens. The upper levels of the visible Cl_2, Br_2, and I_2 bands, according to Mulliken's[4,7] interpretation, are $^3\Pi_{O^+}$ levels, with coupling either Hund's case *c* or something intermediate between case *a* and case *c*, and derived from one normal and one excited atom. Transitions from the normal state to such a state result in bands having *P* and *R* branches only, in agreement with the observed structure. In the case of ICl Curtis has shown that *P*, *Q*, and *R* branches are present. The recent work of Schlapp[8] on intersystem intensities

[4] R. S. Mulliken, Phys. Rev. **36,** 1413 (1931).

[5] D. M. Yost and J. McMorris, J. Am. Chem. Soc., forthcoming paper. We are indebted to these authors for communicating their results to us in advance of publication.

[6] O. Darbyshire, Phys. Rev. **39,** 162 (1932).

[7] R. S. Mulliken, Phys. Rev. **36,** 669, 1440 (1930). Also Rev. Modern Phys. **4,** 17, 70 (1932).

[8] R. Schlapp, Phys. Rev. **39,** 806 (1932).

shows that such structure can arise from a $^3\Pi_1 \leftarrow {}^1\Sigma$ transition, but not from a $^3\Pi_0 \leftarrow {}^1\Sigma$ transition. This, together with the existence of additional states predicted by the theory, establishes the upper state of the visible ICl bands (system I) as a $^3\Pi_1$ state. These bands are thus analogous in every respect save intensity with the infrared, rather than the visible, bands of Br_2 and I_2.

The upper level of the bands of system II must be a O^+ level since only P and R branches appear. These bands are apparently analogous to the Cl_2, Br_2, and I_2 bands. The fact that the r_e and ω_e values are of the same order of magnitude as for the $^3\Pi_1$ level is strongly suggestive of a multiplet relation between them, or in other words this O^+ level is a component of the $^3\Pi$ multi-

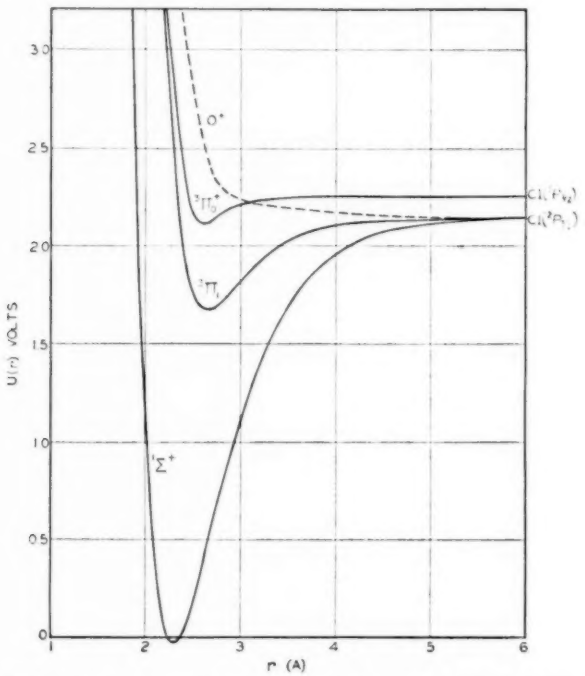

Fig. 2. Potential energy curves for the $^1\Sigma$ (normal) and $^3\Pi$ states of ICl. The $^3\Pi_{0+}$ state is shown here as derived from normal iodine and excited chlorine atoms, and crossed by a repulsive state derived from two normal atoms. See Fig. 4.

plet. Also, the upper level of system III has the character of a O^+ state if our analysis of the sporadic fine structure is correct.

The relative positions of these states, omitting for the time being the upper level of system III, is shown by means of the approximate potential energy of Fig. 2. These curves have been sketched by means of the Morse formula, using the data of Curtis and Patkowski[3] and Darbyshire[6] for the $^3\Pi_1$ level.

Mulliken[4] assumed that the total width of the ICl $^3\Pi$ multiplet would be roughly the same as for Br_2, which he estimated at 2400 cm^{-1}, or a half width ($^3\Pi_0 - {}^3\Pi_1$) of about 1200 cm^{-1}. Actually it seems to be more closely related to that of iodine. If, as seems likely, the upper level of the infrared iodine

absorption bands is the $^3\Pi_1$ level, then the splitting of the 0^+ and 1 components is 3800 cm^{-1} or greater. Our data indicate that the splitting of the two levels for ICl is about 3600 cm^{-1}, while the data for Br_2 indicate a splitting somewhat greater than 1100 cm^{-1}. The separation of the $^3\Pi_{0+}$ and the $^3\Pi_1$ is probably somewhat greater than the half width of the $^3\Pi$ multiplet, however, because of the splitting of the $^3\Pi_{0+}$ and $^3\Pi_{0-}$ states.

In general, these developments in connection with ICl provide good experimental confirmation of the theory of the electronic states of the halogens outlined by Mulliken.

Before proceeding to a discussion of the predissociation phenomena it is of interest to consider the question of relative intensities. The spectrum of ICl exhibits, in addition to a strong band system (I) and a weaker one (II), a very strong continuum with a maximum at about 4700A. On application of the Franck-Condon principle to the potential energy curves of Fig. 2, it is to be observed that the transition $^3\Pi_{0+}\leftarrow{}^1\Sigma$ provides a more satisfactory explanation of the observed continuum at 4700A than does the transition $^3\Pi_1\leftarrow{}^1\Sigma$. The maximum for the latter should occur in the neighborhood of the convergence, resulting in an intensity distribution like that of the visible iodine bands. An additional region of continuous absorption,[9] having a maximum at 2400A, is perhaps due to transitions to the repulsive O^+ state shown in Fig. 2. Thus it appears that the transition $^3\Pi_{0+}\leftarrow{}^1\Sigma$ is really stronger than the transition $^3\Pi_1\leftarrow{}^1\Sigma$, just as in Br_2 and I_2, although the difference is not as marked as in the latter cases. Van Vleck,[10] extending Schlapp's discussion of $^3\Pi\leftarrow{}^1\Sigma$ intensities, has given an explanation for the difference in intensities of these two transitions, and has shown that the relative intensity may differ widely for different molecules.

VII. Predissociation

The experimental facts relating to predissociation are summarized as follows:

(1) The bands of system II ($^3\Pi_0\leftarrow{}^1\Sigma$) apparently end abruptly at $v'=4$, transitions to $v'=4$ being diffuse. The level $v'=4$ lies 600 cm^{-1} above the point of dissociation of the $^3\Pi_1$ state (normal atoms).

(2) The rotational levels of the vibrational state $v'=3$ are well defined to at least $J'=52$. Lines due to transitions to levels above $J'=52$ appear to be broadened but this has not been definitely established. The level $J'=52$ ($v'=3$) lies 680 cm^{-1} above the point of dissociation into two normal atoms.

(3) Beginning very slightly above the $v'=4$ level of system II a new series of closely spaced levels begins. The first six of these give rise to diffuse band heads. Three following band heads (higher levels) appear much sharper. The bands of this group are referred to as system III and converge to give normal iodine and excited chlorine on dissociation.

(4) All rotational structure of system III appears diffuse under high

[9] Cordes and Sponer, Zeits. f. Physik **63,** 338 (1930).

[10] J. H. Van Vleck, Phys. Rev. **40,** 544 (1932). We are indebted to Professor Van Vleck for the privilege of reading his paper in manuscript.

dispersion except characteristic groups belonging, apparently, to three different v' levels. Each group consists of two incomplete branches in which only the central lines are sharp. Analyzing these as P and R branches gives combination differences for the lower level which agree satisfactorily with those obtained from other band systems. Approximate B' and ν' values are thus obtained.

(5) The value of $(r'-r'')$ for system III bands is so large that such transitions, according to the Franck-Condon principle, should be extremely weak. While the band heads referred to in (3) above are actually very faint, the fine structure groups mentioned in the preceeding paragraph are quite strong, nearly as strong as individual lines in the (*3, 1*) band of system II.

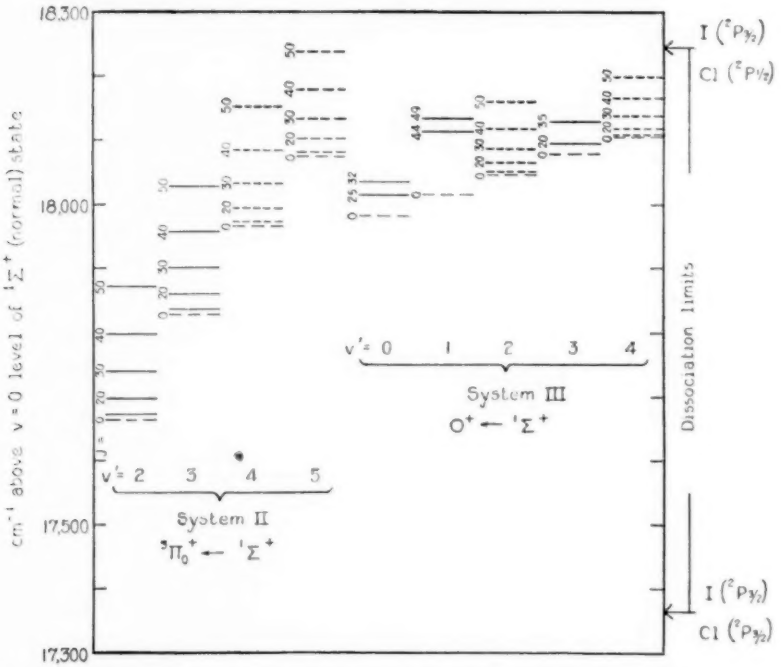

Fig. 3. Energy level diagram for the upper states of systems II and III. Note the correspondence of the observed system III levels (shown by solid lines) with hypothetical levels of the $^3\Pi_{0^+}$ state (dotted lines) with the same J values.

(6) The rotational levels of system III which give rise to sharp spectral lines appear to be closely related to the rotational levels of $v'=4$, and $v'=5$ of the $^3\Pi_0$ state, even though the $v'=4$ band of system II (except for the sharpest of these lines) appears only as a narrow region of continuous absorption, and $v'=5$ bands are not otherwise observed. That is, rotational levels which can be construed as common to the upper states of system II and III are sharp, and no other lines of system III are sharp. This can be shown best by means of an energy level diagram (Fig. 3). Here the predicted levels of $v'=4$ and $v'=5$ (calculated from the data for the $v'=2$ and $v'=3$ levels) are shown as dotted lines together with the observed energy levels.

(7) The ν^0 values calculated from the lines in these groups of fine structure with the B' values obtained from the combination differences agree well with observed band heads of system III. Such agreement would be fortuitous if the upper rotational levels here were merely perturbed $v'=4$ and $v'=5$ rotational levels, for in this case B' values obtained from the combination differences would be without significance.

To account for these phenomena we suppose the following state of affairs. A repulsive O^+ state, derived from normal atoms, crosses the $^3\Pi_{0^+}$

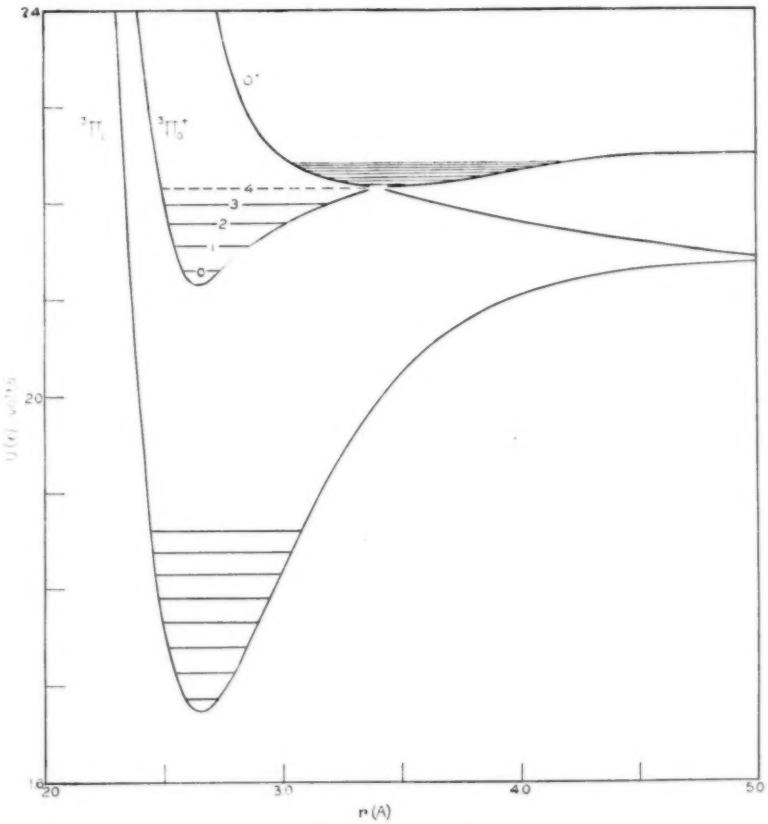

Fig. 4. Potential energy curves for the $^3\Pi$ states ($U(r)$ scale greatly increased over Fig. 2) showing how the $^3\Pi_{0^+}$ state may predissociate above the level $v=3$. The upper levels of system III are shown as a series of closely spaced levels above the point of predissociation.

state at an energy corresponding to the $v'=4$ level of system II, i.e., 17,960 cm^{-1} above the $v''=0$ level, or about 600 cm^{-1} above the energy of two normal atoms. The interaction between the two O^+ states is such as to produce, in effect, two new but not independent states (Fig. 4). The $^3\Pi_{0^+}$ state, formerly leading to dissociation into normal iodine and excited chlorine atoms, now may pass over a potential energy hump and so predissociate into two normal atoms. In the minimum formed by the intersection of the original pair of O^+ curves a new set of quantized levels, rotational and vibrational, is formed. We

note, from the potential energy curves, that this accounts fairly well for the large r_e and small ω_e values of the upper level of system III.

Herzberg[11] was the first to point out that the predissociation in this spectrum is probably a result of interaction with a repulsive state.

It is more difficult to explain the peculiar fine structure, but the conclusion that the observed lines of system III are in some way related to the $^3\Pi_{0^+}$ state is difficult to escape. The rule enunciated in paragraph (6) above not only accounts for the existence of series I–IV, but also for the fact that no lines of the *2,1* band of system III are observed since (see Fig. 3) no levels with the same J coincide. Qualitatively, it explains the number of lines in each of these series, and the greater sharpness of the system III band heads near their convergence.

On the other hand it is difficult to see how discrete levels of $^3\Pi_{0^+}$ can exist above the point of predissociation when the interaction with the repulsive O^+ state is so great that a new set of levels is formed. As a matter of fact, no levels which can be unambiguously identified as $^3\Pi_{0^+}$ have been observed above this point, but one is lead to postulate that the quantization of this

Fig. 5.

state above the point of predissociation is not entirely destroyed, or at least not for certain quantum numbers. This is represented schematically by Fig. 5 which illustrates the proposed type of interaction at the point of intersection of the two O^+ curves. Thus while the $^3\Pi_{0+}$ levels are unstable and not sharply defined above this point we suppose that the rotational quantization still exists to some degree, and that where these levels coincide with levels of the new O^+ state with the same rotational quantum number a "transition" to the latter is possible, resulting in greatly increased life and, in absorption, an observable spectrum line. The absorption process is then not a simple one and it is now less strange that the lines of series I–IV appear with about the same intensity as the lines of the *3,1* band of system II, while the band heads of system III, in accordance with the Franck-Condon principle, are very weak.

No rigid theoretical justification of these assumptions is attempted, nor do we insist on too great an emphasis being placed on our interpretation. Van Vleck (private communication) prefers to regard the observed levels of system III as vestigial remains of the original $^3\Pi_{0^+}$ state. This designation is apt, and perhaps no closer inquiry as to the nature and origin of these levels is warranted by the limited amount of experimental data.

[11] G. Herzberg, Ergebnisse der Exakten Naturwissenschaften **10,** 272 (1931).

One further point is worthy of comment. In section IV it was remarked that the maximum at 4700A in the continuous absorption of iodine chloride is probably due to the transition $^3\Pi_{0^+} \leftarrow {}^1\Sigma$. It is now clear that the dissociation products corresponding to this absorption are normal iodine and both normal and excited chlorine atoms, since the $^3\Pi_{0^+}$ state can yield normal chlorine atoms by predissociation. The relative amounts of normal and excited chlorine atoms probably depend to some extent on experimental conditions (pressure, and wave-length of incident radiation) and an escape from the conflicting photochemical experiments is thus provided by this interpretation of the spectrum. The experiments performed at low pressures[12] tend to show, however, that mainly normal chlorine atoms are produced.

ACKNOWLEDGMENT

One of us (W.G.B.) has had the opportunity of discussing these results with Professors R. S. Mulliken and J. H. Van Vleck. For their valuable comments we are deeply grateful.

[12] G. K. Rollefson and F. F. Lindquist, J. Am. Chem. Soc. **52**, 2793 (1930); **53**, 1184 (1931).

The Theory of the Magnetic Quenching of Iodine Fluorescence and of Λ-Doubling in $^3\Pi_0$ States

By J. H. VAN VLECK
University of Wisconsin

(Received April 4, 1932)

A theoretical basis is given for Turner's proposal that the magnetic quenching of iodine fluorescence is a predissociation phenomenon. To this end it is shown that a magnetic field introduces matrix elements in the Hamiltonian function between the $^3\Pi_{0^+}$ and $^3\Pi_{0^-}$ (or possibly the $^3\Pi_{0^+}$ and $^3\Sigma_{0^+}$) states, respectively stable and unstable in I_2. This confirms Mulliken's assignment of $^3\Pi_{0^+}$ to the upper state of the halogen visible bands. The magnetic field has a unique role for so-called 0^+, 0^- levels because perturbations between these particular states cannot arise from rotational distortion, the cause of the usual Kronig predissociation, or from electric fields unless they are very large or else markedly inhomogeneous. The magnetic quenching should be independent of the rotational quantum number (section 5) and should depend on field strength in the form $b\mathfrak{H}^2/(a+b\mathfrak{H}^2)$. The observed mode of frequency dependence demands that in I_2 the potential curves of $^3\Pi_{0^+}$, $^3\Pi_{0^-}$ states, which are the two components of a Λ-doublet, be extremely close for certain values of r or else actually cross each other. This crossing is shown to be theoretically possible under certain conditions. The possibility of magnetic predissociation in other molecules is also discussed. The predissociation due to collision observed by Turner, Kaplan, and others probably arises because electric fields can blend u and g states, and also 0^+ and 0^- states if inhomogeneous.

Incidental points in halogen band spectra are discussed. Schlapp's intensity theory confirms Brown's assignment of $^3\Pi_1$ to his new level in I_2, Br_2. A calculation is given showing why the $^3\Pi_{0^+}$ level in ICl appears derived from $^2P_{3/2}(I)+{}^2P_{1/2}(Cl)$ when configuration theory (the non-crossing rule) suggests $^2P_{3/2}+{}^2P_{3/2}$. An explicit mechanism is thus furnished for Brown and Gibson's interpretation of the predissociation of ICl published elsewhere in this issue.

The writer's previous formulas for the width of Λ-doublets in $^3\Pi_0$ states are extended to include investigation of the sign of the doublet and the perturbations from $^1\Sigma$, $^5\Sigma$ states previously omitted although coordinate in importance with those from $^3\Sigma$. The need of considering these inter-system interactions is caused by the fact that the doubling is a second rather than first order spin-orbit effect. The structural form of the secular determinants inclusive of spin-orbit terms is exhibited for molecules arising from $^2P+{}^2P$, $^2P+{}^2P'$, and $^2P+{}^2S$.

1. INTRODUCTION

THE fluorescence of iodine vapor is considerably quenched by application of a magnetic field. This effect was first discovered by Steubing, and has been the subject of considerable subsequent experimentation.[1] The most recent experimental work is that of Turner.[2] He finds that the magnetic quenching is quite sensitive to the frequency of the exciting light. When the latter is

[1] W. Steubing, Verh. d. D. Phys. Ges. **15,** 1181 (1913); Ann. der Physik **58,** 55 (1919); **64,** 673 (1921); R. W. Wood and G. Ribaud, Phil. Mag. **27,** 1009 (1914); O. Oldenberg, Zeits. f. Physik **57,** 186 (1929).

[2] L. A. Turner, Zeits. f. Physik **65,** 464 (1930).

below 17,300 cm^{-1}, the field is without effect, while the quenching is greatest (almost 50 percent at 12,500 gauss) in the neighborhood of 18,500 cm^{-1}, gradually diminishing at still greater exciting frequencies.

The theory of the effect has been suggested in bold outline by Turner.[2] He interprets the effect as predissociation, i.e. as dynamical interaction between stable and unstable molecular states. Such interaction causes a sort of communism in the properties of the states involved. The originally stable state partakes partially in the instability of the other state, and vice versa, because, of course, the perturbed wave functions are linear combinations of the two

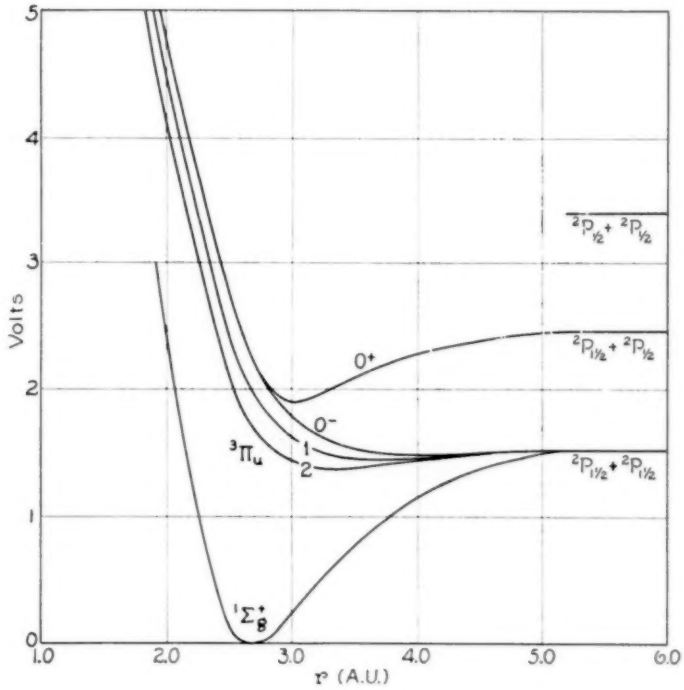

Fig. 1.

The curves marked 0^- and 0^+ in the figure are for the $^3\Pi_{0u}^-$ and $^3\Pi_{0u}^+$ states respectively. These states are often for brevity called the M and N states elsewhere in the article.

The figure shows only a very small portion of all the molecular states derived from $^2P+{}^2P$. We are particularly interested in the states having $\Omega=0$. There are ten states of this category; viz.

$^1\Sigma_g^+$, $^3\Pi_{0g}^+$, $^3\Sigma_g^-$, $^1\Sigma_g^+$ (all type 0_g^+); $^3\Pi_{0g}^-$(type 0_g^-);
$^3\Pi_{0u}^-$, $^3\Sigma_u^+$, $^1\Sigma_u^-$, $^3\Sigma_u^+$ (all type 0_u^-); $^3\Pi_{0u}^+$ (type 0_u^+).

Of these, three are shown in Fig. 1. The derivation of these ten states must be apportioned in accordance with the following scheme:

$^2P_{3/2} + {}^2P_{3/2}$:0_g^+ (twice) 0_u^- (twice). $^2P_{3/2} + {}^2P_{1/2}$:0_g^+, 0_g^-, 0_u^+, 0_u^-. $^2P_{1/2} + {}^2P_{1/2}$:0_g^+, 0_u^-.

That this enumeration and apportionment of possible states is proper can be seen from the Wigner-Witmer correlation rules in the extended form given by Mulliken.[4]

unperturbed ones. There is hence a finite probability that an otherwise stable excited state will dissociate. If this probability is comparable with the proba-

bility of radiation the molecule may dissociate after optical excitation instead of reverting with radiation to the normal state. There will clearly then be a quenching of the fluorescence. For instance in Fig. 1, if the Hamiltonian function contains matrix elements connecting 0^+ and 0^-, a molecule excited to the 0^+ state may dissociate without radiation via the 0^- state instead of returning to the ${}^1\Sigma_g^+$ state.

If, following Turner, the magnetic quenching in iodine thus be ascribed to predissociation, the big theoretical problem is to show that in certain molecular configurations the predissociation is peculiarly important in magnetic fields, i.e., that such fields can introduce previously non-existent matrix components between a stable and unstable state in the Hamiltonian function. This Turner did not do, as his paper did not aim to include the necessary mathematical analysis and so incidentally could not identify correctly the character (i.e., spectroscopic nomenclature) of the unstable level which wrecks the stable one. In the present paper we shall show that the predissociation is due to the interaction between a ${}^3\Pi_{0^+}$ and an unstable ${}^3\Pi_{0^-}$ (or possibly a ${}^3\Sigma_{0^+}$) state, corresponding to the states labelled 0^+, 0^- in Fig. 1, and that a magnetic field does indeed have the effect of creating an interaction between these states. In fact this is the only pair of states available in iodine for which a magnetic field can cause predissociation not otherwise present. All other pairs are either not appreciably intermixed by the magnetic field, or else intermingle and so permit predissociation even in the absence of the field (cf. p. 548). With a 0^+, 0^-, pair we have what may be termed magnetic predissociation, to be contrasted with the usual Kronig[3] predissociation due to rotational distortion, in which the molecular rotation is the agency for creating new matrix elements. The magnetic quenching phenomena thus nicely confirm Mulliken's previous assignment[4] of a ${}^3\Pi_{0^+}$ configuration to the upper state of the visible iodine bands.

Rough Model. If one does not wish to wait for the more exact analysis in later sections, the following very sketchy two dimensional model may be used to illustrate roughly the *modus operandi* of the magnetic field in blending the two components of ${}^3\Pi_0$, which constitute a "Λ-type doublet". Consider two "dumb-bells" or dipoles rotating in the same plane and having a mutual potential energy $f\{\cos(\phi_1-\phi_2)\}$. The wave equation is then of the form $d^2\psi/d\phi_1^2+d^2\psi/d\phi_2^2+a(W-f)\psi=0$. If each dumb-bell has originally one quantum of angular momentum and the combined angular momentum is zero, the "zeroth approximation" wave functions for $|f|\ll W$ are $\psi^+=\cos(\phi_1-\phi_2)$ and $\psi^-=\sin(\phi_1-\phi_2)$, since f will involve no matrix elements at all between states which are respectively even and odd in $\phi_2-\phi_1$. Apply now perpendicular to the plane of rotation a magnetic field sufficiently powerful to

[3] R. de L. Kronig, Zeits. f. Physik **50**, 347 (1928); **62**, 300 (1930).

[4] R. S. Mulliken, Phys. Rev. **36**, 699, 1440 (1930); **37**, 1412 (1931). The subsequent theoretical work of R. Schlapp (ibid. **39**, 806, 1932) has confirmed Mulliken's conjecture that the upper state of the visible halogen bands could not be ${}^3\Sigma_{0,\pm1}^+$ (a conceivable though unlikely alternative to ${}^3\Pi_{0^+}$) without contradicting observed intensities, especially the absence of a Q branch. The intensity relations would be proper, the same as for ${}^3\Pi_{0^+}$, if the upper state were ${}^3\Sigma_{0^-}$, but this configuration is not derivable from unexcited iodine atoms (cf. caption of Fig. 1).

produce Zeeman effects large compared to $W^+ - W^-$, which is of the same order as f. If one of the dumb-bells has an anomaly 2 in magnetic moment, the proper wave functions become $e^{i(\phi_1-\phi_2)}$, $e^{-i(\phi_1-\phi_2)}$, as exponentials rather than trigonometric functions diagonalize the operator $\partial \cdots/\partial\phi_1 + 2\partial \cdots/\partial\phi_2$ though at the expense of diagonalizing f. When the exponentials are utilized all traces of the original even and odd properties are lost, and hence the states are thoroughly intermingled, the desired result. In this model, the two dumb-bells represent symbolically spin and orbit respectively, and $\cos(\phi_1-\phi_2)$, $\sin(\phi_1-\phi_2)$ the ${}^3\Pi_0{}^+$, ${}^3\Pi_0{}^-$ states.

2. Symmetry Considerations

The existence or non-existence of matrix elements between different states involved in perturbations is conditioned largely by the following symmetry types[5] and constants of the motion.

(A) A complete state inclusive of molecular rotation is called + or − by band spectroscopists according as its wave function is even or odd when the coordinates of *all* particles are reflected in the origin.

(B) In molecules of the type X_2 a state is called g or u according as there is evenness or oddness under reflections of the coordinates of all electrons in the origin, without a similar reflection for the nuclear coordinates. The origin must here be taken as the mid-point of the inter-nuclear axis.

(C) For molecules having $\Omega = 0$, there is the further classification 0^+, 0^- (not to be confused with +, − in A) according as the wave function is even or odd as regards reflection of orbital and spin coordinates together in any plane containing the two nuclei. We follow approved[5] spectroscopic nomenclature and so let Λ, Σ, Ω be quantum numbers determining respectively the orbital, spin, and orbital plus spin angular momentum about the figure axis. Molecules having $\Omega = 0$ we shall call 0 states. A 0 state is not necessarily a Σ state. For example, ${}^3\Pi_0$ states are 0 states, as they have $\Lambda^2 = \Sigma^2 = 1$ with $\Lambda + \Sigma = 0$. The ${}^3\Pi_0$, ${}^1\Sigma$, ${}^3\Sigma_0$ states of types 0^+ and 0^- are labelled respectively ${}^3\Pi_0{}^+$, ${}^1\Sigma^+$, ${}^3\Sigma_0{}^-$ and ${}^3\Pi_0{}^-$, ${}^1\Sigma^-$, ${}^3\Sigma_0{}^+$. The paradoxical notation ${}^3\Sigma_0{}^-$ for ${}^3\Sigma$ states of type 0^+ has arisen because the sign behavior is different exclusive and inclusive of spin. (See p. 559. The 0^+, 0^- classification has a meaning only for the component of ${}^3\Sigma$ which has $\Omega = 0$ and which we denote by ${}^3\Sigma_0$ whereas the purely orbital symmetry properties envisaged in the approved notation apply to $|\Omega| = 1$ as well as $\Omega = 0$.)

(D) If the nuclei are regarded as fixed attracting centers the combined orbital plus spin angular momentum about the figure axis is a constant of the motion, *i.e.* Ω is rigorously what Mulliken calls a "good quantum number."

(E) In the absence of external fields the total angular momentum of the molecule is a constant of the motion, *i.e.* J is a good quantum number.

There is no interaction possible between states of different symmetry in (A) or in (B). This is true even in a magnetic field, as such a field does not

[5] For further exposition of molecular symmetry types and the approved spectroscopic notation, which we use, see R. S. Mulliken Phys. Rev. **36,** 611 (1930); Rev. Modern Physics **2,** 60, 506 (1930); **3,** 90 (1931); **4,** 1 (1932).

destroy the invariance of the wave equation under the reflections (A) or (B). An electric field, however, destroys the invariance and may lead to interaction. These statements follow since $\Sigma e_i(x_i\partial/\partial y_i - y_i\partial/\partial x_i)$ is invariant under $x\rightarrow -x$, $y\rightarrow -y$, $z\rightarrow -z$, whereas $\Sigma e_i z_i$ is not. When molecular rotation is admitted, the premise (D) of fixed nuclei is not met, and interaction between states of different Ω (differing by unity in the first approximation) is possible, provided the states have the same J. This is the cause of the usual Kronig[3] rotational predissociation.

Notation. To facilitate printing, we shall henceforth usually refer to the $^3\Pi_0^-$ and $^3\Pi_0^+$ levels as the M and N states respectively instead of using the Greek symbols. (Remember which is which by fact M stands for minus). It is to be further understood that if the molecule is of the symmetrical type X_2, the M and N states here considered are odd with respect to symmetry (B), *i.e.*, are $^3\Pi_{0u}^-$, $^3\Pi_{0u}^+$.

Magnetic Field Applied to Stationary Molecule. The symmetry property (C) is not rigorously maintained under molecular rotation, and so can be used only in describing phenomena in which molecular rotation is not vital. The magnetic quenching in iodine is essentially a phenomenon of this category. The important thing to note is that a magnetic field destroys the property (C) even in a stationary molecule, since $x\partial\cdots/\partial y - y\partial\cdots/\partial x$ is not invariant under $x\rightarrow -x$, $y\rightarrow y$, $z\rightarrow z$. This situation alone is not enough to insure a new interaction due to the magnetic field. For instance, a magnetic field does not blend $^1\Sigma^-$, $^1\Sigma^+$ pairs, as such states have no Zeeman terms. The states $^3\Sigma^-$, $^3\Sigma^+$ have Zeeman terms, but not with inter-connecting elements. On the other hand Zeeman amplitudes really do exist connecting levels of the form $^3\Pi_0^-$, $^3\Pi_0^+$. This will be shown in section 5, and is also fairly obvious from the rough model at the end of section 1.

There is, however, one alternative to the above attribution of the quenching to the pair M, N which cannot be overlooked entirely, although it is somewhat unlikely. This alternative is that the new interaction due to the magnetic field be between N and a $^3\Sigma_0^+$ state[6]. We here use case a notation for the $^3\Sigma$ state (i.e., subscript gives Ω), which is allowable in iodine since the multiplet structure of $^3\Sigma$ levels is of the same order as the Λ-doubling in $^3\Pi_0$ states, and hence large compared to the rotational structure in very heavy atoms. Rotational distortion does not cause interaction between the pair N, $^3\Sigma_0$, but does lead to interaction of N with $^3\Sigma_1$ (more precisely, after the molecular rotation is added, with the component of $^3\Sigma$ which has $|\Omega|=1$ and is + with respect to symmetry A when J is even). Usually the various components of a $^3\Sigma$ level are regarded as constituting virtually a single state, and if this is done, this alternative explanation of the magnetic quenching will not work, for then the predissociation due to rotational distortion via $^3\Sigma_1$ will completely overshadow that due to the magnetic predissociation via $^3\Sigma_0$. Indeed, if we neglect the difference in the shape of the potential curves for $^3\Sigma_1$ and $^3\Sigma_0$, the former predissociation is of the order $q=4B^2J^2/\mathfrak{H}^2\beta^2$ times the latter, where $B=h^2/8\pi^2I$, $\beta=he/4\pi mc$. With the abnormally large moment of inertia in iodine, q is of the order $J^2/100$ in a field of 10,000 gauss, but it is found experimentally[7] that the rotational quantum number J can be over 100 without any sign of impairing the magnetic quenching. It is just possible that in iodine the curves for $^3\Sigma_0$ and $^3\Sigma_1$ are so widely separated that the Franck-Con-

[6] The magnetic field could also cause interaction between M and $^3\Sigma_0^-$, and so cause an otherwise stable $^3\Sigma_0^-$ state to decay, but a state of this character is not found in iodine (see end of note 4).

[7] L. A. Turner, Zeits. f. Physik, **65**, 480 (1930).

don effects (crossing at a suitable r) happen to be unduly preferential to $^3\Sigma_0$ as compared to $^3\Sigma_1$, thus greatly handicapping the rotational predissociation. The whole alternative considered in this paragraph seems particularly unlikely in that the M, N curves are naturally fairly close for a large range of values of r, whereas $^3\Sigma_0^+$, N would be near only accidentally, and then presumably only for a particular value of r. In favor of the alternative, on the other hand, must be balanced the fact that the $^3\Sigma_0^+$ and N levels undoubtedly do cross, whereas we shall see that M and N can be made to cross only with rather artificial hypotheses. The crossing of $^3\Sigma_0^+$ and N is a consequence of the Mulliken-Hund configuration theory, which indicates that $^3\Sigma_0^+$ is higher than N at small r, but lower at $r=\infty$ as it is derived from $^2P_{3/2}+{}^2P_{3/2}$ on account of being the second lowest 0_u^- level. It appears impossible at present to determine the value of r at which this crossing takes place; if it is greater than about 5 A.U. it is clearly too large to cause appreciable predissociation (cf. Fig. 1).

It is to be noticed that in any case the magnetic quenching must be attributed to interaction between a pair of states of the form 0^-, 0^+. In quintet spectra, for instance, $^5\Delta_0^+$, $^5\Delta_0^-$ would be a possible pair. Whether in the particular case of iodine the members of the pair are both $^3\Pi_0$ or one each $^3\Sigma_0$, $^3\Pi_0$ is in a certain sense a rather meaningless question, for in molecules as heavy as iodine, Λ ceases to be a good quantum number, and there is no sharp dividing line between the $^3\Pi_0$ and $^3\Sigma_0$ states.

Magnetic Field applied to Rotating Molecule. With molecular rotation, symmetry (C) is lost, and the behavior is as shown in Fig. 2, since 0^+ states are

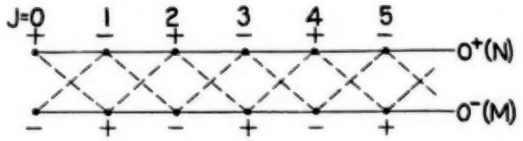

Fig. 2.

$+$ or $-$ as regards symmetry (A) according as J is even or odd, while the reverse is true of 0^-. The matrix elements proportional to the magnetic field $\mathfrak{H}$ in the Hamiltonian function are exclusively of the form $\Delta J=\pm 1$ since $\Delta J=0$ disappears on account of $\Omega'=\Omega''=0$ (cf. also p. 562). These elements are shown by dotted lines in Fig. 2. Hence the field is able to blend the $^3\Pi^+$ and $^3\Pi^-$ (or $^3\Sigma_0^+$) states. On the other hand it is very vital that rotational distortion cannot blend this pair, for the rotational perturbative elements are by (A) and (E) exclusively of the form $+\rightarrow+$ or $-\rightarrow-$, with $\Delta J=0$ and hence cannot appear in Fig. 2. The important thing is thus that the magnetic field breaks down the "J rule" (E), whereas the rotational effects do not.

Absence of Primary Effect in Homogeneous Electric Fields. The unique role of the magnetic field is evidenced not only by this absence of the ordinary Kronig rotational predissociation, but also by the fact that a homogeneous electric field cannot cause the predissociation in question unless exceedingly powerful. This feature seems rather necessary, for otherwise the inevitable stray electric fields might give considerable predissociation even in the absence of the magnetic field. To see that a uniform electric field cannot introduce direct interaction between the $^3\Pi_0$ components, in a homopolar molecule such as I_2, we need only note that such molecules have no permanent electric moment, and so the potential due to an electric field can only introduce matrix

elements connecting two different orbital electronic configurations, whereas the two components of $^3\Pi_0$ belong to the same configuration. Uniform electric fields are likewise ineffective even in heteropolar molecules such as ICl. To prove this, we note that here the permanent electric moment is parallel to the figure axis and so has exclusively elements of the form $\Delta J = \pm 1$; further the potential $\Sigma e_i z_i$ is odd as regards reflection (A) and so there can only be elements connecting states of unlike $+$ $-$ symmetry (A). Thus the matrix elements of the permanent electric moment are represented by the solid rather than dotted lines in Fig. 2 and so do not connect the two doublet components. There can, however, be electric predissociation when we consider the secondary rather than primary effects of the field E, which means the part of the predissociation proportional to E^4 rather than E^2. The reason is that the second approximation in any perturbation calculation introduces as new matrix elements the products of the matrix elements calculated in the unperturbed system. A product such as $a(n_+J; n_-' J \pm 1)b(n_-' J \pm 1; n_+J \pm 1)$, for instance, can then give a predissociating effect, as a, b can be elements connecting two different electron configuration n, n', and so can be of the form $\Delta J = 0$ $(\Omega' \neq 0)$ as well as $\Delta J = \pm 1$ and furthermore need not vanish in homopolar molecules. Moreover, if the electric field is not uniform the electric potential is not linear in the coordinates and so all the preceding considerations fail. Hence there can be a predissociating effect by sufficiently inhomogeneous fields even in the first approximation.

It is quite satisfactory that the predissociating effect of electric fields, especially the inhomogeneous ones, does not disappear completely. Indeed, Turner[8] finds that the iodine fluorescence is greatly diminished by admixture of argon as a foreign gas. The first excited state of the argon atom is so high that there can be no possibility of energy transfers in which argon atoms are excited, and the results can only mean that the intense and highly inhomogeneous electric fields from the argon atoms at the time of collision introduce new matrix elements which permit predissociation. Essentially this point has been emphasized by Turner.[8] He finds further that the critical primary frequency region in which the fluorescence is quenched is approximately the same in quenching by argon as in quenching by a magnetic field,[9] showing that the pair of states involved in the predissociation is presumably the same in both cases.[10]

[8] L. A. Turner, Phys. Rev. **38,** 574 (1931); cf. also J. Kaplan, *ibid.* **38,** 1079, 1792 (1931), F. W. Loomis and H. G. Fuller, *ibid.* **39,** 180 (1932) (abstract).

[9] M. Eliashevich, however, apparently finds less sensitivity to the frequency of the primary source than does Turner. See Phys. Rev. **39,** 532 (1932).

[10] It is not the purpose of the present paper to discuss the general subject of predissociation due to electric fields, but we may note that the important new interactions introduced by such fields are probably usually either blending of u and g states in symmetrical molecules or of 0^- and 0^+ states in symmetrical or unsymmetrical ones. Interaction between most other pairs of states can arise from rotational distortion without the necessity of external fields. It is often mentioned that external fields intermingle states of unlike J, but this effect is important only insofar as it blends electronic states not otherwise interacting (cf. dotted lines in Fig. 2). Unless we care to differentiate between different predissociation rates for different rotational members, the disturbances must be expressible in terms of a breaking down of the classifications (B), (C), (D) without invoking (A) or (E).

3. Further Discussion of Magnetic Predissociation

Dependence on Field Strength. The rate of predissociation is proportional to the square of the interaction matrix elements (cf. section 5). Since these are linear in the field strength $\mathfrak{H}$, the probability that a molecule in the N state dissociates via the M state is $b\mathfrak{H}^2$, where b is a constant, while we shall let a denote the probability factor for a radiation transition from N to the normal state. The fractional amount Q by which the resonance radiation is quenched is thus

$$Q = b\mathfrak{H}^2/(a + b\mathfrak{H}^2) \tag{1}$$

since this is merely the ratio of the number of predissociating molecules to the total number leaving the N state either by radiation or predissociation. The form of dependence predicted by (1) should be capable of experimental verification without undue difficulty.

Shape of M and N Potential Curves. Unfortunately it is impossible at present to predict except in a qualitative way how the amount of quenching should depend on the frequency of the incident light. Accurate predictions would require, for one thing, exact knowledge of the form of the potential energy curves for the M and N states. Actually the M state, which theory tells us must be not far from N, is not observed spectroscopically at all. However, this is not surprising, since a radiation transition from M to the normal state would be of the form $0^- \rightarrow 0^+$ and so is forbidden regardless of the magnitude of the spin-orbit forces.[11] A state discovered by Brown[12] which he thought might conceivably be M is undoubtedly $^3\Pi_1$. The constants of the N level are known quite well,[13] and this level is found to arise from the union of atoms in $^2P_{3/2}$ and $^2P_{1/2}$ states, in accordance with theory, whereas the M level very probably arises from two atoms both in $^2P_{3/2}$ (cf. Fig. 1). The doublet width for the ^2P configuration of the iodine atom is .94 volts, with $^2P_{3/2}$ deepest, and this width is doubtless sufficient to make N stable and M unstable at ordinary values of the inter-nuclear distance r (cf. Fig. 1). Although the separation of the M, N curves is .94 volts for $r = \infty$, it is doubtless much smaller when r is near the usual values. In fact, appreciable predissociation is possible only if the potential curves come close together. The general theory of Λ-doubling in $^3\Pi_0$ states (§4) shows that the separation in question should be not more than of the order $a^2/h\nu(\Pi, \Sigma)$ provided the molecular binding is large compared to the usual constant a of the atomic spin doublet. In iodine the constant a has the value 5067 cm,$^{-1}$ and so this upper limit is roughly of the order 10^3 cm^{-1} if we assume that the $\Pi - \Sigma$ separations are about 2.5×10^4

[11] See R. Schlapp Phys. Rev. **39,** 806 (1932). The transition $0^- - 0^+$ is no longer rigorously forbidden if the correction for rotational distortion is important, as then the classification (C) of section 2 is lost, and a Q (but not P or R) branch can appear. This correction is, however, insignificant for molecules as heavy as iodine.

[12] W. G. Brown, Phys. Rev. **38,** 1187 (1931) (I_2); *ibid.* **38,** 1179 (Br_2). Brown originally rejected the $^3\Pi_1$ assignment to his new level in I_2 and Br_2 because it would yield a tremendous disparity in intensity between $^1\Sigma - ^3\Pi_0$ and $^1\Sigma - ^3\Pi_1$. As we outline above, this disparity is, however, to be expected for inter-system combinations, and Brown himself has recently proposed the $^3\Pi_1$ classification (see paper by Brown and Gibson in this issue).

[13] F. W. Loomis, Phys. Rev. **29,** 112 (1927); also W. G. Brown, *ibid,* **38,** 709 (1931).

cm^{-1}. In Fig. 1, reproduced from one of Prof. Mulliken's papers, the M, N curves are represented as practically coincident when the inter-nuclear distance is sufficiently small. This may not be correct, as they pass over into two components of a spin multiplet when one collapses the molecule into the "united atom." However, it has not seemed advisable to redraw the curves to show the finite separation of the M, N curves at small distances, as the precise amount of the separation is so uncertain. It is quite possible, and rather necessary for our predissociation theory, that in the vicinity of some critical value of r the separation be much smaller than the above upper estimate 10^3 cm^{-1}.

Do the M and N Curves Cross? In the usual forms of predissociation one deals with levels whose potential energy curves cross. It is possible that the M and N states in iodine actually do cross. These states have different symmetries, and so this is not precluded by the "non-crossing" rule for the roots of an irreducible secular determinant. If more were known about the location of all the energy levels, both stable and unstable, of the iodine molecule, it might be possible to decide theoretically whether or not the two levels do cross. Some of the mathematical analysis connected with this point, *i.e.* the sign of the Λ-doublet, will be given in sections 4 and 6, and leads to the general conclusions stated in the next paragraph.

The two doublet components coincide when we neglect the spin-orbit interaction. The M component is unaffected by ${}^1\Sigma_u^+$, ${}^3\Sigma_u^-$, or by g levels, is depressed by higher ${}^1\Sigma_u^-$ or ${}^3\Sigma_u^+$, and elevated by lower ${}^1\Sigma_u^-$ or ${}^3\Sigma_u^+$ levels. Similar remarks apply to N if the plus and minus signs are everywhere interchanged. Even without appealing to the mathematical analysis to be given in sections 4 and 6, these statements are fairly obvious consequences of the fact that spin-orbit action exists only between states of the same Ω and (if $\Omega=0$) of like symmetry (C), section 2, and that interaction between two levels has the effect of separating them further. In this connection one must remember that ${}^3\Sigma_0^-$, ${}^3\Sigma_0^+$ are really 0^+, 0^- states.

When one applies the foregoing rules to iodine, one is tempted to first assume that the important spin-orbit interactions are those between states which are derived from the normal atomic configurations ${}^2P+{}^2P$ inclusive of the various multiplet components. The N level is the only 0_u^+ state so derived and is hence undisplaced by such interactions. On the other hand there are three 0_u^- states so derived in addition to the M state viz. one ${}^1\Sigma_u^-$ and two ${}^3\Sigma_u^+$ states. If M is to cross above N when r becomes sufficiently small it is necessary that one of these three states lie below M in energy and that its interaction with M elevate M more than M is depressed by interaction with the other two of the three states, presumably because of closer proximity. These other two must be above M in energy because only two of the four 0_u^- states are derived from ${}^2P_{3/2}+{}^2P_{3/2}$, and because M is so derived by our interpretation of predissociation. The other two 0_u^- states are derived from ${}^2P_{1/2}+{}^2P_{3/2}$, ${}^2P_{1/2}+{}^2P_{1/2}$ (one each) and so must be above M by the non-crossing rule.

Existing data do not seem adequate to decide whether there really is a

0_u^- state below M. If there were such a state, it might easily escape detection, as it could not combine spectroscopically with the normal state or with the N level since $0^- - 0^+$ and $u - u$ transitions are both forbidden.[14] However, the study of electron configurations in the way developed by Mulliken and Hund,[15] makes it exceedingly doubtful if there is any O^- state more firmly bound than $^3\Pi_0^-$.

In case M is the lowest 0^- state, one can still obtain the desired crossing if one assumes that the N level is strongly depressed by spin-orbit interaction with $^1\Sigma_u^+$ or $^3\Sigma_u^-$ levels derived from excited iodine atoms, *i.e.* from a pair of iodine atoms of more energy than $^2P + ^2P$. The word strongly is inserted because N would need to be more displaced by this interaction than M is by interaction with levels derived both from $^2P + ^2P$ and from excited atoms. For this reason, such an attempt to obtain crossing would appear rather forced were it not for one fact; viz. that the bands $^1\Sigma_g^+ - N$ involved in the fluorescence are inter-system combinations. Such combinations exist only in virtue of the failure of S to be a good quantum number, so that singlet and triplet states begin to share properties. Furthermore it seems altogether probable that in iodine the inter-system radiation is due to the incipient singlet characteristics of N rather than incipient triplet properties of the normal level.[16]

[14] If the 0^- state is $^3\Sigma_0^+$ it must, however, be remembered that one of the other components $^3\Sigma_1^+$ of the same multiplet can combine with $^1\Sigma^+$.

[15] See the most illuminating figure given by Mulliken on p. 40 of Rev. Modern Physics, vol. 4. In the instance of F_2, the ten $2p$ electrons of the separated atoms undoubtedly pass over into his molecular configuration $x\sigma^2 w\pi^4 v\pi^4$ in the case of the $^1\Sigma_g$ state, and $x\sigma^2 w\pi^4 v\pi^3 u\sigma$ in that of $^3\Pi_u$ (or $^1\Pi_u$). Reference to this figure shows that the Σ_u configurations would have to be of the form $x\sigma^2 w\pi^3 v\pi^3 u\sigma^2$ or $x\sigma w\pi^4 v\pi^4 u\sigma$ both of which represent higher energies than $^3\Pi_u$ as they yield "more promoted" configurations of the united atom. Similarly one finds that all the Σ_g configurations except the normal state have higher energies than $^3\Pi_g$. Another figure (no. 44) of Mulliken's article can be used in the case of unsymmetrical molecules like ICl, and here also the indications are that $^1\Sigma^+$ is the lowest 0^+ state, with $^3\Pi_0^+$ next above, whereas $^3\Pi_0^-$ is the lowest 0^- state. Hence in the secular determinants of section 6, one is presumably justified in supposing that the lowest 0^+ level is derived from $^2P\sigma + ^2P\sigma$, with $^3\Pi_0^+$ from $^2P\sigma + ^2P\pi$ next above, while the lowest 0^- is $^3\Pi_0^-$ derived from $^2P\sigma + ^2P\pi$, provided the spin-orbit corrections be neglected. Here the notation $^2P\sigma$ means that the isolated atom has $L = 1$, $\Lambda = \Sigma\lambda = 0$. It is, of course, possible for a $^1\Sigma^+$ configuration to arise from $^2P\pi + ^2P\pi$, but it would be one of higher energy than that from $^2P\sigma + ^2P\sigma$, as it would entail the electron assignment $x\sigma^2 w\pi^4 v\pi^2 u\sigma^2$ or some still higher configuration. This is on the assumption that the atomic state is of the form p^5, so that $^2P\pi$ and $^2P\sigma$ furnish respectively three and four π electrons. However, the result that $^2P\sigma + ^2P\sigma$ is below $^2P\pi + ^2P\pi$ also holds for $p + p$ as well as $p^5 + p^5$, for the assignment $x\sigma^2$ is lower than $w\pi^2$. Mulliken's figures are explicitly for $2p$ orbits, whereas in iodine they are $5p$, but the results on the relative positions of states are the same in both cases, as the underlying qualitative arguments are the same.

[16] This does not necessarily mean that the normal state interacts less strongly with triplet states than does N with singlet levels. The reverse could even be true without contradicting Brown's results if the incipient triplet characteristics of the normal state are acquired from a triplet level which does not combine intensely with N as regards radiation transitions, and if at the same time the incipient singlet properties of N are acquired from a singlet level which radiates very intensely to the normal state. In this connection it is well to remember that in the limiting case of nearly isolated atoms, which may be a fairly good approximation in iodine, radiation is forbidden between molecular levels derived from the same dissociation products, as the Laporte rule for isolated atoms is then a good approximation, and this prohibits transi-

Particularly strong evidence to this effect is furnished by the work of Brown. He finds[17] that in I_2 the transition ${}^1\Sigma_g^+ - {}^3\Sigma_{1u}$ is very much less intense than ${}^1\Sigma_g^+ - N$, the difference being greater than can be ascribed to diversity in Franck-Condon relations. If the inter-system radiation were due to incipient triplet characteristics of the normal state, one would expect these two transitions to be of the same order of magnitude in intensity, whereas they could differ greatly if this radiation is due to incipient singlet properties of ${}^3\Pi_{1u}$ and N. Namely, since spin-orbit coupling is diagonal in Ω, the singlet tendency of ${}^3\Pi_{1u}$ comes from robbing a ${}^1\Pi_u$ level, while that of N comes at the expense of ${}^1\Sigma_u^+$, and so may be entirely different from that of the former in order of magnitude, especially if ${}^1\Pi_u$ and ${}^1\Sigma_u^+$ have widely different energies or moments of inertia. If the so-called D state of the iodine molecule[18] (too high to show in Fig. 1) is of the form ${}^1\Sigma_u^+$, it would have just the desired depressing effect on N, although this interaction might prove too faint on account of the wide energy separation of N and D. At any rate the great intensity of the visible iodine bands shows that there is surely some higher singlet level which strongly perturbs N. Possibly this perturbing level is unstable and so does not show up at all in the ordinary spectral analysis.

It is conceivable that the magnetic predissociation via M might be sufficiently intense even if the M, N curves do not cross but instead are very close to each other and sensibly parallel for a considerable interval of r values. It is hard to determine quantitatively how close the curves would need to be but doubtless the separation would have to be much less than the upper limit 10^3 cm^{-1} previously estimated. The Franck-Condon principle of course precludes an appreciable predissociating interaction between states whose potential energy curves are not very close to each other. It is this fact that, for instance, explains why the N state does not predissociate due to rotational distortion without a magnetic field. There are two 1_u states (*i.e.* states having $\Omega = 1$ and odd with respect to symmetry B) derived from ${}^2P_{3/2} + {}^2P_{3/2}$. One of these levels, viz. ${}^3\Pi_1$ has already been mentioned and falls so far below N that it is unstable when its vibrational energy is sufficient to equalize its

---

tions within the same atomic configuration. Thus the visible halogen bands might very easily owe their intensity to spin-orbit perturbations from levels derived from excited electronic levels of iodine, too high to show in Fig. 1. In particular the D level would be apt to be an important perturber as regards the radiative but necessarily energetic properties of N, since D dissociates into one normal iodine atom and one excited atom in the upper state of the intense atomic iodine resonance line.

[17] W. G. Brown, *l.c.*[12] He further informs the writer that the disparity in intensity in favor of N is less pronounced in IBr and BrCl than in Br_2 and I_2, while in ICl ${}^1\Sigma - {}^3\Pi_1$ is more intense than ${}^1\Sigma - N$. Such variations from molecule to molecule are not disquieting, as diversity in the location of states and in the multiplet constant may make the spin-orbit perturbations widely different. Also the Franck-Condon effects may vary.

[18] Cf. Weizel, p. 381 of "Bandenspektren" vol. of Wien-Harms Handbuch. Weizel's energy level diagram also shows the so-called B state less than one volt above the normal level. This state was proposed by Pringsheim and Rosen (Zeits. f. Physik, **50,** 1, 1928) but its existence has been seriously questioned by Sponer and Watson (*ibid.* **56,** 184 (1929)). Even if there really is a B state, it is of no particular interest for us, as it is a g level, and so cannot perturb the M or N levels. On the other hand the D state is known to be of the u type.

total energy with that of the lowest vibrational member of N. Hence the N state could predissociate rotationally via $^3\Pi_1$ except in so far as the intensity of the effect is reduced by the separation of the potential energy curves. In general, reduction from this cause must be very important as otherwise molecules would have excessively few stable excited states.

Variation of the Magnetic Quenching With Frequency of Incident Beam. This variation can easily be understood in a qualitative way. The sharp cut-off on the low frequency side is clearly due to the fact that unless the molecule is excited to an N state with a considerable amount of vibration, it will not oscillate with sufficient amplitude to traverse the portion of the N curve near the M one (cf. Fig. 1). Turner finds that the cut-off on the high frequency side is not nearly as sharp as that on the low . (His experiments on the high side are not very comprehensive and merely show that the quenching is somewhat diminished if the frequency is raised above about 19,000 cm). This blunter cut-off on the high side is readily comprehensible if the M and N states really do cross, for, as r is diminished, they probably do not separate as rapidly after crossing as they come together before crossing. This follows from the fact that for fairly small r the separation is not more than of the order 10^3 cm^{-1} previously estimated, whereas for $r=\infty$ the separation is the doublet interval 7.6×10^3 cm^{-1} of the iodine atom. If the predissocation is due to close proximity rather than crossing of the curves, one at first thought might not expect the quenching to be diminished at all on the high frequency side. However, as pointed out to me by Prof. Mulliken, too much vibration might augment the time the molecule spends on the right side of the N potential curve at the expense of the left side where the predissociation effects are important. This situation is conceivable, as the left side of the curve is much steeper than the right (cf. Fig. 1).

Possibility of Magnetic Predissociation in Other Molecules. As far as I am aware this type of predissociation has not been reported or probed in other molecules than iodine.[19] Clearly it should be expected whenever one of the M, N states is stable and the other unstable, provided these states cross or are very close for certain values of r. In general, the effect is less probable for lighter atoms than for I_2, as the spin-orbit interaction may easily become too feeble to be the deciding factor between stability and instability. Examination of the potential curves [20] for Br_2 and Cl_2 shows that only the higher vibrational members of N in Br_2, and the almost dissociated members in Cl_2, have greater energy than $^2P_{3/2}+^2P_{3/2}$, and so overlap the continuous rather

[19] It is found that the band fluorescence of mercury excited by a mercury lamp is altered by application of a magnetic field (Franck and Grotrian, Zeits. f. Physik, **6,** 35 (1921); H. Niewodniczanski, *ibid.* **55,** 676 (1929); also unpublished thesis of F. Studer at Wisconsin). This, however, is probably a different effect than the one which we are considering. The usual interpretation of the behavior of mercury is that the Zeeman effect on the hyperfine components of 2537 affects the ability of mercury to absorb its own radiation by displacing slightly the absorption frequencies in the field relative to the emission frequencies of the lamp not situated in the field. The bands are interpreted as radiations of molecules formed by union of an unexcited mercury atom with an optically excited ^3P atom.

[20] Cf., for instance, R. S. Mulliken, Rev. Mod. Phys. **4,** 17 (1932).

than discrete levels of M. Only such members should exhibit the magnetic predissociation, but no experimental data are available.

Likewise no magnetic data are available for molecules such as ICl, IBr, etc. formed from two different ^2P atoms. Here the theoretical situation is particularly interesting, as one no longer has the u-g distinction (B of section 2) and so symmetry considerations no longer preclude N being derived from the lowest dissociation product $^2P_{3/2}+{}^2P_{3/2}$. In fact it is quite probable that for ordinary values of r the N state is really one of the two lowest 0^+ states and so is derived formally from $^2P_{3/2}+{}^2P_{3/2}$, for the latter combination yields two 0^+ states now no longer specialized to 0_g^+. Nevertheless according to measurements of Brown and Gibson[21] given elsewhere in this issue, vibrational extrapolation for the N level in ICl yields a heat of dissociation corresponding to $^2P_{1/2}(\mathrm{Cl})+{}^2P_{3/2}(\mathrm{I})$. As noted by Brown and Gibson, this paradox can be explained by supposing that the potential curve has the shape shown in our Fig. 3 or their Fig. 4. If I is the ordinary vibrational region, then

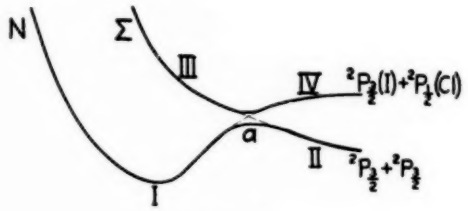

Fig. 3.

clearly the usual extrapolation will follow I+IV rather than I+II. It is not unreasonable that there should be a peak in the curve as shown in Fig. 3. Let us suppose that the secular determinant factors if certain matrix elements are neglected. If then N and Σ belong to different factors, their potential curves can cross, and be approximately of the form I-IV and II-III. If now these matrix elements are reintroduced there will no longer be any factoring, and the "non-crossing rule" will apply, making the curves of the shape I-II and III-IV. As emphasized by Hund,[22] the correlation I-II and III-IV is a purely formal matter as long as the separation at a in Fig. 3 is small, for then the characteristic features of I are really continued more along IV than II. Essentially this principle is utilized in Brown and Gibson's article, but it does remain to verify, explicitly, and this is our only new contribution, that the secular determinant really does factor under reasonable simplifying assumptions. Mathematical analysis relating to this point will be given in section 6, where the secular determinant will be set up explicitly. It will there be shown that the N and Σ curves for molecules derived from $^2P+{}^2P'$ really do cross if we neglect certain matrix elements which would vanish were the atomic Λ's

[21] The writer is indebted to Dr. Brown for communication of results in advance of publication in this issue of the Physical Review. The N state in our notation is the same as the C level in Weizel's. Its dissociation products are often erroneously given in the literature (e.g. Weizel, l.c.[18]) as $^2P_{3/2}(\mathrm{Cl})+{}^2P_{1/2}(\mathrm{I})$ rather than $^2P_{3/2}(\mathrm{I})+{}^2P_{1/2}(\mathrm{Cl})$.

[22] F. Hund, Zeits. f. Physik, **52**, 601 (1929).

rigorously good quantum numbers. It may be mentioned that when the crossing is destroyed by including all elements, molecules vibrating in the region I are unstable, in principle, because of the possibility of leakage through the peak out to the region II, giving a predissociation similar in mechanism to the well-known quantum theory of radioactive disintegration. However, both theoretically and experimentally the predissociation due to this cause is small. The experimental evidence is that Brown and Gibson find the levels of the M state do not "fuzz" unless their energy is greater than the peak a in our Fig. 3 (cf. especially their Fig. 4). The importance of all this for us is that there is thus the possibility of a magnetic predissociation effect in ICl if the M curve (not shown in Fig. 3) crosses or nearly coincides with the N one somewhere in the region I. Without the anomalous peak there could be no magnetic predissociation, as both M and N have the same formal dissociation product $^2P_{3/2}+{}^2P_{3/2}$ and hence the same degree of stability except for the anomaly.[23]

The preceding discussion has all been for molecules derived from the atomic configuration $p^5\,{}^2P+p^5\,{}^2P$. For molecules derived from $p\,{}^2P_{1/2}+p\,{}^2P_{1/2}$ the situation is somewhat different as the atomic multiplets are regular and the lowest dissociation product is $^2P_{1/2}+{}^2P_{1/2}$. Now with symmetrical molecules $^2P_{1/2}+{}^2P_{1/2}$ and $^2P_{1/2}+{}^2P_{3/2}$ each yield one 0_u^- term, and $^2P_{3/2}+{}^2P_{3/2}$ yields two, while $^2P_{1/2}+{}^2P_{3/2}$ gives the sole 0_u^+. Hence the M and N states will dissociate into different atomic multiplet components (a necessary but not sufficient condition for magnetic predissociation) provided M is not the second lowest 0_u^- state. Configuration theory shows that M is very probably usually the lowest rather than second lowest, such level.[24] In molecules derived from $^2S+{}^2P$ (HI etc.) the M and N terms will dissociate into different multiplet components provided the order of energy levels is $^1\Sigma^+<{}^3\Pi<{}^3\Sigma^+$ or $^3\Sigma^+<{}^3\Pi<{}^1\Sigma^+$. This follows since $^2S+{}^2P_{1/2}$, $^2S+{}^2P_{3/2}$ each yield one 0^+ and one 0^- level.

It seems impossible to say at present whether or not the iodine molecule is a fortuitous case involving closer proximity of the M and N components than usual for heavy molecules. If it is, the magnetic predissociation may not be observable in other molecules mentioned above which permit the effect in principle.

[23] Dr. Brown informs the writer that the same predissociation phenomenon is found in IBr and BrCl as in ICl and that the mode of dissociation of N and $^3\Pi_1$ is similar in all three molecules. He will publish details in the near future.

[24] See Fig. 43 of Mulliken's article.[15] According to the calculations of Bartlett on $2p+2p$, the $^3\Sigma_u^+$ level is the lowest and M the next lowest 0_u^- state (Phys. Rev. **37**, 507; 1931; note corrections given in Phys. Rev. **38**, 211, footnote 11 and p. 225). The reason for this disparity is probably that for the actual equilibrium values of r in stable molecules Bartlett's method of approximation based on the Heitler-London method and hydrogenic $2p$ wave functions may be insufficient, while for large values of r the curve for $u\sigma$ should be drawn somewhat lower than in Mulliken's Fig. 43. Then M would still be the lowest u state at the usual values of r (about $\xi=.75$ to 1.5 in Fig. 43) in stable molecules.

4. Theory of Λ-Doubling in $^3\Pi_0$ States

In a previous paper [25] the writer considered Λ-doublets in $^3\Pi_0$ states. These doublets are due to spin-orbit interaction in heavy atoms and hence different in origin from the usual Λ-doublets due to rotation distortion in states having $\Omega \neq 0$. We shall now extend the theory by examining the sign of the doublet separation and specially shall show that the expression for the magnitude of the separation given in the earlier paper was incomplete because it omitted the interaction of $^3\Pi$ with $^1\Sigma$, $^5\Sigma$ states, keeping only that with $^3\Sigma$ states. We shall defer until section 5 inclusion of an external magnetic field.

It will be sufficient to consider as usual the spin-orbit interaction to arise entirely from the coupling of each spin to its own orbit, yielding the well-known energy expression

$$H = \sum a_i \boldsymbol{l}_i \cdot \mathbf{s}_i. \qquad \left(a_i = \frac{e}{2m^2c^2} \frac{1}{r} \frac{dV}{dr} \right). \tag{2}$$

Our previous omission consisted in following the customary procedure of replacing (2) by $A\boldsymbol{L}\cdot\mathbf{S}$, which is tantamount to retaining only matrix elements connecting states of like S and L. This, however, is not allowable for our purposes, as the Λ-doubling is a second rather than first order effect in the spin-orbit couplings, so that other elements are comparable in final importance with the usual ones.

Let us start with an initial system of representation (not at all the correct final one) in which one of the two $^3\Pi_0$ states, say a, has $\Lambda = +1$, $\Sigma = -1$, the other, b has $\Lambda = -1$, $\Sigma = +1$. This we shall call the a, b representation. The transformation matrix for the perturbation problem associated with (2) is to a first approximation $S = 1 + S_1$ where

$$S_1(\alpha\alpha') = -\frac{H(\alpha\alpha')}{h\nu(\alpha\alpha')} \tag{3}$$

with $\alpha = a$ or b and $\alpha' = {}^1\Sigma$, $^3\Sigma_0$, $^5\Sigma_0$, $^3\Pi_0{}'(\neq {}^3\Pi_0)$, $^5\Pi_0$, or $^5\Delta_0$ inasmuch as the matrix elements of (2) are easily seen to be entirely of the form $\Delta\Omega = 0$, $\Delta S = 0, \pm 1$, $\Delta\Lambda = 0, \pm 1$, $\Delta\Sigma = 0, \pm 1$. The Hermitean property makes $H(\alpha'\alpha) = H(\alpha\alpha')^*$. To obtain the energy to a second approximation one must solve the secular problem connected with the transformed Hamiltonian function $H' = S^{-1}HS$. If we neglect third order terms, one finds that the determinantal equation of this is

$$\begin{vmatrix} W_0 + H'(aa) - W & H'(ab) \\ H'(ba) & W_0 + H'(bb) - W \end{vmatrix} = 0 \tag{4}$$

where

$$H'(xy) = \sum_{\alpha'} \frac{H(x\alpha')H(\alpha' y)}{h\nu(\alpha\alpha')} \qquad (x, y = \text{either } a \text{ or } b).$$

The important thing to note is that $H'(ab) \neq 0$; in other words the second ap-

[25] J. H. Van Vleck, Phys. Rev. **33**, 467 (1929), especially section 7. See section 4 of this ref. for somewhat fuller exposition of the perturbation technique which we now use.

proximation removes the initial identity of energies for a, b and so leads to the secular equation (4). This degeneracy was not removed in the first approximation as $H(ab) \neq 0$ would require $\Delta\Lambda = -\Delta\Sigma = 2$.

Before writing down the solution of (4) explicitly it is necessary to examine the phase relations between $H'(a\alpha')$ and $H'(b\alpha')$. These are as follows

$$\begin{aligned} H(a;{}^1\Sigma^\pm) &= \pm H(b;{}^1\Sigma^\pm), & H(a;{}^3\Sigma^\pm) &= \mp H(b;{}^3\Sigma^\pm), \\ H(a;{}^5\Sigma^\pm) &= \pm H(b;{}^5\Sigma^\pm), & H(a;X_a) &= H(b;X_b), \end{aligned} \tag{5}$$

where X_a, X_b are the components of a ${}^3\Pi_0'$, ${}^5\Pi_0$, or ${}^5\Delta_0$ "Λ-type-doublet" in the a, b representation. To obtain these results one notes that reflection in a plane containing the figure axis (operation C of section 2) reverses the sense of rotation about this axis and so interchanges the wave functions ψ_a and ψ_b if the arbitrary phases in these functions be properly chosen. Furthermore the operator corresponding to (2) is even under this reflection. If α' is a Σ state one sees by making a change of variables corresponding to the above reflection that the matrix element $H(a\alpha') = \int \psi_a^* H \psi_{\alpha}' d\tau$ is identical with $H(b\alpha')$ or else the negative thereof according as ψ_{α}' is even or odd under the reflection. Here the integration is to be understood to include the spin summation, and it is necessary to reflect the complete wave functions inclusive of the spin parts. In the approved notation Σ^+, Σ^- the superscript gives the symmetry under a reflection of merely the orbital portion. When the spin is included the symmetry of ${}^3\Sigma$ is reversed. This is because the spin functions for the states ${}^1\Sigma$, ${}^5\Sigma_0$ are even, while that for ${}^3\Sigma_0$ is odd under the reflection.

These properties of the spin functions can be implicitly seen for triplets from the case (a)–case (b) correlation diagrams given by Mulliken.[26] It is perhaps illuminating to verify them explicitly for a two electron system, where these functions are

$$\delta(\tfrac{1}{2};\sigma_1)\delta(\tfrac{1}{2};\sigma_2), \qquad 2^{-1/2}\left[\delta(-\tfrac{1}{2},\sigma_1)\delta(\tfrac{1}{2};\sigma_2) \pm \delta(\tfrac{1}{2},\sigma_1)\delta(-\tfrac{1}{2}\sigma_2)\right], \qquad \delta(-\tfrac{1}{2},\sigma_1)\delta(-\tfrac{1}{2},\sigma_2), \tag{6}$$

corresponding respectively to $\Sigma = +1, 0, -1$. The upper and lower signs give $S=1$, and $S=0$ respectively, and σ_1 is the component of spin of electron 1 in the direction z of the axis of figure. A reflection in a plane containing the axis of figure can be regarded as a reflection in the origin followed by a rotation through 180° about the x axis. Now reflection in the origin does not change the sign of any of the three Cartesian components of angular momentum and so may be regarded as leaving the spin wave functions invariant. On the other hand one verifies from the usual Cayley-Klein transformation scheme[27] obeyed by the spin that the above rotation replaces $\delta(\pm\frac{1}{2},\sigma)$ by $-i(\delta\mp\frac{1}{2},\sigma)$ making (6) exhibit the sign behavior noted above. The extension of the proof to include quintets and configurations with more than two electrons can be obtained from the general theory of the transformation coefficients of the rotation group.[28]

From (5) it follows that $H'(aa) = H'(bb)$ and that the roots of (4) are

$$W({}^3\Pi_0^\pm) = W_0' + 2\sum\left\{\frac{|H({}^3\Pi_0;{}^1\Sigma^\pm)|^2}{h\nu({}^3\Pi_0;{}^1\Sigma^\pm)} + \frac{|H({}^3\Pi_0;{}^3\Sigma^\mp)|^2}{h\nu({}^3\Pi_0;{}^3\Sigma^\mp)} + \frac{|H({}^3\Pi_0;{}^5\Sigma^\pm)|}{h\nu({}^3\Pi_0;{}^5\Sigma^\pm)}\right\}. \tag{7}$$

[26] R. S. Mulliken, Phys. Rev. **36**, 1444 (1930).

[27] Cf., for instance, Eq. (8) of ref.[25] with $\theta = \pi$, $\Omega = 0$.

[28] See F. Hund, Zeits. f. Physik, **63**, 722 (1930).

Here $W_0' = W_0 + \sum |H(^3\Pi_0, \cdot X)|^2/h\nu(^3\Pi_0, \cdot X)$ (with X defined as after (5)) is a term common to both roots, and the upper or lower sign is to be read consistently. The summation is over all the electronic states of the various types indicated after each semicolon and is inclusive of the various vibrational members if we care to allow for the vibrational structure (Franck-Condon effects) which we have not done explicitly. In symmetrical molecules the elements H will vanish for u-g transitions. In (7) we have classified the roots according to their symmetry under reflection (C). The correlation is as given because the transformation matrix connected with (4) has the elements

$$S(a; \mathrm{I}) = S(b; \mathrm{I}) = S(a; \mathrm{II}) = -S(b; \mathrm{II}) = 1/2^{1/2} \tag{8}$$

and with our choice of phases $\psi_a + \psi_b$, $\psi_a - \psi_b$ are respectively even and odd, so that I, II mean $+$, $-$ with respect to (C). It is clearly to be understood that although (7) gives the energies in the ultimate, even-odd representation, the matrix elements on the right side are to be calculated for the initial a, b, representation.

The difference $W(^3\Pi_0^+) - W(^3\Pi_0^-)$ is, of course, the width $h\Delta\nu$ of the Λ-doublet. When one takes into account the different possible signs of the denominators, one is led to the statements regarding sign and the depressing and elevating effects on the different components given on p. 552.

Explicit Calculations. If there are only two electrons not in closed shells, one may calculate the matrix elements of $\mathbf{s}_1$, $\mathbf{s}_2$ from (6) and the properties of the spin operators. Using the phase relations between l_x and l_y characteristic of an axial field, one finds that then

$$H(^3\Pi_0; {}^{2\pm1}\Sigma) = 2^{-1/2}\left[a_1 l_{1x}(^3\Pi; {}^{2\pm1}\Sigma) \pm a_2 l_{2x}(^3\Pi; {}^{2\pm1}\Sigma)\right]$$

with the z axis taken as that of figure. This relation is quite general for two electron systems, as it only supposes S, Σ, and Λ to be good quantum numbers, but is not particularly helpful, since the matrix elements of l_1, l_2 are unknown except with special models involving in each case some rather drastic hypothesis.

One such hypothesis is that the two electrons may be considered in so nearly a central field that their individual and resultant angular momenta l_1, l_2, L are all good quantum numbers. The matrix elements of l_{1x}, l_{2x} for this model in the a, b, system of representation can be deduced by non-commutative algebra[29] or by proper adaptation[30] of the Kronig intensity rules (with phases inserted) and have been tabulated by Johnson.[31] One finally finds that (7) gives

$$W = W_0' + \frac{[a_1 f(L, l_1, l_2) \pm a_2 f(L, l_1, l)]^2}{h\nu(L^3\Pi; L\,{}^{2\pm1}\Sigma)} + \frac{L(L+1)(a_1 \pm a_2)^2 F(L+1; l_1, l_2)}{h\nu(L^3\Pi; L+1\,{}^{2\mp1}\Sigma)} + \frac{L(L+1)(a_1 \pm a_2)^2 F(L, l_1, l_2)}{h\nu(L^3\Pi; L-1\,{}^{2\mp1}\Sigma)}. \tag{9}$$

with the abbreviations

$$f(L, l_1, l_2) = \frac{L(L+1) + l_1(l_1+1) - l_2(l_2+1)}{4(L^2+L)^{1/2}},$$

$$F(L, l_1, l_2) = \frac{(l_2 + l_1 + 1 - L)(l_1 + l_2 + 1 + L)(L - l_1 + l_2)(L + l_2 - l_1)}{16L^2(2L-1)(2L+1)}.$$

[29] Güttinger and Pauli, Zeits. f. Physik **67,** 743 (1931).

[30] See p. 170 of the writer's "Theory of Electric and Magnetic Susceptibilities" for resumé of how this can be done.

[31] M. H. Johnson, Jr., Phys. Rev. **38,** 1628 (1931); Eqs. (3), (4), (5), but replace J, L, S by L, l_1, l_2 to adapt to our problem.

The first index of ν in (9) gives the value of L, and $^{2+1}\Sigma$ means $^3\Sigma$ etc. The $+$, $-$ superscripts for the Σ states have been omitted but for any given value of L, l_1, l_2, they can be determined from the Hund[28] rule that with the present model the orbital wave function for a Σ state of azimuthal quantum number L is even or odd under reflection (C) according as $L-l_1-l_2$ is even or odd. This shows that the upper choice of sign in (9) (not to be confused with the upper choice in (7)) yields $W(^3\Pi_0^+)$ or $W(^3\Pi_0^-)$ according as $L+1-l_1-l_2$ is even or odd. Eq. (9) is valid even when the electrons are equivalent; the members then representing transitions to non-existent states vanish in virtue of $a_1=a_2$.

Another model which can be used is that in which the individual λ's and l's of the electrons are good quantum numbers. Let us suppose that all electrons but two are in closed shells, and that the Π state is of the type $m_1\pi m_2\sigma^3\Pi$. If the two electrons are not equivalent, i.e. $m_1 \neq m_2$, one finds from elementary construction of the wave functions that

$$W(^3\Pi_0^{\pm}) = W_0' + \left[\frac{a_1^2 l_1(l_1+1)}{4h\nu(^3\Pi; m_1\sigma m_2\sigma\ ^{2\mp1}\Sigma^+)} + \frac{a_2^2 l_2(l_2+1)}{8h\nu(^3\Pi; m_1\pi m_2\pi\ ^{2\mp1}\Sigma^+)} + \frac{a_2^2 l_2(l_2+1)}{8h\nu(^3\Pi; m_1\pi m_2\pi\ ^{2\pm1}\Sigma^-)}\right]. \tag{10}$$

If the two electrons are equivalent the complete bracketed expression should be multiplied by a factor 2 and the terms discarded which would involve non-existent states. The latter states are $\sigma^2\,^3\Sigma^+$, $\pi^2\,^1\Sigma^-$, $\pi^2\,^3\Sigma^+$ if the "united atom" approximation is being used (i.e. l_1, l_2 measured relative to the same center) and $\sigma^2\,^3\Sigma_g^+$, $\pi^2\,^1\Sigma_g^-$, $\pi^2\,^3\Sigma_g^+$, $\sigma^2\,^1\Sigma_u^+$, $\pi^2\,^1\Sigma_u^+$, $\pi^2\,^3\Sigma_u^-$ if the molecule is symmetrical and the "separated atom" approximation is used, wherein two electrons are to be considered equivalent for our purposes if their orbits are identical except for being referred to different centers of similar type.

Eqs. (8–9–10) replace (69,70) of our previous paper. We must caution that (9) and (10) apply only when the effect of L, Λ and λ_1, λ_2 respectively upon the energy is small compared to that of the principal quantum numbers n_1, n_2, since in (9–10), though not in (7), we have discarded the portion of (2) not diagonal in n_1, n_2, In (2) a_1, a_2 are in general functions of r_1, r_2, and it is only when we discard the non-diagonal matrix elements that they can be treated as ordinary numbers as in (9–10). It must be remembered that the Λ-doubling is a second order effect, and so the non-diagonal part of (2) (i.e. part of the spin-orbit interaction not diagonal in the principal quantum number) makes a contribution to (7) of the same order as the more usual diagonal part except insofar as the latter yields smaller denominators in (7).

5. Effect of a Magnetic Field upon the Λ-Doubling

Stationary Molecule. Let us first neglect molecular rotation and suppose that a magnetic field is applied parallel to the axis of figure. The extra term introduced into the Hamiltonian function is then $\mathfrak{H}\beta(L_z+2S_z)$ where β is the Bohr magneton $he/4\pi mc$. In the a, b system of representation, this expression is a diagonal matrix whose elements are $\pm\mathfrak{H}\beta$ as then one (the "a" component) has $\Lambda=1$, $\Sigma=-1$, while the other has $\Lambda=-1$, $\Sigma=+1$. Hence the magnetic field merely has the effect of adding $-\mathfrak{H}\beta$ and $\mathfrak{H}\beta$ respectively to the two elements on the principal diagonal of (4) and so the roots of (4) become

$$W = \tfrac{1}{2}\left[W(^3\Pi_0^+) + W(^3\Pi_0^-)\right] \pm \tfrac{1}{2}(4\,\mathfrak{H}^2\beta^2 + h^2\Delta\nu^2)^{1/2}, \tag{11}$$

where $h\Delta\nu$ is the field-free doublet width $W(^3\Pi_0^+) - W(^3\Pi_0^-)$. Eq. (11) has the

[28] The small Greek letters as used here and also later in Eqs. (16) and (18) in the "separated atom model" relate to the one rather than two-center problem and hence are less specific than those in Mulliken's usage. He would, for instance, write $\sigma_u\sigma_g\Sigma_u$ in place of our $\sigma^2\Sigma_u$. In our united atom approximation, the electron is u or g according as l is odd or even.

same structure as the familiar expression for the Paschen-Back effect on doublets. The important thing to note is that after addition of the magnetic terms the transformation matrix associated with (4) no longer has the precise form (8), as (8) demands equal elements along the principal diagonal of (4) (previously secured in virtue of $II(aa) = II(bb)$). Any departure from (8), however, means loss of the even-odd property, in agreement with statements made in section 1. The analogy to the crude model at the end of section 1 is obvious. In the limit $\mathfrak{H}\beta \gg |h\Delta\nu|$ the field demands the a, b representation. In the more usual limit $\mathfrak{H}\beta \ll |h\Delta\nu|$ the roots of (11) are approximately $W(^3\Pi_0^{\pm}) \pm \mathfrak{H}^2\beta^2/h\Delta\nu$.

The assumption of a stationary molecule has permitted particularly simple exhibition of the Paschen-Back effect on the doubling, but is not a good approximation to reality unless perchance the magnetic field is so extremely powerful as to align the molecular axis parallel to the field. Such an alignment would require $\mathfrak{H}^2\beta^2 \gg h|\Delta\nu|(2J+2)h^2/8\pi^2 I$ as the Zeeman effect cited in the last sentence of the preceding paragraph would need to be bigger than the rotational structure. In iodine $h/8\pi^2 Ic$ has the abnormally low value[13] 0.029 cm^{-1}, but, even so, satisfaction of the above inequality at the band origin $J = 0$ in a field of 20,000 Gauss would require $|\Delta\nu/c| \ll 15$ cm.$^{-1}$

Effect of Molecular Rotation. This rotation profoundly modifies the Zeeman effect but will not impair the field-free theory of §4 if we suppose, as we shall, that the molecule is heavy enough so that Hund's case a is a good approximation. With the rotation, the perturbing matrix elements due to the magnetic field are

$$H_1(^3\Pi_0^+ vJ;\ ^3\Pi_0^- v'J') = \tfrac{1}{2}\mathfrak{H}\beta\left[\frac{(J+J'+1)^2 - 4M^2}{(2J'+1)(2J+1)}\right]^{1/2} 1(v;v') \text{ with } J' = J \pm 1.$$

This can be seen by noting that in the a, b system of representation, these matrix elements are of the same structure as those of the potential energy of a rotating dipole,[33] with the moment along the axis of figure taken as β. As usual, M is the magnetic quantum number determining the component of angular momentum in the direction of the field. The factor $1(v; v')$ denotes $\int R_v^+ R_{v'}^- dr$, and has been inserted to allow for the vibrational structure;[34] here R_v^+ and $R_{v'}^-$ are the vibrational parts of the wave function for $^3\Pi_0^+$ and $^3\Pi_0^-$ states of vibrational quantum number v, v' respectively. Unless the field is so very strong as to give much Paschen-Back effect, one can use perturbation theory, and the energy levels in the field are, to the second order

[33] See, for instance, R. de L. Kronig, Proc. Nat. Acad. Sci. **12,** 488 (1926).

[34] This vibrational factor results from the fact that in calculating the matrix elements of the Hamiltonian function H, there is an integration over the radial wave function. It is possible to take H outside the integration particularly since H is a Zeeman term independent of r; or more generally in other problems, since the variation of H with r is usually "blunt," compared to that of the radial wave functions themselves. The function $1(v; v')$ is a Kronecker delta function only in case the initial and final states have the same vibrational constants, etc. so that R^+, R^- belong to exactly the same set of orthogonal functions. In our problem the difference between $1(v; v')$ and a Kronecker delta will presumably not be great, for the potential curves for M and N are quite close for a considerable range of values of r (cf. Fig. 1).

$$W = W(^3\Pi_0^{\pm}) + \sum_{v'}\sum_{J'=J\pm1} \frac{\mathfrak{H}^2\beta^2[(J'+J+1)^2 - 4M^2]\,|\,1(v;v')\,|^2}{4h\nu(^3\Pi_0^{\pm}vJ;\,^3\Pi_0^{\mp}v'J')(2J+1)(2J'+1)}. \quad (12)$$

It is to be noticed that there is only a second order Zeeman effect. A first order effect[35] would require both $\mathfrak{H}\beta \gg |h\Delta\nu|$ and $\mathfrak{H}\beta \gg Jh^2/4\pi^2I$ (except for fortuitous near-coincidences of two states involved in the denominator ν of (12), due to counterbalancing of the stationary doublet width $\Delta\nu$ by rotational or vibrational changes). If one assumes that the effect of the rotational quantum number J on the energy is small compared to the Λ-doublet width $h\Delta\nu$, one can replace $\nu(\,.\,.)$ in (12) by an expression independent of J. This assumption is not an automatic consequence of Hund's case a, as the latter merely insures that the ordinary multiplet constant a_1 be $\ll Jh^2/4\pi^2I$, whereas $\Delta\nu$ is of the second order in a_1 (cf. Eq. 10). Still further simplification can be effected if we assume that both components have nearly the same potential energy curve, making $1(v;v') = \delta(v, v')$ where δ is the usual Kronecker symbol, or if, going to the other extreme, we suppose that the effect of vibration is small compared to the doublet width. The latter supposition, unlike the former, is not usually warranted, but would permit one to take ν outside the v' summation sign and use the relation $\Sigma_{v'}|\,1(v;v')\,|^2 = 1$ proved elsewhere by the author.[36] If either case (12) then reduces to

$$W = W(^3\Pi_0^{\pm}) + \mathfrak{H}^2\beta^2\left[\frac{2J^2+2J-1-2M^2}{(2J-1)(2J+3)h\Delta\nu}\right] \quad (13)$$

provided the rotational structure is small compared to the doublet width.

Rate of Magnetic Predissociation. So far we have ostensibly supposed both doublet components to be stable. If, as in iodine, the $^3\Pi_0^-$ component is unstable, we may index and normalize its vibrational wave function with respect to the energy W. Wentzel, Dirac, and others[37] have shown that the rate at which a stable level 1 predissociates due to interaction matrix element $V(12)$ with a continuous level 2 is $4\pi^2|\,V(12)\,|^2/h^2$ provided that 2 be normalized with respect to energy, and that its energy be given the same value as for the discrete level. Hence in our case the probability of predissociation of the vibrational member v is

$$\sum_{J'=J\pm1} \frac{\pi^2\mathfrak{H}^2\beta^2[(J'+J+1)^2 - 4M^2]}{h^2(2J'+1)(2J+1)}\,|\,1(v, W)\,|^2. \quad (14)$$

In iodine the moment of inertia is probably so large that one is amply warranted in neglecting the rotational modulation of the vibrational potential

[35] It is to be emphasized that we throughout assume Hund's case (a). A linear effect, to be studied in a forthcoming paper by R. Serber, appears as soon as there is an appreciable rotational distortion, i.e., tendency towards case (b) or (d).

[36] J. H. Van Vleck, Proc. Nat. Acad. **15,** 754 (1929); especially pp. 757–758. Note especially that our R^+, R^- denote different sets of orthogonal functions, so that the matrix multiplication is not of the usual type.

[37] G. Wentzel, Zeits. f. Physik, **43,** 524 (1927); Dirac, "The Principles of Quantum Mechanics," p. 166.

energy curves, permitting us to regard $1(v, W)$ as independent of J'. If we do this and average over the various allowed values of the magnetic quantum number, (14) becomes

$$\frac{4\pi^2 \mathfrak{H}^2 \beta^2}{3h^2} \left| 1(v, W) \right|^2 \tag{15}$$

As mentioned in section 3, existing data do not permit evaluation of the factor $1(v, W)$. Different incident frequencies excite the iodine molecule to different vibrational levels v, and hence the dependence of this factor on v would be necessary in order to determine the sensitivity of the quenching to the frequency of excitation.

One point is quite clear. Experimentally the amount of magnetic predissociation does not seem to depend at all on the rotational quantum number, although Turner[7] calculates that enormous values of J are excited in some cases. This accords nicely with the absence of J in (15).

Magnetic Susceptibility in $^3\Pi_0$ *States.* As no gas is known having a $^3\Pi_0$ normal level, we shall merely state the results obtained by adapting to such states the author's general quantum theory of magnetic susceptibilities.[38] If we assume the vibrational structure can be eliminated as in going from (12) to (13), the formula for the susceptibility is $(2N\beta^2/3h\Delta\nu)\tanh(h\Delta\nu/2kT)$ which reduces to $N\beta^2/3kT$ in the limit $h\left|\Delta\nu\right| \ll kT$.

6. Some Secular Determinants for Molecules inclusive of Spin-Orbit Coupling

The writer has found it instructive to actually set up some of these determinants, for their structure is interesting even though insufficient data are available to permit numerical solution. Except for addition of the spin-orbit terms we shall make the usual Heitler-London approximations and so neglect any errors incurred because two wave functions belonging to different atoms are not rigorously orthogonal.

$^2P+^2P$. The orbital wave functions for a molecule derived from two identical $p\,^2P$ atoms have been listed by Bartlett[39] and so need not be given here. One must, of course, multiply them by the proper spin functions (6), and in the case of the $^3\Pi_0$ states pass from the a, b representation to the even and odd states by using the transformation (8). The matrix elements of (2) can be calculated from the well-known properties of the angular momentum operators. We are interested primarily in the dependence of the secular structure on the spin-orbit terms, and so shall not attempt to solve the rather laborious electrostatic part of the problem, instead merely denoting the various electrostatic terms by small Greek letters. We shall use the letter a to denote the atomic multiplet constant, which is the same as $a_1 = a_2$ in (2) and is half the corresponding molecular constant.[40] The various electrostatic

[38] J. H. Van Vleck, "The Theory of Electric and Magnetic Susceptibilities," Chaps. VII and X.

[39] J. H. Bartlett, Jr., Phys. Rev. **37**, 509 (1931).

[40] For general discussion of the relation between atomic and molecular multiplet constants see R. S. Mulliken, Rev. Mod. Phys. **4**, 34 ff, (1932).

terms, and to much less extent also a, are of course functions of the internuclear distance r. The caption below Fig. 1 lists ten 0 states derived from $^2P+^2P$ but because of the symmetry properties the secular equation factors into two biquadratics and two isolated states. One of each are the following[32]

$$\begin{array}{lc|cccc|} \sigma\pi\ {}^3\Pi_u^+ & W=\alpha-\tfrac{1}{2}a & & & & \\ \sigma\pi\ {}^3\Pi_u^- & \alpha-\tfrac{1}{2}a-W & a & 2^{-1/2}a & 2^{-1/2}a & \\ \sigma^2\ {}^3\Sigma_u^+ & a & \beta-W & \epsilon & 0 & \\ \pi^2\ {}^3\Sigma_u^+ & 2^{-1/2}a & \epsilon & \gamma-W & -a & \\ \pi^2\ {}^1\Sigma_u^- & 2^{-1/2}a & 0 & -a & \delta-W & \end{array} = 0 \quad (16)$$

The others are identical except that the labels are $\sigma\pi\ {}^3\Pi_g^-$; $\sigma\pi\ {}^3\Pi_g^+$, $\sigma^2\ {}^1\Sigma_g^+$, $\pi^2\ {}^1\Sigma_g^+$, $\pi^2\ {}^3\Sigma_g^-$ and that the constants $\alpha, \beta, \cdots, \epsilon$ all have new values. The off-diagonal electrostatic term ϵ arises because the individual λ's of the separate atoms are not good quantum numbers even without the spin-orbit distortion, so that certain Σ states can be part π^2 and part σ^2.

As a check on the accuracy of the work, one may verify that (16) simplifies properly in limiting cases. When $\alpha, \beta, \cdots, \epsilon$ vanish, the atoms are uncoupled, and the roots of (16) become $a, a, -\frac{1}{2}a, -2a$, in agreement with the fact that the spin-orbit energies of a ^2P atom are $\frac{1}{2}a, -a$. When $\alpha, \beta, \cdots, \epsilon$ are specialized appropriately for a central field,[41] the problem becomes a one rather than two center one, and one can verify that then (16) yields essentially the secular determinant of the p^2 atomic configuration, studied elsewhere by Bartlett and by Goudsmit.[42]

If one knew the numerical values of the various constants, one could solve (16) numerically for W and so determine the Λ-doubling and spin-orbit distortion even though the latter is of the same order of magnitude as the electrostatic binding, which incidentally is the case in iodine. Eqs

[41] The specialization of (16) to central fields is accomplished by setting $2(\beta-\alpha)=-2^{1/2}\epsilon=\gamma-\alpha=-(\delta-\alpha)$. This can be seen by noting that when $a=0$ the roots must agree with known electrostatic energies for p^2 or p^4 (e.g. Slater, Phys. Rev. **34,** 1293 (1929); Condon and Shortley, *ibid.* **37,** 1025 (1931)) and further with the Wigner rules for the compounding of orbital wave functions (e.g. Bartlett, *ibid.* **38,** 1623 (1931)). Making this specialization, but assuming $0<|a|\ll|\epsilon|$ one finds that the roots of (16) become

$$F_0+F_2-\frac{3}{2}a, \qquad F_0+F_2+a, \qquad F_0-5F_2, \qquad F_0+10F_2$$

in agreement with the energies of $^3D_1$, $^3D_2$, ^1P, ^3S respectively in Russell-Saunders coupling. The isolated root above (16) gives $^3D_2$. The notation $F_2=(\gamma-\alpha)/6$, $F_0=\alpha-F_2$ has been introduced to make our usage agree with Condon and Shortley's. The terms ^3D, ^1P, ^3S are not really allowed by the exclusion principle, but this discrepancy is a formal one which arises because our model is too simple to take cognizance of the "promotions" which take place when the limiting case of central fields is achieved by coalescence of two attracting centers. In the determinant for g^+ configurations which as mentioned above is similar in form to (16) the specialization appropriate to central fields is $\alpha=\delta$, $4(\beta-\alpha)=6\times2^{1/2}\epsilon=3(\gamma-\alpha)$, which makes (16) factor into two quadratics, and then the roots for $0<|a|\ll|\epsilon|$ reduce to the energies of $^3P_0$, $^3P_2$, ^1D, ^1S in Russell-Saunders coupling. (With the g configurations, $F_2=(\gamma-\alpha)/12$, $F_0=\alpha+5F_2$ and the isolated root gives $^3P_1$.)

[42] J. H. Bartlett, Jr., Phys. Rev. **34,** 1247 (1929); S. Goudsmit, *ibid.* **35,** 1325 (1930).

(7-9-10), on the other hand, were derived by perturbation theory and so presupposed this separation to be small. In iodine one has p^5+p^5 rather than $p+p$ (used to obtain 16) but as far as the secular structure is concerned the two cases are entirely similar except for reversal of the sign of a and different numerical values of the various constants. The small Greek letters σ, π in (16), etc. then specify $\Sigma\lambda$ for an atom rather than the λ of a single electron. It may be noted that Eq. (16) may be written in the form

$$W - \alpha + \tfrac{1}{2}a = \frac{(\theta_1 a + 2^{-1/2}\theta_2 a)^2}{W - \beta'} + \frac{(\theta_2 a - 2^{-1/2}\theta_1 a)^2}{W - \gamma'} + \frac{a^2}{2(W - \delta)} \cdot \quad (17)$$

in which it is to be observed that unfortunately the unknown W appears on the right as well as left side. Substitution of approximate values of W on the right reduces (17) to (7), and further to (10) if $\theta_1 = 1, \theta_2 = 0$. Here β', γ' denote the characteristic values $\frac{1}{2}(\beta+\gamma)+\frac{1}{2}[(\beta-\gamma)^2+4\epsilon^2]^{1/2}$ of the β, γ pair of states under omission of the spin-orbit distortion, while θ_1, θ_2 are defined by $\theta_1(\beta-\beta')+\theta_2\epsilon=0$, $\theta_1^2+\theta_2^2=1$. If one uses the root corresponding to $^3\Pi_u^-$, the right side of (17) is the width of the Λ-doublet, since the isolated state above (16) is undisplaced. With this root, the right side has the value $3a/2$ for $r=\infty$ if $^3\Pi_u^-$ is derived from $^2P_{3/2}+{}^2P_{3/2}$. Let us suppose that $a<0$, as is the case in I_2. Then if the Λ-components cross at some intermediate value of r, it is necessary that at least one of the denominators in (17) be positive, for otherwise the right side of (17) could never be positive for any r. This means that one of the $^3\Sigma_u^+$ or $^1\Sigma_u^-$ levels, say κ, exclusive of the spin-orbit correction, must lie below the $^3\Pi_{0u}^-$ level, inclusive of this correction. This agrees with statements on p. 552 except that the condition $W(^3\Pi_{0u}^-) - W_\kappa > 0$ given on that page is less severe than the more rigorous criterion $W(^3\Pi_{0u}^-) - W_\kappa{}^0 > 0$, for the spin-orbit interaction terms will depress κ since κ comes from $^2P_{3/2}+{}^2P_{3/2}$. The purely electrostatic energy $W_\kappa{}^0$ of κ is, of course, the same as the least of the three quantities β', γ', δ. It is to be emphasized that all the conclusions on the size and sign of the doublets in this paragraph apply only if it is legitimate to neglect interaction with configurations derived from excited atoms not included in (16).

$^2P+{}^2P'$. When now we turn to molecules (e.g. ICl) derived from different rather than similar ^2P atoms, the u-g classification is lost, and the factorization is into two quintics, one of which is

$$\begin{array}{l|ccccc|} \pi\sigma\ {}^3\Pi_0^+ & \alpha - \frac{1}{2}a_1 - W & \xi & 2^{-1/2}a_1 & \frac{1}{2}a_1 & \frac{1}{2}a_1 \\ \sigma\pi\ {}^3\Pi_0^+ & \xi & \beta - \frac{1}{2}a_2 - W & 2^{-1/2}a_2 & \frac{1}{2}a_2 & \frac{1}{2}a_2 \\ \sigma\sigma\ {}^1\Sigma^+ & 2^{-1/2}a_1 & 2^{-1/2}a_2 & \gamma - W & \eta & 0 \\ \pi\pi\ {}^1\Sigma^+ & \frac{1}{2}a_1 & \frac{1}{2}a_2 & \eta & \delta - W & -\frac{1}{2}(a_1+a_2) \\ \pi\pi\ {}^3\Sigma_0^- & \frac{1}{2}a_1 & \frac{1}{2}a_2 & 0 & -\frac{1}{2}(a_1+a_2) & \epsilon - W \\ \end{array} = 0 \quad (18)$$

The other quintic is like (18) except that the electrostatic constants $\gamma, \cdots, \eta$ (but not α, β) have different numerical values and that the labels are $\pi\sigma\ {}^3\Pi_0^-, \sigma\pi\ {}^3\Pi_0^-, \sigma\sigma\ {}^3\Sigma_0^+, \pi\pi\ {}^3\Sigma_0^+, \pi\pi\ {}^1\Sigma^-$.

Eq. (18) suggests the following explanation of the pseudo-crossing behavior discussed in connection with Fig. 3, section 2. Application of the transformation (8) to the two $\pi\pi$ states in (18) throws Eq. (18) into a form differing from (18) in that the elements of the fourth row and column become $2^{-1/2}a_1$, $2^{-1/2}a_2$, $2^{-1/2}\eta$, $\frac{1}{2}(\delta+\epsilon)-\frac{1}{2}(a_1+a_2)-W$; $\frac{1}{2}(\delta-\epsilon)$ and those of the fifth 0, 0, $2^{-1/2}\eta$, $\frac{1}{2}(\delta-\epsilon)$, $\frac{1}{2}(\delta+\epsilon+a_1+a_2)-W$. Hence if we set $\eta=\delta-\epsilon=0$ the determinant factors into a biquadratic and a single root $W=\frac{1}{2}(\delta+\epsilon+a_1+a_2)$. The latter is obviously then derived from ${}^2P_{3/2}+{}^2P_{3/2}$, since the magnetic terms for ${}^2P_{3/2}$, ${}^2P_{1/2}$ are respectively $\frac{1}{2}a$, $-a$. Let us assume that at ordinary values of r the energy order is $\sigma\sigma<\sigma\pi<\pi\sigma<\pi\pi$, as seems probable in ICl, and that $a_2<a_1<0$ (i.e. p^5 atoms). Then an extrapolation by means of the biquadratic will make the $\sigma\pi$ level appear derived from ${}^2P_{1/2}+{}^2P_{3/2}$ despite being the second lowest 0^+ level, for the two available 0^+ states obtained from ${}^2P_{3/2}+{}^2P_{3/2}$ will be absorbed by $\sigma\sigma\,{}^1\Sigma^+$ and the isolated root, whose potential curve will be crossed by $\sigma\pi\,{}^3\Pi_0{}^+$ at some large value of r. This crossing is, of course, removed when η, $\delta-\epsilon\neq 0$, and $\sigma\pi{}^3\Pi_0{}^+$ then comes from ${}^2P_{3/2}+{}^2P_{3/2}$, as explained on p. 556. Clearly the usual vibrational extrapolation will make this state appear derived from ${}^2P_{1/2}+{}^2P_{3/2}$ if the low roots of (18) are insensitive to η, $\delta-\epsilon$ at ordinary values of r. It appears quite likely that this is really the case. In the first place, η and $\delta-\epsilon$ both vanish if the λ's (or rather $\Sigma\lambda$ over an atom) are good quantum numbers. At ordinary values of r, to be sure, it may well be that $|\delta-\epsilon|\gg|a_1+a_2|$, meaning that the $\pi\pi$ states have a quantized resultant spin rather than much tendency towards J-J atomic coupling. Application of the transformation (8) to $\pi\pi$ is then a very bad approximation, for (8) diagonalizes spin-orbit terms at the expense of putting electrostatic exchange terms off the diagonal. Nevertheless the potential curve for $\sigma\pi\,{}^3\Pi_0{}^+$ would not be materially affected by η, $\delta-\epsilon$ if $|\beta-\gamma|$, $|\beta-\delta|\gg|\delta-\epsilon|$, $|\eta|$ i.e. if the $\pi\pi$ singlet-triplet separation and interaction with σ^2 is small compared to the distance between $\pi\pi$ and other configurations.[43] The Mulliken-Hund theory of united atoms lends considerable plausibility to this possibility, for the $\pi\pi$ configurations of p^5+p^5 seem to pass into states of the united atom representing a high degree of promotion. At large values of r, on the other hand $|\delta-\epsilon|$, $|\eta|$ may be small compared to $|a_1+a_2|$, and the above factorization into the biquadratic and isolated root is then clearly allowable except in the immediate vicinity of the crossing point.

When one considers the quintic for the five 0^- states, configuration theory suggests that $\sigma\sigma$ as well as $\pi\pi$ is higher than $\sigma\pi$ or $\pi\sigma$. Hence $\sigma\pi{}^3\Pi_0{}^-$, if less than $\pi\sigma{}^3\Pi_0{}^-$, extrapolates into ${}^2P_{3/2}+{}^2P_{3/2}$ even when a lone root is

[43] It is to be noted that the Π states are connected with the other states of (18) only by spin-orbit terms. Hence even if η, $\delta-\epsilon$ are not particularly small in magnitude compared to $\beta-\gamma$, $\beta-\delta$ at small values of r, the error made by setting $\eta=\delta-\epsilon=0$ may still be quite small as far as the Π roots of (18) are concerned, for with very small r the spin-orbit terms may be subordinate to $\beta-\gamma$, $\alpha-\gamma$, etc. At larger values of r, the spin-orbit interaction cannot, of course, be considered small, for it is of the same order as the separation between the two dissociation products between which we wish to differentiate.

factored off, for $\sigma\pi\,{}^3\Pi_0^-$ is then still the lowest root of the biquadratic. If this were not so and there were a lower 0^- level of the form $\sigma\sigma$, it is hard to see how the ${}^3\Pi_0^-$ component in iodine could be unstable, unless perchance the corresponding "hill" in Fig. 3 is very low. Indeed, if $W(\pi^{2\,2\mp1}\Sigma_u^{\mp}) > W({}^3\Pi_{0u}^-) > W(\sigma^2\,{}^3\Sigma_u^+)$ the same type of argument as used in the preceding paragraph could be used to remove a root from (16) instead of (18) and make ${}^3\Pi_{0u}^-$ appear derived from ${}^2P_{3/2}+{}^2P_{1/2}$. Hence in order to make the ${}^3\Pi_{0u}^-$ level unstable in I_2, as needed for our theory of magnetic predissociation, it is necessary to exclude the possibility of $\sigma^2\,{}^3\Sigma^+$ falling below ${}^3\Pi_{0u}^-$, even though such an arrangement might give the much-desired crossing of the Λ-doublet components (cf. page 552).

${}^2S+{}^2P$. The secular equation for ${}^2S+{}^2P$ is formally equivalent to that of the atomic configuration $sp\,{}^{1,3}P$ in an axially symmetrical electric field and hence is a generalization of Houston's[44] well-known equation for field-free atoms in this configuration. Only quadratics are involved, and the solution is

$$ {}^3\Pi_0^-,\ {}^3\Sigma^+\colon W = f(\alpha,\beta), \qquad\qquad {}^3\Pi_0^+,\ {}^1\Sigma^+\colon W = f(\alpha,\gamma) $$

with

$$ 2f(x,y) = x + y - \tfrac{1}{2}a_2 \pm \left[(x - y - \tfrac{1}{2}a_2)^2 + 2a_2^2\right]^{1/2} $$

Here α, β, γ denote the energies of ${}^3\Pi$, ${}^3\Sigma$, ${}^1\Sigma$ without the spin-orbit correction.

We have given only the secular equations characteristic of $\Omega = 0$, but those appropriate to other values of Ω can be constructed without undue difficulty.

The writer wishes to thank Professors R. S. Mulliken and L. A. Turner, also Dr. W. G. Brown for helpful discussions and correspondence.

[44] W. V. Houston, Phys. Rev. **33**, 297 (1929).

Relativity and the Uncertainty Principle

By N. ROSEN AND M. S. VALLARTA
Massachusetts Institute of Technology

(Received March 29, 1932)

A simple ideal experiment to measure simultaneously the position and momentum of a free electron, also its kinetic energy and the instant when this kinetic energy is measured, taking into account the finite velocity of propagation of light as embodied in the Lorentz transformation, is proposed. This experiment is as follows: an observer sends out a light signal which strikes a given free electron and returns along its own track. From measurements made on the outgoing and returning signals the required quantities, and the uncertainties in their measurement, are calculated. In the absence of detailed knowledge concerning the nature of the interaction between the signal and the electron, it is found that for any electron velocity between 0 and c, $\Delta p \Delta x$ and $\Delta E \Delta t$ have an upper and a lower bound. The upper bound depends only on the initial electron velocity and the lower bound is a function of the electron velocity and the outgoing frequency. These bounds come close together for low electronic velocities and low frequencies, but their separation increases as the initial electron velocity increases becoming infinite in the limit $v=c$. In the limit $c \to \infty$ the upper and lower bounds coalesce for all frequencies and all electron velocities giving Heisenberg's results. The possibility, but not the necessity, of a relativistic quantum mechanics with $\Delta p \Delta x = h$ (and $\Delta E \Delta t = h$) is, we believe, established by the present results.

1.

CLASSICAL nineteenth century mechanics may be characterized from the contemporary point of view by the statement that it takes cognizance neither of the finite velocity of propagation of light nor of the dualism between particles and waves. The recognition of the significance of the first fact gave birth to relativistic mechanics, that of the second to quantum mechanics. Historically these two far-reaching theories have been built up successively and rather independently; that this independence could not logically be preserved was strongly felt from the earliest stages of the development of quantum mechanics, but that the finite velocity of propagation of the electromagnetic field plays a prominent rôle in atomic physics was first forcibly brought out by Dirac's theory of the electron spin.

It is well known that the introduction of a finite velocity of propagation into the body of quantum mechanics is beset with grave difficulties and sometimes leads to conclusions (e.g., energy interchange between field and electron) grossly at variance with experiment. While some of these difficulties (e.g., infinite self-energy of the electron) have now been throughly analyzed, it has become increasingly apparent in the course of these investigations that it is not enough to fasten as an afterthought the requirement of Lorentz invariance on the equations of quantum mechanics. Relativistic mechanics and quantum mechanics are in point of fact generalizations of classical mechanics along very different directions, so that *a priori* there is nothing to insure their common consistency. The present paper is intended as an elementary contribution to the analysis of this fundamental question.

Just as relativistic mechanics follows from Einstein's definition of simultaneity, so the kernel of quantum mechanics is found in Heisenberg's uncertainty principle. Hence any attempt to prove the inner consistency (or inconsistency) of relativistic and quantum mechanics reduces in essence to an investigation of whether or not the relativistic definition of simultaneity is consistent with the uncertainty relations, or vice versa. The suggestion has already been made by Schrödinger[1] that these two are incompatible, and to this source might then be ascribed the difficulties mentioned above. *A priori* there is nothing to insure the validity of the uncertainty relations when relativistic notions are taken into account, nor is there any reason to accept *a priori* the relativistic method of measuring time intervals and synchronizing clocks if the measurement of time by means of a clock is to be placed on an equal footing with other physical measurements. This remark opens up two possible methods of attack of the problem of discovering a suitable guiding principle in relativistic quantum mechanics: either one postulates the validity of Einstein's definition of simultaneity (and hence of the Lorentz transformation) and tries to devise an ideal experiment, of the nature of Heisenberg's experiment with a gamma-ray microscope, to deduce the uncertainty relations, or one assumes the uncertainty relations and then attempts to see what modifications are necessary in the definition of simultaneity. The latter is the method chosen by Schrödinger,[1] the former the method of the present paper. Still another conceivable procedure would be to give up both and try to build up a more general theory in which the present quantum theory and the present relativity theory would appear in the limits $c\rightarrow\infty$ and $h\rightarrow 0$, respectively. This requirement, incidentally, applies just as well to either of the above methods of approach. The absence of a sufficiently secure starting point, however, seems to preclude for the present the effective use of the last method of attack.

There are as a matter of fact good reasons to suppose that the Lorentz transformation plays a fundamental part in atomic phenomena and therefore should be taken as the starting point of any new discussion. Experimentally we know that such phenomena play their parts in the same space-time as other physical processes, we further know that gravitational forces play a very small part in the atomic world and, on the theoretical side, that the laws governing atomic processes must be independent of the frame of reference. As already intimated previously, and for the reasons just stated, in this paper we take the standpoint that the Lorentz transformation is valid for elementary processes and attempt to devise a simple experiment to measure simultaneously the momentum and position of a free electron, also its kinetic energy and the instant when this kinetic energy is measured. The difference between our analysis and previous ones is that we try in this way to take into account the finite velocity of propagation of light in an experiment otherwise similar to Heisenberg's experiment with a gamma-ray microscope. His results should then appear here in the limit $c\rightarrow\infty$.

[1] E. Schrödinger "Spezielle Relativitätstheorie und Quantenmechanik," Sitz. der preuss. Akad. der Wiss. p. 238, 1931.

2.

We propose the following ideal experiment: An observer O sends a spectral line, emitted by a single atom, of mean frequency ν_1 and natural width $\Delta\nu_1$ (hereafter called the "signal") towards a remote free electron (i.e., moving in a straight line with uniform velocity). The signal may or may not return to the observer; we may, however, assume without incurring logical difficulties that it does return. The returning signal is a spectral line of mean frequency ν_2 and natural width $\Delta\nu_2$, arriving after a time T. In general $\nu_1 \neq \nu_2$ and $\Delta\nu_1 \neq \Delta\nu_2$ because of the interaction between signal and electron (Doppler and Compton effects). It is required, first, to find the momentum p and the position x of the electron at the time when it received the signal, and the product $\Delta p \Delta x$ of the uncertainties in the measurement of p and x; second, the kinetic energy E and the instant t when this kinetic energy was measured, and the product $\Delta E \Delta t$ of the uncertainties in the measurement of E and t.

Two essential methodical remarks may properly find expression at the outset. The first refers to the use of the Lorentz transformation. For reasons already stated we assume the validity of the latter in order to correlate events in the electron's reference system with events in the observer's frame of reference. While doing so we are fully aware of the difficulties attending the synchronization of clocks considered as quantum mechanical systems which have already been discussed by Schrödinger.[1] However, whereas he is interested in fitting relativity into the framework of quantum mechanics, we take here the converse point of view and therefore his difficulties do not concern us here.

The second remark refers to the general argument for the calculation of the uncertainties of our experiment.[2] We start from the particle picture, assuming a head-on collision between a photon (or a group of photons) and an electron governed by the classical laws of conservation of energy and of momentum. Secondly we introduce the wave picture assuming that the observer sends out a finite wave train which returns to him, after the interaction with the electron, as a finite wave train. Thirdly we show that the observation reacts on the observed object so as to spoil the initial state. The fourth and most important point is to see why the reaction is indeterminate within certain limits.

Finally, since the signal reaches the observer *after* the interaction has taken place, our determination of the momentum and position necessarily refers to an event which has taken place in the past, and so do the corresponding uncertainties. From the relativistic point of view it seems unavoidable that the uncertainty relations, if valid, must hold for the past as well as the future.

In the present example the combination of the wave picture with the particle picture gives the Doppler and Compton effects, the observation unavoidably spoils the initial state because of the collision between signal and electron, and the reaction is indeterminate within limits to be presently calcu-

[2] See C. G. Darwin, "Examples of the Uncertainty Principle", Proc. Roy. Soc. of London **A130,** 632 (1931).

lated because we do not know just where within the finite wave train the photons are, nor as a consequence just where or when within the wave trains the collisions take place.

3.

The spectral line of mean frequency ν_1 and natural width $\Delta\nu_1$, due to a quantum emission from a single atom may be described from the corpuscular point of view either as a single photon of energy $h\nu_1$ or as a group of photons of energies roughly between $h(\nu_1-\Delta\nu_1/2)$ and $h(\nu_1+\Delta\nu_1/2)$ and total energy $h\nu_1$. From the wave standpoint our signal is described as a finite wave train of n waves, and from simple optical considerations it follows that

$$\Delta\nu_1/\nu_1 \doteq 1/n \tag{1}$$

where the symbol $\doteq$ is used for "approximately equal to".

Let now the frequency of the outgoing signal as measured by the observer in his own reference system be ν_1. Applying a Lorentz transformation we find for the frequency ν_1' of this signal in the electron's frame of reference S'

$$\nu_1' = \nu_1\mu, \quad \mu = (1-\beta)^{1/2}/(1+\beta)^{1/2} \tag{2}$$

where $\beta=v/c$ as usual and v is the electron's velocity relative to S. After the collisions the photons (or photon) return to the observer along their own track, by hypothesis. The frequency ν_2' in S' after the interaction is, by the ordinary theory of the Compton effect

$$\nu_2' = \nu_1'/(1+2\alpha\nu_1'), \quad \alpha = h/m_0c^2. \tag{3}$$

Transforming back to S we find for the frequency of the returning signal[3]

$$\nu_2 = \nu_1\mu^2/(1+2\alpha\mu\nu_1). \tag{4}$$

Eq. (3) is derived on the assumption that the electron is initially at rest in S', that is, that it is moving with its initial velocity v_1 with respect to S. The factor μ in (4) therefore refers to the initial velocity v_1 and we may solve (4) for μ to find this initial velocity. We obtain

$$\mu_1 = \alpha\nu_2 + (\alpha^2\nu_2^2 + \nu_2/\nu_1)^{1/2}, \tag{5}$$

where $\mu_1=(1-\beta_1)^{1/2}(1+\beta_1)^{1/2}>0$. From this we obtain the momentum p,

$$p = \frac{m_0c\beta_1}{(1-\beta_1^2)^{1/2}} = \frac{m_0c}{2}\,\frac{1-\mu_1^2}{\mu_1}. \tag{6}$$

If the outgoing and returning frequencies were known exactly, the exact value of the initial momentum would be given by (6) and there would be no uncertainty in its measurement in terms of ν_1 and ν_2. But all that we do know is that ν_1 lies somewhere within a frequency range of width $\Delta\nu_1$, and similarly ν_2. Hence the value of p is also uncertain by an amount Δp which from elementary calculus is given by

[3] Of course the same result is obtained starting from the conservation of energy and momentum with respect to S.

$$\Delta p = \left|\frac{\partial p}{\partial \nu_1}\right| \Delta\nu_1 + \left|\frac{\partial p}{\partial \nu_2}\right| \Delta\nu_2. \tag{7}$$

We now inquire what is the relation between the widths $\Delta\nu_1$, $\Delta\nu_2$ of the outgoing and returning signals. If we start from the classical picture (the signal is a finite wave train of n waves, the electron is a corpuscle) we immediately obtain the relation $\Delta\nu_1/\nu_1 = 1/n \doteq \Delta\nu_2/\nu_2$ or $\Delta\nu_1/\Delta\nu_2 = \nu_1/\nu_2$ for then classical electrodynamics gives the result that the number of oscillations in the incident wave train is the same as the number of waves in the returning wave train, and relativistically this number is an invariant. If, however, we assume that (4) is a relation holding for each component frequency of the outgoing and returning signals, in other words that each frequency band of infinitesimal width is shifted by an amount given by (4), then we may differentiate (4) with μ_1 constant to find the relation between $\Delta\nu_1$ and $\Delta\nu_2$ obtaining,

$$\frac{\Delta\nu_1}{\Delta\nu_2} = \frac{\nu_1/\nu_2}{1 + 2\alpha\mu\nu_1}. \tag{8}$$

Eq. (8) means that the ratio $\Delta\nu_2/\nu_2$ of the shifted Compton line (i.e., the returning signal) depends upon the velocity of the scattering electron; the classical formula $\Delta\nu_2/\nu_2 = \Delta\nu_1/\nu_1$ says that it is independent of this velocity. It is immediately seen that (8) reduces to the classical result in the limit $h \to 0$. Experimentally there does not seem to be any definite evidence as to whether or not $\Delta\nu_2/\nu_2$ depends on the velocity of the scattering electron, but in spite of this it seems that (8) has more in its favor than the classical formula.

From (5), (6), (7) and (8) we find for the uncertainty Δp

$$\Delta p = \frac{m_0 c}{(1 - \beta_1^2)^{1/2}} \frac{1}{1 + \alpha\mu_1\nu_1} (\Delta\nu_1/\nu_1). \tag{9}$$

4.

We now turn our attention to the measurement of the position x of the electron at the instant when the interaction takes place and the uncertainty in the measurement of x.

The wave picture of the interaction leads at once to the result that the latter lasts a finite time τ. Suppose now that a rough average velocity of the electron during the interaction is given by $c\beta$. Then the total elapsed time T measured by the observer between the instant when the signal is sent out and that when it returns is, approximately,

$$T = x/c + \tau + (x + c\beta\tau)/c. \tag{10}$$

From which we find for x

$$x = \frac{c}{2}(T - (1 + \beta)\tau). \tag{11}$$

Again we see immediately that x would be exactly known if we could measure T with an arbitrary precision and if we could find β and τ. Assuming that T

can be so measured, since according to our formulation of the problem there is nothing in principle to prevent measuring a time interval with any arbitrary accuracy, it remains to discuss the determination of β and τ.

In the absence of a detailed theory concerning the nature of the interaction between the electromagnetic field of the outgoing wave and the electron, neither the "mean velocity" βc nor the duration of the interaction τ can be calculated. But even if we had complete and detailed information on the nature of the interaction we could not thereby find the exact value of $(1+\beta)\tau$ because it depends essentially on a knowledge of where within the wave packet the interacting particles are, and this in its nature is unknowable. Roughly one could say that this term would be greatest if the interacting particles were near the head end of the wave packet and smallest if near the tail end. Eq. (11) thus consists of two parts, one $cT/2$ which in principle can be measured as accurately as we like and another $(1+\beta)c\tau/2$ which contains elements which fundamentally cannot be known exactly, but to which only a greatest and a smallest value can be assigned. The latter term therefore causes an uncertainty in our knowledge of x.

We now proceed to estimate the value of Δx. Let $\beta_1 c$ and $\beta_2 c$ be the initial and final electron velocities respectively. Then obviously β_1 and β_2 are the smallest and largest values of β. The duration of the interaction can be roughly estimated by noting that it is equal to the time it would take for the wave train to go past the electron if no interaction had taken place. Referred to the electron's frame of reference S' this time is

$$\tau' = n\lambda_1'/c = 1/\Delta\nu_1'. \tag{12}$$

At this point a peculiar relativistic difficulty makes its appearance. Referred to the electron's reference system S' the duration of the interaction is immediately seen from (12) to be independent of its own motion, but referred to the observer this duration depends on its relative velocity with respect to the electron. We may easily assign upper and lower limits to the value of this quantity as it appears to the observer. If the velocity of the electron throughout the time had been the initial velocity $\beta_1 c$ then, transforming back to S, we find that with respect to the observer this time is

$$\tau_1 = n\lambda_1/c(1-\beta_1) = \tau_{\min} \tag{13}$$

and if the velocity had been the final velocity $\beta_2 c$ then

$$\tau_2 = n\lambda_1/c(1-\beta_2) = \tau_{\max}. \tag{14}$$

Using (11) we may now caculate the greatest and the least values of x. The greatest value is obtained when $(1+\beta)\tau$ has its smallest value $(1+\beta_1)\tau_{\min}$ which gives

$$x_{\max} = \frac{c}{2}(T - n\lambda_1/c\mu_1^2) \tag{15}$$

and the least value is similarly

$$x_{\min} = \frac{c}{2}(T - n\lambda_1/c\mu_2^2). \tag{16}$$

Hence

$$\Delta x_{\max} = x_{\max} - x_{\min} = \frac{n\lambda_1}{2}(1/\mu_2^2 - 1/\mu_1^2). \tag{17}$$

A more moderate estimate would be reached as follows: Suppose that τ has its greatest value $\tau_{\max}$ given by (14). Then if the electron had moved with its initial velocity throughout this time, x would be

$$x_1 = \frac{c}{2}(T - (1 + \beta_1)\tau_{\max}) \tag{18}$$

instead of (15) ($x_1 < x_{\max}$), and if it had moved with its final velocity through this time, then x would be

$$x_2 = \frac{c}{2}(T - (1 + \beta_2)\tau_{\max}) = x_{\min} \tag{19}$$

which is the same as (16). Hence on this assumption

$$\Delta x = \frac{n\lambda_1}{2}(\beta_2 - \beta_1)/(1 - \beta_2) \tag{20}$$

and of course $\Delta x < \Delta x_{\max}$.

A minimum value of Δx would be obtained if the time τ had its least value $\tau_{\min}$ given by (13). The same argument then gives

$$\Delta x_{\min} = \frac{n\lambda_1}{2}(\beta_2 - \beta_1)/(1 - \beta_1). \tag{21}$$

Thus from a relativistic point of view the best we can do is to assign upper and lower bounds to the value of Δx. It follows immediately that only upper and lower bounds can be assigned to $\Delta p \Delta x$.

5.

From (9), (17) and (21) we find

$$\Delta p \Delta x_{\max} = \frac{m_0 c^2}{2(1 - \beta_1^2)^{1/2}} \frac{1}{\nu_1(1 + \alpha\mu_1\nu_1)}(1/\mu_2^2 - 1/\mu_1^2), \tag{22}$$

$$\Delta p \Delta x = \frac{m_0 c^2}{2(1 - \beta_1^2)^{1/2}} \frac{1}{\nu_1(1 + \alpha\mu_1\nu_1)}(\beta_2 - \beta_1)/(1 - \beta_2), \tag{23}$$

$$\Delta p \Delta x_{\min} = \frac{m_0 c^2}{2(1 - \beta_1^2)^{1/2}} \frac{1}{\nu_1(1 + \alpha_1\mu_1\nu_1)}(\beta_2 - \beta_1)/(1 - \beta_1). \tag{24}$$

The initial and final velocities of the electron are related by the conservation of energy $m_1c^2+h\nu_1=m_2c^2+h\nu_2$ (m_1 = electron mass at velocity $\beta_1 c$; m_2 = electron mass at final velocity $\beta_2 c$). Solving this equation for β_2 we have

$$\beta_2 = [1 - 1/(\alpha(\nu_1 - \nu_2) + (1 - \beta_1^2)^{-1/2})^2]^{1/2}$$

which upon substitution in (22), (23) and (24) gives

$$\Delta p \Delta x_{\max} = h/(1 - \beta_1), \tag{26}$$

$$\Delta p \Delta x = h, \tag{27}$$

$$\Delta p \Delta x_{\min} = h(1+ \mu_1^2)/[(1+ 2\alpha\mu_1\nu_1)^2 + \mu_1^2]. \tag{28}$$

We note at once that in the limit $c\to\infty$ all these values coalesce to the value h in agreement with Heisenberg's results.

A plot of (26), (27) and (28) as a function of ν_1 is given in Fig. 1. From (26) we see that $\Delta p \Delta x_{\max}$ becomes infinite as $\beta_1\to 1$. This of course means physically

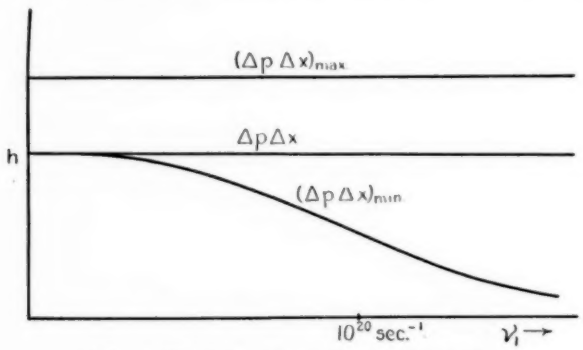

Fig. 1. Typical curves of $\Delta p \Delta x$ for $\beta_1 < 1$.

that in this limit the signal never overtakes the electron and consequently its position becomes wholly uncertain. Taking (26) as the upper bound of the uncertainty relation, it is seen from the plot that the upper and lower bounds diverge as the frequency increases and as the electron velocity increases, but always enclose between them a value of $\Delta p \Delta x$ of the order of magnitude of h. Up to frequencies of the order of magnitude of the Compton frequency $m_0c^2/h \doteq 10^{20}$ sec^{-1} and for moderate electronic velocities the upper and lower bounds define a region where $\Delta p \Delta x$ is of the order of magnitude of h; it is only beyond this frequency that $\Delta p \Delta x$ may have a different order of magnitude. It thus seems as if the electron might begin to behave abnormally when the energy of the colliding photon becomes comparable with its own intrinsic energy or when it has a very high kinetic energy. As the initial electron velocity increases, (27) and (28) become more nearly equal until in the limit $\beta_1\to 1$, (27) and (28) coalesce for all frequencies.

It need hardly be emphasized that the present results contain nothing against the validity of the Heisenberg uncertainty relation in relativistic quantum mechanics. It merely goes to establish the *possibility* but not the *necessity* of a relativistic quantun. mechanics with $\Delta p \Delta x \doteq h$. The possibility

of a relativistic quantum mechanics with $\Delta p \Delta x$ a function of the electron velocity and the frequency remains as yet open. It may be that a more complete knowledge of the nature of the interaction between field and electron will lead to $\Delta p \Delta x \doteq h$ uniquely. In principle, the self-consistency of a relativistic quantum mechanics with $\Delta p \Delta x \doteq h$ is, we believe, established by the present investigation.

6.

It remains now to find the kinetic energy E, the time t when this kinetic energy was measured and the product $\Delta E \Delta t$ of the uncertainties in the measurement of these two quantities. Now any measurement which determines the momentum of a free electron in principle also determines its kinetic energy, and any measurement to find the position fixes the time when this position was occupied in the experiment. By the same argument the uncertainty in the energy is fixed by the uncertainty in the momentum, and the uncertainty in the time is fixed by the uncertainty in the position. An argument which is essentially a repetition of the above method of reasoning and involves the relation $\Delta t \doteq \Delta x / v_1$ leads to the results

$$\Delta E \Delta t_{\max} = \Delta p \Delta x_{\max} \tag{29}$$

$$\Delta E \Delta t = \Delta p \Delta x \tag{30}$$

$$\Delta E \Delta t_{\min} = \Delta p \Delta x_{\min}. \tag{31}$$

The details add nothing essential to our previous results and are omitted.

Notes on the Luminescence of Glass and Fluorite

By THEODORE LYMAN
Jefferson Physical Laboratory, Harvard University
(Received April 1, 1932)

In the first part of this paper a simple method for showing the relation between the absorption of light and the resulting luminescence in glass is described. The second part contains some observations on the luminescence of clear and colored fluorites and of quartz in the extreme ultraviolet. In the case of clear colorless fluorite light on the short wave-length side of the absorption limit at λ1230 is responsible for luminescence in the visible and also in the ultraviolet. This ultraviolet luminescence seems to consist of two parts. In the first place, there is a rather strong, broad band extending from the neighborhood of λ2450 to λ3810. Secondly, in the second there are sharp lines at λ3812, λ3144 and λ3133.

IT IS a commonplace in physics that absorption is necessary to the emission of light by luminescent substances. The following experiment affords a simple means of demonstrating this fact.

The only apparatus required is a small quartz spectrograph and a condensed spark between metal terminals. A piece of microscope cover glass about 0.1 mm thick is placed inside the plate-holder in contact with the photographic plate. A second piece of the same glass may be placed in front of the slit when required.

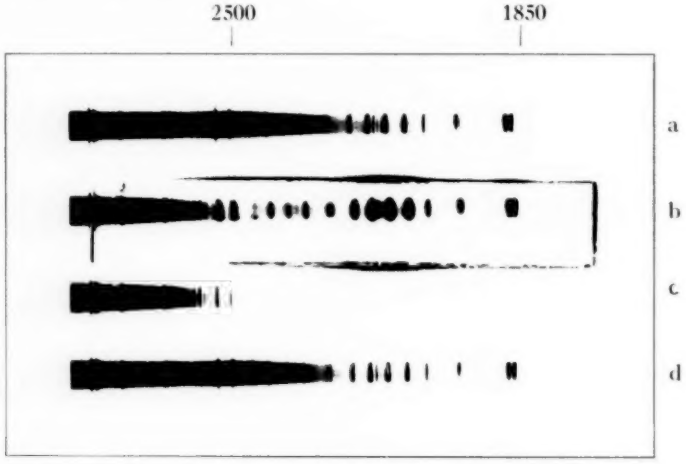

Fig. 1.

Fig. 1. illustrates the nature and results of the experiment; (a) Is the spark spectrum of aluminium and zinc. (b) Is this same spectrum taken through the strip of glass in contact with the plate. (c) Shows the result of placing a bit of cover glass in front of the slit. With a "Seed 23" plate the time of exposure was thirty seconds in each case.

If attention is fixed on (b) it is obvious that the spectrum lines are transmitted through the glass up to the limit set by absorption; in this region they are quite sharp. On the violet side of this point the broader impressions on the photographic plate are due to the luminescence of the glass. A broad line corresponds to each sharp line in the spark spectrum; the effect continues throughout the length of the plate to the aluminum pair at λ1862–54.

This simple experiment demonstrates that the luminescent light is due to the part of the spectrum which lies within the absorption band of the glass.

The same effect is shown by clear colorless fluorite. All the specimens of this quality which have been used were from Zell in Baden. When tested in a vacuum spectroscope they were all found to be of excellent transparency down to the limit of the Schumann region near λ1230. A given specimen was placed in contact with the photographic plate, usually a "Seed 23", sensitized with Nujol and this plate in turn was introduced into a vacuum spectroscope. A hydrogen tube served as source. In the resulting spectrum the lines on the long wave-length side of λ1230 were transmitted through the fluorite, but on the other side of the absorption limit each spectrum line gave rise to luminescence in the fluorite which was recorded on the photographic plate in a number of broad lines.

It is well to note that the effect with glass differs from that with fluorite in one particular. For while with the former substances every strong line in the spectrum excites luminescence throughout the spectral range of the quartz spectrograph, with fluorite the action is confined to a rather limited region from about λ1230 to the neighborhood of λ990. Beyond this point strong spectral lines excite no luminescence. This fact has been checked by substituting a continuous and a disruptive discharge in helium and a hot spark, for the hydrogen tube source.

One is reminded of some results of Gudden and Pohl[1] on the electric conductivity produced in solids by the action of light. These investigators found that the group of wave-lengths which was responsible for the observed result was situated within the optical absorption band of the solid in question, but was limited to a region near the long wave-length side of this band. The luminescence of clear fluorite seems to obey the same general rule. This relation may prove true even for glass if the spectral area is extended into the extreme ultraviolet.

The position in the spectrum of the ultraviolet light excited in clear fluorite by radiations in the extreme ultraviolet was determined in the following manner.

A discharge tube of the internal capillary type was used closed at the end opposite the capillary by a plate of clear, colorless Zell fluorite some 2 mm thick. Matters were so arranged that a number of screens of different materials could be interposed in turn between the end of this capillary and the fluorite window. The essential feature of the device by which this was accomplished consisted in a windlass-like arrangement operated from outside by means of a stopcock. The screens were of course entirely within the discharge

[1] Gudden and Pohl, Phys. Zeits. **23,** 419 (1922).

tube, their distance from the internal capillary being about 14 millimeters, and from the window about 4 millimeters. The discharge tube was filled with hydrogen at a pressure of a few millimeters. The luminescence was studied by means of the small quartz spectrograph already mentioned arranged to view the fluorite window edge on. The first experiment was made with the light from the end of the capillary falling directly on the flurite window. With a "Seed 23" plate an exposure of one half hour showed a broad band extending from λ2450 to λ3810 with a maximum near λ2900 and also certain fairly sharp lines at λ3812, λ3144 and λ3133. To make sure that these radiations were really due to the luminescence of fluorite, another series of exposures were made on the same plate. In the first a piece of cover glass was interposed between the capillary and the window; in the second, a screen of fused quartz was interposed and in the third a piece of fluorite transparent to the Schumann region was employed. In the first two cases, the band just mentioned was absent, in the last case the band was very feeble but the lines were relatively strong. Now experiment had shown that the cover glass transmitted to λ2500, while the quartz and fluorite cut off the spectrum near λ1525 and λ 1230 respectively. The glass was therefore fairly transparent to the region occupied by the band in question while both the quartz and fluorite were very transparent to this region. All the screens were opaque to light of shorter wave-length than λ1230.

Since the band was very feeble even when fluorite was used as a screen, we may conclude that it is chiefly excited by light of shorter wave-length than λ1230. Since the lines did not appear when quartz was used and as they were present when fluorite was employed as a screen, it seems probable that these radiations are partly due to light lying between the absorption limit of the specimen of fused quartz at λ1525 and that of fluorite at λ1230.

In this connection it is interesting to recall that Winkelmann and Straubel[2] have shown that fluorite, excited by x-rays, gives out a luminescent radiation in the form of a band extending from near λ2330 to λ3960 with a maximum near λ2800.

Line spectra in the luminescent light from fluorite were observed by H. W. Morse[3] many years ago. He worked almost entirely with colored specimens. Curiously enough he found that the character and position of the lines depended not only on the particular specimen of the mineral employed but also upon the character of the exciting source; an observation rather at variance with the results of some later experimenters.

The work of Urbain[4] on the presence of rare earths in fluorite is well known. It is probable that the lines which I have observed in the luminescent spectrum of clear, colorless specimens of this mineral are due to traces of these rare earths. On the other hand it is just possible that the presence of these lines has a more fundamental meaning.

Lau and Reichenheim[5] have found that the visible phosphorescence of

[2] Winkelmann and Straubel, Wied. Ann. **59,** 339 (1896).

[3] H. W. Morse, Astrophys. J. **21,** 83 (1905); Proc. Am. Acad. XLI, 590 (1906).

[4] Urbain, Ann. de Chem. et de Physique **18,** 222 and 289 (1909).

[5] Lau and Reichenheim, Ann. d. Physik **12,** 69 (1932).

colorless fluorite is strongly excited by light near the short wave-length limit of the Schumann region. I have checked this observation for Zell fluorite. Visible phosphorescence is also excited in this mineral but to a much feebler degree by light from a condensed spark between aluminium terminals in air. Since the effect is cut off by cover glass but is only slightly weakened by quartz, and since the phosphorescence occurs even when the spark is distant several centimeters from the fluorite, it would seem that the wave-lengths of the stimulating light must lie between the limit of transparency of cover glass and that of two or three centimeters of air, i.e., between λ2500 and say λ1800. As far as I am aware no strong absorption of fluorite has been discovered in this region. The action then is probably due to light only slightly absorbed over a wide range of wave-lengths.

One specimen of fluorite from Derbyshire described as white and investigated by Nichols and Merrill,[6] had a slight but well-marked absorption near λ4240 and was luminescent in the visible. The material however may well have been of very different composition from that which I have investigated.

One fact is important to remember. The brightness of the phosphorescence excited by the spark in air is no indication of the transparency of the particular specimen of fluorite in the extreme ultraviolet. This fact was demonstrated by testing the transparency of a number of pieces of clear, colorless fluorite with a vacuum spectroscope and then observing the brightness of the luminescence from the same pieces when excited by the light from an aluminum-zinc spark. A number of specimens all cut from crystals coming from the same source, namely from Zell in Baden, showed nearly the same transparency in the extreme ultraviolet but exhibited great differences in the intensity of their visible luminescence.

The phenomenon exhibited by fluorite of poor transparency are somewhat different from those just described. A piece of clear and apparently colorless fluorite when examined in the vacuum spectroscope showed very marked absorption between λ1600 and λ1300, but in this region no luminescence appeared to be excited. Total absorption occurred beyond λ1250. Beyond this region the specimen behaved much like the excellent Zell mineral, that is to say, strong lines in the hydrogen spectrum near the absorption limit produced luminescence. In this case therefore absorption is a necessary but not a sufficient condition for luminescence.

Three specimens of colored fluorite were next examined. In nearly all cases a strong absorption began near λ1700. On the short wave-length side of this limit and near it, luminescence was excited. Then followed a region of complete absorption without luminescence or with only the faintest trace, extending to near λ1250, and then a region in which each strong spectral line gave rise to secondary radiation very much as in the case of the colorless fluorite just described.

It seems likely therefore that in the case of these colored fluorites two regions of absorption exist one beginning near λ1700 the other near λ1250. Near both these regions luminescence is excited.

[6] Nichols and Merritt, Phys. Rev. [1] **19,** 31 (1904).

A number of specimens of crystalline quartz were also examined. The limit of absorption was in the neighborhood of λ1500. Only very feeble luminescence seemed to be excited; in fact it is doubtful if the phenomenon exists at all.

With fused quartz the case is different. Absorption begins strongly near λ1525; luminescence is excited but only for a very limited region close to the edge of this absorption band.[7]

I am much indebted to Mr. H. W. Leighton who has carried out much of the experimental work described in this paper.

[7] Compare Webb and Messenger, Phys. Rev. **34,** 1463 (1929).

The Dielectric Behavior of Colloidal Particles with an Electric Double-Layer

By J. B. Miles, Jr. and H. P. Robertson
Experimental Station, E. I. du Pont de Nemours and Company
and
Department of Physics, Princeton University

(Received March 19, 1932)

The dielectric behavior of colloidal particles is treated mathematically. The particles are assumed to be spheres and the electric double-layer is represented by a concentric conducting shell. Assuming that the conductivity of the shell is large compared with that of the particle and that its thickness is small compared with the radius of the particle, the relaxation time in sec. is given by $3\epsilon a/8\pi c^2\lambda_2 d$ where ϵ is the dielectric constant of the material of the particle, a its radius in cm, c the ratio of the e.m.u. to the e.s.u., λ_2 the conductivity of the shell in e.m.u., and d its thickness in cm. A distribution of particle size is assumed, and by the use of Wagner's treatment of non-homogeneous media expressions are obtained for the capacity and power factor as functions of the frequency. It is thus shown that the dielectric behavior predicted by Wagner for an assemblage of spheres having different specific conductivities may also result from an assemblage of colloidal particles of non-uniform size.

Introduction

A CONSIDERABLE number of theories have been proposed in explanation of the mechanism of power loss in liquid and solid dielectrics under alternating electric stress. Some materials behave in a simple manner in that the power loss can be calculated from the dielectric constant and the direct-current conductivity. Many materials are not so simple and the theories proposed for them follow one of two general lines. They consider either that the material is made up of a mixture of substances which separately behave in a simple manner, or that the material itself has an inherently complex behavior.

The theories dealing with the complex behavior of the material are based on the assumption of anomalous conductivity, dielectric hysteresis, or, more recently, the rotation of dipoles acted upon by viscous forces as treated by Debye.[1]

Maxwell[2] treated the case of a non-homogeneous material consisting of layers of simple dielectrics with different dielectric constants and conductivities and showed that an absorption current was to be expected. Grover[3] has shown that this would result in a change of the dielectric constant with frequency and a power factor different from that which would be calculated using the direct-current resistance.

* Contribution No. 57 from the Experimental Station of E. I. du Pont de Nemours and Company.

[1] P. Debye, "Polar Molecules," Chemical Catalog Co., p. 77, New York, 1929.

[2] J. C. Maxwell, "Treatise on Electricity and Magnetism," Oxford University Press, New York, 1928.

[3] F. W. Grover, Bull. Bur. Stand. **7**, 519 (1911).

By assuming the material to be made up of elements of different relaxation times, whose nature is no more specifically described, von Schweidler[4] has shown that the dielectric behavior of certain materials can be explained. Using the experimentally determined charge and discharge currents, he has developed by means of the superposition principle (Hopkinson-Curie) expressions for the behavior of the power factor and capacity as functions of frequency.

Wagner[5] has considered a distribution law for the time constants proposed by von Schweidler and then has made use of this distribution in an extension of Maxwell's theory[6] in which the medium is supposed to consist of spheres of differing conductivities imbedded in a non-conducting medium. It should be remarked that the radii of the spheres play no part in the expression for the time constants of the material.

Murphy and Lowry[7] have proposed a mechanism to explain power loss in solid and liquid dielectrics. They assume (a) that the material contains insulating particles on which are adsorbed ions of both charges, (b) that under

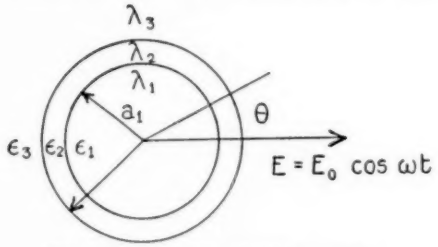

Fig. 1. Model of colloidal particle.

the influence of a field an ion can move freely over the surface, (c) that the ion cannot leave the surface until a critical voltage is attained, and (d) that the concentration of ions decreases at increasing distance from the interface. They consider that the particle alone is electrically equivalent to a pure capacity and that the ions beyond the interface are equivalent to parallel capacities with series resistances of different values, and therefore with different relaxation times. They then set up expressions for the capacity and power factor of such a system of condensers, but the constants which are involved are not determined.

Theory

We shall here consider a mechanism somewhat similar to that of Murphy and Lowry. The dielectric is assumed to consist of poorly conducting particles surrounded by ionic atmospheres and imbedded in a non-conducting medium. We wish to consider the effect of the size of the particles upon the power factor and dielectric constant. For the purpose of mathematical treatment the particles are represented by spheres and the ionic atmospheres by concentric shells of a certain conductivity. The model is drawn in Fig. 1 and corre-

[4] E. von Schweidler, Ann. d. Physik **24,** 711 (1907).
[5] K. W. Wagner, Ann. d. Physik **40,** 817 (1913).
[6] K. W. Wagner, Arch. Elektr. **2,** 371 (1914).
[7] E. J. Murphy and H. H. Lowry, J. Phys. Chem. **34,** 598 (1930).

sponds roughly to the accepted picture of colloidal particles possessing an electric double-layer. The conductivity of the atmosphere surrounding a colloidal particle undoubtedly varies with the distance from the surface but it is here considered to be lumped into an equivalent conducting layer of a certain thickness.

Wagner has treated a system of conducting spheres in a non-conducting medium. Use will be made of this treatment, which gives expressions for the capacity and power factor, by showing that our model is equivalent to a conducting sphere the conductivity of which depends on the constants of the model. By assuming that the conductivity of the spheres varies in a certain way about a most probable conductivity, Wagner obtained expressions for the power factor and dielectric constant of the system which are functions of the frequency. These expressions give curves which are typical of a great many dielectric materials. It is here shown that a similar sort of behavior would be displayed by a dielectric containing spheres of different radii, each surrounded by a conducting shell. Such a system corresponds roughly to the structure of colloidal dispersions.

An outline of the argument to be used follows. The material is supposed to consist of spheres as shown in Fig. 1. The central sphere of radius a_1, has a conductivity of λ_1 and a dielectric constant, ϵ_1. The concentric shell has a radius a_2, conductivity λ_2, dielectric constant ϵ_2, and the outside medium has conductivity and dielectric constant respectively, λ_3, and ϵ_3.

The dielectric constant and conductivity are combined into a complex conductivity to be represented by $\Lambda = \lambda + i\omega\epsilon/4\pi c^2$, where i is $(-1)^{1/2}$, c the ratio of the e.m.u. to the e.s.u. and $\omega/2\pi$ is the frequency. This sphere with its shell is shown to be equivalent to a single sphere of complete conductivity $\bar{\Lambda}$. It is found that $\bar{\Lambda}$ is a function of Λ_1, Λ_2, and the ratio a_2/a_1, and is independent of the conductivity of the medium, Λ_3. The fact that the equivalence is independent of Λ_3 makes it possible to substitute in Wagner's expression for the conductivity of a single sphere, an expression which involves the conductivities of the sphere and the shell and their respective radii. In this way Wagner's work can be taken over directly. By the use of simplifying assumptions and approximations it is possible to get the equivalent conductivity in terms of a single expression, and then by considering a distribution of particle size, rather than a distribution of conductivity as Wagner did, we obtain expressions for the power factor and the capacity as functions of the frequency.

We will now take up the argument in detail. Referring to Fig. 1, let the potentials in the three media be V_k, where $k = 1, 2, 3$; the corresponding electric field strengths are then

$$\boldsymbol{E}_k = -\operatorname{grad} V_k. \tag{1}$$

We consider the sphere immersed in a uniform alternating electric field, the direction of which is along the z axis; the field is accordingly axially symmetric about this axis. Since there are no free charges in the various media the V_k must satisfy Laplace's equation

$$\Delta V_k = 0 \tag{2}$$

and in virtue of the axial symmetry may, on choosing polar coordinates with z axis as pole, be taken in the form

$$V_k = \sum_{n=0}^{\infty} (A_{kn} r^n + B_{kn} r^{-(n+1)}) P_n(\cos\theta) \tag{3}$$

where $P_n(\cos\theta)$ is the nth Legendre polynomial.

The boundary conditions to be satisfied by the V_k are as follows: (a) the field must become uniform as $r \to \infty$, i.e., $\boldsymbol{E}_3 \to (0, 0, E_0 e^{i\omega t})$. But this requires that

$$A_{31} = -E_0 e^{i\omega t}; \quad A_{3n} = 0 (n > 1) \tag{4}$$

to which we may add the normalizing condition

$$A_{30} = 0. \tag{5}$$

(b) V_1 can have no singularity at the origin, whence

$$B_{1n} = 0 \tag{6}$$

for all n. (c) The potentials must be continuous at the boundaries $r = a_1, a_2$ of the spherical shell, i.e.,

$$V_3(a_2) = V_2(a_2); \quad V_2(a_1) = V_1(a_1). \tag{7}$$

Finally, the normal component *total* current

$$\boldsymbol{i}_k = \left(\lambda_k + \frac{i\omega\epsilon_k}{4\pi c^2}\right) \boldsymbol{E}_k = \Lambda_k \boldsymbol{E}_k \tag{8}$$

must be continuous at the boundaries, i.e.,

$$\begin{aligned} \Lambda_3 \frac{\partial V_3}{\partial r} &= \Lambda_2 \frac{\partial V_2}{\partial r} \text{ for } r = a_2 \\ \Lambda_2 \frac{\partial V_2}{\partial r} &= \Lambda_1 \frac{\partial V_1}{\partial r} \text{ for } r = a_1 \end{aligned} \tag{9}$$

Conditions (4)–(9) are readily solved for the constants A_{kn}, B_{kn} of Eq. (3); since we are only interested in the region exterior to the sphere we only write down the results referring to this medium:*

$$\begin{aligned} B_{31} &= \frac{(\Lambda_3 - \Lambda_2)(2\Lambda_2 + \Lambda_1)a_2^3 + (\Lambda_2 - \Lambda_1)(\Lambda_3 + 2\Lambda_2)a_1^3}{(2\Lambda_2 + \Lambda_1)(2\Lambda_3 + \Lambda_2)a_2^3 + 2(\Lambda_2 - \Lambda_1)(\Lambda_3 - \Lambda_2)a_1^3} a_2^3 A_{31} \\ B_{3n} &= 0 \quad (n \neq 1). \end{aligned} \tag{10}$$

Following Wagner we ask whether it is possible to describe this field as due to a single sphere of radius a_2 and complex conductivity $\bar{\Lambda}$ immersed in

* These results as well as (11) and (12) below may be taken directly from J. C. Maxwell, "Electricity and Magnetism" 3rd Ed. Vol. 1, pp. 437–438 (Oxford 1892) (in particular, from Eqs. (6), (10), and (11)) on noting that the mathematical problem here involved is equivalent to his on replacing the (real) specific resistance k by the reciprocal of the complex conductivity Λ.

a medium of complex conductivity. Under the same conditions as those for the double sphere the potential exterior to the single sphere will be given by

$$V_3 = A_{31}\left(r + \frac{a_2^3}{r^2}\,\frac{\Lambda_3 - \bar{\Lambda}}{2\Lambda_3 + \bar{\Lambda}}\right)\cos\theta. \tag{11}$$

Equating the two expressions (3) and (11) for V_3 and solving for $\bar{\Lambda}$ we find

$$\bar{\Lambda} = \frac{(2\Lambda_2 + \Lambda_1)a_2^3 - 2(\Lambda_2 - \Lambda_1)a_1^3}{(2\Lambda_2 + \Lambda_1)a_2^3 + (\Lambda_2 - \Lambda_1)a_1^3}\,\Lambda_2. \tag{12}$$

The double sphere is therefore equivalent to a single sphere whose conductivity is given by the last equation, expressing the conductivity of the latter in terms of the conductivities and radii of the former. This equivalence is perfectly general and does not depend on the medium surrounding the spheres since Λ_3 no longer appears. Wagner derived expressions for the capacity and power factor of an assemblage of single spheres and from the above argument we see that exactly the same electrical behavior results from an assemblage of spheres with shells. We could at any point in Wagner's discussion substitute for the conductivity of his single spheres by means of Eq. (12).

For our purposes, however, it is convenient to introduce at this point some simplifying assumptions. We assume (A) that the conducting shell is thin compared with the radius of the sphere and that its thickness d is constant, i.e.,

$$d/a \ll 1 \text{ and } a_2 = (a_1 + d) \tag{13}$$

(B) that Λ_2 is large compared with Λ_1 or

$$|\,\Lambda_2/\Lambda_1\,| \ll 1. \tag{14}$$

On dividing numerator and denominator of Eq. (12) by $2\Lambda_2 a_1^3$, substituting from Eq. (13) for a_2^3 and expanding, neglecting higher powers of d/a_1, and dropping the subscript of a, we have

$$\bar{\Lambda} = \frac{(1 + \Lambda_1/2\Lambda_2)(1 + 3d/a) - (1 - \Lambda_1/\Lambda_2)}{(1 + \Lambda_1/2\Lambda_2)(1 + 3d/a) + \frac{1}{2}(1 - \Lambda_1/\Lambda_2)}\,\Lambda_2. \tag{15}$$

Expanding and neglecting the product of the small quantities Λ_1/Λ_2 and d/a, we have

$$\bar{\Lambda} = \frac{3\Lambda_1/2 + 3d\Lambda_2/a}{3/2 + 3d/a} \tag{16}$$

$$\bar{\Lambda} = \Lambda_1 + 2d\Lambda_2/a. \tag{17}$$

We now have this simple expression in place of the more complicated Eq. (12) giving the conductivity of the equivalent single sphere and will use it to substitute in Wagner's equations. He gives for the relaxation time of the single sphere

$$\frac{\bar{\epsilon} + 2\epsilon_3}{4\pi c^2(\bar{\lambda} + 2\lambda_3)}. \tag{18}$$

For the relaxation time of our model we obtain by the indicated substitution

$$T = \frac{\epsilon_1 + 2d/a + 2\epsilon_3}{4\pi c^2(\lambda_1 + 2d\lambda_2/a + 2\lambda_3)}. \tag{19}$$

Further simplification is obtained by following Wagner in assuming that $\epsilon_1 = \epsilon_3$ and in addition that the conductivity of the shell in relation to the sphere is so large that λ_1 can be neglected with respect to $2\lambda_2 d/a$ and that $\epsilon_2 d/a \ll \epsilon_1$. We have, then

$$T = \frac{3\epsilon_1 a}{8\pi c^2 \lambda_2 d} \tag{20}$$

for the relaxation time of a non-conducting sphere surrounded by a thin concentric conducting shell.*

Now in order to interpret the experimental facts for many materials it has been shown by von Schweidler[4] and others that it is necessary to assume that the materials are made up of an assemblage of elements having different relaxation times. Since the relaxation time in Wagner's expression, Eq. (18), does not depend on the radii of his spheres, he considers that the variation in T is due to a variation of conductivity. As the radius appears in our expressions for the relaxation time, Eqs. (19) and (20), we shall consider the variation in T to be due to a variation in the radius. We thus depend on the variation of particle size rather than inhomogeneity in particle constitution for the necessary distribution of relaxation times.

The next step is to choose some function to represent the distribution of particle size. Wagner gives reasons for assuming that the conductivities of the spheres differ in such a way that the relaxation times are distributed according to a logarithmic error function and then uses the analysis of his earlier paper[5] in which such a distribution was taken. Since there is no general function expressing the distribution of particle size in colloidal dispersions we will choose a function which, while representing approximately the distribution in typical colloids, gives the same distribution of relaxation times as used in Wagner's treatment. Such a function results if we assume that the volume per cc occupied by spheres of radius between a and $a+da$ is given by

$$dV_a = \frac{Vb}{(\pi)^{1/2}} \frac{1}{a} e^{-(b\log a/a_0)^2} da \tag{21}$$

where V is the total volume per cc occupied by the spheres and b is a constant which determines the density of grouping about a most probable radius a_0. Curves illustrating this function are given in Fig. 2. The general shape is characteristic of the distribution found for small particles.[8]

* The more complete theory of the relaxation times for our model leads to two such times which in the approximation $d/a \ll 1$ here considered are given by Eq. (20) and $\epsilon/4\pi c^2\lambda$. But the effect of this second term is negligible in comparison to that of the first in our case, for in addition to being short in comparison with (20) it appears with an initial amplitude of relative order $d/3a$.

[8] See for example, R. P. Loveland and A. P. H. Trivelli, J. Franklin Inst. **204,** 193 (1927); S. Odén, Chap. 58, "Colloid Chemistry," J. Alexander, Chemical Catalog Co., New York; J. B. Nichols, Physics **1,** 254 (1931).

We wish to show that the particle size distribution, Eq. (21), gives the time constant distribution assumed by Wagner. Eq. (21) can be written thus

$$dV_a = (Vb/\pi^{1/2})e^{-(b\log a/a_0)^2}d\log a/a_0 \tag{22}$$

which, on substituting for a in terms of T by Eq. (20), becomes

$$dV_a = (Vb/\pi^{1/2})e^{-(b\log T/T_0)^2}d\log T/T_0 \tag{23}$$

Wagner's Eq. (44)[6] gives for the distribution of the volumes occupied by the single spheres of different time constants.

$$3dV_a = (Kb/\pi^{1/2})e^{-(b\log T/T_0)^2}d\log T/T_0 \tag{24}$$

where K is a constant (Nachwirkungskonstant)* appearing in his first treatment of a distribution of time constants[5] and is defined as follows: When a

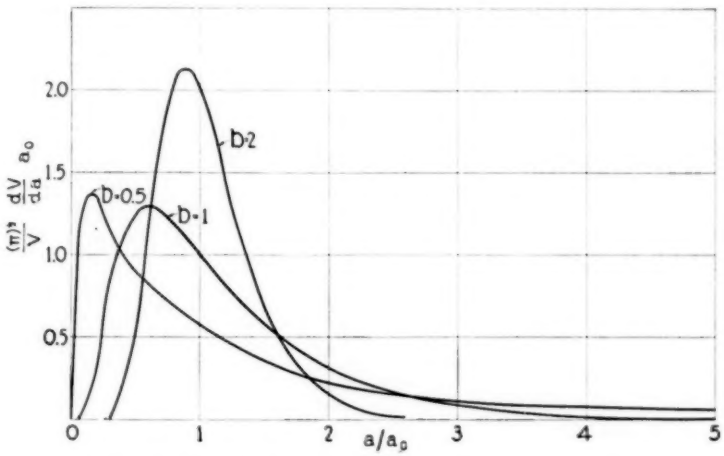

Fig. 2. Assumed volume distribution of particle size.

field is impressed on an imperfect dielectric the electric displacement after a long time, D_∞, is greater than the initial displacement, D_0, and is given by

$$D_\infty = D_0(1 + K). \tag{25}$$

Comparing Eqs. (23) and (24) we see that Wagner's equations may be applied to our case if we substitute $3V$ for k. In his treatment the capacity at any frequency is given by $C+\Delta C$ where C is the capacity at infinite frequency. Making the substitution for k, his equation becomes

$$\frac{\Delta C}{C} = \frac{3Vb}{\pi^{1/2}}e^{-b^2z_0^2}\int_0^\infty e^{-b^2u^2}\frac{\cos(2b^2z_0 - 1)u}{\cos u}du \tag{26}$$

and for the power factor, $\tan\phi$,

$$\left(1 + \frac{\Delta C}{C}\right)\tan\phi = \frac{3Vb}{\pi^{1/2}}e^{-b^2z_0^2}\int_0^\infty \frac{e^{-b^2u^2}\cos 2b^2z_0u}{\cos u}du. \tag{27}$$

Here

$$z = \log T/T_0,\ z_0 = \log T_0,\ \text{and}\ z + z_0 = u,$$

* See "Elektrophysik der Isolierstoffe," A. Gemant, Julius Springer, Berlin, 1930, p. 95, for amplification of the meaning of this constant and also on the pages following for calculation of the relaxation time by a method similar to Wagner's.

Tables and curves illustrating these equations are given in Wagner's paper.[5] In Figs. 3 and 4 are reproduced his curves for capacity and power factor as functions of frequency.

It is of interest to see the order of magnitude to be expected for the value of T_0. Eq. (20) becomes

$$T_0 = 1.33(a/d)\epsilon_1(1/\lambda_2')10^{-13} \tag{28}$$

where λ_2' is expressed in reciprocal ohms. If we assume the electric double-layer[9] of the order of 10^{-7} cm in thickness, a particle radius of 10^{-5} cm, and a conductivity of 10^{-3}, then the relaxation time will be 1.33×10^{-8}. We should not expect the conductivity to be greater than that of a strong acid in aqueous solution, i.e., of the order of 1 and it will probably be less than that. With this value of T_0, a decrease in the dielectric constant and an increase in the power factor should be observed in the range of the high radio frequencies, i.e.,

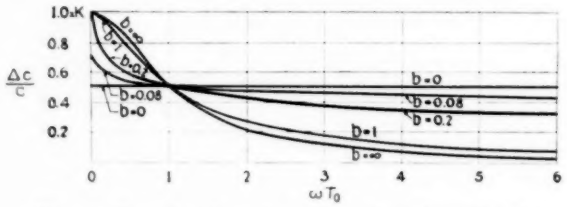

Fig. 3. Capacity increment as a function of ωT_0.

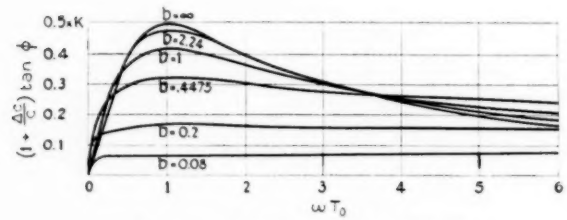

Fig. 4. Power factor as a function of ωT_0.

at about 10^7. In many cases the particle size may be larger than 10^{-5} cm, and as we see from the above expression, the relaxation time increases with increasing particle size, so that for particle sizes of the order of 10^{-4} cm the whole region of anomalous behavior would fall in the range of frequencies in which measurements can easily be made.

In some cases the relaxation time may be so short that it will be experimentally impossible to determine C, the capacity at infinite frequency. In order to make use of Eqs. (26) and (27) this quantity must be known. However, it should be possible to calculate C from the dielectric constants of the medium and the material of the spheres. Methods of doing this are discussed by Piekara.[10]

It should be pointed out that the assumptions made in simplifying Eq. (12) place certain limitations on the applicability of the simple expression

[9] T. Svedberg, "Colloid Chemistry," p. 195, Chemical Catalog Co., New York, 1924.
[10] A. Piekara, Phys. Zeits. **31**, 579 (1930).

for the relaxation time which results, Eq. (20). For small particle sizes of the order of 10^{-7} cm it has been estimated that the thickness of the ionic layer is of the same order as the particle radius.[11] We have assumed that d/a is less than one, so that we can apply our expressions only to the larger particles. Since we have assumed the particles to be relatively non-conducting the results will not be applicable to dispersions of colloidal metals. We have tacitly assumed in expression (14) that

$$\omega\epsilon_1/4\pi c^2\lambda_2 \ll 1$$

or in using Eq. (20) we must have

$$(2/3)\omega T d/a \ll 1.$$

We have assumed d/a small so that the expressions are valid for a frequency as high as $1/T$ and for frequencies above this the validity will depend on the value of d/a.

Speculations of a qualitative nature have often been made as to the effect of adsorbed ions on the alternating current losses in liquid and solid dielectrics and of the effect of colloidal particles on these losses in transformer oils. With the aid of Eq. (20) we can obtain quantitative expression for the frequency at which the maximum power loss is to be expected for one model. For other spherical models with different conditions of shell thickness, conductivity, etc., a similar procedure might be undertaken to obtain the relaxation time by use of the general Eq. (12) and substitution in Wagner's expression for the relaxation time, Eq. (18). In view of the impossibility of obtaining a rigorous mathematical representation of the form of the conducting surfaces, their conductivities, etc. in the case of solid dielectrics and of the lack of knowledge of the nature of the electric double-layer in colloids it does not seem worth-while to undertake the expression of the relaxation time for more general cases of the spherical model. It is evident from the expressions obtained for the model treated in detail that in addition to the recognized effect of the volume concentration and conductivity of impurities on the dielectric behavior, the effect of size is also of importance in certain cases.

In addition to providing an interpretation of dielectric behavoir, this analysis provides means for investigating colloidal structure. For example an indication of the degree of uniformity of particle size could be obtained from the shape of the power factor vs. frequency curve, or the position of a maximum in this curve would give the most frequent relaxation time giving definite relationship between the particle radius, the thickness of the ionic atmosphere and its conductivity.

In conclusion one of the authors (J.B.M.,Jr.) wishes to express his appreciation of the encouragement and helpful criticism which he has received from Dr. E. O. Kraemer during the preparation of this paper.

[11] A. Tiselius, Diss., Upsala, 1930.

Further Data on the Thermal Diffusivity of Nickel[1]

By RICHARD H. FRAZIER
Massachusetts Institute of Technology
(Received March 17, 1932)

Results are given of tests for determining with precision the thermal diffusivity of a specimen of nickel having nearly the same chemical analysis as the one for which results and method of experimental procedure were presented in a former paper. The over-all probable error is shown to be about 0.06 percent. The results and conditions of the tests are discussed in comparison with those for the former specimen.

THE specimen on which the following results were obtained (which will be designated as rod *D*) came from the same manufacturer's batch as the specimen reported upon in the first paper[1] (which will be designated as rod *C*), and hence has nearly the same chemical analysis:[2]

Cobalt	0.01 ± 0.005 percent	Manganese	0.26 ± 0.010 percent
Copper	0.07 ± 0.005	**Nickel**	**99.25 ± 0.030**
Carbon	0.14 ± 0.005	Silicon	0.07 ± 0.010
Iron	0.11 ± 0.015	Sulphur	0.06 ± 0.005

A comparison with the analysis of rod *C* shows the chief difference to be in the iron content, rod *C* containing about 0.14 percent more iron than rod *D*. The only other significant differences are in the carbon and manganese contents, rod *D* containing about 0.02 percent more carbon and about 0.03 percent more manganese than rod *C*.

Seven runs gave the results shown in Table I, uncorrected for pendulum calibration:

TABLE I.

Run	p	ΔT	Average T
28	0.004,218,4 ± 0.000,002,1 sec.$^{-1}$	4.49°C	8.60°C
29	0.004,206,8 ± 0.000,007,8	4.64	8.37
30	0.004,221,3 ± 0.000,001,8	4.99	8.11
32	0.004,209,3 ± 0.000,003,5	4.31	8.48
33	0.004,228,1 ± 0.000,005,7	4.78	8.41
35	0.004,214,8 ± 0.000,007,1	4.30	8.43
36	0.004,213,5 ± 0.000,003,0	4.37	8.77

From these data the most probable value is,

$$p = 0.004,216,0 \pm 0.000,001,9 \text{ sec.}^{-1},$$

[1] See "Precision Method for Determining the Thermal Diffusivity of Solids," Phys. Rev **39**, 515 (1932), referred to elsewhere in this article as "the first paper." The method and apparatus whereby the results reported here were obtained, were explained therein. The symbols used here are defined therein. The results reported here are for one of a series of experiments in a program of thermal measurements aimed toward the measurement of the Thomson effect.

[2] Analysis by Arthur D. Little, Inc. The precision of the determination (which may be taken as applicable also to the analysis for rod *C* reported in the first paper) is only estimated, inasmuch as more exact figures can be determined only by making a very large number of analyses on the same type of material and then making a careful study of the variations.

and the application of the pendulum correction factor of 1.00063 ± 0.00005 gives finally,

$$p = 0.004,218,7 \pm 0.000,001,9 \text{ sec.}^{-1}.$$

For this specimen,

$$L = 9.501 \pm 0.001 \text{ cm}$$

and

$$\rho = 8.840 \pm 0.004 \text{ gm} \cdot \text{cm}^{-3},$$

and since

$$p = \frac{k\pi^2}{4c\rho L^2} = \frac{\alpha^2\pi^2}{4L^2},$$

$$\alpha^2 = 0.15434 \pm 0.00008 \text{ cm}^2 \cdot \text{ sec.}^{-1},$$

and

$$k/c = 1.3643 \pm 0.0009 \text{ gm} \cdot \text{cm}^{-1} \cdot \text{sec.}^{-1}.$$

This result is about 2.8 percent higher than the result for rod C and the average temperature is about 16.3°C lower. According to the International Critical Tables, k changes about -0.053 percent per °C temperature rise and c changes about $+0.10$ percent per °C temperature rise between 0° and 100°C, giving a resultant change of -0.153 percent for the ratio. Applying this figure to the difference in average temperature gives a change of 2.6 percent for comparison with the 2.8 percent obtained. However the data for temperature coefficients suffer from the same shortcomings discussed for conductivities, etc., in the first paper, and it is probable that just as in the case of the temperature coefficient for electrical resistivity, the temperature coefficient for thermal conductivity and the temperature coefficient for specific heat are affected by the chemical composition and internal structure of the specimen. There is in fact one set of data[3] which shows that the thermal conductivity of nickel, contrary to that of other nearly pure metals, apparently has a maximum somewhere in the region between 0° and 18°C. The comparison given therefore is not of great significance, but merely shows that the difference between the values of k/c for the two cases is not widely different from what would be predicted from results obtained by other observers. If the method for the precise determination of specific heat which is in the process of development is successful, the variation of thermal conductivity with temperature over the range from 0° to 100°C will be determinable by means of the proposed Thomson effect apparatus and hence will make possible a direct comparison of the thermal properties of rods C and D. An indication that the thermal properties of these rods are nearly identical (which is essential for the contemplated Thomson effect experiment) is given by the fact that their electrical resistivities are nearly identical. These together with the thermal diffusivities for rods C and D are shown in Table II, and as a matter of incidental interest, in comparison with rod A, the first rod tried, a very impure rod obtained by error which contained only 91.56 percent nickel, the chief impurity being manganese:

[3] C. H. Lees, "Conductivity of Metals at Low Temperatures," Trans. Roy. Soc. London **208,** 381 (1908). The specimen was "turned from a bar supplied by Messrs. Johnson and Matthey as 0.99 Ni."

TABLE II.

Rod	Electrical resistivity	Temperature	Thermal diffusivity	Average temperature
A	19.5 microhm·cm	22.5°C	0.10 $cm^2 \cdot sec.^{-1}$	12.°C
C	10.85	20.6	0.14985	24.78
D	10.84	20.3	0.15434	8.45

Tabular values of the temperature coefficient for the electrical resistivity of nickel are in the neighborhood of +0.4 to +0.6 percent per °C temperature rise which when applied to the difference of 0.3°C between the temperatures for the resistance measurements for rods *C* and *D* still leaves the results in accord within the precision of the determinations.

The runs for rod *D* were made under more difficult conditions than those for rod *C* in that the ambient and water temperatures fluctuated more. The ambient temperature finally was controlled within a few thousandths of a °C as far as the specimen was concerned by means of a motor-driven air blower installation having both speed and damper control. The apparatus was protected from direct draft by a thin sheet-metal shield, the space between it and the outer guard tube of the apparatus being packed with waste. Ambient temperature for the specimen was taken as the temperature of the outer guard tube. This temperature control did not include the galvanometer circuit, however, so more trouble was experienced from stray thermal electromotive forces than in the tests on rod *C*, though the corrections necessary for change in the zero position of the galvanometer during a run due to this cause were very small. The water temperature however was subject to considerable variation due to variations in rate of water flow in the building mains caused by other users. In the summer time when the runs on rod *C* were made this change in water rate was of little consequence because of the building being nearly at the same temperature as the water, but with heat in the building and the water much colder the heat transfer to the water and hence the water temperature varied more with variation in rate of flow. Consequently most of the runs were made at times when little competitive activity was expected, and all runs wherein a fluctuation of over ± 0.02°C was observed were discarded. Approximate corrections were applied to compensate for temperature changes in the runs retained.

The changes in water temperature in the experiments for rod *C* were of the nature of a gradual rise or fall during a run, while in the experiments for rod *D* the changes were more sudden and sometimes in both directions during a run. In the former case the effect was to introduce differences in the decrements of the most probable curves fitted to the observed points for the various runs, while in the latter case the effect was more predominantly one of scattering of points for the individual runs. This is substantiated by the data, for while the values of p for the various runs for rod *D* are more closely clustered than are the values for rod *C*, thus giving the final result for rod *D* the smaller probable error, the probable errors for the individual runs for rod *D* are considerably greater than those for rod *C*; and in fact the greatest observed temperature fluctuations occurred in runs 29, 33, and 35.

It should be said that in computing p for rod C the results for the individual runs were averaged without regard to their individual probable errors since there is no ground for inferring a relation between the probable error of an individual run and the weight which it should have in the average. For rod D however, there is (as explained above) some ground for inferring such a relation. However, when the average is computed by weighting each run inversely as the square of its probable error, the final result is affected by less than 1 part in 2000 and its probable error by about one-eighth, so that the difference lies within the probable error calculated either way.

The only change in design of apparatus from that shown in Fig. 1 of the first paper was in the construction of the water deflector for directing the stream on to the top of the specimen, the type illustrated having been found to be insufficiently secure. Incidentally several rates of water flow have been used, varying from about 3 to 5 meters per second, with no significant difference in the results obtained for p.

The writer wishes to express his thanks to Mr. W. V. A. Kemp for assistance in assembly of apparatus.

The Molecular Process of Crystal Growth in Hexagonal Metals. Deposition upon Monocrystalline Hemispheres of Zinc

By PAUL A. ANDERSON*
Department of Physics, State College of Washington
(Received March 29, 1932)

The growth of a single crystal rod of zinc is allowed to proceed from a small orifice into a mass of molten zinc and the monocrystalline hemisphere thus formed isolated by rotation of the apparatus. The hemisphere is subjected to uniform bombardment by zinc vapor and observation of the growth on its surface forms the basis for a study of the variation of depositional rate with crystal surface structure. It is assumed, with Kossel and Stranski, that the force acting upon an atom which has struck the crystal surface is qualitatively proportional to the number of contiguous lattice atoms and a "force series" is drawn up listing the relative depositional energies for eleven typical positions of different crystal surface structure. With the aid of this force series the macroscopically observed growth on the experimental crystal is interpreted in terms of atom-by-atom deposition.

WE DEFINE the term "molecular process of crystal growth" as the process by which a macroscopic crystal takes atoms or molecules from its environment and incorporates them into its lattice.[1] To describe this process we have to answer the specific question: what is the influence of the geometric arrangement of atoms at any given point of the crystal surface upon the probability that an atom striking the crystal at that point will condense and become an integral part of the lattice? The bombarding atom may come from the gaseous or liquid phase or from an adjacent crystal of different orientation (recrystallization phenomena).

The molecular process of crystal growth has been studied from both the theoretical[2] and experimental[3] angles in the cases of certain heteropolar salts but the investigation of the metals from this point of view has scarcely been begun.[4] Stranski[5] recently has extended his method of theoretical treatment to metals of simple cubic lattice type. With the exception of the work of Volmer and Estermann on mercury[6] little if any experimental work has been done under conditions permitting direct and unambiguous interpretation of the experimental observations.

* During the course of this work, National Research Fellow in Physics.

[1] The mechanism of formation of crystal nuclei is regarded, at least formally, as a distinct problem.

[2] Kossel, Leipziger Vorträge, 1928. Hirzel, Leipzig; Stranski, Zeits. f. physik. Chem. **136,** 259 (1928).

[3] Kossel, reference 2, gives a resumé of this work.

[4] The great mass of information which has been accumulated in metallographic research throws little light upon the fundamental crystal growth mechanism. The initial conditions are generally so imperfectly defined as to preclude analysis of the observations in terms of the fundamental growth process.

[5] Stranski, Zeits. f. physik. Chem. B **11,** 342 (1930).

[6] Volmer and Estermann, Zeits. f. Physik **7,** 13 (1921).

Of all the possible schemes for the study of crystal growth one involving deposition upon a monocrystalline sphere or hemisphere is peculiarly adapted to furnish the maximum amount of information directly interpretable in terms of the elementary process of atom-by-atom growth.[7] If we subject a spherical monocrystalline surface which is free from oxide or other impurities to uniform bombardment from a disperse phase slightly supersaturated with respect to the crystal temperature any observed differences in growth rate at different points of the crystal surface can be traced with some degree of confidence to the structure of the crystal substratum at these points; the initial conditions are otherwise impartial to growth in any given direction.[8] Since, furthermore, every possible crystal zone is potentially developable from a sphere or hemisphere a comprehensive survey of the effect of substratum structure upon growth is obtainable in a single experiment.

Experimental

Method

The essential features of the method may be described as follows: A single crystal rod is grown by Bridgman's method[9] in a narrow tube, *C* Fig. 1, which projects into a mass of molten zinc contained in a wider tube, *B*. The growth of the rod is carried beyond the orifice of *C*; a hemispherical crystal-liquid boundary is thus formed and upon quickly rotating the tube through 180° a monocrystalline hemisphere, strain-free and with an oxide-free mirror-smooth surface, is left exposed to the bombardment of zinc vapor furnished by the pool of metal at the other end of the tube. Regulation of the rate of growth on this hemisphere is effected by a simple regulation of the temperature difference between crystal and vapor source. Continuous visual observation of the growth is secured by using an open-wound glass tube *F* as the heating furnace.

Apparatus and procedure

The apparatus described here is that used in our first experiments. Some obvious refinements, notably the addition of an evacuated glass cylinder for shielding the tube from irregular air currents, and more exact control of the temperature gradient between crystal and vapor source by a thermocouple acting upon a galvanometer-photocell-thyratron circuit[10] so far have been found to have no decided effect upon the results and are not mentioned further.

Fig. 1 is a diagrammatic cross sectional sketch of the essential parts of the apparatus: a Pyrex glass tube *ABC* blown in the form shown and the Pyrex

[7] Kossel, reference 2.

[8] The anisotropic nature of the thermal conductivity in noncubic crystals is probably significant only when the growth rate is rapid. Gliding of "adsorbed" atoms over the crystal surface with final condensation at a point other than the point of impact is a factor which must, however, be considered.

[9] Bridgman, Proc. Am. Acad. Arts Sci. **60**, 307 (1925).

[10] A slight modification of the arrangement described by the writer in Rev. Sci. Insts. **1**, 764 (1930).

furnace tube *F*. *ABC* made a sliding fit in *F*. *F* was wound with 3 mm nichrome ribbon spaced 3 mm between turns, total resistance about 20 ohms, and the winding secured with narrow vertical bands of talc-water glass cement. The winding was divided into two sections, S_1 and S_2, by an adjustable contact clamp. *T* was a thin-walled brass tube cemented over the end of *C*. The open end of *F* was stopped with a transite disk and the whole arrangement mounted on laboratory clamps in such a way that, from an initial vertical position, it could be rotated through 180° about a horizontal axis.

Highly purified zinc[11] in the form of small lumps and in quantity sufficient to fill *C* and about one third of *B* with molten metal, was placed in the chamber *A* and *V* then connected by flexible metal vacuum tubing and cooled sealing wax joints with a Hyvac pump, McLeod gauge, mercury trap, and a reservoir containing nitrogen over liquid sodium-potassium alloy. After re-

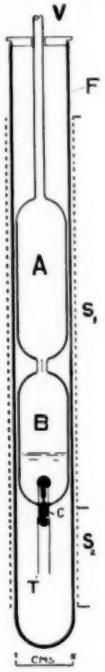

Fig. 1. Experimental arrangement for preparing monocrystalline hemispheres and subjecting them to deposition from the vapor phase.

peated evacuation and washing of *ABC* with nitrogen the zinc was melted in vacuum and degassed by swashing the molten metal about in *A* under full vacuum. After continuing this treatment for two hours enough nitrogen was admitted to force the metal slowly through the 0.2 mm capillary filter connecting *A* and *B*. *A* was reevacuated while the capillary was still sealed by a small quantity of molten zinc and the tube sealed off from the pump. The molten metal in *B* showed no traces of floating oxide and retained the appearance of clean mercury after being held continuously in the molten state

[11] Total impurities under 0.001 percent. Kindly furnished to me by Mr. H. M. Cyr of the New Jersey Zinc Company.

for periods as long as five days. Improvement of the outgassing vacuum from 10^{-3} to 10^{-6} by addition of a three-stage mercury diffusion pump and double liquid air trap had no appreciable effect upon the results.

Crystallization in C was started by slowly decreasing the current in section S_2. The beginning of crystallization and its growth upwards toward the orifice was followed by the characteristic change in light reflection attending solidification and the final stage in the development of the hemisphere determined by trial and error: the tube was rotated sufficiently to expose the orifice and the position of the solid meniscus observed. By suitable readjustment of the heating currents in S_1 and S_2 and of the position of the tube ABC relative to the temperature gradient between S_1 and S_2 the crystal-liquid interface was moved out into the bulk of molten metal until it took the desired position. Two or three trials were usually sufficient and the interface position could then be held practically constant for hours at a time. The heating currents in S_1 and S_2 and the tube position for this steady state, which is designated "setting I", were recorded, the apparatus rotated and fixed in the inverted position, and the currents again adjusted until the crystal was held just below and the pool of zinc just above the melting point, "setting II". This latter adjustment was made by determining the currents for which the crystal just began to melt and the pool to solidify, then slightly decreasing the one and increasing the other. Having once determined these settings growth experiments could be carried out repeatedly on different crystal hemispheres with the same tube.[12] The procedure for each growth experiment was, now, (1) the zinc in C and B was remelted completely, the current in S_1 set at the value for setting I, and the crystal hemisphere grown by gradually decreasing the current in S_2 to the value for setting II. The stem and hemisphere were usually grown in about one hour but the process could be speeded up to half an hour or slowed down to two hours without apparent influence on subsequent observations. (2) The tube was rotated and the currents brought immediately to setting II.

To secure an estimate of the temperature difference between the crystal surface and the vapor source during deposition a dummy tube, identical to ABC with the exception that a thermocouple well was punched in B, and C blown in such a way as to allow of introducing a thermocouple junction just below the surface of the hemisphere,[13] was put through adjustments identical to those in the determination of settings I and II. The temperature difference in this tube was found to be about 5°C and in the actual growth experiments the difference was, presumably, of this order. It should be emphasized at once that an extremely small temperature gradient inducing growth at a rate so low as to approach the equilibrium or zero-growth-rate state is a desirable experimental condition and that the rather primitive apparatus employed here is not capable of the exact control required for the study of extremely slow growth. The results which have been obtained show, however, that infor-

[12] Crystallization and remelting of zinc in a Pyrex tube does not crack the tube provided the temperature is maintained near the melting point.

[13] In this case the hemisphere was polycrystalline.

mation regarding some of the main features of growth may be gotten by this simple method and the consequences of a proposed theory of growth are checked sufficiently to warrant the conclusion that the general method of attack is sound.

Results

Deposition on the hemisphere began immediately after rotation of the tube. The phenomena observed are grouped in stages, progression to a new stage connoting in general the point at which a significant feature of growth first became visually observable.

Stage 1: During the first half-hour the only effect observed was a slight, apparently uniform, dulling of the initially mirror-smooth surface of the hemisphere.

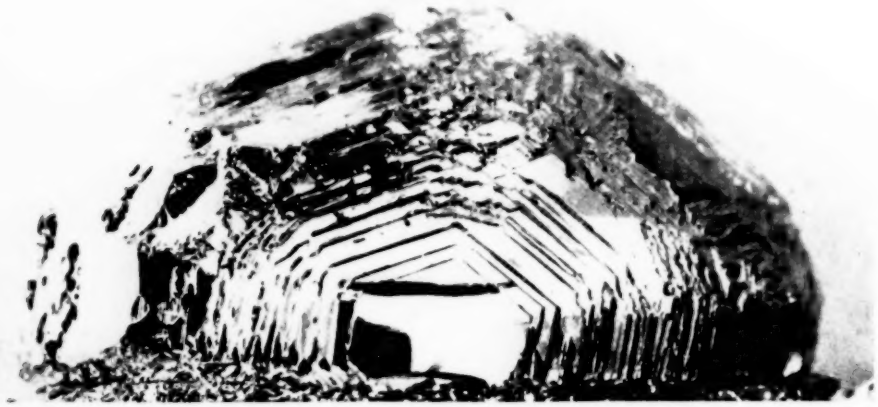

Fig. 2. Photograph of a typical experimental crystal after two and one-half hours deposition. Principal crystal axis approximately normal to plane of paper.

Stage 2: A small patch, about half a millimeter in diameter when first observed, plane, circular, and brilliantly reflecting, appeared against the duller background of the crystal surface.

Stage 3: The small patch increased continuously in diameter and clearly showed itself to be a plane truncating the sphere. After a total elapsed time of an hour three narrow brilliant bands, equidistant and comparable to the longitudinal lines of a terrestrial globe map, appeared. These bands converged at the center of the "polar" plane patch. This stage was especially striking and beautiful to watch.

Stage 4: The polar plane continued to increase in diameter; it was no longer circular but imperfectly hexagonal with the corners of the hexagon undeveloped. Below the polar plane a series of step-like plane-surfaced shoulders developed, each hexagonal in form.

Further growth was a continuation of stage 4 with each feature noted there progressively developing. Fig. 2 is a photograph of a hemisphere after

two and a half hours deposition; the heating current was shut off and the crystal broken out of the cold tube. This crystal was chosen for its particularly favorable orientation and is, otherwise, somewhat less perfect than most of the crystals which have been made. In ten of the twelve hemispheres grown the major crystal axis was approximately normal to the tube axis, a tendency which has been observed in single crystal rods by Bridgman and others and which is consistent with the theory of growth suggested later in this paper.

Interpretation of results

Fig. 3 is a photograph of a model, built up from steel ball-bearings secured with rubber cement, which has proved useful in visualizing the initial surface structure of the zinc hemisphere and in reducing the observed growth to its origin in single-atom deposition. With the aid of suitable guides this model was built in such a way that it duplicated the model which would be obtained by filling a spherical cavity with balls arranged in the system of hexagonal closest packing, dividing this sphere through the equatorial basal crystal

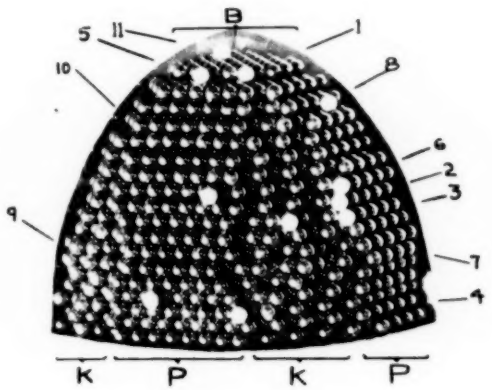

Fig. 3. Model of spherical crystal surface in its initial state. Numbered white balls represent atoms from vapor which have struck at points of different surface structure. Principal crystal axis normal to base of model.

plane, and finally quartering the hemisphere. The exposed side elevation of the model then represents fairly accurately a portion of the surface of a single crystal sphere of ideal close packed hexagonal type some 5 $\mu\mu$ in diameter. The differentiation in surface structure clearly shown between (1) the uniquely regular surface B representing the 0001 basal cleavage plane, (2) the bands P with the characteristic alternate-row regularity of the prismatic and pyramidal zones, and (3) the irregular regions K, furnish the starting point for interpreting the experimental observations. It is clear that in the actual crystal corresponding to a model of impracticable size K spreads out over practically the entire surface; B and P would very nearly but, on purely geometric grounds, never entirely disappear. What, now, is to be expected when a hemisphere of this surface structure is subjected to bombardment by gaseous metal atoms? The white balls in Fig. 3 represent atoms which have struck the

crystal at points of different surface structure. Which of these atoms is most likely to be held, which to reevaporate immediately?

Table I lists these "white" atoms, a description of their positions in terms of the surface geometry of the crystal, and the number of lattice atoms contiguous to each. The effective diameter of a lattice atom is set equal to unit length and only the four innermost shells with radii 1, $2^{1/2}$, $(8/3)^{1/2}$, and $3^{1/2}$ about the condensed atom are taken into account. The environment of any given atom may be described by a symbol of the form 6/3/1/9 which is equivalent to the statement that the atom is question has six "neighbors" at unit distance (direct contact), three at distance $2^{1/2}$, one at $(8/3)^{1/2}$, and nine

TABLE I. *Relative depositional energies as a function of crystal surface structure.*

Designation of position, Fig. 3	Description of position	Number of contiguous atoms at distances: 1	$2^{1/2}$	$2(2/3)^{1/2}$	$3^{1/2}$	Symbol
1	Edge of incomplete 0001 lattice plane.	6	3	1	9	6/3/1/9
2	Edge of incomplete 1012 pyramidal face. position 6 previously filled.	6	3	1	7	6/3/1/7
3	Ditto of 2. Position 2 previously filled.	6	3	1	7	6/3/1/7
4	Edge of incomplete 1010 prismatic face.	6	2	1	9	6/2/1/9
5	Edge of complete 0001 lattice plane.	5	3	1	9	5/3/1/9
6	Edge of incomplete 1012 pyramidal face. Position 2 not previously filled.	5	3	1	7	5/3/1/7
7	Ditto of 6	5	3	1	7	5/3/1/7
8	On 1011 pyramidal face.	5	3	1	7	5/3/1/7
9	On prismatic 1010 face.	4	4	0	7	4/4/0/7
10	On 1012 pyramidal face.	4	2	1	9	4/2/1/9
11	On basal 0001 face.	3	3	1	6	3/3/1/6

at $3^{1/2}$. We now make the assumption, analogous to that previously used by Kossel and by Stranski in their theoretical discussion of growth in cubic crystals, that the force acting upon an atom which has struck the crystal surface is the sum of four force terms, each of which is proportional to the number of neighbors in a given shell and each of which is weighted by the radius of that shell. The symbol 6/3/1/9 then becomes a measure of the relative magnitude of the force acting upon the atom in question. Quantitative weighting, which

would be impossible at present, generally turns out to be unnecessary. Table I is arranged as a force series; it is also an energy series and a condensation probability series. The atom at the head of the table is acted upon by the maximum, that at the foot by the minimum, force and the probability of permanent condensation decreases from top to bottom.

Reexamination of the experimental observations in the light of this force table and the crystal model from which it is derived yields the sought for interpretation of the macroscopically observed growth process in terms of atom-by-atom deposition. If the force table is valid deposition will occur at the maximum rate, position 1, along the edges of the rudimentary polar plane, *B* Fig. 3, and of the 0001 lattice layers which form a series of steps below *B* in the polar region of the hemisphere. The maximum rate is maintained until all except the corner atoms of the hexagon in each of these layers are laid down; the corner atoms are bound by the slightly smaller force 6/3/1/8. For the beginning of a new row along the edge of one of these hexagons the force drops to 5/3/1/9, position 5, and since the force is still less at the corners of the completed hexagons, 5/3/1/7, growth will be directed toward rather than away from these corners. The imperfect corners exhibited by the experimental crystal, Fig. 2, show agreement between theory and experiment on this point. In contradistinction to the maximum rate parallel to the 0001 plane, the growth rate normal to *B* should be a unique minimum, position 11. Isolated atoms initiallly present on *B* will evaporate and atoms striking the face of *B* will either reevaporate relatively rapidly or glide to an edge and there condense.[14] Growth in this region of the hemisphere should be relatively very rapid parallel to, and slow normal to, the 0001 plane; the rudimentary plane *B* should grow until it eventually develops into a uniquely perfect macroscopically visible polar plane truncating the hemisphere, conclusions which are strikingly borne out by the experimental results.[15]

The next most favored positions of growth lie along the edge of a *P* band, positions 4 and 6, or in one of the zigzag furrows which initially cover practically the entire surface of the hemisphere, position 7. Because of the greater depositional energy at position 4 the first atom will most probably be laid down near the "equator". After a single atom is deposited in any one of these positions the force acting upon the next atom jumps to 6/3/1/7, Positions 2 and 3, and this force is maintained until a complete vertical row is deposited. The first effect of this deposition to be observed experimentally is an increase in the width and depth of the furrows. The furrows are initially sufficiently minute to permit specular reflection of visible light and the hemisphere appears optically smooth. As the dimensions of the furrows approach the wave-length of visible light scattering sets in and the hemisphere is "dulled", stage 1 above. The mechanism of this coarsening is indicated in Fig 4, which is a model of part of a single 0001 lattice plane comprising a *K*

[14] The reality of this gliding hypothesis is being investigated by a direct method in this laboratory.

[15] See stages 2 and 3 of the experimental observations. We have here an explanation for the results of Volmer and Estermann on mercury, reference 6.

region bounded by two P bands. Each vertical row deposited at the edge of a P band or in a furrow contributes one atom to each 0001 plane. The black-dotted white balls represent the atoms which are laid down first; deposition then follows along the direction of the arrows. As two columns of condensing atoms, moving toward each other at an angle of 120°, meet at a corner the depositional energy drops sharply and growth at that corner is halted until succeeding columns moving up en echelon meet at the corner and halt in their turn. The net effect is the progressive coarsening observed experimentally.

An atom striking at any point on the face of a P band, positions 8, 9, 10, is held by forces which are everywhere less than the minimum force at the edge of the band and the effect of this differentiation upon growth should be a progressive widening of the rudimentary bands while their surfaces remain "flat", i.e., everywhere parallel to a hexagon circumscribing the equatorial great circle of the sphere. Stage 3 of the experimental observations may be in-

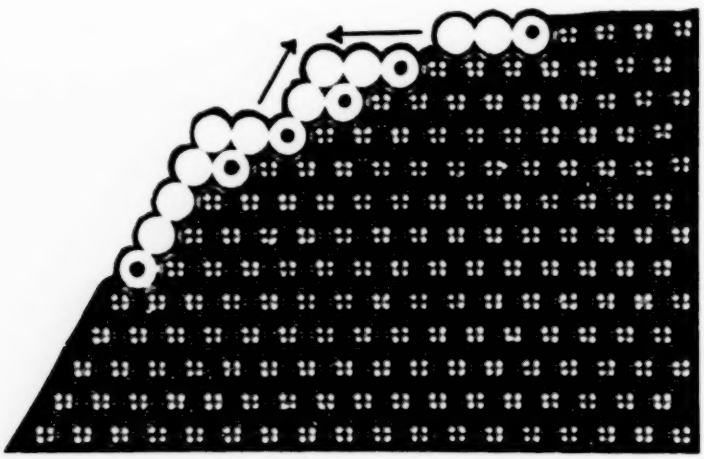

Fig. 4. Model of a single 0001 lattice plane of the hesmisphere. Dark balls: initial structure. White balls: condensed atoms.

terpreted as the stage of growth at which the widening of these bands becomes visible. Since the band surfaces are relatively regular in structure they appear as the brilliant "longitudinal lines" against the duller background of the K regions. The result of continued growth along the preferred tangential direction is shown by the experimental crystal, Fig. 2. Positions 8, 9, and 10 are, of course, only typical of a multiplicity of surface structures which are presumably present initially along a P band. A consideration of the variation in depositional energy between these few positions is, however, sufficient to bring out one or two more important features of growth. From the large value of the force term for position 8 relative to positions 9 and 10 we should conclude that the $10\bar{1}1$ surface structure wherever initially present should be filled in. The filling-in process will leave a minute shoulder or ledge bounded by a 0001 plane and a low-energy pyramidal or prismatic plane. In general

such a ledge will be formed wherever a high-energy surface adjoins a low-energy surface and since, on geometric grounds and as indicated by the model, an alternation of high and low energy surfaces is to be expected along a rudimentary *P* band the first effect of growth on the surface of these bands should be the formation of a series of ledges. The crystal hemisphere is converted, in effect, into a stack of crystal plates, each plate paralleling the 0001 crystal plane. The edge of a shoulder is relatively impregnable to further deposition and growth must be directed from the inner corners of the shoulders toward the edges. The result will be a progressive increase in the width and depth of the shoulders similar to the coarsening of the furrows discussed above. The development of these shoulders was easily followed during deposition on the hemisphere from the first appearance of the longitudinal lines, which under a low-power lens showed a surface structure similar to the edge of an imperfectly aligned pack of cards, to the point at which some of the shoulders attained a depth and width of the order of a millimeter, Fig. 2. A further consequence implicit in this interpretation is: high-energy pyramidal faces should not appear on the final crystal. While goniometric measurements have not been made for lack of the necessary instruments, rough visual examination with a low-power microscope is sufficient to distinguish between pyramidal faces of high d/a axial ratio (low-depositional energy according to our force series) and those of low d/a ratio (high energy). Such examination of the experimental crystals has failed to show a single face of low ratio among hundreds of high ratio.

General significance of the results

The study of the molecular process of crystal growth is essentially a study, under peculiarly simple conditions, of crystal surface forces as a function of surface structure and as such is capable of throwing light on related problems involving the action of the surface forces of solids. The hypothesis of "active centers" which has played such a prominent part in the development of the theory of adsorption and catalysis at solid-gas and solid-liquid interfaces may be given definite form in terms of relative depositional energies. The forces which determine crystal growth, and for which the bombarding atoms are in effect probes, must enter also as the variable factor which, for a given system, determines the effect of surface structure upon adsorption. Stranski[16] has already pointed out that in solids of simple cubic lattice type the high adsorptive power of homopolar relative to heteropolar crystals may be accounted for by the juxtaposition of high energy positions peculiar to the homopolar crystal lattice. It is clear from the preceding discussion that this juxtaposition is characteristic, also, of zinc. In zinc the active centers are of course those positions which rank near the top of the force series, Table I, and the variation of the heat of adsorption with surface structure may be expected to parallel the variation in the depositional energy of zinc atoms themselves.[17]

[16] Stranski, reference 5, p. 348.

[17] Interesting possibilities, not discussed further, are encountered in considering the adsorption of polyatomic molecules; e.g., the modifying effect of the dissociation energy, the influence of the space configuration of the gaseous molecule, and the orienting effect to be expected from fitting one end of the molecule into contiguous positions on the crystal surface.

Particularly significant results may be expected from combining the findings of molecular growth studies with those of the reflection of molecular rays from monocrystalline surfaces, whether the reflection be of specular or of cosine type. Cosine reflection, true condensation succeeded by reevaporation in the sense of the original theory of Langmuir and Wood, may evidently be treated by methods identical to those used in the present work, and the accommodation coefficient, to which the effect of crystal surface structure is relegated in the Langmuir theory, invested with specific physical significance in terms of the relative depositional energy.

The major part of this investigation was done at the Jefferson Physical Laboratory of Harvard University in 1929–30. I should like to record my great obligation to Professor P. W. Bridgman for his interest and advice during the course of the work.

On the Radial Induced Electromotive Force Discovered by Corbino

By CARL A. BECK
Department of Physics, Northwestern University
(Received March 26, 1932)

This effect, which is essentially the Hall effect on induced currents in circular disks, was found in bismuth by Corbino. According to his theory, the quantity of charge transported through the circuit of resistance R is $-(1/8\pi R)c_H SH^2$, where the coefficient, c_H, corresponds to the final field H, and S is the area of the disk. On the other hand, K. K. Smith derived the following formula for the equivalent change of flux, $N=-(S/4\pi)\int_{H_1}^{H_2} cH\,dH$. These expressions agree only if c is independent of H. Our experiments on bismuth show that the value of the coefficient derived from the first formula is always greater than that derived from the second. This discrepancy is explained by the fact that the coefficient c decreases as the strength of the field increases. The ratio of Hall coefficient to resistivity, found for plates cut from the disks, agrees quite well with the coefficient c_2 derived from the second formula. In antimony the induced effect, small and opposite in sign to that in bismuth, is found. In this metal, the coefficients decrease only slightly with the field and no discrepancy between c_H, c_2 and R/ρ has been detected. In the case of bismuth, the graphs relating the induced throws and magnetic field are, for sufficiently strong fields, linear. Hence one can deduce simple expressions for the Hall and Corbino coefficients in intense fields.

INTRODUCTION

BOLTZMANN,[1] in a theoretical study of the Hall effect, pointed out that in a circular metallic disk having one electrode attached to the center while the second electrode is in contact with the entire periphery, the lines of flow are logarithmic spirals when there is a magnetic field normal to the disk. At each point the deviation of a line of flow from the radial direction is a small angle, γ, whose tangent depends upon the strength of the magnetic field and upon the material of which the disk is made. Von Ettingshausen[2] investigated the change in resistance in such a disk of bismuth.

It was Corbino,[3] however, who first demonstrated experimentally the following three related galvanomagnetic effects with circular metallic disks.

(1) Owing to the action of a steady magnetic field on a radial electric current, there is a circular current whose density varies inversely as the distance from the center. On interrupting the radial current many times a second, the inductive effect of the changing circular current is revealed by means of a galvanometer connected to a coil surrounding the disk.

(2) A steady current is sent through a disk which is suspended in a steady magnetic field. A torque acts upon the disk owing to the production of a circular current.

[1] L. Boltzmann, Wien Ber. **94,** 644 (1886); Phil. Mag. **22,** 226 (1886).
[2] Von Ettingshausen, Wien Ber. **94** (2) 560 (1886).
[3] Corbino, Phys. Zeits. **12,** 561 (1911).

(3) The center and periphery of the disk are simply connected to a galvanometer. While a magnetic field normal to the disk is being established, there is a radial electromotive force whose sense is independent of the sense of the field. Corbino pointed out that this effect may be regarded as a Hall effect on the induced currents.

The first effect was investigated by Corbino,[3] and later by Adams,[4] Chapman,[5] and Adams and Chapman.[6] An experimental study of the second effect was made by Smith,[7] and by Smith and O'Bryan.[8] The third effect has hitherto been tried only by Corbino,[3] and he apparently has made only a few observations on one disk of bismuth.

Corbino, and also Adams, showed theoretically that all three effects depend upon a certain coefficient, c, which is closely related to the Hall effect. According to Adams' definition, the Corbino coefficient is the ratio of the transverse electric field to the vector product of the primary electric field and the magnetic field, that is

$$E_T = cE_P \times H. \tag{1}$$

Furthermore, if R denotes the Hall coefficient, and ρ the resistivity, then

$$c = R/\rho. \tag{2}$$

This last relation was verified by Heaps[9] using rectangular plates, and also by Smith and O'Bryan[8] using circular disks (second Corbino effect).

Object of the Experiment

The work to be described was undertaken to investigate the third effect because, as before stated, the existing data were extremely meager. As this effect is the only one of the three which is caused by the changing of a magnetic field, it was of interest to compare the values of the coefficient found in this manner with those found in the same piece of material by measuring the Hall effect and resistivity, using steady currents and steady magnetic fields.

Theory of the Method

Corbino[3] derives the expression for the quantity of charge, Q, passing through the galvanometer in the third effect by using the value of the electromagnetic energy, W, of the disk in the magnetic field, namely,

$$W = cIH^2S/8\pi, \tag{3}$$

where I is the radial current, H the magnetic field perpendicular to the disk and S the area of the disk. The variation of this energy in time dt due to a change in the field is given, *treating I as a constant*, as

[4] E. P. Adams, Phil. Mag. **27,** 244 (1914).
[5] A. K. Chapman, Phil. Mag. **32,** 303 (1916).
[6] Adams and Chapman, Phil. Mag. **28,** 692 (1914).
[7] K. K. Smith, Phys. Rev. **8,** 402 (1916).
[8] K. K. Smith and H. M. O'Bryan, Phys. Rev. **33,** 66 (1929).
[9] C. W. Heaps, Phys. Rev. **12,** 340 (1918).

$$dW = -\frac{1}{8\pi} SI \frac{d(cH^2)}{dt} dt = e_r I dt, \tag{4}$$

e_r being the radial e.m.f.

Therefore,

$$e_r = -\frac{1}{8\pi} S \frac{d(cH^2)}{dt} \cdot \tag{5}$$

If the radial induced e.m.f. acts in a closed circuit of total resistance R, then

$$Q = \frac{1}{R} \int_0^t e_r dt = -\frac{1}{8\pi R} S c_H H^2 \tag{6}$$

where c_H is the value of the coefficient corresponding to the final value of the field. Hence the equivalent change of flux linked with the galvanometer circuit is,

$$N = QR = -\frac{1}{8\pi} S c_H H^2, \tag{7}$$

whence

$$c_H = -8N/r_0^2 H^2 \qquad \text{(Equation I)}$$

where r_0 is the radius of the disk.

Another formula for the radial e.m.f. was derived by K. K. Smith after an attempt to treat I as a variable in the differentiation of Eq. (3) had failed because the resulting expression for N, the change of flux, could not be completely integrated under the experimental conditions. The derivation of his formula is as follows.

The induced e.m.f. round a circle of radius r described about the center of the disk is from Faraday's law of induction,

$$-\pi r^2 dH/dt = \int E_c dl = 2\pi r E_c \tag{8}$$

where E_c is the circular electric intensity. Therefore, $E_c = -(r/2)(dH/dt)$, and from the definition of the Corbino coefficient, the radial electric field is given by

$$E_r = -c(r/2)(dH/dt)H. \tag{9}$$

Hence, the radial e.m.f. in the disk at any instant is,

$$e_r = \int_0^{r_0} E_r dr = -c \int_0^{r_0} \frac{r}{2} \frac{dH}{dt} H dr = -c \frac{dH}{dt} H \frac{r_0^2}{4} \tag{10}$$

assuming H and dH/dt to be independent of r. The lower limit of the integral has been put equal to zero because in practice it is negligibly small, being merely the radius of the wire connected to the center of the disk.

Now

$$N = \int_0^t e_r dt = -\tfrac{1}{4} r_0^2 \int_{H_1}^{H_2} cH dH. \tag{11}$$

Case I. c independent of H

Then if the initial field, H_1, is zero, one has, $c = -8N/r_0^2H^2$. Therefore, by Eq. I., $c_H = c$.

Case II. c not independent of H

Differentiating N with respect to the upper limit of integration, one has,

$$\frac{dN}{dH_2} = -r_0^2 c_2 \frac{H_2}{4}$$

or

$$c_2 = -\frac{4}{r_0^2}\frac{dN}{dH_2}\frac{1}{H_2} \qquad \text{(Equation II).}$$

If one determines experimentally how the value of N changes in a series of observations in which, starting always with the same initial value, the final value of the field varies, one is thus able to find c_2 the value of the coefficient corresponding to the field H_2.

Description of Apparatus and Experimental Procedure

For the purpose of obtaining strong magnetic fields, we used a Weiss electromagnet, manufactured by the Société Genevoise. The pole faces were 50 mm or 100 mm in diameter, depending upon the size of the disk. Fields up to 22,000 gauss were used. The maximum magnetizing current was about 65 amperes and this could be regulated very closely, if necessary, by means of a potentiometer. The electromagnet was water-cooled, but no especially accurate control of the temperature of the magnet was attempted, the range being about two or three degrees. In every set of observations, the field H was repeatedly measured on reversal with a Société Genevoise search coil whose effective area was accurately known.

The disks were cast in graphite molds from c.p. bismuth and antimony obtained from Eimer and Amend, and from Mallinckrodt. No particular attention was given to the formation of any definite crystalline structure. Some disks were cooled rapidly, others slowly. The dimensions are given in Table I.

Table I. *Dimensions of various disks.*

Disk	Radius (cm)	Thickness (mm)	Source	Disk	Radius (cm)	Thickness (mm)	Source
Bi A_1	1.8	1.09	M.	Bi B_2	2.25	0.77	M.
A_2	1.8	0.94	M.	C_1	4.37	1.22	M.
A_3	1.8	1.08	M.	C_2	4.37	1.22	E.A.
A_5	1.8	1.02	E.A.	Sb A_1	1.78	1.11	E.A.
B_1	2.25	0.80	M.	A_2	1.78	1.11	E.A.

M—Mallinckrodt E.A.—Eimer and Amend

In order to measure the third effect, the disks were mounted in a circular brass form (Fig. 1). This is merely a hollow flat cylinder, C, with a groove in the edge into which the disk B was soldered with Wood's metal. The leads to the disks consisted of an insulated brass wire, E, of diameter 0.8 mm or less, soldered into a hole at the center of the disk. This wire passed through a

brass tube, D which screwed into the back of the mounting. Brass has a very small Corbino coefficient, -1.4×10^{-8} e.m.u.,[8] which was neglected in comparison with the coefficients of bismuth and antimony. A Leeds and Northrup high sensitivity ballistic galvanometer, Type 2285-e, with a coil resistance of 12.6 ohms, was used as an aperiodic fluxmeter. The circuit consisted of the mounted disk, the coil of the fluxmeter, F, a small resistance used in a potentiometer to control the zero reading, and also the secondary coil (29.25 ohms) of a Brooks' inductometer, I, used for calibration. The sensitivity of the fluxmeter was 498 maxwells per cm at the actual scale distance which was 4.86 meters.

Since there is, necessarily, a cylindrical hole in one of the pole pieces, the field at the center is slightly weakened by an amount depending on the distance between the pole faces. In this work the search coil was placed halfway between the center and edge of the disk. A simple calculation, involving Eq. (10) in the theory, shows that the assumption that the field, as measured, is uniform over the disk's surface, does not lead to appreciable error. Also, the residual field was found to be comparatively small, and it was neglected in applying Eq. I since the throw varies with the square of the field. It is to be noted that if the residual field is constant, its value has no effect whatever on the determination of c_2 in Eq. II.

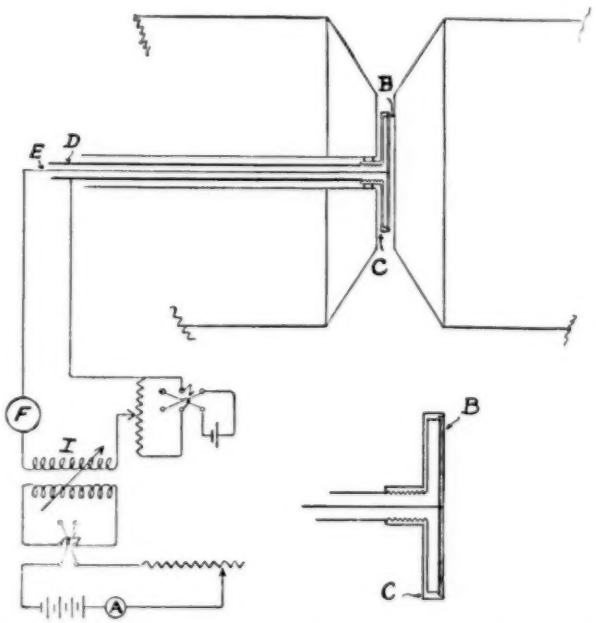

Fig. 1. Diagram of apparatus used for measuring the induced throws.

If the Corbino e.m.f. is the cause of a throw Θ on the fluxmeter, and a known change of flux, N', gives a throw, Θ', on the same instrument, then $N=N'\Theta/\Theta'=K\Theta$ and, if Eq. I is valid, $c_H=-8K\Theta/r_0^2H^2$, where K is a constant.

On the other hand, the use of Eq. II involves the determination of the slopes of a graph of Θ against the final field, H_2. That is,

$$c_2 = -\frac{4}{r_0^2}\frac{dN}{dH_2}\frac{1}{H_2} = -\frac{4K}{r_0^2}\frac{d\Theta}{dH_2}\frac{1}{H_2}. \tag{14}$$

Observations of Θ were taken in sets of four, that is, two on the establishment and two on the removal of the field. Furthermore, several such sets were taken at each field used. The effect is not very large, although with bismuth disks in strong fields, throws amounting to nearly 20 cm were obtained.

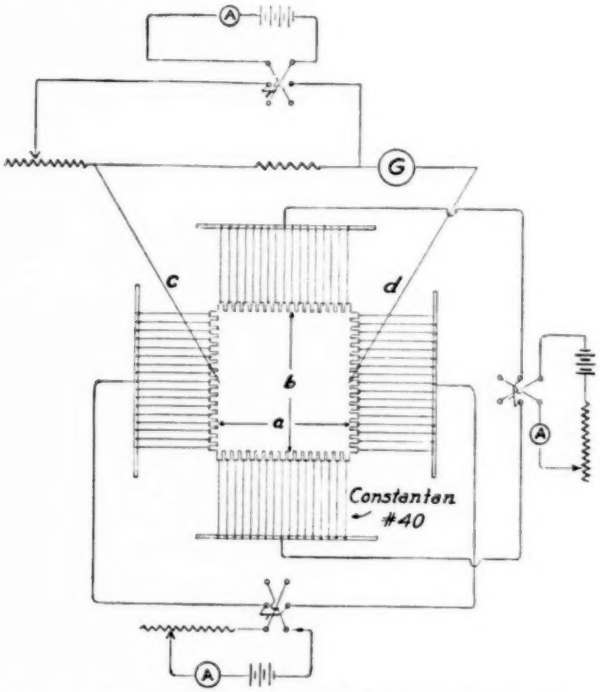

Fig. 2. Diagram of apparatus used for measuring R and ρ.

Since it appeared impracticable to increase the sensitivity of the fluxmeter, several vacuum tube circuits were tried, including one similar to Kellogg's[10] arrangement for amplifying the kick produced by the discharge of a condenser. All these attempts failed, and it may be surmised that, since the quantity of electricity which flows radially in the disk varies inversely as the resistance of the circuit, a successful ballistic amplifier in this case must have a low resistance.

In order to find the Hall coefficient, each disk was removed from the mounting and waxed to a glass plate. Four wires of the same material as that of the disk served as leads, two of these being connected to a galvanometer which measured the Hall e.m.f. generated. Not many readings were taken as this method served merely as a check on the value of R which, to-

[10] J. M. B. Kellogg, Thesis: "A Ballistic Amplifier," State University of Iowa, 1929.

gether with ρ, was found by a method used by Heaps.[9] For this purpose, the disk was cut into rectangular form (Fig. 2) with an odd number of teeth formed in each edge by careful sawing. The leads to these teeth were of constantan wire No. 40, which provide enough resistance to prevent stray currents. The wires, c and d, were of the same material as that of the disk itself and sufficiently long to extend outside of the field. Measurements of R and ρ were first made with these wires in the position shown. They were then removed, and soldered to the midpoints of the other two sides, after which

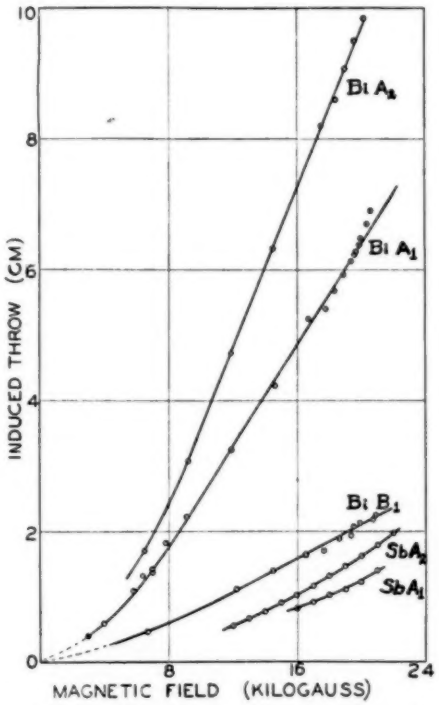

Fig. 3. Curves showing the induced throws, the initial field being zero.

similar measurements were again taken. Several sets of observations were taken at each field in order to obtain R and ρ by the equations,

$$R = D'st/I_yH \tag{15}$$

$$\rho = D''sbt/aI_x \tag{16}$$

where D' and D'' are deflections, s is the voltage sensitivity of the d'Arsonval galvanometer used, t is the thickness of the plate, and I_x and I_y are currents parallel to the length, a, and breadth, b, of the plate. It was necessary, when finding these values for antimony to use a galvanometer of very high sensitivity. Thermal effects, in this case, were especially annoying and, for that reason, the whole specimen, mounted on a piece of bakelite, was placed in a narrow cell containing transformer oil. This removed all unsteadiness, and left only a small drift.

Experimental Results

The writer worked with eight bismuth disks and two antimony disks. The throws observed in the Corbino effect are plotted in Figs. 3 and 4 against the final field. Except in the case of Bi B_1, throws at a given field are in the order of the sizes of the disks. For bismuth the graphs are linear in strong fields, but in weaker fields, they curve toward the origin. However, in the weaker fields, the observed throws do not decrease as rapidly as the square of the field decreases.

Fig. 5 shows the throws obtained with Bi C_1, (A) with the initial field always about zero and (B) with the initial field always about 9000 gauss. The

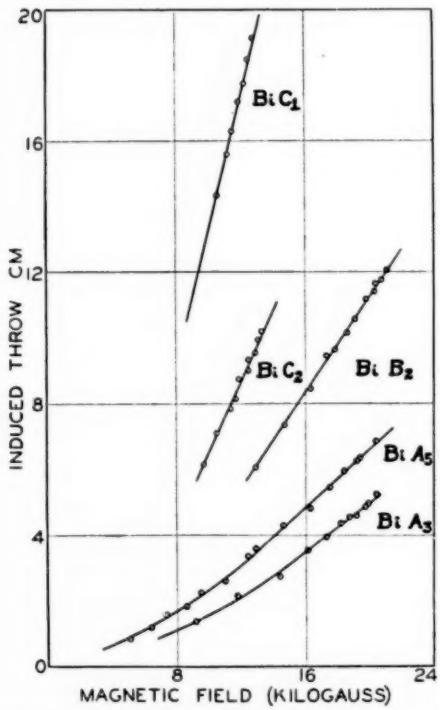

Fig. 4. Additional curves showing the induced throws, with initial field zero.

parallelism of the two graphs shows that for any final field, the value of the coefficient c_2 in Eq. II does not depend upon the initial field.

On account of limitations of space, only a small part of the calculated results can be exhibited here. The Hall coefficient, the Corbino coefficient and the resistivity vary considerably from disk to disk, the variation of the Hall coefficient being greatest, and that of the resistivity least. The larger part of these variations is probably to be attributed to differences in the crystalline structure. The main interest, however, is in comparing c_H, c_2 and R/ρ for one and the same disk. It was not thought necessary to include graphs showing the variations of the Hall coefficient, since the value of R was of interest only because it appears in the ratio, R/ρ. The resistivity curves, (Fig. 6), for bismuth are straight lines at high fields.

The coefficients, c_H and c_2, and also R/ρ as functions of H are plotted for comparison in Figs. 7, 8, and 9 for Bi A_1, Bi A_5 and Bi B_2, respectively. As in the case of the other disks, there is a good agreement between c_2 and R/ρ while the value of c_H is considerably higher than R/ρ. Since the Corbino

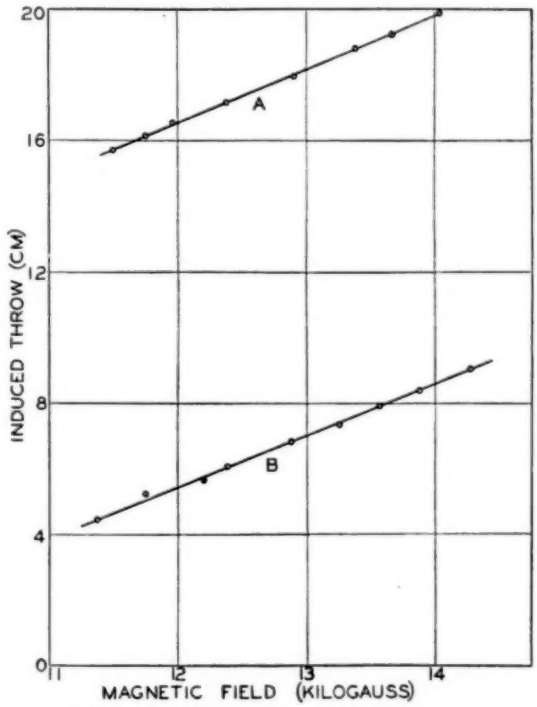

Fig. 5. Curves showing the induced throws for Bi C_1, the initial field zero for the upper and about 9000 gauss for the lower curve.

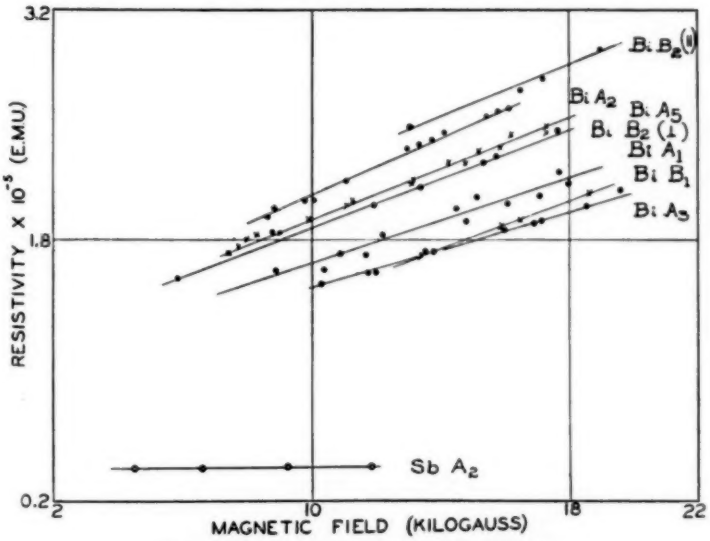

Fig. 6. Resistivity of the various disks.

coefficient decreases as the field increases, the value of c_H as found from Eq. I is not the true coefficient at the final field, but rather at a field between zero and the final field. In the case of Bi B_2 as shown, there is a good agreement between c_2 and R/ρ when the leads c and d are in one position, but some divergence when these leads are connected to the other sides. This is probably due either to a lack of isotropy in the specimen or to a change produced by handling or heating, although previous tests made on other disks had

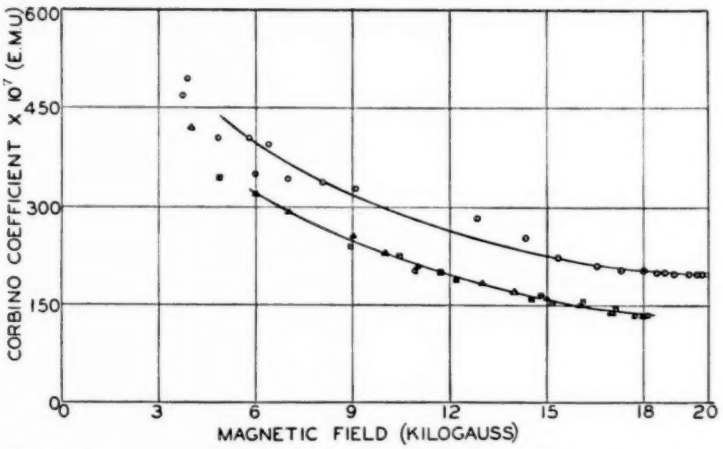

Fig. 7. A comparison of c_H, c_2 and R/ρ for Bi A_1. Circles c_H from Eq. I; Triangles, c_2 from Eq. II; squares, R/ρ.

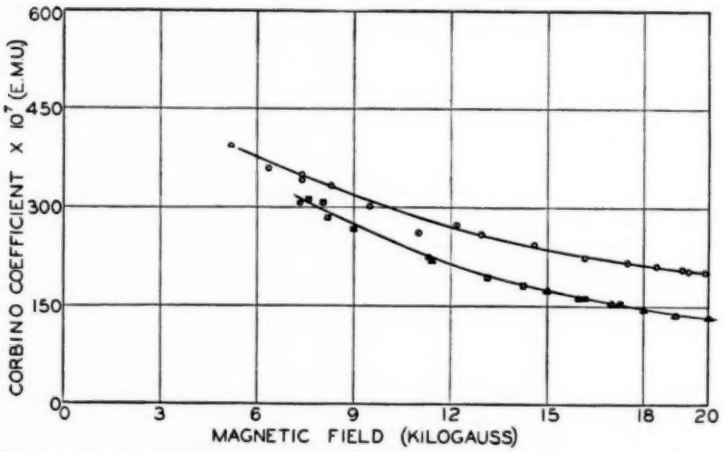

Fig. 8. A comparison of c_H, c_2 and R/ρ for Bi A_5. Circles, c_H from Eq. I; triangles, c_2 from Eq. II; squares R/ρ.

proved that the leads c and d could be removed and replaced without appreciable effect upon the measurements. There is a similar discrepancy also in one of the other disks, but, on the whole, the agreement of c_2 and R/ρ can be considered quite good.

In Table II, we see the disagreement between c_H and c_2 for Bi A_1 while the results in Table III prove the agreement of R/ρ with the c_2.

The values which are given by Corbino[3] for the third effect in bismuth are:

H (gauss) :	3700	6100	7250	8100	8650
$c \times 10^7$ (e.m.u.) :	2×770	2×490	2×450	2×440	2×430

The factor 2 was introduced after an error was discovered by Corbino.[11] These values are much higher than any found in this work, or by observers

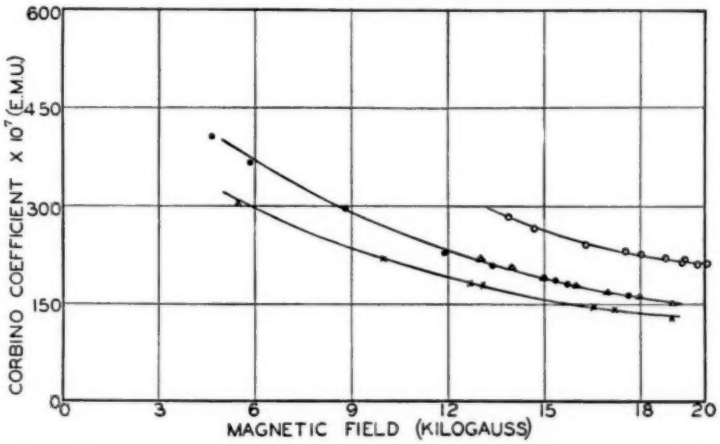

Fig. 9. A comparison of c_H, c_2 and R/ρ for Bi B_2. Circles, c_H from Eq. I; triangles c_2 from Eq. II: black dots and crosses, Hall primary current first in one direction, then in the perpendicular direction.

TABLE II. *Bi* A_1.

H (gauss)	throw (cm)	$c_H \times 10^7$ (e.m.u.) (Eq. I)	Slope $d\Theta/dH_2$ cm/kilogauss	$c_2 \times 10^7$ (e.m.u.) (Eq. II)
20,400	6.71	−199		
19,700	6.24	199		
19,000	5.93	202		
18,000			0.39	−133
18,000	5.55	211		
17,000			0.39	140
16,600	5.00	224		
16,000			0.39	149
15,000			0.39	159
14,300	4.25	255		
14,000			0.39	171
13,000			0.39	184
11,900	3.25	283		
11,000			0.38	210
9,100	2.20	328		
7,000	1.37	344		
6,400	1.32	396		
6,000			0.31	320
4,900	0.78	405		
3,800	0.54	470		
3,000			0.20	420

of the first and second effects. L. L. Campbell[12] gives values which lie in the same region as those in the present work.

[11] Corbino, Phys. Zeits. **12,** 845 (1911), footnote.

[12] L. L. Campbell, "Galvanomagnetic and Thermomagnetic Effects." p. 132, 1923.

TABLE III. *Bi* A_1. *R and* ρ *by rectangle method.*

Field (gauss)	Hall deflection (cm)	R (e.m.u.)	Resistivity deflection (cm)	$\rho\times10^{-5}$ (e.m.u.)	$c=R/\rho\times10^{7}$ (e.m.u.)
18,100	5.08	2.92	8.47	2.15	−136
17,100	4.86	2.96	8.14	2.06	143
16,100	4.76	3.08	7.95	2.01	153
14,800	4.49	3.15	7.55	1.91	165
11,700	3.89	3.46	6.71	1.70	203
10,400	3.60	3.63	6.40	1.62	224
		Electrodes joined to the other sides.			
17,700	5.12	2.98	8.04	2.21	135
15,100	4.575	3.11	7.5	2.06	151
14,500	4.49	3.19	7.2	1.98	161
12,200	4.08	3.44	6.64	1.83	188
10,900	3.79	3.58	6.25	1.72	208
8,900	3.35	3.87	5.84	1.61	240
4,900	2.21	4.67	4.95	1.36	344

$I_y=1.02$ amperes. $I_x=0.4$ amperes.

For antimony in strong fields, the curves (Fig. 3), representing the throws are not linear as in the case of bismuth. They are nearly parabolic in form which is, of course, the form that will yield, by Eq. II, a constant value of the coefficient c_2. The resistivity is practically constant, within the limit of experimental error, over the range of fields used. The comparison of the three coefficients, c_H, c_2 and R/ρ for one of the antimony disks is shown in Fig. 10 and in Tables IV and V. Since there is not much variation with strength of field, all three show the expected fair agreement.

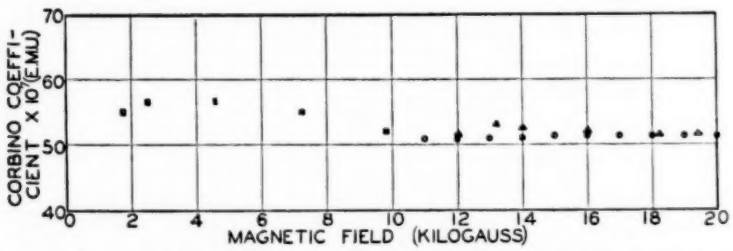

Fig. 10. Sb A_2. Circles, C_H from Eq. I; triangles C_2 from Eq. II, squares R/ρ.

It must be noted here, however, that the Corbino deflections are very small, and it is therefore difficult to obtain precise results. The average value of the coefficient for antimony is given by Campbell[12] as $+40\times10^{-7}$ e.m.u. One of the disks (Sb A_1) yields a value over the range of fields used of about 40×10^{-7} while the other gives a little over 50×10^{-7}.

SUMMARY AND DISCUSSION

It has been shown that (1) in the case of bismuth, in which the Corbino coefficient varies with the strength of the field, the value of the coefficient found from Corbino's equation for the induced effect does not agree with the value of R/ρ. (2) The expression for the induced throw, derived by K. K.

TABLE IV. *Sb* A_2.

H (gauss)	Induced throw (cm)	$c_H \times 10^7$ (e.m.u.) (Eq. I)	Slope $d\Theta/dH_2$ (cm/kilogauss)	$c_2 \times 10^7$ (e.m.u.) (Eq. II)
22,000	1.98	51		
20,000	1.63	51	0.16	51
18,000	1.33	51	0.15	52
16,000	1.04	51	0.13	52
15,200				53
14,000	0.79	50	0.13	52

TABLE V. *Sb* A_2.

H (gauss)	R (e.m.u.)	$\rho \times 10^{-5}$ (e.m.u.)	$c = R/\rho \times 10^7$ (e.m.u.)
11,980	0.21		
11,850		0.41	52
9,270	0.22	0.41	55
6,600	0.23	0.40	57
4,500	0.23	0.40	57
3,720	0.22	0.40	55

$I_y = 100.5$ milliamps. $I_x = 21.4$ milliamps.

Smith, yields for both bismuth and antimony a good agreement between the Corbino coefficient and R/ρ. (3) In the case of antimony, in which the coefficient varies only slightly with the strength of the field, the use of Corbino's equation leads to no observable discrepancy. (4) For fields sufficiently strong the graphs for bismuth relating the induced throws and the magnetic fields are straight lines. Since for this region the slope is independent of the field, it follows that $c_2 H_2 = k$, a constant for a given disk. In this same region, the resistivity graphs are also linear, that is, $\rho = aH_2 + b$, and therefore the Hall coefficient is $R = ka + kb/H_2$. Table VI shows the values of k, a and b for five of the bismuth disks.

Now if the graphs for the induced throw and resistivity, respectively, continue to be straight indefinitely, then the conclusion that the limiting value of R is ka seems to be justifiable. And it would follow from Eq. II that the Corbino coefficient would then approach zero asymptotically in very intense fields. Mazzari[13] found that for the bismuth disk he used, the Hall coefficient above 29,000 gauss had the *constant* value, -2.63 e.m.u. It would be of interest to determine experimentally the limiting value of the Corbino coefficient in very intense fields.

TABLE VI. (*Values in e.m.u.*)

Disk	k	a	ka	b
Bi A_2	-0.36	8.9	-3.2	1.18×10^5
A_5	-0.26	7.8	-2.0	1.13×10^5
B_2	-0.29	7.6	-2.2	1.10×10^5
A_1	-0.24	6.7	-1.6	0.97×10^5
A_3	-0.23	5.9	-1.4	0.92×10^5

[13] A. Mazzari, N. Cimento **5**, 215 (1928).

Now Kapitza[14] has found as the result of extensive experiments on a large number of elements, that the resistance of a metal increases according to a quadratic law in weak fields, and according to a linear law in stronger fields. This seems to be in agreement with Mazzari's observation on bismuth, and also with our experiments which indicate that the Corbino coefficient in strong fields varies inversely as the strength of the field.

On the other hand, N. H. Frank,[15] on the basis of Sommerfeld's theory of metallic conduction, deduced the following expression for change of resistance, namely

$$\frac{\Delta\rho}{\rho} = \frac{BH^2}{1 + CH^2}$$

where B and C are constants for a given metal. Sommerfeld and Frank[16] state that "in the transition region between the quadratic law and the approach to saturation, this function represents all of Kapitza's results fully as well as this linear law." According to the theoretical formula the relative change of resistance approaches a saturation value, B/C, in very strong fields. The "constant" C is R^2/ρ^2, the square of the Corbino coefficient. Hence one would not expect that the Frank formula would be applicable in the anomalous case of bismuth. And our experiments in antimony, for reasons stated above, are by no means precise enough to reveal the slight variations of R, c and ρ as the strength of the field increases.

In conclusion the writer wishes to acknowledge his indebtedness to the Physics Department of Northwestern University and, in particular, to express a deep appreciation of the constant interest and suggestions of Professor K. K. Smith, who proposed the problem and kindly permitted the publication in this paper of the equation he developed.

[14] P. Kapitza, Proc. Roy. Soc. **A123,** 292 (1929).
[15] N. H. Frank, Zeits. f. Physik **64,** 650 (1930).
[16] A. Sommerfeld, and N. H. Frank, Rev. Mod. Phys. **3,** 1 (1931).

Note on the Transmission and Reflection of Wave Packets by Potential Barriers

By L. A. MacColl
Bell Telephone Laboratories

(Received January 14, 1932)

In previous studies, by the methods of wave mechanics, of one-dimensional motion of particles in cases in which there are intervals in which the value of the potential energy function $V(x)$ exceeds the value of the total energy E, attention has been confined to wave functions of the form $f(x, E) \exp(-2\pi iEt/h)$. In the present note wave packets are considered, instead of these trains of waves.

The function $V(x)$ is taken as follows:

$$V(x) = 0 \text{ for } x < 0 \text{ and for } x > a,$$
$$= V_0 > 0 \text{ for } 0 < x < a.$$

A wave function is set up which initially represents a wave packet moving toward the point $x=0$ from the left. The separation of the incident packet into a reflected packet and a transmitted packet is studied. It is found that the transmitted packet appears at the point $x=a$ at about the time at which the incident packet reaches the point $x=0$, so that there is no appreciable delay in the transmission of the packet through the barrier.

THE recent literature on wave mechanics contains a large number of papers dealing with the one-dimensional motion of particles in cases in which the potential energy function, $V(x)$, has various arrangements of large and small values. According to classical mechanics, if the value of $V(x)$ at each point of a certain interval exceeds the value of the total energy, E, of the particle, the particle can neither enter nor pass through that interval. It is for this reason that such an interval, or the function $V(x)$ in such an interval, is called a "potential barrier." According to quantum mechanics a potential barrier is not an absolute barrier to particles with small total energy; such a particle may either be reflected or transmitted by the barrier.

Apparently, in all of the work which has been done hitherto on problems concerning potential barriers, attention has been confined to solutions of the wave equation which are of the form

$$\Psi = f(x, E) \exp(-2\pi iEt/h).$$

As is known, such solutions apply to cases in which the particle has the precisely determined value E of total energy and in which the relative probabilities of finding the particle in various intervals are independent of the time. The typical problem which has been considered heretofore may be stated as follows: Assuming that the particle is moving toward a certain potential barrier with total energy E, what is the probability that it will pass through the barrier?

The solution of such a problem can give no information about the manner in which the particle traverses the barrier, when it does. It has been pointed out by Condon[1] that it would be interesting to consider problems, involving

[1] Condon, Revs. Mod. Phys. **3**, 76 (1931).

potential barriers, in which the relative probabilities of finding the particle in various intervals are not independent of the time. It is only in the sense of studying such probabilities that we can investigate, by the methods of wave mechanics, the transmission of a particle through a barrier. The present note is devoted to the study of a simple typical problem of the kind suggested by Condon.

We shall employ the potential energy function which is defined by the equations

$$\left.\begin{aligned} V(x) &= 0 && x < 0, \\ &= V_0 > 0 && 0 < x < a, \\ &= 0 && x > a. \end{aligned}\right\} \tag{1}$$

We shall take a suitable elementary wave function of the form $f(x, E)$ $\exp\left[-2\pi iEt/h\right]$ and effectively integrate it with respect to E over a certain range, thus producing a new wave function. It is required that at $t=0$ this wave function shall form a wave packet, the bulk of which lies to the left of the point $x=0$ and is moving toward the barrier. The problem is to study the way the wave function changes with time, and, in particular, to study the development of the function in the interval $x>a$. There arises the question of whether we should select the elementary wave function and the interval of integration so that the resulting wave function shall initially be identically zero in the interval $x>a$, or so that no values of E greater than V_0 shall occur in the composition of the function, that is, so that the function $V(x)$ shall be definitely a barrier. The second of these choices is the one made here, because it seems on the whole to represent the more interesting situation, and because it leads to the simpler analysis. Of course, this choice gives us initially a certain non-zero value of the probability that the particle be in the interval $x>a$. But, as this value is small compared with the initial value of the probability that the particle be in the interval $x<0$, and compared with the final value of the probability that the particle be in the interval $x>a$, no real difficulty is created by the fact that this initial value is not zero.

As the exact solution of the problem is expressed in terms of definite integrals which are difficult to evaluate numerically, the discussion is confined to the simpler qualitative features of the wave function. This discussion suffices to give a rather clear idea of the properties of the solution.

The chief result of the study can be stated as follows: The probability that the particle be in the interval $x>a$ is initially small; as time goes on this probability increases, rather slowly at first, much more rapidly in the neighborhood of the time at which the bulk of the incident wave packet reaches the point $x=0$, and then more slowly again; the time interval during which this probability undergoes its chief variation is substantially independent, both as to location and as to length, of the height and width of the barrier.

Consider the function $\Psi(x, t)$ which is defined by the following sequence of equations:

$$\left.\begin{aligned} \Psi &= \Psi_1 + \Psi_2, && x < 0, \\ &= \Psi_3 + \Psi_4, && 0 < x < a, \\ &= \Psi_5, && x > a; \end{aligned}\right\} \tag{2}$$

$$\left.\begin{aligned} \Psi_1 &= \int_{w_1}^{w_2} \exp\left[-(w - E_0^{1/2})^2/(4\lambda^2) + ik(x + x_0)w - 2\pi i t w^2/h\right]dw, \\ \Psi_2 &= \int_{w_1}^{w_2} \beta_1(w^2) \exp\left[-(w - E_0^{1/2})^2/(4\lambda^2) - ik(x - x_0)w - 2\pi i t w^2/h\right]dw, \\ \Psi_3 &= \int_{w_1}^{w_2} \alpha_2(w^2) \exp\left[-(w - E_0^{1/2})^2/(4\lambda^2) + kx(V_0 - w^2)^{1/2}\right. \\ &\quad \left. + ikx_0 w - 2\pi i t w^2/h\right]dw, \\ \Psi_4 &= \int_{w_1}^{w_2} \beta_2(w^2) \exp\left[-(w - E_0^{1/2})^2/(4\lambda^2) - kx(V_0 - w^2)^{1/2}\right. \\ &\quad \left. + ikx_0 w - 2\pi i t w^2/h\right]dw, \\ \Psi_5 &= \int_{w_1}^{w_2} \alpha_3(w^2) \exp\left[-(w - E_0^{1/2})^2/(4\lambda^2) + ik(x + x_0 - a)w - 2\pi i t w^2/h\right]dw; \end{aligned}\right\} \tag{3}$$

$$\left.\begin{aligned} \beta_1(w^2) &= -1 - 2i \sin\theta \frac{ch\left[ka(V_0 - w^2)^{1/2} - i\theta\right]}{sh\left[ka(V_0 - w^2)^{1/2} - 2i\theta\right]}, \\ \alpha_2(w^2) &= -i \sin\theta \frac{\exp\left[-ka(V_0 - w^2)^{1/2} + i\theta\right]}{sh\left[ka(V_0 - w^2)^{1/2} - 2i\theta\right]}, \\ \beta_2(w^2) &= -i \sin\theta \frac{\exp\left[ka(V_0 - w^2)^{1/2} - i\theta\right]}{sh\left[ka(V_0 - w^2)^{1/2} - 2i\theta\right]}, \\ \alpha_3(w^2) &= \frac{-i \sin 2\theta}{sh\left[ka(V_0 - w^2)^{1/2} - 2i\theta\right]}, \\ \theta &= \arctan\left[w/(V_0 - w^2)^{1/2}\right]. \end{aligned}\right\} \tag{4}$$

Here λ, x_0, w_1, E_0, and w_2, are positive numbers, and

$$0 < w_1 < E_0^{1/2} < w_2 < V_0^{1/2}.$$

We write

$$8\pi^2 m/h^2 = k^2,$$

where m is the mass of the particle under consideration.

It is easy to verify that the function $\Psi(x, t)$ satisfies the Schrödinger non-relativistic wave equation

$$\frac{\partial^2 \Psi}{\partial x^2} - k^2\left[V(x) + \frac{h}{2\pi i}\frac{\partial}{\partial t}\right]\Psi = 0,$$

and that, for any fixed value of t, Ψ and $\partial\Psi/\partial x$ are continuous functions of x.[2]

[2] Of course, the solution is set up by the familiar device of obtaining an elementary solution of the form $f(x, w) \exp(-2\pi i t w^2/h)$, and then integrating with rsepect to w. The limits of integration are taken as w_1, w_2, rather than 0, $V_0^{1/2}$, merely in order to make the problem of verifying the solution a little simpler.

The integrals in Eqs. (3) are difficult to evaluate numerically; we shall merely discuss them qualitatively, avoiding certain extreme values of the parameters a, V_0, E_0, λ, w_1, w_2. To state the complicated facts rather loosely, it will be shown that when $t=0$ the function Ψ is a packet of waves concentrated about the point $x=-x_0$. As t increases the packet moves to the right, gradually spreading out. The bulk of the packet strikes the barrier, that is, reaches the point $x=0$, at about the time $t=x_0[2E_0/m]^{-1/2}$ and the packet then separates into a reflected packet and a transmitted packet. The reflected packet moves indefinitely to the left. The transmitted packet starts to the right from the point $x=a$ when the original packet strikes the barrier. The transmitted packet, as it leaves the point $x=a$, is of substantially the same form, except for a constant factor, as the original packet when it reaches the point $x=0$. In the interval $0<x<a$ the function Ψ is nearly a monotonic decreasing function of x multiplied by a function of t which is small when $t=0$, has appreciable values in the neighborhood of the instant $t=x_0[2E_0/m]^{-1/2}$, and ultimately becomes small again.

To a great extent, the qualitative properties of Ψ can be deduced from those of the function Ψ_1. Hence, we shall first consider the latter function.

If $E_0^{1/2}-w_1$ and $w_2-E_0^{1/2}$ are fairly large, and if λ is not too large, we can write approximately

$$\Psi_1 = \int_{-\infty}^{\infty} \exp\left[-(w-E_0^{1/2})^2/(4\lambda^2) + ik(x+x_0)w - 2\pi i t w^2/h\right]dw. \quad (5)$$

In order that this approximation shall be legitimate we must assume that the numbers

$$(E_0^{1/2}-w_1)/(2\lambda),\quad (w_2-E_0^{1/2})/(2\lambda),$$

are sufficiently large, say somewhat greater than unity. We make this assumption.

From (5) one obtains the following relation by means of some elementary transformations.

$$\exp\left[E_0/(4\lambda^2) - [E_0^{1/2}+2i\lambda^2k(x+x_0)]^2/[4\lambda^2(1+8\pi i\lambda^2 t/h)]\right]\Psi_1$$
$$= 2\lambda[-(1+8\pi i\lambda^2 t/h)]^{-1/2}\int_{-\infty[-(1+8\pi i\lambda^2 t/h)]^{1/2}}^{\infty[-(1+8\pi i\lambda^2 t/h)]^{1/2}} \exp w^2 dw.$$

The limits of integration indicate that the path of integration is the entire straight line passing through the points $w=\pm[-(1+8\pi i\lambda^2 t/h)]^{1/2}$. It can be shown without difficulty that the value of the integral in the right-hand member of the preceding equation is $i\pi^{1/2}$. Hence, we have the following approximate expression for the function defined by the first of Eqs. (3):

$$\Psi_1 = 2\lambda\pi^{1/2}(1+8\pi i\lambda^2 t/h)^{-1/2}\exp\left[-E_0/(4\lambda^2)\right.$$
$$\left.+[E_0^{1/2}+2i\lambda^2k(x+x_0)]^2/[4\lambda^2(1+8\pi i\lambda^2 t/h)]\right]. \quad (6)$$

The principal qualitative properties of the function Ψ_1 can be obtained readily from the approximation (6). Let us consider the absolute magnitude of Ψ_1. We have, approximately, by (6),

$$|\Psi_1| = 2\lambda\pi^{1/2}(1 + 64\pi^2\lambda^4t^2/h^2)^{-1/4} \exp\left[(1 + 64\pi^2\lambda^4t^2/h^2)^{-1}\right.$$
$$\left.\cdot\left[E_0 - 4\lambda^4k^2(x + x_0)^2 + 32\pi\lambda^4k(x + x_0)E_0^{1/2}t/h\right](4\lambda^2)^{-1} - E_0/(4\lambda^2)\right].$$

This shows that, for any fixed value of t, $|\Psi_1|$ has its greatest value near the point determined by the equation

$$x + x_0 = 4\pi k^{-1}E_0^{1/2}t/h = (2E_0/m)^{1/2}t.$$

At the point where $|\Psi_1|$ is a maximum we have approximately

$$|\Psi_1| = 2\lambda\pi^{1/2}(1 + 64\pi^2\lambda^4t^2/h^2)^{-1/4}.$$

It is to be observed that we have approximately

$$\Psi_1(x, 0) = 2\lambda\pi^{1/2} \exp\left[-\lambda^2k^2(x + x_0)^2 + ik(x + x_0)E_0^{1/2}\right].$$

The chief qualitative properties of the function Ψ_1 are now apparent. When $t=0$ the function is a packet of complex waves which is extremely small except in the neighborhood of the point $x=-x_0$. As t increases the packet moves to the right with speed which can be estimated as equal to $(2E_0/m)^{1/2}$. As the packet moves forward it spreads out, and the maximum absolute value of the function Ψ_1 diminishes.

If, as we assume, E_0 and V_0-E_0 are large, and a is not too large, the functions $\beta_1(w^2)$ and $\alpha_3(w^2)$ vary only slowly in the neighborhood of the point $w=E_0^{1/2}$, which is the important part of the interval of integration $w_1 \leqq w \leqq w_2$. Hence, we can write, approximately,

$$\Psi_2(x, t) = \beta_1(E_0)\Psi_1(-x, t), \tag{7}$$
$$\Psi_3(x, t) = \alpha_3(E_0)\Psi_1(x - a, t). \tag{8}$$

According to (7), the function Ψ_2 is approximately, aside from a constant factor, merely the function Ψ_1 with the sign of x changed. We now perceive the qualitative nature of the function Ψ in the interval $x<0$. Initially we have a packet of waves concentrated about the point $x=-x_0$. As t increases the packet travels to the right, gradually spreading out and diminishing in maximum absolute magnitude. The bulk of the packet reaches the barrier at $x=0$ at about the instant $t=(2E_0/m)^{-1/2}x_0$. Thereafter, the packet is multiplied by a nearly constant factor, and it travels indefinitely to the left, gradually spreading out as before.

Eq. (8) displays the nature of the function Ψ in the interval $x>a$. Initially the function is small throughout the interval. In the neighborhood of the instant $t=(2E_0/m)^{-1/2}x_0$ the function begins to have appreciable values in the neighborhood of the point $x=a$. Thereafter we have a wave packet moving off indefinitely to the right, and gradually flattening out. As the function $\alpha_3(w^2)$ is small throughout the more important part of the interval of integration, the packet which moves to the right from the barrier is smaller than the packet which impinges on the barrier from the left.

It is significant that $\Psi(x, t)$ first attains appreciable values in the interval $x>a$ when the bulk of the incident packet reaches the point $x=0$. In this connection it is interesting to compute the probability $P(t)$ that the particle be in the interval $x>a$ at the instant t. It is easily found, on the basis of the approximations already made, that

$$P(t) = \int_a^\infty |\Psi_5(x, t)|^2 dx = 2^{3/2}\pi\lambda k^{-1} |\alpha_3(E_0)|^2 \int_\Omega^\infty e^{-u^2} du, \tag{9}$$

where

$$\Omega = 2^{1/2}\lambda[hkx_0 - 4\pi E_0^{1/2}t][h^2 + 64\pi^2\lambda^4 t^2]^{-1/2}. \tag{10}$$

These equations show that, to within the accuracy of the qualitative discussion given, the probability $P(t)$ does not depend on the height or width of the barrier, except through the constant factor $|\alpha_3(E_0)|^2$. In particular, the instant of most rapid increase of $P(t)$ is independent of V_0 and a.

It remains to examine $\Psi(x, t)$ in the interval $0<x<a$.

On the assumption that $ka(V_0-E_0)^{1/2}$ is fairly large, the function $\beta_2(w^2)$ is much larger, numerically, than $\alpha_2(w^2)$ throughout the more important part of the interval of integration. It follows that Ψ_4 is larger than Ψ_3 in the interval $0<x<a$, except, possibly near the point $x=a$ where both functions are small. Hence, throughout most of the interval $0<x<a$ the function Ψ is nearly equal to Ψ_4.

Now, throughout the more important part of the interval of integration $\exp[-kx(V_0-w^2)^{1/2}]$ is a slowly varying function of w. Therefore, we can write approximately,

$$\Psi_4 = \exp[-kx(V_0 - E_0)^{1/2}] \int_{w_1}^{w_2} \beta_2(w^2) \exp[-(w - E_0^{1/2})^2/(4\lambda^2) + ikx_0 w - 2\pi i t w^2/h] dw. \tag{11}$$

This equation shows that $|\Psi_4|$ is approximately a monotonic function of x multiplied by a function of t. The fact that Ψ is a continuous function of x, together with the facts which we have already deduced concerning Ψ in the intervals $x<0$ and $x>a$, shows that the function of t must be small when $t=0$, must attain appreciable values in the neighborhood of the instant $t=(2E_0/m)^{-1/2}x_0$, and must ultimately become small again.

In conclusion a word should be said about two physically important limiting cases which immediately come to mind. These are the cases in which we have $V_0=0$ and $V_0=\infty$, respectively.

The present theory is in no way applicable to the case $V_0=0$. In order to treat this case we would have to consider cases in which the wave packet contains elementary wave functions pertaining to values of E which are greater than V_0. However, for the sake of simplicity, and in order to confine the discussion to those problems that seem to possess the most interesting features, such cases have been explicitly excluded from consideration in this paper.

On the other hand, the theory does apply to the case in which $V_0=\infty$. We need only observe what happens when we take V_0 greater and greater without limit, E_0 being left unchanged. It results that the magnitude of the transmitted wave packet (measured in any convenient way) becomes smaller and smaller, and vanishes in the limit. Thus, in the limit the wave function is identically zero on the far side of the barrier, so we have perfect reflection. It is interesting to observe that the perfect reflection is explained simply by the vanishing of the magnitude of the transmitted packet, and not by the packet suffering an infinite delay.

Surface Energy and Heat of Vaporization of Liquids[1]

By LOUIS S. KASSEL[2] AND MORRIS MUSKAT[3]
The Pittsburgh Experiment Station of the U. S. Bureau of Mines, and the Gulf Research Laboratory, Pittsburgh, Pa.

(Received March 28, 1932)

An approximate calculation of the total surface energy of nonpolar liquids is made, by using forces obtained from quantum theory. The formula obtained is somewhat different from that previously used by Margenau, and it is suggested that his calculation gives either the free surface energy, or some closely related quantity. The calculations are made by assuming both that the positions of the molecules obey the simple Maxwell-Boltzmann distribution law appropriate to a dilute gas, and that the distribution is uniform outside of the excluded regions caused by the (approximate) impenetrability of the molecules. For argon, neon, nitrogen, and oxygen the experimental values lie between those computed on these two extreme assumptions; for helium the calculated value is too great, even when uniform distribution is assumed, due probably to the importance of zero-point energy for liquid helium. The heat of vaporization has been calculated in a similar way and for it also the experimental values lie between those based on the two different distributions, except for helium, where the zero-point energy shows up still more prominently, as would be expected.

INTRODUCTION

IT IS possible to derive from quantum mechanics[4,5] approximate expressions for the polarization attraction between nonpolar molecules. This calculation, taken in conjunction with experimental values for the kinetic theory diameter, gives a rough picture of the interaction of such molecules. The actual repulsion at small distances, which is due to exchange interactions, does not, of course, suddenly become infinite, as is implied by the use of the term "diameter"; this repulsion does rise very rapidly, however, as the separation is decreased, and hence the model of a rigid sphere surrounded by an attractive field is not wholly unreal. It is of some interest to see whether or not the properties of liquids can be accounted for by this model. We shall consider here the calculation of the surface energy and of the heat of vaporization of nonpolar liquids.

THEORY OF SURFACE ENERGY

This problem has been treated by Margenau,[6] but his results are not entirely satisfying, as we shall show presently.

When the surface area of a liquid is increased in an isothermal system, there will in general be mechanical work done and heat absorbed. The sum of

[1] Published by permission of the Director, U. S. Bureau of Mines. (Not subject to copyright.)

[2] Associate physical chemist, U. S. Bureau of Mines, Pittsburgh Experiment Station, Pittsburgh, Pa.

[3] Gulf Research Laboratory, Pittsburgh, Pa.

[4] Eisenschitz and London, Zeits. f. Physik **60**, 491 (1930).

[5] London, Zeits. f. Physik **63**, 245 (1930).

[6] Margenau, Phys. Rev. **38**, 365 (1931).

these gives the increase in the total surface energy of the system. The quantity that is ordinarily measured is the surface tension σ; σ is related to the total surface energy U, by the thermodynamic equation

$$U = \sigma - T(\partial\sigma/\partial T) - p(\partial\sigma/\partial p). \tag{1}$$

The last term on the right, which corresponds to $p\Delta V$, is usually quite negligible. The surface tension itself corresponds to the free energy of the surface. A detailed theory should therefore be compared with experiment in terms of σ, but since this quantity varies greatly with temperature a crude theory can scarcely be expected to give a satisfactory temperature dependence. Hence its results may be more suitably compared with U, which is almost independent of temperature.

To calculate the total surface energy of a liquid, imagine an infinite body of it divided into two portions by a geometrical plane. Suppose that every

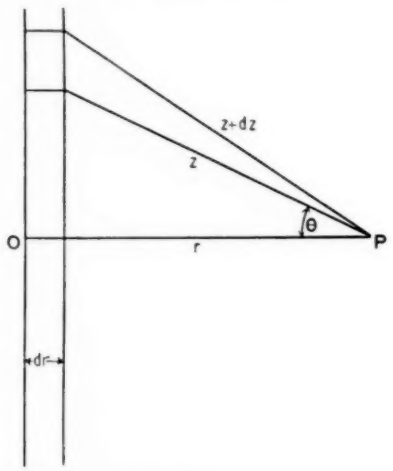

Fig. 1.

molecule in the liquid remains fixed in position in its proper half as the two halves are separated; the work necessary to carry out this separation is then merely the mutual potential energy of the two portions of liquid. The separation having been completed, permit the surfaces formed to rearrange themselves; in this process, the surface layers will expand, and will absorb heat. The work done in the separation plus the heat absorbed in the rearrangement give the total surface energy. Since, however, we have not carried out an equilibrium process, and the separate work and heat terms have no direct thermodynamic interpretation, all we can say is that the work done is greater than σ, and the heat absorbed less than $[-T(\delta\sigma/\delta T)]$. Although we are not able to calculate the heat term, since we do not know the variation in density near the surface of the liquid, the work term is easily found as follows.

Suppose that there are n molecules per cc in the interior of the liquid, and that the mean number of molecular centers per cc at a distance z from the center of a chosen molecule is $nf(z)$. Let the mutual potential energy of two molecules at this distance be $E(z)$. The mutual potential energy of a molecule with respect to the molecules in an annulus located as shown in Fig. 1 is then

readily seen to be $2\pi nzf(z)E(z)dzdr$. By integrating from $z=r$ to ∞ and from $r=y$ to ∞ we obtain the mutual potential energy between a molecule and a body of liquid at the distance y. Furthermore, since the number of molecules per cm^2 of interface at a distance between y and $y+dy$ from the interface is ndy, the total mutual potential energy of the two halves per cm^2 is finally:

$$W = 2\pi n^2 \int_0^\infty dy \int_y^\infty dr \int_r^\infty zf(z)E(z)dz. \tag{2}$$

By successive integrations by parts, proceeding from left to right, it follows that:

$$\begin{aligned} W &= 2\pi n^2 \int_0^\infty rdr \int_r^\infty zf(z)E(z)dz \\ &= \pi n^2 \int_0^\infty z^3 f(z)E(z)dz. \end{aligned} \tag{3}$$

This equation is evidently valid even though the integrand in the integral be discontinuous, as will be presently supposed, since nothing except convergence requirements was assumed in the reduction of Eq. (2) to Eq. (3).

The contribution, U, to the total surface energy per cm^2 of either half is then:

$$U = -\pi n^2/2 \int_0^\infty z^3 f(z)E(z)dz. \tag{4}$$

As already suggested, the potential field $E(z)$ will be taken as appropriate to a rigid sphere molecule surrounded by an attractive polarization field. Specifically, then

$$\left.\begin{aligned} E(z) &= +\infty : z < R_0 \\ &= -\beta/z^6 : z \geqq R_0 \end{aligned}\right\}. \tag{5}$$

With regard to the distribution function $f(z)$ the following two extreme assumptions will be investigated:

$$\left.\begin{aligned} \text{(a)} : f(z) &= 0 : z < R_0 \\ &= 1 : z \geqq R_0 \end{aligned}\right\} \tag{6}$$

$$\text{(b)} : f(z) = e^{-E(z)/kT}. \tag{7}$$

Assumption (b) is that used by Margenau and implies a treatment of the liquid as if it were a dilute gas.

The corresponding values of U are evidently:

$$\text{(a)} : \quad U = \frac{\pi}{4}\frac{n^2\beta}{R_0^2} \tag{8}$$

$$\begin{aligned} \text{(b)} \qquad U &= \frac{\pi n^2\beta}{2} \int_{R_0}^\infty \frac{e^{\beta/kTz^6}}{z^3} dz \\ &= \frac{\pi n^2\beta}{12}\left(\frac{kT}{\beta}\right)^{1/3} \int_0^{\beta/kTR_0^6} \frac{e^u}{u^{2/3}} du. \end{aligned} \tag{9}$$

The integration in case (b) is easily carried out graphically. A single curve of $e^u/u^{2/3}$ suffices for the integrand for all values of T, R_0 and β, and only the upper limit changes from case to case.

According to the Eisenschitz and London theory, an approximate value for β is $(3/4)(\alpha^2 V)$, where α is the polarizability and V the ionization potential. The calculations thus depend upon α, V, R_0 and n; only the last of these is known with much certainty. The values which we have used for the others are, so far as we know, about the same as adopted by Margenau. Both his results and those of the present calculation are shown in Table I.

TABLE I.

	T (°K)	$\alpha \cdot 10^{24}$	V volts	$R_0 \cdot 10^8$	$n \cdot 10^{-22}$	U calc. (ergs/cm²) Eq. (8)	Eq. (9)	Marg.	$U_{exp.}$	$\sigma_{exp.}$
He	4	0.20	24.5	2.11	1.94	0.78	$>7.10^5$	0.78	0.6	0.12
Ne	26	0.39	21.5	2.60	3.60	5.88	26.3	20	15.0	5.15
A	87	1.63	15.7	2.13	2.11	17.76	145.1	50	35	12.5
N_2	80	1.74	17.0	3.42	1.75	12.63	55.8	26	25.8	8.27
Cl_2	233	4.60	13.2	3.30	1.37	45.11	6688.	100	73	29.2
O_2	80	1.57	13.0	3.30	2.27	14.21	40.4	21	35	15.7

It will be observed that for argon, neon, nitrogen, and oxygen the experimental values of U lie between the calculated values for uniform and Boltzmann distributions. When it is remembered that the calculated values in both cases are low because of the unavoidable omission of a noncalculable heat term, it may be seen that the hypothesis of uniform distribution gives rather more satisfactory results. It is fortunate that this is so, since the simple Boltzmann formula gives concentrations which are physically absurd. Thus for liquid oxygen at 70°K, this formula gives an average of 42 molecules between 3.3 and 6.6×10^{-8} cm from the center of a given molecule; hexagonal close packing of spheres of diameter 3.3×10^{-8} cm would permit only 12 molecules within this space. The density of liquid oxygen at this temperature corresponds to close packed spheres of 3.9×10^{-8} cm diameter; and it is thus fairly evident that if the actual molecules may be approximately represented by spheres of 3.3×10^{-8} cm diameter, there is not room for much departure from uniformity.

For helium, the calculated values of U are much too large. It seems quite certain that for very light molecules the zero point vibrational energy plays an important rôle; thus we shall find that the low heat of vaporization of helium can only be accounted for by the use of zero-point energy, and we must invoke this energy also to account for the low density of the liquid. Its effect on surface energy is of course less direct, but apparently by no means unimportant.

For chlorine, also, the value calculated from (9) is hopelessly high, though that from (8) is satisfactory. If we adopt the ionization potential used by Margenau, the agreement is much improved, but we have been unable to find support for this value.

It is to be noted that the entire treatment of this problem, as presented

here, differs from that given by Margenau.[7] He calculated the force necessary to separate the liquid into two parts as a function of the distance between the halves, and then integrated this force to get the work of separation. This calculation is not as clear physically as that given here, but it apparently corresponds to an equilibrium process, and hence should give, not the total surface energy, but only the free energy of formation of the surface.

Margenau gives his calculation as a way of obtaining U. In the present notation his result may be expressed as:

$$U_M = -\pi n^2 \int_0^\infty dx \int_x^\infty dy \int_y^\infty r dr \int_r^\infty E'(z) f(z) dz. \tag{10}$$

It may be readily shown that when

$$f(z) = \Phi[E(z)/T] \tag{11}$$

this quantity is related to the U of Eq. (4) by:

$$U = U_M - T(\partial U_M/\partial T) \tag{12}$$

which is the relation that must hold if U is the total energy and U_M the free surface energy.[8] The condition (11) is fulfilled when the distribution is uniform, or when it follows the simple Boltzmann formula, and it has besides a plausible appearance. We do not fully understand, however, just why it is necessary. When Margenau's calculated values are compared with experimental values of σ instead of with U as Margenau did, they are seen to be rather too large.[9] The agreement with experiment of the present calculations, while superficially worse than that erroneously obtained by Margenau, is actually considerably better, and by inventing plausible functions $f(z)$ one could obtain even exact agreement; it is to be hoped that experimental values of $f(z)$ will soon be available, at least for monatomic liquids, from analysis of x-ray diffraction data. It will be of considerable interest to see how the results are affected when these empirical values are used.[10]

The Heat of Vaporization

The heat of vaporization per molecule is composed of the energy necessary to remove the molecule from the liquid plus that required to expand the surrounding atmosphere; that is

$$\Delta H = \Delta U + \Delta(pv). \tag{13}$$

[7] Margenau's calculation, like ours, applies to a surface of uniform density; there is thus an unknown correction for the actual surface, which will, however, affect U more than F.

[8] We wish to thank Professor F. Zwicky for pointing out this relation to us.

[9] Margenau's agreements in the cases of He, O_2, Cl_2, and Hg appear to depend upon fortunate choices of temperature, since if he had made the calculations at about 2°K, for He, and near the freezing points for the others, he would have found surface energies much too high.

[10] For liquid mercury, Debye and Menke, Ergebnisse der technischen Röntgenkunde, **2,** 1 (1931), have determined such values; the maximum reached by $f(z)$ is only about 3, and as z increases, $f(z)$ falls rapidly to 1. The general form of their $f(z)$ curve is in satisfactory agreement with the requirements of our calculations; since liquid mercury exhibits metallic properties, a computation of its surface tension from the forces between the neutral atoms appears to us to be a questionable procedure, and hence no direct use is made of Debye and Menke's result.

We can compute the part of ΔU due to potential energy; there is certainly some difference in the mean kinetic energy of the molecules in gas and liquid, but except at low temperatures where zero point energy comes into prominence, this is a relatively small effect. The potential energy part of ΔU is found as follows:

Consider a quantity of liquid containing N molecules, where N is very large. The mutual potential energy of a molecule with respect to all the others is

$$W = \int_0^\infty - 4\pi n r^2 f(r) E(r) dr.$$

The mutual potential energy of all the molecules is $\frac{1}{2}NW$, since the energy of each pair must be counted only once. Hence the potential energy per mol is $\frac{1}{2}N_0 W$ where N_0 is Avogadro's number, or:

$$U = 2\pi n N_0 \int_0^\infty r^2 f(r) E(r) dr. \tag{14}$$

In terms of the two above assumptions for $f(z)$ we get:

$$\text{(a)}: \quad \Delta U = -\frac{2}{3}\frac{\pi n N_0 \beta}{R_0^3} \tag{15}$$

$$\text{(b)}: \quad \Delta U = -\frac{2}{3}\pi n N_0 (kT\beta)^{1/2} \int_0^{(\beta/kTR_0^6)^{1/2}} e^{z^2} dz \tag{16}$$

provided the vapor formed is so dilute that attractive forces in it may be ignored. Again, Eq. (16) can be readily evaluated graphically. The term $\Delta(pv)$ of Eq. (13) is, of course, easily seen to be RT. Table II shows how the calculated values of ΔH compare with experimental ones. The values of α, V, R_0, and n are the same as those in Table I.

TABLE II.

Gas	T (°K)	ΔH calc. cal./mol.		$\Delta H_{exp.}$
		Eq. (15)	Eq. (16)	
He	4	81.3	$>10^{10}$	24
Ne	34	310.4	922	380
A	87	1213	11900	1500
N_2	80	975	4860	1400
Cl_2	240	4334	694000	2400
O_2	90	913	2300	1730

For helium the agreement is very poor, and it is clear that a large part of the energy needed must be supplied by the zero point vibration of the liquid. For chlorine, also, our choice of ionization potential again leads to calculated values too high. But for the other liquids the observed values of the heat of vaporization lie between the values calculated by Eqs. (15) and (16). And as in the case of the surface energy, in all cases except O_2, the agreement with the assumption of a uniform distribution is much better than with that of a Boltzmann distribution. It thus appears that here, too, a slight modification of the distribution function from uniformity would lead to values as accurate as can be obtained with the quantum mechanical approximations to the intermolecular forces.

LETTERS TO THE EDITOR

Prompt publication of brief reports of important discoveries in physics may be secured by addressing them to this department. Closing dates for this department are, for the first issue of the month, the twenty-eighth of the preceding month; for the second issue, the thirteenth of the month. The Board of Editors does not hold itself responsible for the opinions expressed by the correspondents.

Line Broadening and the Imprisonment of Resonance Radiation

Applications of existing theories of resonance radiation diffusion[1] have, in the main, employed classically predicted values of absorption coefficients, or values of this quantity predicted from measurements at low gas pressures (of the order 1 micron). Zemansky,[2] and Webb and Messenger[3] found that at larger vapour pressures, Hg resonance radiation escaped from a body of gas faster than could be accounted for on the basis of the known (low pressure) value of the atomic absorption coefficient—and indeed the more was this so the higher the vapor pressure. These authors attributed the effect to line broadening due to absorption or other causes.

Bearing on this question are some experiments of the writer, similar to experiments already reported,[4] which show that when the resonance radiations of Ne at a pressure of 1.5 mm pass a considerable distance away from a discharge and are absorbed, only a small fraction (1–3 percent) of this energy is converted into metastable atoms,[5] the remainder escaping to the walls as scattered resonance radiation.

It has been calculated from these results, assuming a mean life of the excited atoms of 10^{-7} sec. and reasonable tentative values (1–0.1 percent) for the (quenching) efficiency of gas kinetic collisions transferring excited Ne atoms to the metastable state that the mean free path (reciprocal of absorption coefficient) of the scattered resonance quanta must be of the order of 0.2–2 cm. This may be compared to the value 6.5×10^{-6} cm calculated for the cores of the resonance lines of Ne for 1 mm pressure by Found and Langmuir[6] from a formula of Ladenburg, or to the value 2×10^{-4} cm for the core of the mercury resonance line predicted for a pressure of 1 mm from the atomic absorption coefficient of Hg for this radiation as known for low pressures.[7] It is suggested that the great discrepancy here involved is caused by a broadening of the resonance lines as a result of coupling forces (Holtsmark[8] broadening), or of molecule formation.[9]

It is well known that the absorption breadths of the resonance lines of Na, Cs, etc. at pressures of the order of 1 mm are very great compared with the Doppler breadths. Hopfield[10] found a large broadening of the He resonance line in emission which was explained by Weizel[9] as due to molecule formation between excited He atoms and normal He atoms.

Abnormal broadening of the visible lines of the rare gases has not been observed: from the standpoint of the coupling theory[8] none would be expected since there are no *resonators* among the normal gas molecules which can respond to the frequencies concerned; from the standpoint of molecule formation it may be that a possible shortness of life of the upper

[1] K. T. Compton, Phys. Rev. **20,** 283 (1922); E. A. Milne, Journ. Lond. Math. Soc. Vol. 1 (1926).

[2] M. W. Zemansky, Phys. Rev. **29,** 513 (1927).

[3] Harold W. Webb and Helen A. Messenger, Phys. Rev. **33,** 319 (1929).

[4] Carl Kenty, Phys. Rev. **38,** 377 (1931).

[5] I. Langmuir and C. G. Found, Phys. Rev. **36,** 604 (1930).

[6] C. G. Found and I. Langmuir, Phys. Rev. **39,** 248 footnote (1932).

[7] See for example, M. W. Zemansky, Phys. Rev. **36,** 229 (1930).

[8] J. Frenkel, Zeits. f. Physik **59,** 198 (1930).

[9] Walter Weizel, Phys. Rev. **38,** 642 (1931).

[10] J. J. Hopfield, Astrophys. J. **72,** 133 (1930).

excited states, compared with the effective[11] life of the resonance states, renders such formation relatively unlikely.

Penning[12] calculated from Dorgelo's and Washington's measurements of the mean lives of metastable Ne atom at 7.1 mm pressure that only about 1 collision in 10^5 was of the first kind (resulting in transfer from the metastable state to the resonance state). It has frequently been suggested on the other hand, that the atoms go continually up and down between these states,[13] the efficiency of collisions of the first and second kinds being supposed to be relatively very high and the mean free path of the resonance lines being supposed to be very short (classically predicted values). Obviously, under such circumstances a calculation like that of Penning would be meaningless. But, the present results show that once a metastable Ne atom is raised to the resonance state there will be little chance of a new metastable atom being formed and hence Penning's calculation is confirmed (as are also the essentially similar calculations of a number of other observers on the lives of metastable atoms.[14]

The present results are in agreement with the direct observation of Meissner and Graffunder[15] that metastable Ne atoms are powerfully destroyed by strong Ne light (an abnormally long mean free path of the scattered resonance lines of Ne might have been inferred from this alone) and with Penning's interpretation that metastable atoms were strongly destroyed in his experiments[16] by irradiation and with the irradiation experiments of the writer.[4]

The previous results that the currents here dealt with (in the case of pure rare gases) are mainly of photoelectric origin[4,17] have been confirmed. Complete details of the experiments will be given in a paper now in preparation.

Found and Langmuir (private communication) have recently confirmed by direct means that the free paths of the scattered resonance radiations in Ne at 1 mm pressure are very great (of the order of magnitude of the tube diameter or larger) compared with the classically predicted values.

CARL KENTY

Research Laboratory,
General Electric Vapor Lamp Co.,
Hoboken, N. J.,
April 6, 1932.

[11] Repeated reabsorptions are here taken into account.

[12] F. M. Penning, Zeits. f. Physik **46,** 342–343 (1928).

[13] P. D. Foote, Phys. Rev. **30,** 288 (1927); M. W. Zemansky, Phys. Rev. **34,** 226 (1929); see also C. G. Found and I. Langmuir, reference 6, pp. 250, 251.

[14] See an excellent summary of data of this kind by Zemansky, Phys. Rev. **34,** 213 (1929).

[15] K. W. Meissner and W. Graffunder, Ann. d. Physik **84,** 1009 (1927).

[16] F. M. Penning, Phil. Mag. **11,** 961 (1931) and other papers.

[17] Carl Kenty, Phys. Rev. **38,** 2079 (1931).

The New Effect Produced by the Action of X-rays on Matter

G. I. Pokrowski (Phys. Rev. **38,** 925 (1931)) has reported a series of experiments which indicate that some of the heavier elements (Pb, Bi, Hg, etc.) after irradiation with x-rays (90 and also 140 k.v.) acquire feeble radioactive properties. A sample of Pb which had been irradiated for 30 minutes was found to produce a measurable ionization current up to 90 minutes after irradiation. This experiment has been repeated by Gingrich (Phys. Rev. **39,** 748 (1932)) who used as detector a Lindemann electrometer of high sensitivity. Although Gingrich's experimental arrangement would probably have been able to detect one one-hundredth of the maximum effect reported for Pb, yet he found no difference for the ionization produced by various metals before and after irradiation with x-rays whose voltage was varied between 45 and 160 k.v. Gingrich's periods of irradiation appear to have been comparable with those of Pokrowski (30 to 40 minutes).

Pokrowski also reported an effect which was built up after continued irradiation with x-rays. This effect was detected by scintillations produced on a zinc sulphide screen. This effect was found to persist for many days after irradiation and corresponded with about one scintillation per cm^2 per second. From a knowledge of the total ionization produced he calculated that the particles from Pb which were responsible for the scintillations had an average energy of 1.1×10^6 e.v. If these were α-particles, then they should have a range in

air at N.T.P. of about 6 mm and since range is inversely proportional to pressure, a range of about 4.5 cm at 10 cm pressure.

The writer, whose experiments were well under way at the time of Gingrich's letter, repeated Pokrowski's work employing a Geiger point counter as detector. The point of the counter was a platinized plantinum sphere 0.3 mm in diameter, while the house, which was 2 cm in diameter and 6 cm long was a cylinder of copper gauze (10 wires to the cm, each 0.17 mm diameter).

The counter was operated at 2000 volts, with the house negatively charged, a cabinet of batteries being the source of potential. The counter was enclosed in a glass tube 5 cm in diameter which could be opened by means of a large glass joint and after closing be kept at any desired pressure. The passage of ionizing radiation through the counter was detected by one valve amplification in a telephone (transformer coupled) and a microammeter. The passage of one secondary β-ray due to γ-rays from uranium through the counter caused a defection of 400 microamperes and a loud click in the telephone.

A sample of sheet lead (unirradiated) in the form of a cylinder (2.5 cm diameter) was slipped over the house of the counter and after shielding with 5 mm Pb the natural count determined and found to be 2.8 ± 0.5 counts per minute, this being the average of readings taken over 100 minutes. (Under these same conditions with the shield removed the counter would record secondary electrons from γ and x-rays.) The sample of Pb after removal from the counter and rolling out flat was irradiated with x-rays from a tungsten target at 110 k.v. and 1.2 m.a., the sample being 10 cm from the target. The sample was irradiated for a total of 200 hours with counts being taken at various intervals, however even after this length of irradiation the sample still showed practically the same count of 3.0 ± 0.5 counts per minute. Five minutes elapsed between shutting off the x-rays and the start of the counter, so that any effect which did not last longer than this period would not have been detected. The counter was operated at 10 cm pressure of air so that α-particles of the order of 1 million electron volts should have easily passed through the counter since the point of the counter was only 1.5 cm from the surface of the lead cylinder. It is difficult to estimate the sensitivity of this method but it seems highly probable that much as one α-particle per minute per cm^2 of lead would have been detected, however no change greater than 0.5 counts per minute was found, a value which is about one one-hundredth of the effect found by Pokrowski. Check experiments indicated that β-particles or γ-rays would have been detected if they had been responsible for the effect reported by Pokrowski.

Because of the great interest connected with Pokrowski's results other experiments were carried out using different counters operating at a lower pressure, different samples of lead and x-rays of a voltage range between 50 and 140 k.v., however in no case was the irradiation found to produce any determinable radioactivity. This failure, together with that of Gingrich, is difficult to correlate with the positive results reported by Pokrowski.

NORMAN S. GRACE

Department of Chemistry,
University of California,
April 14, 1932.

Note on the Discovery of the Photoelectric Effect in a Copper-Oxide Rectifier

Under "Letters to the Editor," **39,** 531 (1932), a letter signed by Professors Frenkel and Joffé has in it the following statement: "The illumination of the place of contact between a metal and a semiconductor, Cu and Cu_2O say, produces, as has been first shown by Lange, an unusual photoelectric effect," etc.

They may have had reference only to the outer contact, but it is not quite clear that that is the case and it may be worth while to point out that the effect at the inner boundary between cuprous oxide and the mother copper was first discovered in our laboratory before 1926. It was demonstrated in the Scientific Exhibition given at Philadelphia in December, 1926, during a meeting of the American Association for the Advancement of Science. It was also mentioned in an article entitled "A New Electronic Rectifier," by Grondahl and Geiger, (Transactions of the A.I.E.E., **XLVI,** 357 (1927)), where it is stated that illumination of a rectifier not only changes the resistance, but produces a small e.m.f. in the rectifier, so that it has to be avoided when measuring very small currents. The effect was

discovered by Dr. P. H. Geiger and the writer in cooperation and consists in an e.m.f. produced at the junction between the cuprous oxide and the mother copper on which the oxide is formed. Dr. Lange later discovered the effect at the outer contact made to the free surface of the cuprous oxide. By the German writers the former effect has been called the "hinterwandeffekt" and the latter, the "vorderwandeffekt." Professor W. Schottky has on various occasions recognized our priority in the discovery; see, for instance, Phys. Zeits. **31,** 913 (1930).

L. O. GRONDAHL

Research Department,
Union Switch and Signal Company,
April 12, 1932.

A Correction to Wave-length Measurements with the Double-Crystal Spectrometer

The measurement of the diffraction angles from calcite for certain x-ray lines by the double-crystal x-ray spectrometer is now established as one of the precision methods of measuring x-ray wave-lengths. However, there is a correction to be made to the observed angle due to the effective height of the slits or the effective vertical spread of the beam. The formula previously given by Compton[1] is in error, giving too large a correction. Professor Compton and the writer recently derived the corrected formula, which is:

$$\delta\theta_{\text{eff}}=\frac{a^2+b^2}{24L^2}\tan\theta$$

where a and b are the vertical stops at a distance L apart and θ is the Bragg angle. This is to be compared to Eq. (3) in reference 1.

The wave-length of the Mo $K\alpha_1$ line as previously determined by this method is now to be calculated from the angles

$$\theta_1=6^\circ\ 42'\ 35.9_5''$$

and

$$\theta_4=27^\circ\ 51'\ 35.0''.$$

The index of refraction calculated from these angles by the usual method give

$$\delta=(2.08\pm0.15)\times10^{-6}$$

The wave-length of Mo $K\alpha_1$ calculated from θ_4 by the same method[1] is 707.843 ±0.002 x.u. This is to be compared with Larsson's[2] value of 707.831 ±0.003 x.u. calculated on the same basis from photographic measurements. Bearden's[3] value of θ_4 is 27° 51′ 34.4″ ±0.2″ on the basis of the incorrect formula, and the new correction would increase this angle slightly. There is thus good agreement between Compton's and Bearden's measurements in the fourth order with the double-crystal x-ray spectrometer.

The correction is seen to be very small but these changes are appreciable in view of the accuracy with which the diffraction angles can be measured. Where the original data are available it would be well worth while recalculating the angles on the basis of this correction.

I appreciate the collaboration of Professor Compton on this calculation and regret that his absence necessitates the publication without his signature.

JOHN H. WILLIAMS

National Research Fellow,
University of Chicago,
Chicago, Illinois,
April 18, 1932.

[1] A. H. Compton, R.S.I. **2,** 365 (1931).
[2] A. Larsson, Phil. Mag. **3,** 1136 (1927).
[3] J. A. Bearden, Phys. Rev. **38,** 2089 (1931).

Factors Influencing Ionization Produced by Cosmic and Gamma-Rays

Since the mechanism of ionization by gamma-rays is known, a study of the factors influencing ionization produced by gamma and cosmic radiations respectively should give information regarding the process of ionization by cosmic rays.

Accordingly, an experimental study of the following factors is in progress: pressure, temperature and molecular weight of the gas used in the ionization chamber; the material of inner walls as well as the volume and interior area of, and the voltage applied to the ionization chamber.

An ionization chamber was constructed in which the volume, interior area and wall material could be varied. It was designed by R. D. Bennett, Massachusetts Institute of Technology.

The experimental procedure was as follows:

1st. The ionization current was measured when cosmic radiation was the only ionizing agent.

2nd. The ionization current was determined when the ionization was produced by cosmic rays and the radiation from 0.2 milligrams of radium at a fixed position. The ratio of the

former to the latter, denoted by R, was determined when the factors enumerated above were varied.

Experiment shows that this ratio remains constant for pressures varying from 5 to 70 atmospheres, when air, oxygen or carbon dioxide is used in the chamber. This is in accord with the preliminary results[1] obtained with pressures varying from 10 to 50 atmospheres.

R is independent of the volume of the chamber within the limits of the volume available in the chamber used. The volume was varied by a factor of four. It is also of interest to note that the shape of the ionization chamber seems to have no effect upon the ionization current per unit volume.

The effect of temperature upon the ionization by gamma-rays has been reported.[1] We were interested in finding whether temperature was a factor in the case of ionization produced by cosmic rays. The chamber was subjected to various temperatures, while the batteries and other parts, by means of which temperature might cause a change in the sensitivity of the electrometer, were kept at a constant temperature. It was found that, within experimental error, R remained constant. Separate tests showed temperature to be a factor in each case. Hence, the temperature coefficient is the same for cosmic as for gamma-rays.

It is hard to interpret the results when different liners are used. This is complicated by several factors, of which local radiation due to contaminations of the liners is difficult to determine. There is a variation of R after corrections are made for absorption. Further work is in progress on this point.

At present the value of R is being determined for applied chamber voltages varying from 6 to 450 volts over the same range of pressures used when the effect of pressure was being studied. It is hoped that this may help to determine whether saturation with pressure is due to the rate of recombination of ions becoming equal to that of diffusion[1] or to the complete absorption[2] by the gas of the beta-particles ejected from the walls of the ionization chamber.

These results indicate the process of ionization is the same for cosmic as for gamma-rays and that the cosmic rays are gamma in nature.

This work was done with the aid of a grant from the Rumford Committee.

J. C. Stearns
Wilcox Overback

University of Denver,
April 21, 1932.

[1] A. H. Compton, R. D. Bennett and J. C. Stearns, Phys. Rev. **39,** 873 (1932).
[2] J. W. Broxon, Phys. Rev. **37,** 1320 (1931)

Paramagnetic Susceptibilities in Crystals

Following a suggestion of Professor Van Vleck, we have investigated the influence of electric fields of different symmetries[1] on the paramagnetic susceptibilities of atoms in crystals. Experimentally, the susceptibility can often be represented by the Curie-Weiss law $\chi = C/(T+\Delta)$, provided the temperature is not too low. We find that if the energy levels are all either high or low compared with kT then the rigorous expansion for the susceptibility averaged over all directions is of the form $\chi = C_1/T + C_3/T^3 + \cdots$, the term in $1/T^2$ being absent. This means that if we measure the susceptibility of a crystal powder and plot $1/\chi$ against T, the curve tends to an asymptote passing through the origin and not through the point $(0, -\Delta)$. At lower temperatures it is necessary to use exact expressions and it is found that the susceptibility may simulate the law $\chi = c/(T+\Delta)$ over a wide range of temperature. This is the case, for example, with Pr and Nd, where the splitting produced by the crystal field is comparable with kT at room temperatures.

The rare earths lend themselves very readily to exact calculations, which have been carried out for Pr and Nd. At room temperatures and lower, the only normal states are those arising from the lowest multiplet level; the other multiplet levels can be neglected. Assuming a field of cubic symmetry $A(x^4+y^4+z^4)$ and a magnetic field H one can solve the related secular problem up to and including terms in H^2. The secular determinants are of order 9 and 10 respectively; when $H=0$, that for Pr factors into a singlet and four quadratics; that for Nd factors into two quintics on account of the Kramers two-fold degeneracy, and each quintic factors into a singlet and two

[1] Cf. Kramers, Proc. Amst. Acad. **32** and also Bethe, Ann. d. Physik **3,** 133 (1929).

quadratics. The lowest multiplet level of Pr splits up into two triply degenerate and one non-degenerate level. Agreement with experiment is obtained when the nonmagnetic, single level is placed lowest. The lowest multiplet level of Nd splits up into two quadruply degenerate and one doubly degenerate level, and here the doubly degenerate level must be placed lowest. The results agree satisfactorily with the measurements of Gorter and de Haas.[2] The over-all splitting produced by the crystal field is about 360 cm^{-1} for Pr and 840 cm^{-1} for Nd.

Calculations have also been made for Ni. Here the separation of energy levels due to the crystal field is much larger than the multiplet separation. The close equality of the observed principal susceptibilities suggests that the field is nearly cubic. If we neglect the spin, the ground state is split by the cubic field into one nonmagnetic and two magnetic levels; the nonmagnetic level must, for agreement with experiment, lie so far below the others that it alone is a normal state. The orbit-spin interaction is incapable of splitting this level which now has three coincident components. Thus the spin remains entirely free, and the susceptibility is rigorously proportional to $1/T$. The orbit-spin interaction, however, introduces an orbital contribution, so that the magneton number has a value intermediate between the Bose-Stoner value $[4S(S+1)]^{1/2}$ and the Laporte-Sommerfeld value $[4S(S+1)+L(L+1)]^{1/2}$. From the known value of the magneton number, we deduce an over-all separation of some 20,000 cm^{-1} due to the cubic field. If now a rhombic term is introduced into the Hamiltonian, the degeneracy of the lowest level is removed, the separation being of the order of a few wave numbers, and it is possible to explain the small differences in the principal susceptibilities. The dependence on temperature is now of the form $\chi = C_1/T + C_2/T^2 + \cdots$ with different values of C_1, C_2, and Δ for the three axes. The average Δ is zero down to very low temperatures, in agreement with the very small observed value.

We have also considered Cu. Here the principal susceptibilities are so different as to preclude a cubic field. On the basis of a rhombic field producing a splitting large compared with the multiplet width, it is found that the law $\chi = C/T$ is obeyed by the susceptibility down to very low temperatures (cf. the experiments of de Haas and Gorter[3]). Thus the rhombic field alone does not introduce a correction to Curie's law, although it gives different Curie constants for the three axes.

These quantitative results are in general agreement with the qualitative predictions of Van Vleck (Quantum Theory of Electric and Magnetic Susceptibilities, Oxford University Press, Chap. XI), the chief difference being that the crystal fields are usually more nearly cubic than was there supposed, and also that the condition given for the spin to be free, namely (orbit-spin interaction)^2/(crystal field separation)$\ll kT$, is often too stringent.

The experimental material indicates that substances of high magnetic dilution, as for example the hydrated sulphates, have smaller values of Δ than the corresponding anhydrous salts. In these latter substances of very low magnetic dilution the effect of crystal fields on the deviation from Curie's law is probably subordinate to the influence of coupling between the angular momentum vectors of neighboring atoms, which will also give rise to a term Δ.

Further computations are in progress on cerium, cobalt and iron. Details of the work will be published shortly.

O. M. Jordahl
W. G. Penney
R. Schlapp

Department of Physics,
University of Wisconsin,
April 22, 1932.

[2] Gorter and de Hass, Leiden Com. 218b.

[3] de Haas and Gorter, Leiden Com. 210d.

The Production of Multiple Secondaries in Lead by Cosmic Radiation

Recently Rossi[1] has shown that triple coincidences occur in three G.M. counters placed out of line if these are surrounded by lead. We have observed a similar phenomenon with two G.M. counters arranged as shown in the accompanying diagram, Fig. 1.

Coincident discharges of the two counters were recorded on a telephone message register, operated by circuits soon to be described. The resolving time of the circuits was such that the accidental coincidences amounted to only two or three per hour and hence could be

[1] Bruno Rossi, Phys. Zeits. **33**, 304 (1932).

entirely neglected. At the spacing used the real coincidences averaged 1.71 per minute with a probable error of ± 0.03 per minute

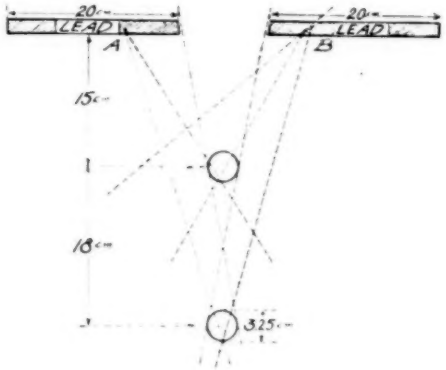

Fig. 1.

over a counting time of 1568 minutes. When blocks of lead $20 \times 32 \times 1$ cm were placed on either side of the counters in positions such that straight line paths through both counters were impossible for secondary rays originating in the lead, then the counting rate *increased* to 1.84 ± 0.03 over a counting time of 1312 minutes. The difference in the counting rates of 0.13 ± 0.04 must be attributed to some process by means of which the same primary ray ejects two or more secondaries from the lead at slightly different angles, some of these passing through one counter and others through the other counter. These secondaries may arise from the spraying out of distingegration products from a single nucleus as illustrated at *A* in the figure or they may be emitted as recoil electrons or protons at different points along the path of the primary ray as illustrated at *B*.

THOMAS H. JOHNSON
J. C. STREET
The Bartol Research Foundation of The Franklin Institute,
Swarthmore, Pa.,
April 25, 1932.

The Crystal Structure of Insulin

It has been known for some time that insulin exhibited certain optical properties of a true crystal.[1] Although numerous attempts have been made by Freudenberg[2] and others, no x-ray diffraction pattern could be obtained beyond the usual ring due to the 3.5A spacing common to proteins. Work of this kind employing the usual lengths of x-radiation, (copper $K\alpha$, 1.54A) has been done in this laboratory over a period of two years.

Recently insulin has been investigated by means of long wave x-rays, using the $K\alpha$ radiation of magnesium and aluminum. The method employed was essentially the same as previously used,[3,4] but a new type of apparatus was designed for the purpose.

The spacings found for insulin by this method are approximately 130, 100, and 80A, giving an axial ratio of 4/3:1:4/5. With the aid of microscopic data the crystal form was found to be monoclinic, with one angle between 88 and 90 degrees, the individual crystals frequently assuming a pseudo hexagonal form. The crystals were positive.

On the basis of the approximate molecular weight of 35,000 proposed by DuVigneaud,[5] and checked by others,[2] and the density of 1.315 determined by Freudenberg[2] and checked by us, the number of molecules per unit cell was found to be 26.

More complete data will be prepared for publication in the very near future, and the method will be applied to other proteins.

G. L. CLARK
K. E. CORRIGAN
Chemistry Department,
University of Illinois,
May 2, 1932.

[1] E. B. Mathews, Reported by Wintersteiner, DuVigneaud, and Jensen. Jour. Pharm. and Exp. Therapeutics **31,** 84 (1927).

[2] Freudenberg, Hoppe-Seyler's Zeits. f. physiol. Chem. **204,** 233 (1927).

[3] Clark and Corrigan, Radiology **15,** 117 (1930).

[4] Clark and Corrigan, Jour. Ind. and Eng. Chem. **23,** 815 (1931).

[5] DuVigneaud Jour. Bio. Chem. **70,** 393 (1927).

Erratum: Dissociation of the Carboxyl Group in Amino Acids and Related Substances, Produced by Absorption of Ultraviolet Light

Three typographical errors occurred in the printing of the above mentioned letter to the Editor (Phys. Rev. **40,** 115 (1932)). To correct these the word "cystine" should replace

"cysteine" in the sentence on page 115 which explains the figure, under (6′) and (8′), which refer to water and HCl solutions of cystine, respectively.

The importance of the corrections is apparent from a consideration of the reaction which occurs when light of the 2500A range breaks the S-S linkage in cystine, $COOH \cdot CHNH_2 \cdot CH_2 \cdot S \cdot S \cdot CH_2 \cdot CHNH_2 \cdot COOH$, which in the presence of HCl will produce cysteine, $COOH \cdot CHNH_2 \cdot CH_2 \cdot SH$, and cysteine chloride, $COOH \cdot CHNH_2 \cdot CH_2 \cdot SCl$.

GLADYS A. ANSLOW

Smith College,
Northampton, Mass.,
April 24, 1932.

BOOK REVIEWS

Lichtelektrische Zellen und Ihre Anwendung, H. Simon and R. Suhrmann. Pp. 373+vii, figs. 295. Verlag von Julius Springer, Berlin, 1932. Price RM 34.20, bound.

This volume is at least the eighth which has been published during the past four years in the field of photoelectricity. Striking evidence for the recent rapid development and extension of this field is seen in the fact that these eight treatises show surprisingly little overlapping. Each occupies itself primarily with certain particular phases of the field and only when all are combined does one obtain a complete panorama of this branch of physics. The present volume, written by two authors who need no introduction to students of photoelectricity, offers the most comprehensive review of the practical and technical aspects of the subject which has yet appeared. While it might be judged from the title that the book confines itself to the technical applications of photoelectric cells, it is in reality a treatise on the whole field of photoelectric technique, giving as much—or more—attention to problems which arise in laboratory research as to those common to industrial developments. It will be valuable alike to physicists and engineers.

The first four chapters present a concise discussion of the fundamental laws and phenomena in photoelectricity. The authors disclaim any attempt to make this an exhaustive review, referring the reader to the other books on the more physical and theoretical aspects of the subject. The discussion is nevertheless an adequate introduction to the more practical phases of photoelectricity and includes a short review of photoconductivity and the photoelectric effect in rectifying layers, as well as a much longer discussion of the ordinary surface effect.

Chapter V (64 pages) is a detailed account of the methods of construction and manufacture of photoelectric cells of all types. It includes such topics as the design of cells for various purposes, vacuum technique and outgassing methods, methods of preparing photoelectric materials (particularly the alkali metals) and of introducing them into the cell, gas-filling construction of selenium cells and cuprous oxide cells, etc. Chapter VI (112 pages) describes rather completely the apparatus and methods used in photoelectric investigations. Methods of measuring photoelectric currents are first discussed, the methods involving the use of electrometers being given particular attention. The amplification of both steady and rapidly varying photocurrents is taken up in detail, and finally there is a most exhaustive review of sources of light and their characteristics, light filters, monochromators, and methods of measuring light intensities. The last chapter (130 pages) is devoted to descriptions of the technical applications of photoelectric cells, including photoelectric photometers of all types (lamp photometers, microphotometers, spectro-photometers, etc.), photo-telephony, facsimile transmission, television, sound films, and the numerous applications of photoelectric relays. The treatment in each case includes a discussion of the general principles underlying the various methods as well as a description, with many excellent diagrams and photographs, of the practical details of design and construction of the instrument. The book is profusely illustrated throughout, containing nearly 300 figures, a large number of which are half-tones.

On the whole the book is compiled with the amazing thoroughness which we have come to expect of German writers. The American reader will be disappointed to find in a few cases that instruments and methods which have been developed and are widely used in this country are given only passing mention. For example, in the rather detailed discussion of electrometer technique no mention at all is made of the Compton electrometer, which in this country has almost completely supplanted the Dolezalek form for photoelectric work. Similarly, in the discussion of amplifying tubes and of monochromators and light sources, it is only the German-made instruments which are described. This is to be expected, of course, for authors in any country will naturally give prime consideration to the instruments and methods with which they are most familiar. In the present volume the disadvantage to readers in this country will be largely offset by the fact that they will gain an introduction to apparatus and technique which are in many cases superior to our own. In any case the book will certainly be invaluable to anyone working in either the physical or technical branches of photoelectricity.

LEE A. DU BRIDGE
Washington University

Le Soleil. Georges Bruhat. Pp. 235+xvi, figs. 47 and 16 plates. Librairie Felix Alcan, Paris, 1931. Price 20 fr.

This clearly written small volume brings together the more important known physical data regarding the sun and discusses in convenient outline their theoretical interpretation. Even though the internal constitution of the sun appears to be fairly well known, the author, perhaps wisely, avoids its discussion and the subject matter of the book relates almost entirely to the surface features of the sun and the properties of its atmosphere. The selection of the material, the relative space allotted to each subject and the arrangement seem fortunate. The value of the book would be enhanced by the inclusion of guiding references to important literature.

Ross Gunn
Naval Research Laboratory

Kolloidwissenschaft, Elektrotechnik und Heterogene Katalyse. W. Ostwald. Pp. 113, figs. 63. Verlag Theodor Steinkopff, Dresden, 1930. Price RM 5.

This little book has been reprinted from the Kolloidchemischen Beiheften. It expresses very well the author's ideas concerning the importance of a knowledge of colloid chemistry in the complete understanding of insulators, electrodes, rectifiers, photoelectric cells, and heterogeneous catalysis. After discussing briefly the properties of matter in colloidal state of dispersion, the author presents the evidence which shows that the colloidal state of matter is found in and contributes markedly to the successful operation of insulators, electrodes, rectifiers, photoelectric cells and catalysts. To anyone interested in the above mentioned subjects this book will serve as an introduction to the science of colloids as applied in those fields.

L. H. Reyerson
University of Minnesota

Handbuch der Experimentalphysik Erg. Band I. Bandenspektren—W. Weizel. Pp. 461+xi figs. 139. Akademische Verlag m.b.H., Leipzig, 1931. Price RM 43.—bound, RM 45.

The study of the spectra of diatomic molecules has now approached a certain stage of completion as is evidenced by the number of reviews of it which have appeared of late. The book under review, by Professsr Weizel, is itself more than a review, it is a complete treatise on the subject, and while it naturally covers much the same ground as Professor Mulliken's well known articles in English in the Reviews of Modern Physics differences in style and content make both works indispensable.

The method of attack is somewhat unusual and will undoubtedly meet with the hearty approval of all who have experienced difficulties in following the quantum theory of molecules. The frank acceptance of "models," however inexact, while still not providing the royal road to knowledge at least smooths out some of the bumps. The theoretical analysis is put first and is founded on separation of the wave function in elliptic coordinates, considerable emphasis being placed on the separability into individual wave functions for the electrons. The various symmetry properties of the wave functions are completely explained so far as this can be done without invoking even the elements of group theory. Vibration and rotation are treated in the absence of spin which appears as a perturbation. Perturbation theory, uncoupling phenomena and such special topics as predissociation nuclear spin, etc. are given extended treatments.

From the discussion of the theoretical terms the second chapter passes on to the predicted band types, intensities, selection principles, band structures, etc. The third chapter is devoted to polyatomic molecules, and naturally gives only a brief introduction to this already extensive subject within its limited bounds. The final chapter, covering about one half of the book is given over to a very valuable resumé of the spectra of particular molecular groups, both diatomic and polyatomic. References are carried up to the end of 1930 and partially into 1931.

What seems to be a rather large number of slips and misprints have been detected but none of them promise to be particularly troublesome. Everything is presented in such detail and with such uniform excellence that we can only give Professor Weizel's book the highest recommendation.

E. L. Hill
University of Minnesota

CURRENT LITERATURE OF PHYSICS

Extracts from the Tables of Contracts of Some of our Contemporaries

PROCEEDINGS OF THE ROYAL SOCIETY

SERIES A, VOL. 135, NO. 828 — APRIL 1, 1932

Reactions between Carbon and Certain Gases. By **W. E. J. Broom and M. W. Travers**.. 512
Study of the Magnetic Properties of Matter in Strong Magnetic Fields. Part III. Magnetostriction. By **P. Kapitza**.... 537
Study of the Magnetic Properties of Matter in Strong Magnetic Fields. Part IV. The Method of Measuring Magnetostriction in Strong Magnetic Fields. By **P. Kapitza**.. 568
Study of the Magnetic Properties of Matter in Strong Magnetic Fields. Part V. Experiments on Magnetostriction in Dia- and Para-magnetic Substances. By **P. Kapitza**.. 568
On the Analysis of Experimental Observations in Problems of Elastic Stability. By **R. V. Southwell**.... 601
Fluorescent Excitation of Mercury by the Resonance Frequency and by Lower Frequencies. III. By **Lord Rayleigh**.... 617
Permanent Magnet for β-Ray Spectroscopy. By **J. D. Cockroft, G. D. Ellis and H. Kershaw**.... 628
Sensitivity of Atomic Analysis by X-rays. By **C. E. Eddy and T. H. Laby**.... 637
Examination of Turbulent Flow with an Ultramicroscope. By **A. Face and H. C. H. Townend**.... 656
Note on the Distribution of Turbulent Velocities in a Fluid near a Solid wall. By **G. I. Taylor**.... 678
Transport of Vorticity and Heat through Fluids in Turbulent Motion. By **G. I. Taylor**.. 685

NATURE

VOL. 129, NO. 3258 — APRIL 9, 1932

Letters to the Editor
Gill-Morrell and Barkhausen-Kurz Oscillations. By **E.C. S. Megaw; R. Cockburn**.... 542
Polish on Metals. By **F. Kirchner; C. A. Murison, N. Stuart, and G. P. Thomson**.... 545
Anomalous Diamagnetism of Bismuth. By **S. Ramachandra Rao**.... 545
Photochemical Decomposition of Phosphine. By **H. W. Melville**.... 546
Structure of the Third Positive Group of CO Bands. By **G. H. Dieke and J. W. Mauchly**. 546

NATURE

VOL. 129, NO. 3259 — APRIL 16, 1932

Survey of Radioactivity. By **A. S. R.**.... 560
Letters to the Editor:
Variation of Penetrating Radiation with Zenith Distance. By **Gilberto Bernardino**.... 578
Automatic Recording of Heaviside Layer Heights. By **Eric L. C. White**.... 579
Photoconductivity of Diamonds. By **R. Robertson, J. J. Fox, and A. E. Martin**.... 579
Hydrogen Chromosphere. By **J. Woltjer, Jr.**.... 580
Polarization of Raman Scattering. By **S. Bhagavantam and S. Venkaleswaran**.... 580
Constitution of the Keratin Molecule. By **Claude Remington**.... 580

ZEITSCHRIFT FÜR PHYSIK

VOL. 75, NOS. 3 AND 4 — MARCH 31, 1932

Electrical Breakdown Strength and Crystal Structure (The Mechanism of Electrical Breakdown in Solid Insulators. III). By **A. v. Hippel**.... 145
Remarks on the Theory of the Positive Column in Diatomic Gases. By **R. Holm**.... 171
On the Theory of Fine Structure in Roentgen Absorption Spectra. II. By **R. de L. Kronig**. 191
Remarks on the Theory of Rapidly Oscillating Charges. By **Guido Beck**.... 211
Hyperfine Structure of Thalium Arc Lines. By **D. A. Jackson**.... 223
Nuclear Moment of Gallium. By **D. A. Jackson**.... 229

Absolute Measurement of Roentgen Rays with the Electron Tube Counter. By **A. Huppertsberg** 231
Dependence of the Photoelectric Emission of Potassium on the Arrangement of Atomic Hydrogen and Potassium Layers on Its Surfaces. By **P. I. Lukirsky and S. Rijanoff** 249
On Double Refraction Due to Fluid Flow. By **Paul Boeder** 258
On the Spectral Distribution of the Deplorization Current in the Photoelectric Conductance of Rock Salt Exposed to Roentgen Rays. By **N. Kalabuchow and B. Fischelew** .. 282

ZEITSCHRIFT FÜR PHYSIK

VOL. 75, NOS. 5 AND 6 — APRIL 6, 1932

On the Theory of the Width of Spectral Lines (Kopplungsbreite) and Collision Damping. By **V. Weisskopf** 287
Band Spectra of Calcium Hydride. By **Birger Grundström** 302
On the Applicability of Heated Wires for Ultrasonic Measurements. By **H. Müller and T. Kraefft** 313
On Absorption Bands of Iodine and Tellurium. By **E. Hirschlaff** 315
Resonance Spectra of Iodine Vapor at High Temperatures. By **E. Hirschlaff** 325
On the Photodissociation of Molecules into Ions. By **A. Terenin and B. Popow** 338
On the Atomic Structure Factor for X-rays in the Region of Anomalous Dispersion. By **D. Coster and K. S. Knol** 340
Proof of the Uniqueness of the Resolution of Intensity Curves into Their Components. By **Ernst Lonn** 348
Molecular Scattering of Light in Solid Bodies. V. The Theory of Light Scattering (Abstract). By **M. Leontowitsch and S. Mandelstam, Jr.** 350
On the Molecular Field of Weiss. By **Kotarô Honda** 352
On the Molecular Moment of Three Lead Isotopes. By **Hans Kopfermann** 363
On the Growth of a Space Charge in Electrical Discharge through a Gas. By **N. Kapzov** ... 380
Dependance of the Intensity Relations of Secondarily Produced X-ray Lines on the Exciting Wave-Length. By **E. Alexander** 391
On the Reflection of Absorption of Long Wave X-rays. By **E. Dershem and M. Schein** .. 395
Separation between ^2F Levels of Ce IV. By **R. Brunetti and Z. Ollano** 415
On the Burning Out in Vacuum of Incandescent Wires. By **Leopold Prásnik** 417
Remark on the Work of M. Wolfke and J. Mazur: On Two Different Liquid States. By **Lothar Meyer** 421

DIE NATURWISSENSCHAFTEN

VOL. 20, NO. 15 — APRIL 8, 1932

Magnetic Properties of Iron and of its Most Important Alloys. By **O. v. Auwers** 257
Short Original Contributions:
Spectograms of Infrared Lines in the Aurora. By **L. Vegard** 268
Remark on the Radius of the Electron. By **M. Born** 269
Spectrum of the Sun's Corona. By **T. L. De Bruin** 269
News and Proceedings of the Gesellschaft der Wissenschaften zu Göttingen 1931 270

DIE NATURWISSENSCHAFTEN

VOL. 20, NO. 16 — APRIL 15, 1932

Short Original Contributions:
Rotational Motions of Chain Molecules in Normal Paraffins in the Neighborhood of Their Melting Points. By **Alex Müller** 282

DIE NATURWISSENSCHAFTEN

VOL. 20, NO. 17 — APRIL 22, 1932

Short Original Contributions:
Predissociation of the Benzol Molecule in the Lowest Electronic State. By **F. Almasy** .. 296
On the Nature of the Contact Surface [Sperrschict] in Copper Oxide Rectifiers. By **F. Waibel and W. Schottky** 297

PHYSIKALISCHE ZEITSCHRIFT

VOL. 33, NO. 7 — APRIL 1, 1932

Mechanism of the Positive Column in Monatomic Gases. By **R. Seeliger** 273–294
New Method for Measuring Mobilities of Ions. By **G. Stetter** 294–296
Behavior of Hybrid Ions and of multiple Valued Ions with Widely Separated Charges in Electrolytic Solutions. By **G. Scatchard and J. G. Kirkwood** 297–300
On the Choice of a Basis for Atomic Weights. By **St. Meyer** 301–302
Optical Method for the Determination of Vapor Densities. By **H. A. Stuart and M. Weiss** 302–304
Proof of a Secondary Radiation of the Penetrating Corpuscular Radiation. By **B. Rossi** 304–305
Doppler Effect in Piezoquartz. By **H. Müller and T. Kraefft** 305–306
Difference Between Oak and Beech Trees in Respect to Danger from Lightning. By **B. Walter** 306–307

COMPTES RENDUS

VOL. 194, NO. 11 — MARCH 14, 1932

Speaking Clock Designed for the Telephonic Distribution of Time. By **Ernest Esclangon** . 921
Optical Properties of Nitrobenzene in Thin Layers Under an Electrostatic Tension. By **A. Cotton and H. Mouton** 924
On a High Frequency Method for the Study of Vibrations. By **Paul Santo Rini** 955
Some Examples of Non-Linear Oscillations. By **Nicolas Kryloff and Nicolas Bogoliuboff** .. 957
Infrared Absorption Spectrum of Ring Hydrocarbons. By **P. Lambert and J. Lecomte** .. 960
Absorption Spectra of the Rare Earth in the near Infrared. By **R. Freymann and S. Takvorian** 963
New Methods for the Study and Regulation of Television Transmission. By **Maurice Robert** 965
On the Fine Structure of the α-Rays from ThC. By **S. Rosenblum and M. Valadares** 967

COMPTES RENDUS

VOL. 194, NO. 12 — MARCH 21, 1932

Simple Relations between Molecular Spectra and Molecular Structure. By **H. Deslandres** 1033
Ionization Effects Observed in the Presence of Rays from Beryllium Under Excitation by α-Rays from Radium Emanation. By **M. de Broglie, F. Dupré La Tour, L. Leprince-Ringuet and J. Thibaud** 1037
Cyclic Impedances of a Polyphase Line Connected with the Earth. By **André Blondel** ... 1044
Upon the Similitude of a Vortex. By **C. Camichel, L. Escande and G. Sabathe** 1048
Deduction of Maxwell's Equation from the Wave Tensor of Eddington. By **Jean J. Placinteanu** 1054
On the Phenomena of Entrainement in Radio Technique. By **Nicolas Kryloff and Nicolas Bogoliuboff** 1064
Phonic Sound for Measuring the Mechanical Intensity of Sound. By **J. F. Cellerier** ... 1067
New Type of Accumulator. By **François Boissier** 1069

COMPTES RENDUS

VOL. 194, NO. 13 — MARCH 29, 1932

On the Energy of Matter. By **Émile Sevin** 1116
Phenomena of Demultiplication of frequencies in Radio Technique. By **Nicolas Kryloff and Nicolas Bogoliuboff** 1119
On a Peculiar Method of Activation of Matter. By **G. Reboul** 1122
Photovoltaic Properties of Cadmium Sulphide. By **René Audubert and Cécile Stora** 1124

JOURNAL OF RHEOLOGY

VOL. 3, NO. 2 — APRIL, 1932

Thixotropy and Plasticity. II—An Empirical Equation Expressing Thixotropic Fluidity Changes. By **Elliott L. McMillen** 163

Thixotropy and Plasticity. III—The Effect of Thixotropy upon Plasticity Measurements. By **Elliott L. McMillen** 179
Future Problems of Theoretical Rheology. By **Mayo D. Hersey** 196
Purification of Materials by Vacuum Distillation. By **Earl W. Flosdorf and Arthur E. Palmer** 205
Elastic After-Effect in Metals. By **M. F. Sayre** 206
Engler Viscometer and the Theory of Laminar Flow at the Entrance of a Tube. By **L. Schiller** 212
Approximate Calibration of Apparatus for Measuring Absolute Viscosity. By **C. H. Weiss and M. Louis** 217
Fluidity Method for the Determination of Association I. By **Eugene C. Bingham and Laurence W. Spooner** 221
Outline of a Systematic Survey of Rheological Theories. By **Markus Reiner** 245

PROCEEDINGS OF THE NATIONAL ACADEMY OF SCIENCES

VOL. 18, NO. 4 APRIL, 1932

Interatomic Distances in Covalent Molecules and Resonance between Two or More Lewis Electronic Structures. By **Linus Pauling** 293
Critique of Recent Quantum Theories. II. By **R. J. Seeger** 303
Ionization of Argon and Neon by Neutral Argon Beams. By **Otto Beeck** 311
Ionization in Gases by Ions and Atoms. By **F. Zwicky** 314
Mass of the Electron. By **William Duane** 319
Instrument for the Photometering of the New X-ray Lines. By **William Duane** 322
Pressure Variation of the Heat Function as a Direct Measure of the van der Waals Forces. By **Frederick G. Keyes and Samuel C. Collins** 328
Proof of Gibbs' Hypothesis on the Tendency toward Statistical Equilibrium. By **Eberhard Hopf** 333

BUREAU OF STANDARDS JOURNAL OF RESEARCH

VOL. 8, NO. 6 JUNE, 1932

Method for Determining the Most Favorable Design of Gas Burners. By **John H. Iseman, Elmer R. Weaver and Francis A. Smith** 446
Photographic Emulsion: Analysis for Nonhalide Silver and Soluble Bromine. By **Burt H. Carroll and Donald Hubbard** 447
International Comparison of Electrical Standards. By **George W. Vinal** 448
Method for the Purification of Rubber and Properties of the Purified Rubber. By **A. T. McPherson** 449
Tests of a Balanced Thermocouple and Filter Radiometer as a Standard Ultraviolet Dosage Intensity Meter. By **W. W. Coblentz, R. Stair and J. M. Hogue** 450
The Isoelectric Point of Wool. By **Milton Harris** 451
An Optical Method for Measuring Temperature and Convective Heat Transfer. By **R. B. Kennard** 452

JOURNAL OF THE FRANKLIN INSTITUTE

VOL. 213, NO. 5 MAY, 1932

Design Materials and Erection of the Kill Van Kull (Bayonne) Arch. By **Leon S. Moisseiff** 465
Piezoelectric Gage for Recording the Instantaneous Pressure in Shotguns. By **C. T. Ervin** 503
Early Ship Building on the River Delaware. By **Charles Lyon Chandler** 515
Effect of Certain Monochromatic Ultraviolet Radiation on Euglena Cells. By **W. F. G. Swann and C. del Rosario** 549

PHYSICS

VOL. 2, NO. 5 MAY 1932

Dielectric Properties of Some Glycols. By **A. H. White and S. O. Morgan** 313
Development of Polar Characteristics in Insulating Oils. By **W. N. Stoops** 322

Potential Distributions in Large Cylindrical Disks with Partially Penetrating Electrodes. By **Morris Muskat** 329
Chemical Treatment of Rotary Drilling Fluids. By **H. C. Lawton, H. A. Ambrose and A. G. Loomis** 365
Radon Content of Soil Gas. By **Holbrook G. Botset and Paul Weaver** 376
Speed, Speed Factor and Power Input of Different Designs of Diffusion Pumps, and Remarks on Measurements of Speed. By **T. L. Ho** 386
A. C. Wheatstone Bridge for Audio and Radio-frequency Measurements. By **A. Hemingway and J. F. McClendon** 396